frontiers | Research Topics

Immune response to respiratory viruses and respiratory viral infections in susceptible populations

Edited by
Paraskevi C. Fragkou, Roy Chemaly, Giulia De Angelis,
Dimitra Dimopoulou, Giulia Menchinelli and Chrysanthi Skevaki

Published in
Frontiers in Immunology
Frontiers in Medicine

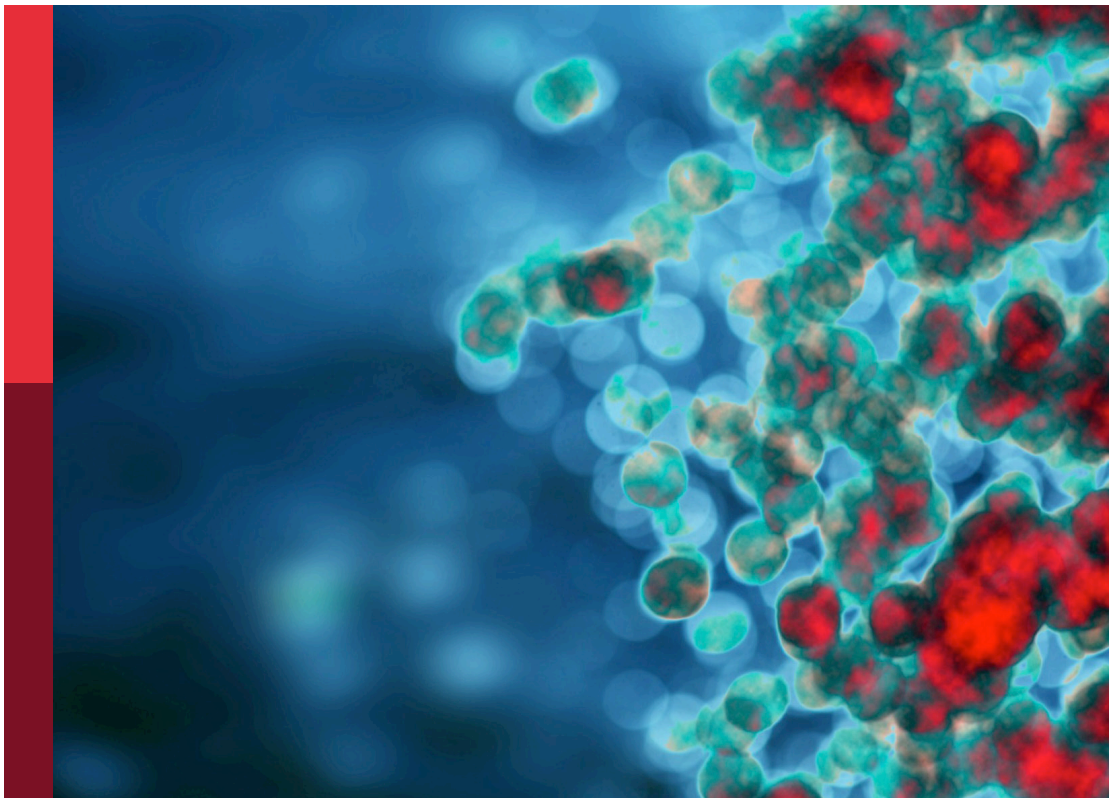

ISSN 1664-8714
ISBN 978-2-8325-4045-9
DOI 10.3389/978-2-8325-4045-9

About Frontiers

Frontiers is more than just an open access publisher of scholarly articles: it is a pioneering approach to the world of academia, radically improving the way scholarly research is managed. The grand vision of Frontiers is a world where all people have an equal opportunity to seek, share and generate knowledge. Frontiers provides immediate and permanent online open access to all its publications, but this alone is not enough to realize our grand goals.

Frontiers journal series

The Frontiers journal series is a multi-tier and interdisciplinary set of open-access, online journals, promising a paradigm shift from the current review, selection and dissemination processes in academic publishing. All Frontiers journals are driven by researchers for researchers; therefore, they constitute a service to the scholarly community. At the same time, the *Frontiers journal series* operates on a revolutionary invention, the tiered publishing system, initially addressing specific communities of scholars, and gradually climbing up to broader public understanding, thus serving the interests of the lay society, too.

Dedication to quality

Each Frontiers article is a landmark of the highest quality, thanks to genuinely collaborative interactions between authors and review editors, who include some of the world's best academicians. Research must be certified by peers before entering a stream of knowledge that may eventually reach the public - and shape society; therefore, Frontiers only applies the most rigorous and unbiased reviews. Frontiers revolutionizes research publishing by freely delivering the most outstanding research, evaluated with no bias from both the academic and social point of view. By applying the most advanced information technologies, Frontiers is catapulting scholarly publishing into a new generation.

What are Frontiers Research Topics?

Frontiers Research Topics are very popular trademarks of the *Frontiers journals series*: they are collections of at least ten articles, all centered on a particular subject. With their unique mix of varied contributions from Original Research to Review Articles, Frontiers Research Topics unify the most influential researchers, the latest key findings and historical advances in a hot research area.

Find out more on how to host your own Frontiers Research Topic or contribute to one as an author by contacting the Frontiers editorial office: frontiersin.org/about/contact

Immune response to respiratory viruses and respiratory viral infections in susceptible populations

Topic editors

Paraskevi C. Fragkou — 1st Department of Critical Care Medicine & Pulmonary Services, Evaggelismos General Hospital, Greece

Roy Chemaly — University of Texas MD Anderson Cancer Center, United States

Giulia De Angelis — Catholic University of the Sacred Heart, Rome, Italy

Dimitra Dimopoulou — Panagiotis & Aglaia Kyriakou Children's Hospital, Greece

Giulia Menchinelli — Catholic University of the Sacred Heart, Rome, Italy

Chrysanthi Skevaki — Universities of Giessen and Marburg Lung Center, Germany

Citation

Fragkou, P. C., Chemaly, R., De Angelis, G., Dimopoulou, D., Menchinelli, G., Skevaki, C., eds. (2023). *Immune response to respiratory viruses and respiratory viral infections in susceptible populations*. Lausanne: Frontiers Media SA.

doi: 10.3389/978-2-8325-4045-9

Table of contents

frontiers | Frontiers in Medicine

TYPE Editorial
PUBLISHED 17 November 2023
DOI 10.3389/fmed.2023.1330265

OPEN ACCESS

EDITED AND REVIEWED BY
Marc Jean Struelens,
Université Libre de Bruxelles, Belgium

*CORRESPONDENCE
Paraskevi C. Fragkou
✉ evita.fragou@gmail.com

†These authors have contributed equally to this work

RECEIVED 30 October 2023
ACCEPTED 02 November 2023
PUBLISHED 17 November 2023

CITATION
Fragkou PC, Dimopoulou D, De Angelis G, Menchinelli G, Chemaly RF and Skevaki C (2023) Editorial: Immune response to respiratory viruses and respiratory viral infections in susceptible populations. *Front. Med.* 10:1330265. doi: 10.3389/fmed.2023.1330265

Editorial: Immune response to respiratory viruses and respiratory viral infections in susceptible populations

Paraskevi C. Fragkou[1,2*†], Dimitra Dimopoulou[2,3†], Giulia De Angelis[2,4,5], Giulia Menchinelli[2,4], Roy F. Chemaly[2,6] and Chrysanthi Skevaki[2,7] On behalf of the European Society of Clinical Microbiology Infectious Diseases (ESCMID) Study Group for Respiratory Viruses (ESGREV)

[1]1st Department of Critical Care Medicine and Pulmonary Services, Evaggelismos General Hospital, Athens, Greece, [2]European Society of Clinical Microbiology and Infectious Diseases (ESCMID) Study Group for Respiratory Viruses (ESGREV), Basel, Switzerland, [3]2nd University Department of Pediatrics, Panagiotis & Aglaia Kyriakou Children's Hospital, Athens, Greece, [4]Dipartimento di Scienze Biotecnologiche di Base, Cliniche Intensivologiche e Perioperatorie, Università Cattolica del Sacro Cuore, Rome, Italy, [5]Dipartimento di Scienze di Laboratorio e Infettivologiche, Fondazione Policlinico Universitario A. Gemelli IRCCS, Rome, Italy, [6]University of Texas MD Anderson Cancer Center, Houston, TX, United States, [7]Institute of Laboratory Medicine, Universities of Giessen and Marburg Lung Center, Marburg, Germany

KEYWORDS

respiratory viral infections, immunology, critical illness, immunodeficiency, immunosuppression

Editorial on the Research Topic
Immune response to respiratory viruses and respiratory viral infections in susceptible populations

Introduction

Respiratory viruses are ubiquitous pathogens that cause infections of varying severity depending on attributes of the host and the virus itself (1). Data from the influenza pandemic in 2009, seasonal influenza epidemics and, more recently, the COVID-19 pandemic, underlie the importance of certain host risk factors that are associated with severe viral infections (1). Besides primary and iatrogenic/secondary immunosuppression that constitutes well known risk factors for basically any infection, other conditions such as pregnancy, obesity, diabetes mellitus, hypertension, cardiovascular disease, asthma, chronic obstructive pulmonary disease and extremes of age have been associated with high mortality and morbidity from respiratory viral infections (1).

The pathogenesis of immune dysregulation that is triggered by these host factors remains largely inexplicable. Revealing the differences and deciphering the commonalities among these conditions that render the host susceptible to severe viral infections will lead us a step closer to the development of more individualized therapeutic targets and

preventative strategies. It is, therefore, vital to congregate the available evidence (including recent advances) and highlight the current research gaps in order to attest potential future therapeutic and preventative options.

The current Research Topic aims to highlight interdisciplinary research approaches that explore the role of host risk factors in the pathogenesis, progress and outcome of respiratory viral infections. Ultimately, the scope of this topic is to generate evidence on improved management and prevention of viral infections in susceptible populations, by assembling current knowledge and addressing potential gaps in research.

Cell culture model and diagnosis of respiratory viral infections

Cell culture models are essential laboratory tools for studying *in vitro* models of host-pathogen interactions and the molecular mechanisms that are involved in the pathogenesis of viral infections. Fukuyama et al. presented their study on the establishment of a new porcine bronchial epithelial cell line from the respiratory tract of a neonatal pig. Through their experiments they concluded that porcine bronchial cells may represent a useful *in vitro* tool to investigate treatments that both potentiate antiviral immunity in the respiratory epithelium of the porcine host and can regulate Toll Like Receptor (TLR) 3- and TLR4-mediated inflammatory injury in the porcine airway which protects the host against harmful immune over responses.

In clinical context, early diagnosis and severity stratification of respiratory viral infections remains challenging in many cases as diagnostic molecular assays are not readily available in all clinical settings and routinely used biomarkers, such as C-reactive protein and white blood cell count, are not sensitive and specific for viral infections (2). Research is increasingly focusing on molecules that can be potentially used as biomarkers with high sensitivity and specificity for viral infections. Herzog et al. conducted a literature review on the surface adhesion molecule on human myeloid cells CD169 (also known as Siglec1 or Sialoadhesin), as a candidate screening biomarker for viral diseases. The authors concluded that even though CD169 shows a promising potential as a biomarker in acute viral diseases so far, universal laboratory standards and methodological groundwork are imperative to generate comparable and reliable results on its diagnostic performance in the context of viral infections.

Severe acute respiratory syndrome coronavirus 2 infection

Severe Acute Respiratory Syndrome Coronavirus 2 (SARSCoV-2) cell entry is achieved through binding of the surface Spike (S) protein into its main host receptor angiotensin converting enzyme 2 (ACE2) (3). SARS-CoV-2 triggers inflammatory responses by affecting multiple cell types including type II alveolar epithelial cells and activating molecular pathways via its S protein, which have been shown to participate in the pathogenesis of COVID-19 (4–7). Al-Qahtani et al. showed that SARS-CoV-2 S protein suppressed inflammatory responses by decreasing the expression and secretion of interleukin (IL)-8, IL-6 and Tumor Necrosis Factor alpha (TNF-α) in alveolar type II cells during the early stages of infection, through activation of the PI3K/AKT pathway. The authors also suggested that at the early stages of the infection, S protein signals inhibit immune responses to the virus, which allows the propagation of the infection. Moreover, S protein signals in combination with TLR2 signals enhance Plasminogen Activator Inhibitor-1 (PAI-1) expression, which potentially affects the local coagulation cascade. The findings of this study propose the potential use of AKT/mTOR inhibitors for the regulation of inflammatory responses during SARS-CoV-2 infection.

SARS-CoV-2 infection has been considered as a trigger for autoimmune diseases through different mechanisms, including bystander activation, cross-reactivity, molecular mimicry, epitope spreading, and cryptic antigen unmasking (8). Tonutti et al. presented a case of anti- Melanoma differentiation antigen 5 (MDA5) syndrome with skin manifestations, constitutional symptoms, and cardiomyopathy following a confirmed SARS-CoV-2 infection in a 70-year-old Caucasian woman and then, they systematically searched for publications on inflammatory myositis associated with COVID-19, focusing on the anti-MDA5 syndrome. MDA5, a pattern recognition receptor, along with type I interferon (IFN) are important components of the immune response against viral infections. The activation of MDA5 induces the synthesis of type I IFN, which is inversely correlated with COVID-19 severity. A strong IFN signature has been associated with disease activity in various connective tissue diseases, including anti-MDA5 syndrome and might have protective effects against viral infections, including COVID-19. Finally, they concluded that SARS-CoV-2 may trigger the synthesis of autoantibodies and elicit an autoimmune response involved in inflammatory myositis pathogenesis, associated to the type I IFN rich molecular milieu promoted by the virus itself. In addition, Luo and Zhou identified common differentially expressed genes (DEGs) for COVID-19 and primary Sjogren's syndrome and performed enrichment and Protein-protein interaction network analysis. They found that COVID-19 and Sjogren's syndrome have common pathogenic mechanisms and pathways, that may be mediated by specific hub genes.

Diversity in response to SARS-CoV-2 exposure among elderly people may be related to differences in their innate immune responses (9). The gel-forming mucin 5B (MUC5B) is part of the mucus that covers the surface of the respiratory epithelium and plays a key role in the control of respiratory infections, the maintenance of immune homeostasis and the mucociliary clearance (10, 11). The decreased expression of MUC5B leads to declined mucociliary clearance, which has been correlated with aging (12). Moreover, constitutive expression of MUC5B levels is associated with the MUC5B promoter polymorphism rs35705950, while the high expressing T-allele is a risk factor for the non-infection-related aging lung disease, idiopathic pulmonary fibrosis (13). van Moorsel et al. investigated the association of MUC5B rs35705950 with severe COVID-19, in a retrospective candidate gene case-control study and the findings revealed that carriage of the T-allele of MUC5B rs35705950 may result in the protection from severe COVID-19, providing further evidence for

the existence of trade-offs among optimal expression levels of MUC5B in the aging lung.

Alshammary et al. performed a systematic review and meta-analysis about the role of T-cell subsets and IL-10 levels among COVID-19 patients and their correlation with the disease severity and outcome. The results demonstrated that severe and non-survivor COVID-19 cases had lower counts of CD4/CD8 T-cells and higher levels of IL-10 compared to mild and survivor cases and the immunodepression following SARS-CoV-2 infection is possibly driven by IL-10. Also, they suggested that these clinical parameters may be reliable predictors of severity and mortality in COVID-19 patients.

Pinchera et al. evaluated the impact of mammalian Target of Rapamycin (mTOR) treatment on the evolution and outcome of SARS-CoV-2 infection in 371 kidney transplant recipients. No differences in the risk of acquiring SARS-CoV-2 infection were observed between the various immunosuppressive therapies. In contrast, patients who received mTOR inhibitors, as part of their immunosuppressive therapy, compared to other regimens had a lower chance of developing a moderate or severe disease. It is worth noting that multivariate analysis found that none of the variables considered showed a statistically significant impact regardless of the presence or absence of mTOR inhibitors. Therefore, mTOR inhibitors may be considered a possible treatment for COVID-19 in transplant and non-transplant patients, due to their potential antiviral or immunomodulatory properties.

In addition, it has been reported that vitamin D may be an important component in the prevention of respiratory tract infections, as it plays a signaling role in the modulation of the innate and adaptive immune response and immunoregulation (14). A systematic review and meta-analysis of randomized controlled trials was conducted by Kümmel et al. to assess the potential effects of vitamin D supplementation on the treatment and prevention of COVID-19 and its complications. The authors found that vitamin D supplementation is associated with a trend of decreased COVID-19-related mortality, shorter hospitalization, and less frequent admission to the Intensive Care Unit (ICU), especially in patients receiving repeated vitamin D doses, when vitamin D was given after the diagnosis of COVID-19.

Finally, acute respiratory distress syndrome (ARDS) in COVID-19 is triggered by hyperinflammation, indicating the need of immunosuppressive treatments. The Janus kinase (JAK) inhibitors, including Ruxolitinib, that block cytokine signaling pathways were found to improve outcome in hospitalized COVID-19 patients (15). Völkel et al. investigated the systemic effects of Ruxolitinib in critically ill COVID-19 patients by studying serum proteomes by mass spectrometry and cytokine array analyses at different time points after initiation of treatment. They demonstrated that the mechanism of action of Ruxolitinib in COVID-19 associated ARDS can be related to the SARS-CoV-2-infection and the effects of this drug as a modulator of T-cells.

Other respiratory viruses

Cigarette smoking has been associated with an increased risk of contracting acute respiratory infections, as well as increased risk of developing severe infections and infection-related adverse outcomes (16, 17). Studies have demonstrated the complex interplay between host immune responses to influenza A and cigarette smoking, and how the latter may lead to worse infection outcomes (17). However, data on the effects of cigarette smoking on influenza B infection are limited. Chavez et al. developed an animal model to study how cigarette smoking can affect the course and severity of influenza B infection. The authors demonstrated that cigarette smoke extract reduced the influenza-B specific antibodies without compromising their neutralizing potency. Although they did not find any association between cigarette smoke extract exposure and viral replication, there was a dose-dependent effect of increasing cigarette smoke extract concentrations on mortality, insinuating a potential role of cigarette smoking in influenza B infection-related adverse outcomes in humans.

Besides influenza, Respiratory Syncytial Virus (RSV) represents a major contributor of infection-related hospitalizations with significant mortality and morbidity rates among adults and children, and especially in infants, elderly and immunocompromised patients (18–20). Besides supportive care, specific treatment options for RSV include ribavirin, palivizumab and RSV-immune globulin (only available in the United States), but are reserved for severe cases or at high risk for severe disease, including immunocompromized patients (21). Bindernagel et al. presented their experience of using a single dose of ASCENIV (an intravenous immunoglobulin that is manufactured from blending normal plasma with plasma from donors that possess high antibody titers against RSV and other respiratory pathogens) in three cases of critically ill children of <5 years old, with some form of immune dysregulation. According to the authors, all three cases improved following administration of ASCENIV, concluding however, that well designed randomized controlled trials are needed to investigate whether ASCENIV is safe and effective in RSV infection.

Increasing evidence showed that inflammasomes activated by viral pathogens play a key role in viral clearance and tissue injury recovery (22). Li et al. investigated the role of non-canonical inflammasomes in the context of human adenovirus (HAdV) infection, another important respiratory pathogen that may lead to severe pneumonia, especially amongst susceptible hosts. The researchers found that HAdV infection induce macrophage pyroptosis by triggering non-canonical inflammasome activation via a NF-kB-dependent manner. They also noted that caspase-4 and caspase-5 may represent potential biomarkers associated with the severity HAdV-related pneumonia. These results reveal a new pathogenetic perspective on the pathogenesis of HAdV-related inflammatory tissue damage, that warrant further investigation.

Author contributions

PF: Conceptualization, Data curation, Investigation, Methodology, Writing—original draft, Writing—review & editing. DD: Conceptualization, Data curation, Investigation, Methodology, Writing—original draft, Writing—review & editing. GD: Methodology, Project administration, Supervision, Writing—review & editing. GM: Methodology, Project administration, Supervision, Writing—review & editing. RC: Methodology, Project

administration, Supervision, Writing—review & editing. CS: Methodology, Project administration, Supervision, Validation, Visualization, Writing—review & editing.

Funding

The author(s) declare financial support was received for the research, authorship, and/or publication of this article. CS was supported by the Universities Giessen and Marburg Lung Center (UGMLC), the German Center for Lung Research (DZL), University Hospital Giessen and Marburg (UKGM) research funding according to article 2, section 3 cooperation agreement, and the Deutsche Forschungsgemeinschaft (DFG, German Research Foundation)-SFB 1021 (Project Number 197785619), KFO 309 (Project Number 284237345), and SK 317/1-1 (Project Number 428518790) as well as by the Foundation for Pathobiochemistry and Molecular Diagnostics.

Conflict of interest

CS: Consultancy and research funding, Bencard Allergie and Thermo Fisher Scientific; Research Funding, Mead Johnson Nutrition (MJN).

The remaining authors declare that the research was conducted in the absence of any commercial or financial relationships that could be construed as a potential conflict of interest.

Publisher's note

References

1. Fragkou PC, Moschopoulos CD, Reiter R, Berger T, Skevaki C. Host immune responses and possible therapeutic targets for viral respiratory tract infections in susceptible populations: a narrative review. *Clin Microbiol Infect.* (2022) 28:1328–34. doi: 10.1016/j.cmi.2022.03.010

2. Kapasi AJ, Dittrich S, González IJ, Rodwell TC. Host biomarkers for distinguishing bacterial from non-bacterial causes of acute febrile illness: a comprehensive review. *PLoS ONE.* (2016) 11:160278. doi: 10.1371/journal.pone.0160278

3. Letko M, Marzi A, Munster V. Functional assessment of cell entry and receptor usage for SARS-CoV-2 and other lineage B betacoronaviruses. *Nat Microbiol.* (2020) 5:562–9. doi: 10.1038/s41564-020-0688-y

4. Appelberg S, Gupta S, Akusjärvi SS, Ambikan AT, Mikaeloff F, Saccon E, et al. Dysregulation in Akt/mTOR/HIF-1 signaling identified by proteo-transcriptomics of SARS-CoV-2 infected cells. *Emerg Microbes Infect.* (2020) 12:1748–60. doi: 10.1080/22221751.2020.1799723

5. Mizutani T, Fukushi S, Saijo M, Kurane I, Morikawa S. JNK and PI3k/Akt signaling pathways are required for establishing persistent SARS-CoV infection in Vero E6 cells. *Biochim Biophys Acta Mol Basis Dis.* (2005) 1741:4–10. doi: 10.1016/j.bbadis.2005.04.004

6. Khan S, Shafiei MS, Longoria C, Schoggins JW, Savani RC, Zaki H. SARS-CoV-2 spike protein induces inflammation via TLR2-dependent activation of the NF-κB pathway. *Elife.* (2021) 10:68 doi: 10.7554/eLife.68563

7. Stukalov A, Girault V, Grass V, Karayel O, Bergant V, Urban C, et al. Multilevel proteomics reveals host perturbations by SARS-CoV-2 and SARS-CoV. *Nature.* (2021) 594:246–52. doi: 10.1038/s41586-021-03493-4

8. Liu Y, Sawalha AH, Lu Q. COVID-19 and autoimmune diseases. *Curr Opin Rheumatol.* (2021) 33:155–62. doi: 10.1097/BOR.0000000000000776

9. Rosenberg ES, Dufort EM, Blog DS, Hall EW, Hoefer D, Backenson BP, et al. COVID-19 testing, epidemic features, hospital outcomes, and household prevalence, New York state-March 2020. *Clin Infect Dis.* (2020) 71:1953–1959. doi: 10.1093/cid/ciaa549

10. Roy MG, Livraghi-Butrico A, Fletcher AA, McElwee MM, Evans SE, Boerner RM, et al. Muc5b is required for airway defence. *Nature.* (2014) 505:412–6. doi: 10.1038/nature12807

11. Okuda K, Chen G, Subramani DB, Wolf M, Gilmore RC, Kato T, et al. Localization of secretory mucins MUC5AC and MUC5B in normal/healthy human airways. *Am J Respir Crit Care Med.* (2019) 199:715–27. doi: 10.1164/rccm.201804-0734OC

12. Svartengren M, Falk R, Philipson K. Long-term clearance from small airways decreases with age. *Eur Respir J.* (2005) 26:609–15. doi: 10.1183/09031936.05.00002105

13. Seibold MA, Wise AL, Speer MC, Steele MP, Brown KK, Loyd JE, et al. A common MUC5B promoter polymorphism and pulmonary fibrosis. *N Engl J Med.* (2011) 364:1503–12. doi: 10.1056/NEJMoa1013660

14. Jolliffe DA, Camargo CA, Sluyter JD, Aglipay M, Aloia JF, Ganmaa D, et al. Vitamin D supplementation to prevent acute respiratory infections: a systematic review and meta-analysis of aggregate data from randomised controlled trials. *Lancet Diabetes Endocrinol.* (2021) 9:276–92. doi: 10.1136/thorax-2020-BTSabstracts.105

15. Neubauer A, Wiesmann T, Vogelmeier CF, Mack E, Skevaki C, Gaik C, et al. Ruxolitinib for the treatment of SARS-CoV-2 induced acute respiratory distress syndrome (ARDS). *Leukemia.* (2020) 34:2276–8. doi: 10.1038/s41375-020-0907-9

16. *Smoking in Acute Respiratory Infections - The Centre for Evidence-Based Medicine*. Available online at: https://www.cebm.net/2020/03/smoking-in-acute-respiratory-infections/ (accessed October 21, 2023).

17. Chavez J, Hai R. Effects of cigarette smoking on influenza virus/host interplay. *Pathogens.* (2021) 10:636. doi: 10.3390/pathogens10121636

18. Celante H, Oubaya N, Fourati S, Beaune S, Khellaf M, Casalino E, et al. Prognosis of hospitalised adult patients with respiratory syncytial virus infection: a multicentre retrospective cohort study. *Clin Microbiol Infect.* (2023) 29:943. doi: 10.1016/j.cmi.2023.03.003

19. Bylsma LC, Suh M, Movva N, Fryzek JP, Nelson CB. Mortality among US infants and children under 5 years of age with respiratory syncytial virus and bronchiolitis: a systematic literature review. *J Infect Dis.* (2022) 226:S267–81. doi: 10.1093/infdis/jiac226

20. Li Y, Wang X, Blau DM, Caballero MT, Feikin DR, Gill CJ, et al. Global, regional, and national disease burden estimates of acute lower respiratory infections due to respiratory syncytial virus in children younger than 5 years in 2019: a systematic analysis. *Lancet.* (2022) 399:2047–64. doi: 10.1016/S0140-6736(22)00478-0

21. Gatt D, Martin I, AlFouzan R, Moraes TJ. Prevention and treatment strategies for respiratory syncytial virus (RSV). *Pathogens.* (2023) 12:154. doi: 10.3390/pathogens12020154

22. Cerato JA, da Silva EF, Porto BN. Breaking bad: inflammasome activation by respiratory viruses. *Biology.* (2023) 12:943. doi: 10.3390/biology12070943

frontiers in Medicine

ORIGINAL RESEARCH
published: 23 November 2021
doi: 10.3389/fmed.2021.668024

The *MUC5B* Promoter Polymorphism Associates With Severe COVID-19 in the European Population

Coline H. M. van Moorsel[1,2†], Joanne J. van der Vis[1,3†], Anna Duckworth[4], Chris J. Scotton[4], Claudia Benschop[1,5], David Ellinghaus[6,7], Henk J. T. Ruven[3], Marian J. R. Quanjel[1] and Jan C. Grutters[1,2]*

[1] Department of Pulmonology, St Antonius ILD Center of Excellence, St. Antonius Hospital, Nieuwegein, Netherlands, [2] Division of Heart and Lungs, University Medical Center Utrecht, Utrecht, Netherlands, [3] Department of Clinical Chemistry, St Antonius ILD Center of Excellence, St. Antonius Hospital, Nieuwegein, Netherlands, [4] College of Medicine & Health, Institute of Biomedical & Clinical Science, University of Exeter, Exeter, United Kingdom, [5] Department of Medical Microbiology and Immunology, St Antonius ILD Center of Excellence, St. Antonius Hospital, Nieuwegein, Netherlands, [6] Genetics and Bioinformatics Group, Institute of Clinical Molecular Biology, Christian-Albrechts-University, Kiel, Germany, [7] Faculty of Health and Medical Sciences, Novo Nordisk Foundation Center for Protein Research, Disease Systems Biology, University of Copenhagen, Copenhagen, Denmark

Background: Diversity in response on exposure to severe acute respiratory syndrome coronavirus 2 may be related to the innate immune response in the elderly. The mucin MUC5B is an important component of the innate immune response and expression levels are associated with the *MUC5B* promoter polymorphism, rs35705950. The high expressing T-allele is a risk allele for the non-infectious aging lung disease idiopathic pulmonary fibrosis (IPF). We investigated if *MUC5B* rs35705950 associates with severe COVID-19.

Methods: In this retrospective candidate gene case-control study we recruited 108 Dutch patients (69% male, median age 66 years, 77% white) requiring hospitalization for COVID-19 (22% ICU stay, 24% died). For validation, genotypes were obtained from the UK-Biobank ($n = 436$, 57% male, median age 70 years, 27% died), for replication data from the severe COVID-19 GWAS group from Italy ($n = 835$) and Spain ($n = 775$) was used, each with a control cohort ($n = 356{,}735$, $n = 1{,}255$, $n = 950$, respectively). *MUC5B* association analysis was performed including adjustment for age and sex.

Results: The rs35705950 T-allele frequency was significantly lower in Dutch white patients ($n = 83$) than in controls (0.04 vs. 0.10; $p = 0.02$). This was validated in the UK biobank cohort (0.08 vs. 0.11; $p = 0.001$). While age and sex differed significantly between cases and control, comparable results were obtained with age and sex as confounding variables in a multivariate analysis. The association was replicated in the Italian ($p = 0.04$), and Spanish ($p = 0.03$) case-control cohorts. Meta-analysis showed a negative association for the T-allele with COVID-19 (OR = 0.75 (CI: 0.67–0.85); $p = 6.63 \times 10^{-6}$).

Conclusions: This study shows that carriage of the T-allele of *MUC5B* rs35705950 confers protection from development of severe COVID-19. Because the T-allele is a known risk allele for IPF, this study provides further evidence for the existence of trade-offs between optimal mucin expression levels in the aging lung.

Keywords: *MUC5B*, COVID-19, idiopathic pulmonary fibrosis, innate immunity, mucus, SARS-CoV-2, aging lung

OPEN ACCESS

Edited by:
Laurent Pierre Nicod, University of Lausanne, Switzerland

Reviewed by:
Paola Rottoli, University of Siena, Italy
Marialuisa Bocchino, University of Naples Federico II, Italy

***Correspondence:**
Coline H. M. van Moorsel
c.van.moorsel@antoniusziekenhuis.nl

†These authors have contributed equally to this work and share first authorship

Specialty section:
This article was submitted to Pulmonary Medicine, a section of the journal Frontiers in Medicine

Received: *15 February 2021*
Accepted: *22 October 2021*
Published: *23 November 2021*

Citation:
van Moorsel CHM, van der Vis JJ, Duckworth A, Scotton CJ, Benschop C, Ellinghaus D, Ruven HJT, Quanjel MJR and Grutters JC (2021) The MUC5B Promoter Polymorphism Associates With Severe COVID-19 in the European Population. Front. Med. 8:668024. doi: 10.3389/fmed.2021.668024

INTRODUCTION

The current coronavirus disease (COVID-19) pandemic illustrates the diversity in response on exposure to severe acute respiratory syndrome coronavirus 2 (SARS-CoV-2). Response to infection ranges from asymptomatic to death from organ failure, of which the latter is most commonly observed in the elderly (1). Such differences are associated with aging, but may also be influenced by the genetic constitution of the host.

Diversity in response to SARS-CoV-2 exposure may be related to host factors associated with airway defense. The gel-forming mucin 5B (MUC5B) is part of the mucus that covers the surface of the respiratory epithelium and forms a key barrier defense against respiratory pathogens (2, 3). *In vivo* studies in mice showed that Muc5B deficiency caused accumulation of materials in the upper and lower airways, leading to chronic infection and inflammation that failed to resolve normally. By contrast, in mice that overexpress Muc5B, macrophage function was improved. Hence, the presence of Muc5B in the lung is essential for controlling infections, maintaining immune homeostasis, and mucociliary clearance (4). Aged mice had significantly reduced Muc5b levels in comparison with young mice (5) and decreased expression of Muc5B in mouse models was associated with reduced mucociliary clearance (4, 5). In both humans (6) and mice (5) decreased mucociliary clearance was shown to be associated with aging.

Constitutive expression levels of MUC5B are associated with a common promoter polymorphism, rs35705950 of the encoding gene *MUC5B*. The minor rs35705950 T allele is associated with high expression levels of MUC5B and the major G allele is associated with low expression levels (7, 8). The high expressing T-allele is a known risk factor for idiopathic pulmonary fibrosis (IPF) (7), a fatal aging lung disease of unknown cause predominately affecting older males with a history of smoking. IPF is a non-infectious disease of the distal lung caused by damage of the alveolar epithelium followed by progressive fibrogenesis (9).

Recently it was shown that aging lung diseases such as IPF and chronic obstructive pulmonary disease (COPD) share disease loci but have opposite risk alleles (10). Given the fact that the alleles of these loci influence expression levels we proposed a theory of trade-offs in aging lung disease (11). A trade-off exists whenever a benefit in one context entails a cost in another (12). In aging lungs, the high expressing *MUC5B* T-allele may be important for optimal airway defense against infections while it provides an increased risk for IPF in the alveolar compartment.

Therefore, we examined if *MUC5B* rs35705950 is associated with severe COVID-19. To investigate this, we performed a retrospective candidate rs35705950 case-control study in a Dutch cohort and included an UK cohort for validation and an Italian and Spanish cohort for replication.

MATERIALS AND METHODS

Patients

This is a retrospective candidate gene case-control study. The discovery cohort from the ILD biobank and data registry of the St Antonius Hospital Nieuwegein, the Netherlands, included (n = 108) adult patients hospitalized due to COVID-19 at St Antonius Hospital between March 19, 2020 and May 5, 2020. Diagnosis of COVID-19 was made on the basis of a positive SARS-CoV-2 PCR except for three cases with clinical characteristics and a high-resolution computed tomography (HRCT) of the chest congruent with COVID-19 pneumonia. We collected demographics, clinical characteristics, radiology and survival data from medical hospital records. Severe disease was arbitrarily defined by hospitalization with the need for oxygen supplementation.

The control group consisted of 611 Dutch white healthy controls, from the biobank. The study was approved by The Medical research Ethics Committees United (MEC-U) of St. Antonius Hospital and all patients provided written informed consent (approval number R05-08A).

For validation we obtained data from the UK biobank (13). The validation cohort consisted of unrelated UK Biobank participants (application 44046) of European ancestry with 436 adult patients with a diagnosis of COVID-19 based on a positive SARS-CoV-2 PCR in the period 16 March−14 April 2020. In this period, testing was almost exclusively restricted to patients admitted to the hospital or presenting at emergency services with severe disease plus healthcare workers suffering clinical signs of infection, including fever and cough or shortness of breath. Overall, for the UK, the case fatality rate was highest during the study period (https://ourworldindata.org/mortality-risk-covid?country~GBR). Death due to COVID-19 was calculated using ICD-10 codes U071 and U072 before end of May 2020 and 117 out of 436 (27%) of the UK biobank case cohort died due to COVID-19. This indicates that the test criteria at that time were a reasonable proxy for severe COVID-19. Furthermore, 356,799 UK biobank controls were included. All UK Biobank participants provided written informed consent, the UK Biobank study was approved by the National Research Ethics Service Committee North West-Haydock (REC reference 16/NW/0274), and all study procedures were performed in accordance with the World Medical Association Declaration of Helsinki ethical principles for medical research.

For replication we obtained summary data from the severe COVID-19 GWAS group (14) for white subjects. Replication cohort I consisted of 835 adult patients, of which 30% were female and a median age of 65 (IQR 56–75) years hospitalized with COVID-19 in Italy and 1,255 controls of which 39% is female and a median age of 49 (IQR 33–59) years. Replication cohort II consisted of 775 adult patients, of which 34% were female and a median age of 67 (IQR 58–75) years hospitalized with COVID-19 in Spain and 950 controls of which 33% were female and a median age of 44 (IQR 33–50) years. Severe COVID-19 was defined as hospitalization with respiratory failure. Information about respiratory support and comorbidities were described previously in more detail (14).

Genotyping

For Dutch subjects, DNA was extracted using a Chemagic 360 (PerkinElmer, Waltham, Massachusetts, USA) from whole blood. The discovery cohort was genotyped for *MUC5B* rs35705950 genotype with a pre-designed taqman SNP genotyping assay and

TABLE 1 | Characteristics of Dutch patients hospitalized with COVID-19.

	All	White	Non-white	*p*
N	108	83	25	
Males, *n* (%)	74 (69)	56 (67)	18 (72)	0.67
Age at diagnosis, median (IQR), y	66 (22)	71 (18)	55 (14)	0.001
Stay at ICU, *n* (%), days	24 (22)	18 (22)	6 (24)	0.79
Deaths, *n* (%)	23 (21)	18 (14)	5 (20)	0.86
Age at death, median (IQR), y	75 (15)	76 (14)	64 (24)	0.26
Length of hospitalization survivors, median (IQR), days	9 (10)	11 (14)	7.5 (5)	0.10
Body Mass Index, median (IQR)	28.1 (5)	28.1 (4.6)	28.2 (7.2)	0.72
Diabetes, *n* (%)	8 (7)	7 (8.4)	1 (4)	0.68
Asthma/COPD, *n* (%)	16 (15)	15	1	0.11
Interstitial lung disease, *n* (%)	1 (1)	1 (1)	0(1)	1.00
Pulmonary hypertension, *n* (%)	1 (1)	1 (1)	0 (1)	1.00

N, number; y, years; IQR, inter quartile range; ICU, intensive care unit; COPD, chronic obstructive pulmonary disease.

the QuantStudio® 5 Real-Time PCR system (both ThermoFisher Scientific, Waltham, Massachusetts, USA).

For the UK biobank data, we obtained genotype counts summarized separately for cases and controls for SNP rs35705950, with data from participants who died before the epidemic excluded. SNP data was generated from the Affymetrix Axiom UK Biobank array and the UK BiLEVE array following extensive central quality control (13). We used genetic data from the "v3" release of UKBB containing the full set of Haplotype Reference Consortium (HRC) and 1000 Genomes imputed variants, followed by additional internal quality control to define a cohort of unrelated white European participants (15).

For replication cohort I and II, we obtained genotype counts summarized separately for white cases and controls from the severe COVID-19 GWAS group for SNP rs35705950 at chr11, pos_hg38 1219991, G, T (www.c19-genetics.eu). SNP rs35705950 was directly genotyped, except for 3 out of 2,090 genotypes of the Italian cohort. These were imputed via TOPMed reference panel (14).

Statistical Analysis

SPSS 24 (IBM, Armonk, New York, USA) was used for statistical analysis. Due to ethnic differences in the prevalence of the *MUC5B* rs35705950 alleles, genetic analyses were stratified by ethnicity and only statistically analyzed in white subjects. Differences between white and non-white patients and between carriers and non-carriers of the rs35705950 T-allele were calculated using a Chi square test for categorical data. Differences with continuous data were tested with *t*-test or the Mann-Whitney U test where appropriate. Differences between the allele and genotype frequencies were calculated with the Pearson's goodness-of-fit chi-square test, together with the OR and 95% CI. Binary logistic regression was used to test for *MUC5B* rs35705950 association and COVID-19 with age and sex as confounding variables. Linear regression was used to test for rs35705950 association with age, adjusted for sex. Fisher's exact test was used to test for deviation from Hardy–Weinberg equilibrium. A value of $p < 0.05$ was considered statistically significant. Meta-analyses were performed using the allele contrast and dominant model in the web tool META-Genyo (16). Heterogeneity in the data was evaluated with I^2 statistics and Cochran's Q test was low for both the allele contrast and dominant model. The fixed-effect estimate method, inverse variance was used.

RESULTS

Dutch Participants

In total 108 patients hospitalized with COVID-19 (**Table 1**) in The Netherlands were included in the study of which 74 (69%) were males. Among 108 patients, 83 (77%) were white and 25 patients were non-whites. The median age of the patients was 66 years (range 19.1–92.4) and differed significantly between whites (71 years) and non-whites (55 years; $p = 0.0004$). Of all patients, 24 patients were admitted to the intensive care unit (22%).The median length of hospitalization of patients who survived COVID-19 was 9 days. Twenty-three patients died (21%) and they were significantly older than patients who survived, 74 vs. 63 years, respectively ($p = 0.002$). There was a trend toward significance for a younger age at death in non-whites (**Table 1**).

The control cohort consisted of 611 white subjects with a median age of 59 years, of which 285 (47%) were male.

UK Biobank Participants

In total 436 patients of European ancestry with a diagnosis of COVID-19 were included in the study of which 249 (57%) were males. Characteristics and co-morbidities for UK biobank participants are presented in **Table 2**. The median age of the patients was 70 years. One hundred and seventeen patients (27%) patients died. The control cohort consisted of 356,799 subjects with a median age of 69 years, of which 161,178 (45%) were male. Significantly more male sex, older age, higher number of death, higher BMI, more diabetes, COPD and ILD were observed among COVID-19 cases when compared with controls (**Table 2**).

TABLE 2 | Characteristics of UK biobank participants.

	COVID-19	Controls	$p^{\$}$
N	436	356,799	
Males, *n* (%)	249 (57)	161,179 (45)	<0.001
Age, median (IQR), y^	70 (16)	69 (13)	<0.001
Deaths, *n* (%)*	117 (27)	688 (0.002)	<0.001
Age at death, median (IQR), y	75 (8)	74(8)	0.75
Body Mass Index, median (IQR)	29.1 (6.2)	27.3 (5.7)	<0.001
Diabetes, *n* (%)	38 (8.7)	15,815 (4.4)	<0.001
Asthma, *n* (%)	65 (15)	41,508 (12)	0.015
COPD, *n* (%)	42 (9.6)	8,371 (2.4)	<0.001
Interstitial lung disease, *n* (%)	7 (1.6)	1,262 (0.3)	<0.001

N, number; y, years; IQR, inter quartile range; COPD, chronic obstructive pulmonary disease; Diabetes, any definition of diabetes.

$Linear regression associations observed using available data in white European covid cases vs. controls, adjusted for age and sex where relevant. ^ =age at 15/03/2020

**Deaths were those that occurred between 15/03/20 and 31/5/20 only.*

Association of *MUC5B* Rs35705950 With COVID-19

In the discovery cohort of 108 patients, there were 99 patients with a GG genotype and 9 patients with a GT genotype. The minor T-allele frequency of the *MUC5B* promoter polymorphism was 0.04. In the white subgroup of COVID-19 patients, 76 had a GG genotype and 7 a GT genotype, which was in Hardy-Weinberg equilibrium. The frequency of the T-allele in the white COVID-19 group was 0.04 and this was significantly lower than the T-allele frequency of 0.10 in the control group ($p = 0.023$; OR = 0.42, CI = 0.19–0.91; **Table 3**). Age and sex were significantly different between cases and controls, however multivariate analysis with age and sex as confounding variables showed comparable results ($p = 0.03$; OR = 0.40, CI = 0.18–0.91).

For the UK validation cohort the minor T-allele frequency of *MUC5B* rs35705950 was 0.08 in cases and this was significantly lower than the T-allele frequency of 0.11 in the controls ($p = 0.001$; OR = 0.66, CI = 0.51–0.85; **Table 3**).

This association remained significant after adjustment for age, sex, BMI, asthma, COPD, ILD and diabetes (**Table 4**).

For the UK biobank cohort we separately investigated if the rs35705950 allele frequency associated with age. The association of the rs35705950 allele frequency with age is small with $\beta = -0.0002$ ($p = 0.027$) with a small decrease in T-allele frequency with increasing age. Moreover, if we remove ILD cases, the association for non-ILD UK biobank participants become $\beta = -0.0003$ ($p = 2.8 \times 10^{-4}$). This indicates that there is no survival bias of T-allele carriers. Our data also demonstrates no survival bias for ILD cases during this period of isolation.

In the severe COVID-19 replication cohort I and cohort II, the minor T-allele frequency of *MUC5B* rs35705950 was 0.10 and this was significantly lower than the T-allele frequency of 0.13 in both control cohorts (cohort I: $p = 0.039$; OR = 0.81, CI = 0.67–0.99; and cohort II: $p = 0.030$; OR = 0.79, CI = 0.64–0.98; **Table 3**). Analysis of replication cohort I and II together, adjusted for sex, age and top 10 principal component showed comparable results, OR 0.75 (SD 0.098); $p = 0.003$.

Meta-analyses were performed to analyze the association of *MUC5B* rs35705950 with severe COVID-19, both for comparison of allele contrast and for a dominant T-allele carriage model (GT+TT vs. GG). **Figure 1A** shows the forest plot of the T vs. G allele meta-analysis of the four cohorts. The pooled negative association with COVID-19 for the T allele was significant with an OR of 0.75 (CI: 0.67–0.85); $p = 6.63 \times 10^{-6}$. **Figure 1B** shows the forest plot of the meta-analysis of the dominant model (GT+TT vs. GG) of the four cohorts. The pooled negative association of T allele carriage was significant with an OR of 0.75 (CI: 0.66-0.86; $p = 2.05 \times 10^{-5}$).

DISCUSSION

In this study we used a candidate gene case-control approach to examine whether a genetic polymorphism that influences expression of MUC5B is associated with susceptibility to severe COVID-19. We observed a significant association between the *MUC5B* rs35705950 promoter polymorphism and severe COVID-19 in four white European cohorts. The results of the meta-analyses demonstrate the protective effect of the *MUC5B* T allele against severe COVID-19. The T-allele frequency and T-carrier frequency was lower in severe COVID-19 patients than in controls.

Beneficial effects of carriage of the T-allele have been reported before. In smoking non-Hispanic white COPD patients with interstitial HRCT features, T-allele carriers experienced less acute respiratory disease and a longer time-to-first event (17). Furthermore, in IPF patients, carriers had a lower bacterial burden than non-carriers (18) and better survival (19).

In the human respiratory system, MUC5B is secreted throughout the lung by submucosal glands and the superficial epithelium of trachea, bronchi, bronchioles and alveoli, and by salivary glands and nasal mucosa (3, 4, 20, 21). The T-allele was shown to increase the MUC5B promoter activity and carriers of the T-allele demonstrated increased RNA expression of MUC5B in lung tissue (7, 8, 22). A recent paper shows that MUC5B rs35705950 resides within a gene enhancer that is subject to epigenetic remodeling (23). In the airway epithelium of an explant lung of a severe ICU admitted COVID-19 patient, dramatically reduced MUC5B protein and mRNA expression was found when compared with control lung (24).

The increased MUC5B production in T-allele carriers may protect carriers from adverse events related to airway defense. This may be of particular importance in aging, because mucus production and mucociliary clearance have been described to decrease with aging (5, 6). Furthermore, decreased mucociliary clearance may underlie the observed age-related increase in the incidence of severe community-acquired pneumonia in the elderly (25). Similar to previous reports on COVID-19 (1) we also observed that severe COVID-19 and death from COVID-19 is predominantly found in the elderly.

TABLE 3 | *MUC5B* rs35705950 genotype in white subjects with severe COVID-19 and controls.

	Discovery		Validation		Replication I		Replication II	
	COVID-19	**Controls**	**COVID-19**	**Controls**	**COVID-19**	**Controls**	**COVID-19**	**Controls**
Country	Netherlands	Netherlands	United Kingdom	United Kingdom	Italy	Italy	Spain	Spain
N	83	611	436	356,735	835	1,255	775	950
GG, *n* (%)	76 (92)	501 (82)	369 (85)	281,333 (79)	670 (80)	964 (77)	624 (81)	723 (76)
GT, *n* (%)	7 (8)	103 (17)	67 (15)	70,987 (20)	156 (19)	268 (21)	140 (18)	210 (22)
TT, *n* (%)	0 (0)	7 (1)	0 (0)	4,415 (8)	9 (1)	23 (2)	11 (1)	17 (2)
MAF	0.04	0.10	0.08	0.11	0.10	0.13	0.10	0.13
OR	0.42		0.66		0.81		0.79	
95% CI	0.19–0.91		0.51–0.85		0.67–0.99		0.64–0.98	
p	0.023		0.001		0.039		0.030	

N, number; MAF, minor allele frequency; OR, odds ratio; CI, confidence interval.

TABLE 4 | Multivariate association analysis for COVID-19 in the UK biobank validation cohort.

	Odds ratio	**95% CI**	***p***
rs35705950 T allele	0.67	0.52–0.86	0.002
Sex	1.52	1.26–1.84	<0.001
Age	1.02	1.01–1.03	0.002
Body Mass Index	1.06	1.04–1.08	<0.001
Diabetes	1.22	0.85–1.74	0.28
COPD	3.20	2.26–4.52	<0.001
Asthma	1.11	0.84–1.46	0.47
Interstitial lung disease	2.45	1.08–5.58	0.03

CI, confidence interval; COPD, chronic obstructive pulmonary disease.

Severe COVID-19 is primarily associated with a respiratory system pathology. Autopsy of patients who died from COVID-19 showed presence of diffuse chronic and tracheobronchial inflammation and alveolar type 2 (AT2) cell hyperplasia in the majority of biopsies (26). SARS-CoV-2 virus was detected in both airway epithelium and AT2 cells and the authors concluded that histology suggests progressive disease that begins in the airway and extends to alveolar zones (26). High constitutive levels of MUC5B in the elderly may protect the airway from SARS-CoV-2 viral infection.

Death rates of the Dutch and UK COVID-19 cases are high. The UK biobank positive COVID-19 cases even had a death rate of 27% which is considerably higher than the maximum 15.2% (27) evolving case fatality rate in the UK from mid-March to end May 2020. After community testing was rolled out, the case fatality rate in the UK decreased below 4% (27). The high death rate of affected UK biobank cases may be due to the older age of biobank participants with a median of 69 years old. With increasing age, the lung changes to the extent that alleles which in younger people confer non-essential divergent expression, may influence the risk of disease in aged tissue. In aging lung diseases such as IPF, COPD and lung cancer, a pattern is emerging of shared disease loci. Although loci are shared, it is of considerable interest that the respective diseases associate with opposite risk alleles and with opposing expression levels (10, 11, 28). Previously we summarized findings and presented a theory in which trade-offs in the aging respiratory system exist (11). The present study shows that the *MUC5B* rs35705950 polymorphism may be added to this list of shared loci with opposite risk alleles. The *MUC5B* T-allele, which appears beneficial in this study, is best known as a major risk allele for IPF (7). IPF is a rare non-infectious pulmonary aging disease of unknown cause characterized by insidious onset of disease in patients without a history of pulmonary health problems. Subsequent studies showed that the *MUC5B* T-allele not only predisposes to IPF but to a variety of chronic progressive forms of pulmonary fibrosis (29–32).

Because severe COVID-19 is associated with substantial pneumonitis and shares multiple risk factors with IPF, Fadista et al. recently investigated whether a genetic correlation between IPF and severe COVID-19 exists using a Mendelian randomization approach (33). They found that genetically increased risk of IPF indeed associated with increased COVID-19 severity, except for the *MUC5B* allele. The *MUC5B* risk allele had a different effect compared with other IPF predisposing alleles and protected against COVID-19 hospitalization in the elderly. Because the *MUC5B* results contradicted their hypotheses the authors were concerned that the analysis might have been influenced by possible selection bias: 1) due to the rs35705950 T allele carriers undertaking strict self-isolation, and 2) due to survival bias of the rs35705950 non-IPF T allele carriers (33). With the unique data of the UK biobank cohort, we were able to address these questions. First, the *MUC5B* T allele is only known to be associated with progressive fibrosing ILD. These patients may have been isolating due to clinical vulnerability. However, instead of underrepresentation, we were able to show the significant overrepresentation of patients with ILD in the biobank COVID-19 cases vs. non-cases. These data include 5 IPF cases and 1,014 IPF controls, bias introduced by effective shielding of these patients is therefore not present. Second, it is suggested that *MUC5B* T-allele carriers may have increased survival in the population. This would result in increasing T-allele frequencies with age. However, we found a very slight decrease in the T-allele frequency with age. When we delete ILD subjects

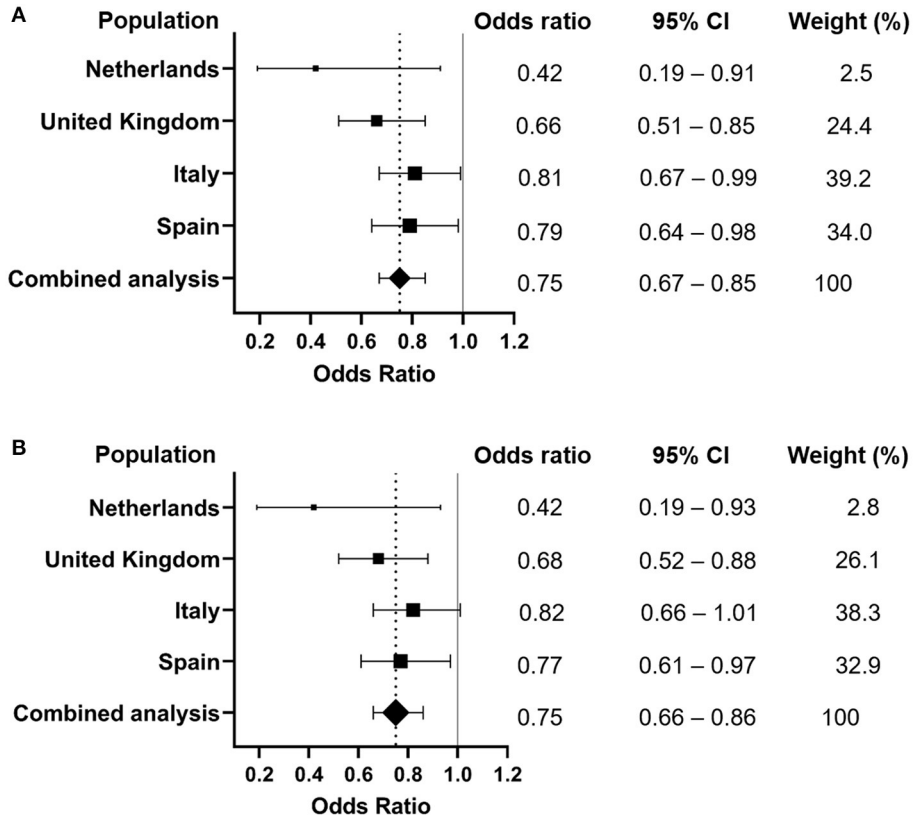

FIGURE 1 | Forest plots of meta-analyses of the association of *MUC5B* rs35705950 with severe COVID-19 in subjects of European ancestry. Dotted line represents the odds ratio from the combined analysis. **(A)** Meta-analysis of allele contrast (T vs. G; P combined analysis = 6.63 e-06). **(B)** Meta-analysis of the dominant T-allele carriage model (GT+TT vs. GG; P combined analysis = 2.05e-05). CI, confidence interval.

from the cohort, the association remained, meaning that there is no survival bias of T-allele carriers in the non-ILD population.

The finding by Fadista et al. is in line with our current findings and we found no evidence for stratification bias driving these results. We performed a candidate allele study because we hypothesized that the IPF predisposing allele would protect against COVID-19 and confirmed this hypothesis. The current finding of protection against severe COVID-19 combined with the established increased risk for pulmonary fibrosis in T-allele carriers may represent a trade-off that becomes apparent with aging. During the first decades of life the effect of both alleles may be neutral while at an older age differences in constitutive expression levels may predispose to disease. The pleiotropic property of the gene polymorphism is expressed only in the older individuals. This idea complements the well-established principle of pleiotropic antagonism, the theory of aging where one gene is involved in multiple traits (pleiotropy) with a beneficial fitness enhancing effect in early life and a detrimental fitness diminishing effect in later life (34).

A limitation of the study is the focus on white European populations. Minor allele frequencies for *MUC5B* rs35705950 are known to differ between populations. The allele frequencies of the control cohorts are congruent with previous reports (32, 35–37). The protective T-allele is known to have the highest frequency in populations of European ancestry, but is less frequent to non-existent in non-European populations. It is tempting to speculate that the increased risk for infection with SARS-CoV-2 and the worse clinical outcome in black, Asian and minority ethnic populations in western societies (38) may be associated with low carriage of the protective *MUC5B* T-allele. Replication cohort I and II are part of the study population used by Fadista et al. (33). In their study, a 89% white patient population and a 99% white control cohort was used, therefor they adjusted the analysis for genetic ancestry principal components (33). We used a white Dutch and UK population, so in order to replicate our findings and allow comparison of the results we included replication cohorts I and II and performed the analysis on white subjects only, which produced similar results. However, future studies aimed at improving understanding of COVID-19 risk in populations worldwide should include genetics of different ethnic groups. Another limitation is the small sample size of the Dutch cohort, yielding a significant result but with a wide confidence interval. Furthermore, specific information on disease severity such as organ involvement, CO-RAD and CT-severity scores are missing. However, all patients in the Dutch cohort were hospitalized for confirmed COVID-19 and had a SpO_2 <94%.

Hospital triage during the study period was restricted because the wards were overcrowded. Furthermore, 22% of patients were admitted to the intensive care unit and 24% of patients died. In addition, the death rates of the UK COVID-19 cases was high (27%), all suggestive of case cohorts with severe COVID-19. However, further studies are needed to investigate if the *MUC5B* polymorphism will associate with specific COVID-19 severity scores.

A strength of our study is the inclusion of the UK Biobank cohort, with cases and controls having been recruited as one cohort 9–13 years prior to the COVID pandemic. This procedure is most ideal to avoid recruitment bias in case-control studies and the cohort yields a highly significant result.

In conclusion, we found that carriage of the T-allele of *MUC5B* rs35705950 confers protection from development of severe COVID-19. Because the T-allele is a known risk allele for pulmonary fibrosis, this study provides further evidence for the existence of trade-offs between optimal expression levels in the aging lung.

DATA AVAILABILITY STATEMENT

The datasets presented in this article are not readily available because they contain potentially identifying or sensitive patient information. Requests to access the datasets can be directed to the corresponding author.

ETHICS STATEMENT

The ILD biobank and data registry of the St. Antonius Hospital was reviewed and approved by the Medical research Ethics Committees United (MEC-U) of St. Antonius Hospital. The UK Biobank study was reviewed and approved by the National Research Ethics Service Committee North West-Haydock. All participants provided their written informed consent to participate in this study.

AUTHOR CONTRIBUTIONS

The study was conceived and designed by CM and JV. CB, CS, AD, DE, and MQ contributed to the conduct of this study. Data were acquired by MQ, JV, AD, and DE and analyzed by AD and JV. CM reviewed the medical literature, oversaw the conduct of the study, participated in the interpretation of data, drafted, and wrote the manuscript. All authors reviewed and contributed to the manuscript during its development and approved it for publication.

FUNDING

This study was funded by ZonMW TopZorg St Antonius Care grant nr 842002001; ZonMW Topspecialistische Zorg en Onderzoek grant no 10070012010004; Nederlandse Vereniging van Artsen voor Longziekten en Tuberculose COVID-19 grant; GW4 BioMed Medical Research Council Doctoral Training Partnership. Funders were not involved in the study design, collection, analysis and interpretation of the data.

ACKNOWLEDGMENTS

The authors are indebted to the severe COVID-19 GWAS group and the UK Biobank for making summarized genotype counts for SNP rs35705950 available. We thank Mirjam Visser (St. Antonius Hospital, Nieuwegein, the Netherlands) for support in the patient informed consent procedure. This research has been conducted using the UK Biobank Resource (application 44046). The authors would like to acknowledge the use of the University of Exeter High-Performance Computing facility. A preliminary version of the manuscript describing only findings in the discovery cohort has been posted on medRxiv.org a nonprofit preprint server for health science (van Moorsel et al. THE MUC5B PROMOTOR POLYMORPHISM ASSOCIATES WITH SEVERE COVID-19. medRxiv 2020.05.12.20099333; doi: https://doi.org/10.1101/2020.05.12.20099333).

REFERENCES

1. Rosenberg ES, Dufort EM, Blog DS, Hall EW, Hoefer D, Backenson BP, et al. COVID-19 testing, epidemic features, hospital outcomes, and household prevalence, New York State-March 2020. *Clin Infect Dis*. (2020) 71:1953–9. doi: 10.1093/cid/ciaa549
2. Knowles MR, Boucher RC. Mucus clearance as a primary innate defense mechanism for mammalian airways. *J Clin Invest*. (2002) 109:571–7. doi: 10.1172/JCI0215217
3. Okuda K, Chen G, Subramani DB, Wolf M, Gilmore RC, Kato T, et al. Localization of secretory mucins MUC5AC and MUC5B in normal/healthy human airways. *Am J Respir Crit Care Med*. (2019) 199:715–27. doi: 10.1164/rccm.201804-0734OC
4. Roy MG, Livraghi-Butrico A, Fletcher AA, McElwee MM, Evans SE, Boerner RM, et al. Muc5b is required for airway defence. *Nature*. (2014) 505:412–6. doi: 10.1038/nature12807
5. Grubb BR, Livraghi-Butrico A, Rogers TD, Yin W, Button B, Ostrowski LE. Reduced mucociliary clearance in old mice is associated with a decrease in muc5b mucin. *Am J Physiol Lung Cell Mol Physiol*. (2016) 310:L860–7. doi: 10.1152/ajplung.00015.2016
6. Svartengren M, Falk R, Philipson K. Long-term clearance from small airways decreases with age. *Eur Respir J*. (2005) 26:609–15. doi: 10.1183/09031936.05.00002105
7. Seibold MA, Wise AL, Speer MC, Steele MP, Brown KK, Loyd JE, et al. A common MUC5B promoter polymorphism and pulmonary fibrosis. *N Engl J Med*. (2011) 364:1503–12. doi: 10.1056/NEJMoa1013660
8. Nakano Y, Yang I V., Walts AD, Watson AM, Helling BA, Fletcher AA, et al. MUC5B promoter variant rs35705950 affects MUC5B expression in the distal airways in idiopathic pulmonary fibrosis. *Am J Respir Crit Care Med Am Thorac Soc*. (2016) 193:464–6. doi: 10.1164/rccm.201509-1872LE
9. Raghu G, Remy-Jardin M, Myers JL, Richeldi L, Ryerson CJ, Lederer DJ, et al. Diagnosis of idiopathic pulmonary fibrosis An Official ATS/ERS/JRS/ALAT Clinical practice guideline. *Am J Respir Crit Care Med*. (2018) 198:e44–68. doi: 10.1164/rccm.201807-1255ST
10. Hobbs BD, de Jong K, Lamontagne M, Bossé Y, Shrine N, Artigas MS, et al. Genetic loci associated with chronic obstructive pulmonary disease overlap with loci for lung function and pulmonary fibrosis. *Nat Genet*. (2017) 49:426–32. doi: 10.1038/ng.3752

11. Van Moorsel CHM. Trade-offs in aging lung diseases: a review on shared but opposite genetic risk variants in idiopathic pulmonary fibrosis, lung cancer and chronic obstructive pulmonary disease. *Curr Opin Pulmonary Med.* (2018) 24:309–17. doi: 10.1097/MCP.0000000000000476
12. Gluckman PD, Low FM, Buklijas T, Hanson MA, Beedle AS. How evolutionary principles improve the understanding of human health and disease. *Evol Appl.* (2011) 4:249–63. doi: 10.1111/j.1752-4571.2010.00164.x
13. Bycroft C, Freeman C, Petkova D, Band G, Elliott LT, Sharp K, et al. The UK Biobank resource with deep phenotyping and genomic data. *Nature.* (2018) 562:203–9. doi: 10.1038/s41586-018-0579-z
14. Ellinghaus D, Degenhardt F, Bujanda L, Buti M, Albillos A, Invernizzi P, et al. Genomewide association study of severe covid-19 with respiratory failure. *N Engl J Med*. (2020) 383:1522–34. doi: 10.1056/NEJMoa2020283
15. Tyrrell J, Mulugeta A, Wood AR, Zhou A, Beaumont RN, Tuke MA, et al. Using genetics to understand the causal influence of higher BMI on depression. *Int J Epidemiol.* (2019) 48:834–48. doi: 10.1093/ije/dyy223
16. Martorell-Marugan J, Toro-Dominguez D, Alarcon-Riquelme ME, Carmona-Saez P. MetaGenyo: a web tool for meta-analysis of genetic association studies. *BMC Bioinformatics.* (2017) 18:563. doi: 10.1186/s12859-017-1990-4
17. Ash SY, Harmouche R, Putman RK, Ross JC, Martinez FJ, Choi AM, et al. Association between acute respiratory disease events and the MUC5B promoter polymorphism in smokers. *Thorax.* (2018) 73:1071–4. doi: 10.1136/thoraxjnl-2017-211208
18. Molyneaux PL, Cox MJ, Willis-Owen SAG, Mallia P, Russell KE, Russell AM, et al. The role of bacteria in the pathogenesis and progression of idiopathic pulmonary fibrosis. *Am J Respir Crit Care Med.* (2014) 190:906–13. doi: 10.1164/rccm.201403-0541OC
19. Peljto AL, Zhang Y, Fingerlin TE, Shwu-Fan M, Garcia JGN, Richards TJ, et al. Association between the MUC5B promoter polymorphism and survival in patients with idiopathic pulmonary fibrosis. *JAMA.* (2013) 309:2232–9. doi: 10.1001/jama.2013.5827
20. Nielsen PA, Bennett EP, Wandall HH, Therkildsen MH, Hannibal J, Clausen H. Identification of a major human high molecular weight salivary mucin (MG1) as tracheobronchial mucin MUC5B. *Glycobiology.* (1997) 7:413–9. doi: 10.1093/glycob/7.3.413
21. Hancock LA, Hennessy CE, Solomon GM, Dobrinskikh E, Estrella A, Hara N, et al., Evans CM, et al. Muc5b overexpression causes mucociliary dysfunction and enhances lung fibrosis in mice. *Nat Commun.* (2018) 9:5363. doi: 10.1038/s41467-018-07768-9
22. Helling BA, Gerber AN, Kadiyala V, Sasse SK, Pedersen BS, Sparks L, et al., Schwartz DA. Regulation of MUC5B expression in idiopathic pulmonary fibrosis. *Am J Respir Cell Mol Biol.* (2017) 57:91–9. doi: 10.1165/rcmb.2017-0046OC
23. Gally F, Sasse SK, Kurche JS, Gruca MA, Cardwell JH, Okamoto T, et al., Schwartz DA, Gerber AN. The MUC5B-associated variant rs35705950 resides within an enhancer subject to lineage- And disease-dependent epigenetic remodeling. *JCI Insight.* (2021) 6:e144294. doi: 10.1172/jci.insight.144294
24. Yin W, Cao W, Zhou G, Wang L, Sun J, Zhu A, et al. Analysis of pathological changes in the epithelium in COVID-19 patient airways. *ERJ Open Res.* (2021) 7:00690-2020. doi: 10.1183/23120541.00690-2020
25. Fung HB, Monteagudo-Chu MO. Community-acquired pneumonia in the elderly. *Am J Geriatr Pharmacother.* (2010) 8:47–62. doi: 10.1016/j.amjopharm.2010.01.003
26. Borczuk AC, Salvatore SP, Seshan S V., Patel SS, Bussel JB, Mostyka M, et al. COVID-19 pulmonary pathology: a multi-institutional autopsy cohort from Italy and New York City. *Mod Pathol.* (2020) 33:2156–68. doi: 10.1038/s41379-020-00661-1
27. Roser M, Ritchie H, Ortiz-Ospina E, Hasell J. *Coronavirus Pandemic (COVID-19)*. OurWorldInData.org (2020). Available online at: https://ourworldindata.org/coronavirus
28. Snetselaar R, van Oosterhout MFM, Grutters JC, Van Moorsel CHM. TERT polymorphism rs2736100: a balancing act between cancer and non-cancer disease, a meta-analysis. *Front Med.* (2018) 5:41. doi: 10.3389/fmed.2018.00041
29. Van Der Vis JJ, Snetselaar R, Kazemier KM, Ten Klooster L, Grutters JC, Van Moorsel CHM. Effect of Muc5b promoter polymorphism on disease predisposition and survival in idiopathic interstitial pneumonias. *Respirology.* (2016) 21:712–7. doi: 10.1111/resp.12728
30. Ley B, Newton CA, Arnould I, Elicker BM, Henry TS, Vittinghoff E, et al. The MUC5B promoter polymorphism and telomere length in patients with chronic hypersensitivity pneumonitis: an observational cohort-control study. *Lancet Respir Med.* (2017) 5:639–47. doi: 10.1016/S2213-2600(17)30216-3
31. Platenburg MGJP, Wiertz IA, van der Vis JJ, Crestani B, Borie R, Dieude P, et al. The MUC5B promoter risk allele for idiopathic pulmonary fibrosis predisposes to asbestosis. *Eur Respir J.* (2020) 55:1902361. doi: 10.1183/13993003.02361-2019
32. Juge PA, Lee JS, Ebstein E, Furukawa H, Dobrinskikh E, Gazal S, et al. MUC5B promoter variant and rheumatoid arthritis with interstitial lung disease. *N Engl J Med.* (2018) 379:2209–19. doi: 10.1056/NEJMoa1801562
33. Fadista J, Kraven LM, Karjalainen J, Andrews SJ, Geller F, Baillie JK, et al., Jenkins RG, Feenstra B. Shared genetic etiology between idiopathic pulmonary fibrosis and COVID-19 severity. *EBioMedicine.* (2021) 65:103277. doi: 10.1016/j.ebiom.2021.103277
34. Austad SN, Hoffman JM. Is antagonistic pleiotropy ubiquitous in aging biology? *Evol Med Public Heal.* (2018) 2018:287–94. doi: 10.1093/emph/eoy033
35. Karczewski KJ, Francioli LC, Tiao G, Cummings BB, Alföldi J, Wang Q, et al. The mutational constraint spectrum quantified from variation in 141,456 humans. *Nature.* (2020) 581:434–43. doi: 10.1530/ey.17.14.3
36. Borie R, Crestani B, Dieude P, Nunes H, Allanore Y, Kannengiesser C, et al. The MUC5B variant is associated with idiopathic pulmonary fibrosis but not with systemic sclerosis interstitial lung disease in the european Caucasian population. *PLoS ONE.* (2013) 8:e70621. doi: 10.1371/journal.pone.0070621
37. López-Mejías R, Remuzgo-Martínez S, Genre F, Pulito-Cueto V, Rozas SMF, Llorca J, et al. Influence of MUC5B gene on antisynthetase syndrome. *Sci Rep.* (2020) 10:1415. doi: 10.1038/s41598-020-58400-0
38. Pan D, Sze S, Minhas JS, Bangash MN, Pareek N, Divall P, et al. The impact of ethnicity on clinical outcomes in COVID-19: a systematic review. *EClinicalMedicine.* (2020) 23:100404. doi: 10.1016/j.eclinm.2020.100404

Conflict of Interest: The authors declare that the research was conducted in the absence of any commercial or financial relationships that could be construed as a potential conflict of interest.

Publisher's Note: All claims expressed in this article are solely those of the authors and do not necessarily represent those of their affiliated organizations, or those of the publisher, the editors and the reviewers. Any product that may be evaluated in this article, or claim that may be made by its manufacturer, is not guaranteed or endorsed by the publisher.

frontiers | Frontiers in Medicine

SYSTEMATIC REVIEW
published: 28 April 2022
doi: 10.3389/fmed.2022.852749

T-Cell Subsets and Interleukin-10 Levels Are Predictors of Severity and Mortality in COVID-19: A Systematic Review and Meta-Analysis

Amal F. Alshammary[1], Jawaher M. Alsughayyir[1], Khalid K. Alharbi[1], Abdulrahman M. Al-Sulaiman[2], Haifa F. Alshammary[3] and Heba F. Alshammary[4]*

[1] Department of Clinical Laboratory Sciences, College of Applied Medical Sciences, King Saud University, Riyadh, Saudi Arabia, [2] Department of Medical and Molecular Virology, Prince Sultan Military Medical City, Riyadh, Saudi Arabia, [3] College of Applied Medical Sciences, Riyadh Elm University, Riyadh, Saudi Arabia, [4] College of Dentistry, Riyadh Elm University, Riyadh, Saudi Arabia

OPEN ACCESS

Edited by:
Pasquale Esposito, University of Genoa, Italy

Reviewed by:
Carmen Silvia Valente Barbas, University of São Paulo, Brazil
Wang-Dong Xu, Southwest Medical University, China

***Correspondence:**
Amal F. Alshammary
aalshammary@ksu.edu.sa

Specialty section:
This article was submitted to Infectious Diseases - Surveillance, Prevention and Treatment, a section of the journal Frontiers in Medicine

Received: *11 January 2022*
Accepted: *01 April 2022*
Published: *28 April 2022*

Citation:
Alshammary AF, Alsughayyir JM, Alharbi KK, Al-Sulaiman AM, Alshammary HF and Alshammary HF (2022) T-Cell Subsets and Interleukin-10 Levels Are Predictors of Severity and Mortality in COVID-19: A Systematic Review and Meta-Analysis. Front. Med. 9:852749. doi: 10.3389/fmed.2022.852749

Background: Many COVID-19 patients reveal a marked decrease in their lymphocyte counts, a condition that translates clinically into immunodepression and is common among these patients. Outcomes for infected patients vary depending on their lymphocytopenia status, especially their T-cell counts. Patients are more likely to recover when lymphocytopenia is resolved. When lymphocytopenia persists, severe complications can develop and often lead to death. Similarly, IL-10 concentration is elevated in severe COVID-19 cases and may be associated with the depression observed in T-cell counts. Accordingly, this systematic review and meta-analysis aims to analyze T-cell subsets and IL-10 levels among COVID-19 patients. Understanding the underlying mechanisms of the immunodepression observed in COVID-19, and its consequences, may enable early identification of disease severity and reduction of overall morbidity and mortality.

Methods: A systematic search was conducted covering PubMed MEDLINE, Scopus, Web of Science, and EBSCO databases for journal articles published from December 1, 2019 to March 14, 2021. In addition, we reviewed bibliographies of relevant reviews and the medRxiv preprint server for eligible studies. Our search covered published studies reporting laboratory parameters for T-cell subsets (CD4/CD8) and IL-10 among confirmed COVID-19 patients. Six authors carried out the process of data screening, extraction, and quality assessment independently. The DerSimonian-Laird random-effect model was performed for this meta-analysis, and the standardized mean difference (SMD) and 95% confidence interval (CI) were calculated for each parameter.

Results: A total of 52 studies from 11 countries across 3 continents were included in this study. Compared with mild and survivor COVID-19 cases, severe and non-survivor cases had lower counts of CD4/CD8 T-cells and higher levels of IL-10.

Conclusion: Our findings reveal that the level of CD4/CD8 T-cells and IL-10 are reliable predictors of severity and mortality in COVID-19 patients. The study protocol is registered

with the International Prospective Register of Systematic Reviews (PROSPERO); registration number CRD42020218918.

Systematic Review Registration: https://www.crd.york.ac.uk/prospero/display_record.php?ID=CRD42020218918, identifier: CRD42020218918.

Keywords: COVID-19, SARS-CoV-2, coronavirus, interleukin 10, CD4, CD8, IL-10

INTRODUCTION

Coronavirus disease 2019 (COVID-19) is a viral infection caused by the severe acute respiratory syndrome coronavirus 2 (SARS-CoV-2), first identified in December 2019 when patients with an unknown type of pneumonia were admitted to Hubei hospital in Wuhan, China (1, 2). The fear of encountering a novel strain from the notorious coronavirus family, of which SARS-CoV-1 and MERS-CoV are members, was thus realized (3). This novel disease spread rapidly from its country of origin to other regions of the world, affecting people in 192 countries and resulting in 280,001,617 confirmed cases and 5,402,083 deaths (4). COVID-19 was declared a global health emergency and a pandemic by the World Health Organization (WHO) in March 2020 (5).

Infection with SARS-CoV-2 does not immediately cause disease, and patients can be divided into four major classes based on their presentation on the clinical spectrum. Patients in the first class are asymptomatic with no clinically reported signs, although anosmia and dysgeusia are common among this group (6–8). The second develop flu-like symptoms with fever, sore throat, and cough (9, 10). Additional signs and symptoms of varying severity are present in the third group, including frequent chest pain, difficulty breathing, and unproductive cough (10, 11). Finally, in the fourth group, life-threatening complications become evident as the disease progresses, and patients begin to exhibit critical signs and symptoms, including pneumonia, acute lung injury (ALI), acute respiratory distress syndrome (ARDS), septic shock, and multiple organ failure (12, 13). Furthermore, the incubation period from infection to the onset of disease varies greatly, ranging from 2 to 14 days (14, 15). The virus's basic reproduction number (R_0) is estimated to be around 1.4 and 3.8, indicating the potential for a pandemic and recurrent infection within populations (1, 16–18).

It is common for patients with COVID-19 to show a marked decrease in their leukocyte counts, specifically their lymphocyte counts, a condition that translates clinically into immunodepression or immunosuppression (19–25). Outcomes depend on lymphocytopenia status, especially patients' T-cell counts. Recovery is more likely when lymphocytopenia is resolved, and severe complications arising from lymphocytopenia may lead to death (25–29). In addition, studies report elevated levels of IL-10 in severe and non-survivor cases relative to mild or survivor COVID-19 cases (23–26, 30–32). Thus, as an anti-inflammatory cytokine, IL-10 may be responsible for the reduced T-cell counts that lead to immunodepression in COVID-19 patients (33).

It is essential for our understanding of the disease course to identify the influence of T-cell subsets and IL-10 in patients with mild and severe COVID-19, as well as in survivor and non-survivor cases. This systematic review and meta-analysis aimed to analyze T-cell subsets (CD4/CD8) and IL-10 in severe and fatal cases of COVID-19. Our understanding of the mechanisms causing the immunodepression observed in COVID-19—and its consequences—may enable the early identification of disease severity predictors and development of more effective interventions.

METHODS

Protocol and Registration

The systematic review and meta-analysis were performed and reported following the guidelines of the Preferred Reporting Items for Systematic Reviews and Meta-Analysis (PRISMA), including the flow diagram (**Figure 1**) and checklist (**Supplementary Table 1.1**) (34). Guidelines provided by the Meta-Analyses Of Observational Studies in Epidemiology (MOOSE), including the checklist (**Supplementary Table 1.2**) (35) were also followed. The study protocol was registered with the International Prospective Register of Systematic Reviews (PROSPERO); registration number CRD42020218918 (36).

Eligibility Criteria

The PICOS framework—problem/patients/population, intervention/indicator, compare, outcome, and study designs—was used to formulate our research question (37, 38) as follows: Patients: confirmed COVID-19 patients; Indicator: T-cell subsets (CD4/CD8) and IL-10; Comparison: mild vs. severe or survivors vs. non-survivors; Outcome: severity or mortality; Study designs: hospital-based published studies including retrospective, cohort, prospective, descriptive or observational studies, and case series, in which T-cell subsets (CD4/CD8) and IL-10 levels are documented across COVID-19 severity and mortality groups.

Our review also included studies reporting clinical laboratory parameters among confirmed COVID-19 patients, in which clinical diagnosis and classification of patients were carried out following either the WHO guidelines or guidelines published by an official national or regional health governing body. We allowed this criterion to be flexible as the majority of studies only followed WHO guidelines after their recognition of COVID-19 as a pandemic on March 11, 2020 (5, 39). However, studies following national or regional guidelines were included if the criteria for COVID-19 classification was outlined clearly and matches the criteria outlined by the WHO.

The selected studies were hospital-based, and those not reporting on CD4/CD8 T-cells and IL-10, or lacking proper

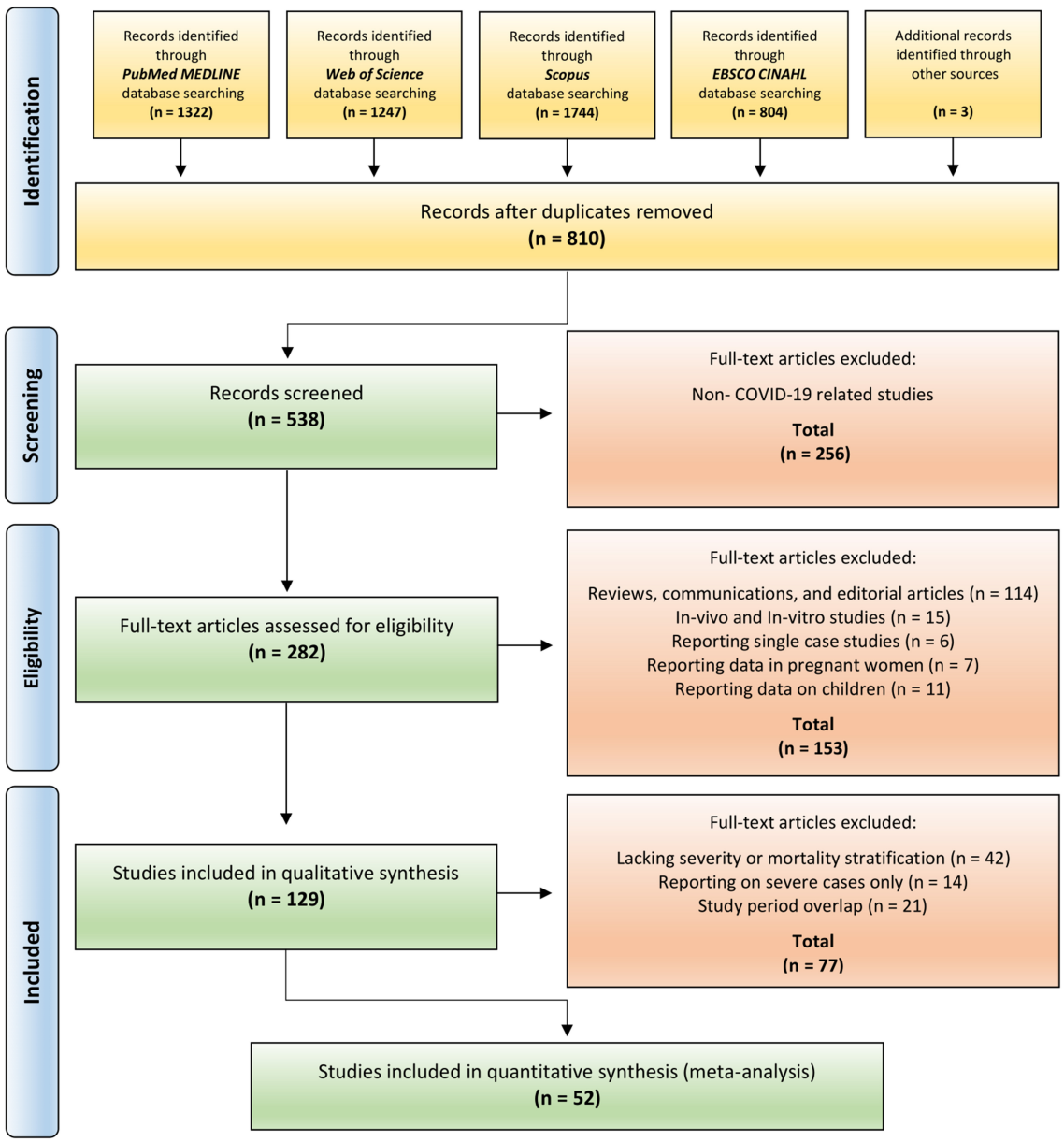

FIGURE 1 | PRISMA flow diagram for T-cell subsets and IL-10 in COVID-19 studies. Figure is adapted from PRISMA flow diagram 2009 (34).

stratification of COVID-19 patients, were excluded. Moreover, to reduce population heterogeneity, we included studies reporting laboratory values for male or female adults and excluded studies reporting on children and pregnant women. However, given that some studies only stratified patients based on sex or provided the mean age of their entire sample, we anticipated a proportion of no more than 10% where studies stated inclusion of children or pregnant women. Furthermore, to eliminate possible differences arising in clinical data obtained from the infection of various SARS-CoV-2 strains, we included studies reported during the first emergence of SARS-CoV-2. Included studies were published in 2020/2021, and data acquisition covered the period from December 2019 to July 2020.

Information Sources

A systematic search was conducted for published journal articles from databases including PubMed MEDLINE, Scopus, Web of Science, and EBSCO CINAHL. Eligible studies identified from the bibliographies of relevant systematic reviews were also included, and a manual search on the preprint server for health sciences, medRxiv, was used to identify unpublished relevant studies. Reviews, opinion articles, editorial material,

communications, conference proceedings and abstracts, *in-vivo*, and *in-vitro* studies were excluded.

Search Strategy

A systematic search was conducted for journal articles published from December 1, 2019 to March 14, 2021. We used the text words (severe acute respiratory syndrome coronavirus 2), or (SARS-CoV-2), or (coronavirus infection disease 19), or (COVID-19), in conjunction with (T lymphocytes), (T-cells), (CD4), (CD8), (lymphocytes), (interleukin 10), and (IL-10) independently (**Supplementary Tables 2.1–2.4**). We also applied filters to our search results specifying journal articles and articles published in English.

Study Selection

Articles obtained from each database were imported into a designated EndNote (Clarivate) folder (40). A new folder was created to combine all articles from each database to eliminate duplicates. Retained articles were then exported into an electronic review manager, Colandr (41), to facilitate title, abstract, and full-text screening using the specified eligibility criteria. While performing full-text screening, we performed a manual search of the full article text, including the **Supplementary Material**, to confirm T-cell subsets (CD4/CD8) and IL-10 were included in each study. This process was carried out independently by six authors, with articles selected by one author being verified by the others. In any cases of disagreement, the final decision about each study was made by consensus from all authors, and decisions were documented in an Excel spreadsheet (Microsoft Corporation) (42).

Data Collection Process

Extracted data from the studies were exported into an Excel spreadsheet. For studies with unclear classification of patients, the corresponding authors were contacted for clarification. Authors were also contacted to request data where studies were missing values for T-cell subsets or IL-10. If no response was received, we performed data extraction from study figures using WebPlotDigitizer, a web-based tool for extracting data from figures (**Supplementary Table 3**) (43).

Data Items

Data items included author name, publication year, study location (country/city/hospital), study period (duration), study design, assessment of COVID-19 severity (WHO or national/regional health care authority guidelines), timing of proposed classification (on admission or later), sample size (number), sample characteristics (sex, age, underlying conditions), number of cases classified as mild or survivor, number of cases classified as severe or non-survivor, T-cell subsets (CD4/CD8), and IL-10 values stratified by severity or mortality. For laboratory values reported on a continuous scale, the mean and standard deviation (SD), the median with minimum/maximum range, or median and interquartile (IQR) values were extracted. This process was carried out independently by three authors, AFA, JMA, and HFA, and data extracted by one author were verified by the others. Consensus was reached by all authors in any instances of disagreement, and decisions were documented in Excel.

Assessment of Quality and Risk of Bias in Individual Studies

The Newcastle-Ottawa Scale (NOS) for cohort studies was adopted to evaluate selected studies independently (44). The NOS scale uses a star system (0–9) to judge a study based on three domains: sample selection, sample comparability against controls, and assessment of outcome. A higher NOS score (above 7 stars) reflects better quality and a lower risk of bias. In contrast, lower NOS scores (below 4 stars) reflect lower quality and a higher risk of bias. NOS scores of 4–6 stars indicate moderate quality and risk of bias (**Supplementary Table 4**). All authors independently rated the included studies. Each author documented their scoring decision and subsequently verified the scoring decision of other authors. The final decision for each study was made by consensus from all authors, and scores were documented in Excel.

Synthesis of Extracted Data

Extracted data values from the selected studies were reported on a continuous scale. The mean and SD from each study were pooled to compute the effect size or the standardized mean difference (SMD) and 95% confidence intervals (CI). In the case of median and IQR (minimum and maximum) reporting, we computed the mean and SD based on Wan et al.'s formula (45). The mean and SD were calculated using Cochran's formula for median and IQR reporting without minimum and maximum ranges (46). Furthermore, the means and SDs of similar subgroups were combined into a single group using Cochran's formula for combining similar subgroups (46). Formulas used in this study are listed in **Supplementary Tables 5.1–5.2**.

Meta-Analysis Summary Measures

Because heterogeneity was expected between individual studies, our meta-analysis used the DerSimonian-Laird inverse variance method for a continuous random-effects model (46, 47). To calculate the SMD, we applied Hedge's g formula to avoid bias in a small study size (48, 49). Statistical analysis of extracted data in this study took place using STATA 17 (StataCorp) (50).

Synthesis of Meta-Analysis Results

The SMD and 95% CI were computed using the mean, SD, and sample size from each study (47). Meta-analysis results were displayed using forest and Galbraith plots following the same meta-analysis computational measures. Statistical analysis of extracted data, including the construction of the forest and Galbraith plots, also used STATA 17 (StataCorp) (50).

Assessment of Heterogeneity

Statistical heterogeneity was assessed using I^2 values to measure the degree of inconsistency of collected results produced from the meta-analysis (51, 52). An I^2 cut-off value of 0% indicates no heterogeneity, 25% is low, 50% is moderate, and 75% indicates a

high level of heterogeneity (52). The Galbraith plot can also be used to assess heterogeneity visually through detecting outliers located outside the 95% CI shaded region (53). STATA 17 (StataCorp) (50) was used to analyze the I^2 cut-off value and the Galbraith plot.

Between-study variations can be further explored through subgroup analysis to identify the source of heterogeneity if due to a specific study-level covariate. Heterogeneity induced by the relationship between specific-study effect size and study-level covariates can be measured by performing meta-regression, where the adjusted R^2 is used to examine the proportion of between-study variance explained by study-level covariates (54). A bubble plot was also generated following meta-regression as a graphical presentation of the relationship between study-level covariates and the effect size of a specific study (54–56). STATA 17 (StataCorp) was used for the statistical analysis of extracted data, including meta-regression and the construction of the bubble plot (50).

Small Study Effects and Publication Bias

Standard funnel plots and non-parametric trim and fill funnel plots were constructed to detect possible cumulative bias in the studies. The standard funnel plot is used to detect small study effects and publication bias (57, 58). A symmetrical funnel denotes the absence of bias, while an asymmetrical funnel indicates clear publication bias (46). Publication bias may arise because smaller studies with non-significant results are suppressed from publication, leading to a biased sample. With the nonparametric trim and fill analysis, smaller studies inducing the funnel plot asymmetry are removed to estimate the funnel plot true center. This is followed by the addition of removed studies and their missing counterparts around the center (46, 59, 60). This method enables detection and measurement of the influence of missing studies on the overall effect size (46, 59, 60).

The regression-based Egger test was also performed to statistically assess plot distribution asymmetry: $P < 0.1$ indicates publication bias, whereas $P > 0.1$ indicates no publication bias (61, 62). Measurement of publication bias was also performed using Begg's non-parametric rank correlation based on correlating the standardized effect with the variance using Kendall's tau b (63). Begg's test investigates whether Kendall's rank correlation between the effect size and its variance equals zero: a significant correlation indicates bias ($P < 0.05$), whereas a non-significant correlation indicates the absence of bias ($P > 0.05$). Standard funnel plots, nonparametric trim and fill funnel plot analysis, regression-based Egger test, and the nonparametric rank correlation (Begg) test were performed using STATA 17 (StataCorp) (50).

Meta-Analysis Sensitivity Test

The influence of studies harboring a high risk of bias was quantified by performing the Leave-One-Out sensitivity test, where each study is omitted sequentially to measure its influence on the overall combined effect size (64). STATA 17 (StataCorp) was again used for this purpose (50).

RESULTS

Study Selection

An outline of the systematic review search results is presented in **Figure 1**. We identified 5,120 studies by searching four major databases, including PubMed (1,322), Web of Science (1,247), Scopus (1,744), and EBSCO CINAHL (804). In addition, three records were identified from the bibliographies of relevant systematic reviews and the manual search on the preprint server medRxiv. After removal of duplicates, 810 records were screened. Of those, 272 were excluded following title and abstract review. Retained articles were assessed for study eligibility. Of these, 256 records were excluded as they were not COVID-19 related studies. A further 153 papers were excluded as they were reviews, communications, editorial articles, *in-vivo*/*in-vitro* studies or studies reporting on pregnant women or children. Included studies were thoroughly assessed for eligibility criteria. Of those, 77 records were excluded because of lack of stratification based on severity/mortality, for reporting on severe cases only (**Supplementary Table 6.1**), and because of overlapping study periods (**Supplementary Table 6.2**). Finally, 52 studies were retained for the synthesis of meta-analysis results (19, 21–25, 27, 30–33, 65–105).

Study Characteristics

The general characteristics of the studies are described in **Table 1**. They were all hospital-based and included 34 retrospective, 1 retrospective case series, 1 retrospective cohort, 1 prospective, 1 prospective observational, 1 prospective cohort, 10 cohort, and 3 observational cohort studies. The majority of studies were from China with 37 investigations across multiple cities [Wuhan (21), Beijing (4), Hangzhou (3), Guangzhou (2), Taizhou (2), Shanghai (1), Wenzhou (1), Nanchang (1), Nanjing (1), and Jiangsu (1)]. The remaining studies were from the United States [New York (1), New Haven (1), and Cincinnati (1)], United Kingdom [London (2), and Manchester (1)], France [Paris (1), and Creteil (1)], Ireland [Dublin (1)], Italy [Brescia/Monza/Pavia (1)], Spain [Madrid (1)], Netherlands [Breda (1)], Brazil [Curitiba (1)], Korea [Seoul (1)], and Singapore [Singapore (1)] (**Figure 2**).

The main characteristics and methods for COVID-19 classification in the selected studies are shown in **Supplementary Table 7.1**. A total of 15 studies classified COVID-19 severity based on WHO guidelines, while 25 studies followed the Chinese National Health Commission or the Chinese Centre for Disease Control and Prevention, and 12 studies used national or local guidelines. With regard to the clinical laboratory tests performed for COVID-19 patients, 37 studies reported sample acquisition within 24 h of admission, 8 reported sample acquisition 1–7 days post-admission, 1 study reported sample acquisition 7–14 days post-admission, and 6 studies did not specify the sample acquisition time (**Supplementary Table 7.2**). All studies confirmed COVID-19 infection through RT-PCR. Comorbidities varied, with most studies reporting cardio-cerebrovascular disease, hypertension, diabetes, renal disease, liver disease, chronic obstructive pulmonary disease (COPD), and cancer (**Supplementary Table 7.3**).

TABLE 1 | General characteristics of included studies.

First author	Abers, Michael	Hospital	ASST Spedali Civili Brescia; Ospedale San Gerardo; Ospedale S. Matteo
Publication year	2021	Study period	February 25–May 09, 2020
Country	Italy	Study design	Retrospective
City	Brescia; Monza; Pavia	NOS score	6
First author	Azmy, Veronica	Hospital	Not Defined: Tertiary Care Hospital
Publication year	2021	Study period	March 10–31, 2020
Country	United States	Study design	Cohort
City	New Haven, CT	NOS score	7
First author	Cantenys-Molina, S	Hospital	Gregorio Maranon General University Hospital
Publication year	2021	Study period	March 26–May 26, 2020
Country	Spain	Study design	Retrospective
City	Madrid	NOS score	7
First author	Carissimo, Guillaume	Hospital	National Centre for Infectious Diseases
Publication year	2020	Study period	February–April 2020
Country	Singapore	Study design	Observational cohort
City	Singapore	NOS score	8
First author	Chen, Jiaxin	Hospital	Nanjing Medical Hospitals
Publication year	2020	Study period	January 23–March 11, 2020
Country	China	Study design	Retrospective
City	Nanjing	NOS score	6
First author	Chi, Ying	Hospital	Hospital not specified; but the region is specified (Jiangsu province)
Publication year	2020	Study period	Not specified
Country	China	Study design	Cohort
City	Jiangsu	NOS score	6
First author	Deng, Fuxue	Hospital	Sino-French New City Branch of Tongi Hospital
Publication year	2020	Study period	January 30–March 30, 2020
Country	China	Study design	Retrospective
City	Wuhan	NOS score	6
First author	Diao, Bo	Hospital	General Hospital of Central Theater Command or Hanyang Hospital
Publication year	2020	Study period	December 2019–January 2020
Country	China	Study design	Retrospective
City	Wuhan	NOS score	6
First author	Feng, Xiaobo	Hospital	Wuhan Union Hospital
Publication year	2020	Study period	January 23–February 22, 2020
Country	China	Study design	Prospective
City	Wuhan	NOS score	7
First author	Flament, Heloise	Hospital	Bichat or Cochin Hospitals
Publication year	2021	Study period	March 23–October 05, 2020
Country	France	Study design	Cohort
City	Paris	NOS score	9
First author	Gadotti, Ana Carolina	Hospital	Hospital not specified; but the region is specified (Curitiba Parana)
Publication year	2020	Study period	June–July 2020
Country	Brazil	Study design	Prospective cohort
City	Curitiba	NOS score	7
First author	Guan, Jingjing	Hospital	Fifth Affiliated Hospital of Wenzhou Medical University
Publication year	2020	Study period	Not specified; no overlap with hospital location
Country	China	Study design	Cohort
City	Wenzhou	NOS score	6
First author	Han, Huan	Hospital	Renmin Hospital of Wuhan
Publication year	2020	Study period	January–February 2020
Country	China	Study design	Retrospective
City	Wuhan	NOS score	6

(Continued)

TABLE 1 | Continued

First author	He, Bing	Hospital	Renmin Hospital of Wuhan
Publication year	2020	Study period	February 01, 2020
Country	China	Study design	Retrospective
City	Wuhan	NOS score	8
First author	He, Susu	Hospital	Taizhou Public Health Medical Centre
Publication year	2020	Study period	January 17–February 12, 2020
Country	China	Study design	Retrospective
City	Taizhou	NOS score	7
First author	Henry, Brandon Michael	Hospital	University of Cincinnati Medical Centre
Publication year	2021	Study period	April–May 2020
Country	United States	Study design	Retrospective
City	Cincinnati	NOS score	8
First author	Huang, Hong	Hospital	Tongji Hospital
Publication year	2021	Study period	February 07–March 27, 2020
Country	China	Study design	Retrospective
City	Wuhan	NOS score	6
First author	Huang, Wei	Hospital	Wuhan Number 1 Hospital
Publication year	2021	Study period	January 20–March 17, 2020
Country	China	Study design	Retrospective
City	Wuhan	NOS score	7
First author	Hue, Sophie	Hospital	Henri Mondor Hospital Intensive Care Unit (ICU)
Publication year	2020	Study period	March 08–30, 2020
Country	France	Study design	Prospective observational
City	Cretil	NOS score	7
First author	Jin, Xiao-Hong	Hospital	Taizhou Hospital of Zhejiang Province and Taizhou Enze Hospital
Publication year	2020	Study period	January 19–March 11, 2020
Country	China	Study design	Retrospective
City	Taizhou	NOS score	7
First author	Keddie, Stephen	Hospital	University College London Hospital (UCLH)
Publication year	2020	Study period	April 06–May 18, 2020
Country	United Kingdom	Study design	Cohort
City	London	NOS score	7
First author	Kwon, Ji-Soo	Hospital	Asan Medical Centre
Publication year	2020		Chung-Ang University Hospital
Country	Korea		Soonchunhyang University Seoul Hospital
City	Seoul		Inje University Sanggye Paik Hospital
		Study Period	February–April 2020
		Study Design	Prospective
		NOS score	7
First author	Laing, Adam	Hospital	Guy's Hospital and St. Thomas Hospital
Publication year	2020	Study period	March 25–May 14, 2020
Country	United Kingdom	Study design	Observational cohort
City	London	NOS score	8
First author	Li, Chenze	Hospital	Tongji Hospital
Publication year	2020	Study period	January 29–April 01, 2020
Country	China	Study design	Retrospective
City	Wuhan	NOS score	9
First author	Li, Mingyue	Hospital	Wuhan Union Hospital
Publication year	2020	Study period	February 25–27, 2020
Country	China	Study design	Retrospective
City	Wuhan	NOS score	7
First author	Li, Qiang	Hospital	Shanghai Public Health Clinical Centre

(Continued)

TABLE 1 | Continued

Publication year	2020	Study period	January 20–June 23, 2020
Country	China	Study design	Retrospective
City	Shanghai	NOS score	6
First author	Li, Xiaolei	Hospital	The First Affiliated Hospital of Nanchang University
Publication year	2020	Study period	January 24–March 12, 2020
Country	China	Study design	Retrospective
City	Nanchang	NOS score	7
First author	Liao, Baolin	Hospital	Guangzhou Eighth People's Hospital
Publication year	2021	Study period	January 22–April 10, 2020
Country	China	Study design	Retrospective
City	Guangzhou	NOS score	8
First author	Liu, Fangfang	Hospital	Fiifth Medical Centre of PLA General Hospital
Publication year	2020	Study period	January 20–February 23, 2020
Country	China	Study design	Cohort
City	Beijing	NOS score	8
First author	Liu, Jian	Hospital	First Affiliated Hospital
Publication year	2020	Study period	January 22–March 20, 2020
Country	China	Study design	Retrospective
City	Hangzhou	NOS score	7
First author	Liu, Jing	Hospital	Wuhan Union Hospital
Publication year	2020	Study period	January 05–24, 2020
Country	China	Study design	Retrospective
City	Wuhan	NOS score	8
First author	Liu, Lei	Hospital	General Hospital of Central Theater Command of the PLA
Publication year	2020	Study period	February 06–21, 2020
Country	China	Study design	Cohort
City	Beijing	NOS score	7
First author	Liu, Yangli	Hospital	Tongji Hospital
Publication year	2021	Study period	February 09–April 06, 2020
Country	China	Study design	Retrospective
City	Wuhan	NOS score	6
First author	Liu, Xue-Qing	Hospital	Leishenshan Hospital
Publication year	2021	Study period	February 23–April 04, 2020
Country	China	Study design	Retrospective Cohort
City	Wuhan	NOS score	8
First author	Luo, Miao	Hospital	Wuhan Pulmonary Hospital and Tongji Hospital
Publication year	2020	Study period	January 09–March 31, 2020
Country	China	Study design	Retrospective
City	Wuhan	NOS score	9
First author	Mann, Elizabeth	Hospital	Four Hospitals in Greater Manchester Area
Publication year	2020	Study period	March 29–May 07, 2020
Country	United Kingdom	Study design	Observational cohort
City	Manchester	NOS score	7
First author	McElvaney, Oliver	Hospital	Beaumont Hospital
Publication year	2020	Study period	June 2020
Country	Irland	Study design	Cohort
City	Dublin	NOS score	7
First author	Rendeiro, Andre	Hospital	New York Presbyterian Hospital and Lower Manhattan Hospital
Publication year	2020	Study period	April–July 2020
Country	United States	Study design	Retrospective
City	New York	NOS score	9
First author	Schrijver, Benjamin	Hospital	The Peripheral Hospital Amphia Breda

(Continued)

TABLE 1 | Continued

Publication year	2020	Study period	March 24–April 14, 2020
Country	Netherlands	Study design	Retrospective
City	Breda	NOS score	7
First author	Shi, Hongbo	Hospital	Beijing Youan Hospital
Publication year	2020	Study period	Not specified
Country	China	Study design	Retrospective
City	Beijing	NOS score	9
First author	Tan, Mingkai	Hospital	Guangzhou Eighth People's Hospital
Publication year	2020	Study period	January–February 2020
Country	China	Study design	Cohort
City	Guangzhou	NOS score	7
First author	Wang, Zhongliang	Hospital	Wuhan Union Hospital
Publication year	2020	Study period	January 16–29, 2020
Country	China	Study design	Retrospective
City	Wuhan	NOS score	7
First author	Xu, Bo	Hospital	Hubie Provincial Hospital of Traditional Chinese and Western Medicine
Publication year	2020	Study period	December 26, 2019–March 01, 2020
Country	China	Study design	Retrospective
City	Wuhan	NOS score	7
First author	Yang, Ai-Ping	Hospital	Not specified: possibly Zhejiang Xiaoshan Hospital
Publication year	2020	Study period	End date of data collection; February 29, 2020
Country	China	Study design	Retrospective
City	Hangzhou	NOS score	7
First author	Yang, Fan	Hospital	Renmin Hospital
Publication year	2020	Study period	January 01–April 15, 2020
Country	China	Study design	Retrospective
City	Wuhan	NOS score	6
First author	Yi, Ping	Hospital	First Affiliated Hospital of Medical College of Zhejiang University
Publication year	2020	Study period	January 19–February 19, 2020
Country	China	Study design	Retrospective
City	Hangzhou	NOS score	7
First author	Zeng, Hao-Long	Hospital	Tongji Hospital
Publication year	2020	Study period	January 17–February 14, 2020
Country	China	Study design	Retrospective
City	Wuhan	NOS score	6
First author	Zeng, Zhilin	Hospital	Tongji Hospital
Publication year	2020	Study period	January 28–February 12, 2020
Country	China	Study design	Retrospective
City	Wuhan	NOS score	7
First author	Zhang, Bo	Hospital	Tongji Hospital
Publication year	2021	Study period	February–April 2020
Country	China	Study design	Retrospective
City	Wuhan	NOS score	6
First author	Zhang, Jun	Hospital	Tongji Hospital
Publication year	2020	Study period	January 01–February 13, 2020
Country	China	Study design	Retrospective
City	Wuhan	NOS score	7
First author	Zhao, Yan	Hospital	Beijing You'an Hospital
Publication year	2020	Study period	January–March 2020
Country	China	Study design	Cohort
City	Beijing	NOS score	7
First author	Zou, Li	Hospital	Renmin Hospital of Wuhan University
Publication year	2020	Study period	January 16–March 03, 2020
Country	China	Study design	Retrospective
City	Wuhan	NOS score	7

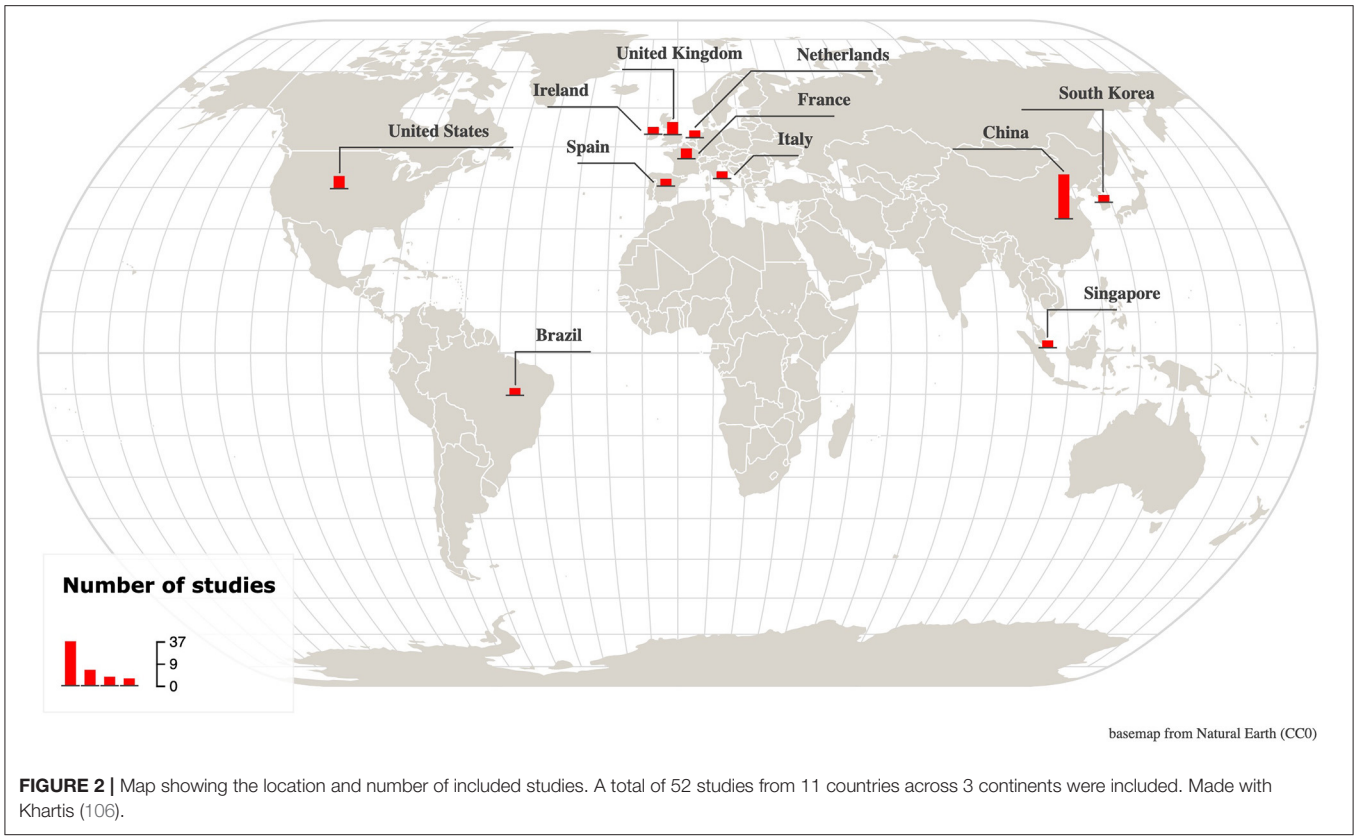

FIGURE 2 | Map showing the location and number of included studies. A total of 52 studies from 11 countries across 3 continents were included. Made with Khartis (106).

Reporting of COVID-19 severity subgroups (e.g., discharged vs. hospitalized; non-ICU vs. ICU) varied greatly between studies. Therefore, each subgroup was assigned to either mild (including moderate) or severe (including critical) categories based on the clinical presentation described in each study. Similarly, the reporting of COVID-19 mortality contained a slight degree of variability (e.g., cured vs. died; hospitalized vs. deceased). Each subgroup was thus classified into either survivors or non-survivors. Some studies reported more than two groups (up to four), and accordingly, we performed a subgroup combination if the stratification for COVID-19 patients was defined clearly in the study. Thus, our meta-analysis only included studies satisfying this criterion. **Supplementary Table 7.4** illustrates the method for subgroup assignment from each study, and **Supplementary Table 5.2** shows the formula used for combining subgroups.

The population size and age of COVID-19 patients from the included studies are shown in **Supplementary Tables 8.1–8.4**. The total number of patients by sex is reported as an approximate number because some studies did not describe gender. The mean population size based on severity was 7,913, including 3,905 males and 3,680 females. Of those, 5,109 (2,357 males/2,493 females) were classified as mild, and 2,804 (1,548 males/1,087 females) were severe. In contrast, the mean population size based on mortality was 3,420, including 1,813 males and 1,508 females. Of those, 2,662 (1,350 males/1,268 females) were sub-grouped as survivors, and 758 (463 males/240 females) as non-survivors. The mean age was 53.03 ± 25.6 for the mild group, and 63.39 ± 22.61 for the severe patients. In contrast, the mean age was 59.36 ± 16.11 for the survivors, and 70.67 ± 12.82 for the non-survivors.

Risk of Bias Within Studies

Studies were examined for quality to avoid bias, and a score was assigned to each study using the NOS scale for quality assessment of cohort studies, shown in **Table 1** and detailed in **Supplementary Table 4**. The majority of studies received scores indicating high quality: 5 studies received a score of 9, 8 studies received scores of 8, and 26 studies received scores of 7. A total of 13 studies received scores of 6, indicating moderate quality. The sensitivity analysis of our results did not differ markedly following the exclusion of moderate quality studies.

Meta-Analysis Results of Individual Studies

For the pairwise comparison between mild and severe COVID-19, 24 studies reported decreased counts for CD4 T-cells in the severe cases compared with mild ones (SMD = −1.39 to −0.11), and only 2 studies reported increased counts for CD4 T-cells (SMD = 0.25 to 0.34) (**Figure 3A** and **Supplementary Table 9.1**). Similarly, 25 studies reported decreased counts for CD8 T-cells in severe cases relative to mild ones (SMD = −1.49 to 0.02), and only 1 study reported increased counts for CD8 T-cells (SMD = 0.55) (**Figure 3B** and **Supplementary Table 9.2**). In contrast, all 38 studies of IL-10 reported increased IL-10 levels in the severe cases relative to mild ones (SMD = 0.19 to 1.57) (**Figure 4** and **Supplementary Table 9.3**).

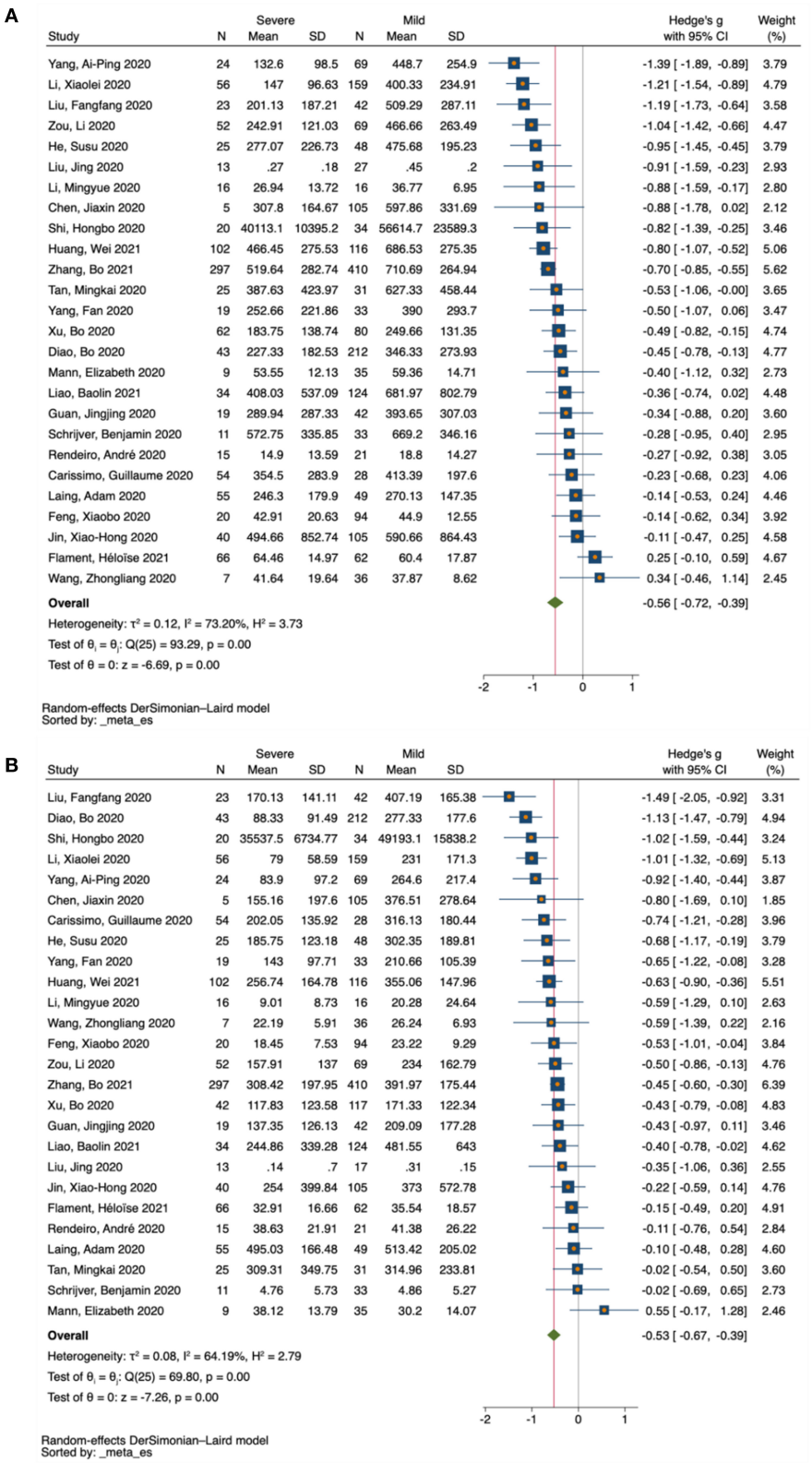

FIGURE 3 | Forest plot of T-cell subsets in COVID-19 severity studies. **(A)** CD4 T-cells in COVID-19 severity studies. **(B)** CD8 T-cells in COVID-19 severity studies. The no-effect line is represented at the value of zero. The diamond symbol represents estimated combined effect size.

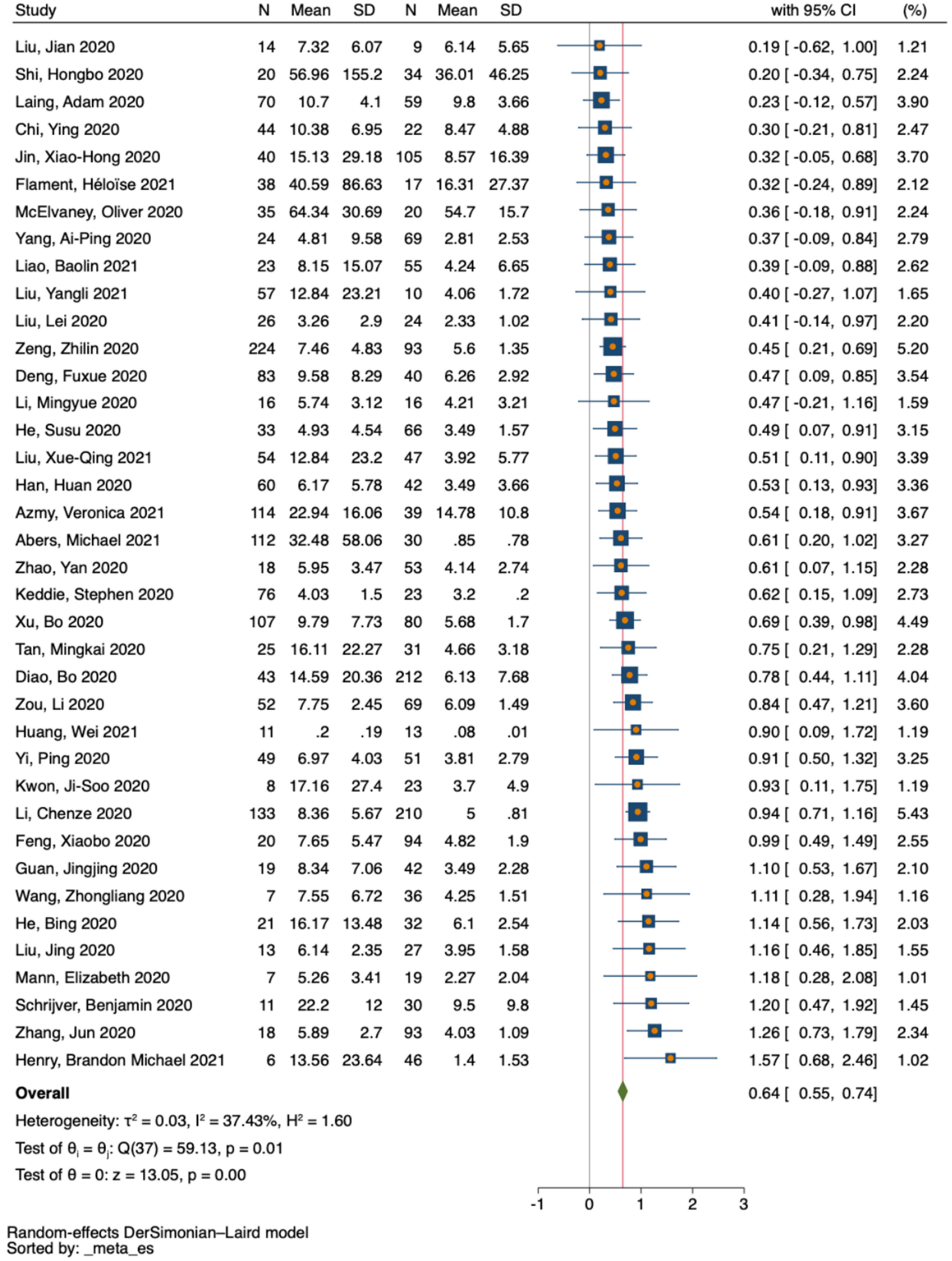

FIGURE 4 | Forest plot of IL-10 in COVID-19 severity studies. The no-effect line is represented at the value of zero. The diamond symbol represents estimated combined effect size.

All included studies for CD4 T-cells (six studies) reported decreased counts in the non-survivors relative to survivors (SMD = −0.99 to −0.03) (**Figure 5A** and **Supplementary Table 9.4**), for the pairwise comparison between COVID-19 survivors and non-survivors. Similarly, four studies reported decreased counts for CD8 T-cells among non-survivors compared with survivors (SMD = −0.89 to −0.47), and only two studies reported increased counts for CD8 T-cells (SMD = 0.17 to 0.36) (**Figure 5B** and **Supplementary Table 9.5**). In contrast, nine studies reported increased levels of IL-10 in the non-survivors relative to survivors (SMD = 0.29 to 1.6), and only one study reported decreased levels of IL-10 (SMD = −0.01) (**Figure 5C** and **Supplementary Table 9.6**).

Meta-Analysis Results of Combined Studies

Forest Plot Meta-Analysis

Based on severity, a total of 26 eligible studies were used for pairwise comparison between mild and severe COVID-19 cases for T-cell subsets. There were 2080 subjects in the mild group vs. 1,112 in the severe group for CD4 T-cells, and 2,107 subjects in the mild group vs. 1,092 in the severe group for CD8 T-cells. Our forest plot meta-analysis revealed an increased effect size of having reduced counts of CD4 and CD8 T-cells in the severe group relative to the mild group (SMD = −0.56, 95% CI = −0.72 to −0.39; SMD = −0.53, 95% CI = −0.67 to −0.39, respectively) (**Figures 3A,B**). Similarly, a total of 38 eligible studies were used for pairwise comparison between mild and severe COVID-19 cases for IL-10, with a total of 1,981 subjects in the mild group vs. 1,731 in the severe group. The forest plot meta-analysis revealed an increased effect size of having elevated levels of IL-10 in the severe group compared with the mild group (SMD = 0.64, 95% CI = 0.55 to 0.74) (**Figure 4**).

In terms of mortality, six eligible studies were used for pairwise comparison between survivor and non-survivor COVID-19 cases for T-cell subsets. A total of 1,680 cases were noted in the survivor group vs. 389 in the non-survivor group for CD4 T-cells, and 537 in the survivor group vs. 95 in the non-survivor group for CD8 T-cells. Our forest plot meta-analysis revealed an increased effect size of having reduced CD4 and CD8 T-cell counts in the non-survivor group compared with the survivor group (SMD = −0.73, 95% CI = −0.94 to −0.53, and SMD = −0.44, 95% CI = −0.84 to −0.04, respectively) (**Figures 5A,B**). Similarly, considering mortality, a total of 10 studies were used for pairwise comparison between survivor and non-survivor COVID-19 cases for IL-10, with a total of 2810 subjects in the survivor group vs. 569 in the non-survivor group. The forest plot meta-analysis revealed an increased effect size of having elevated levels of IL-10 in the non-survivor group compared with the survivor group (SMD = 0.74, 95% CI = 0.42 to 1.06) (**Figure 5C**).

Galbraith Plot Meta-Analysis

A total of 26 studies were used for pairwise comparison between mild and severe COVID-19 cases for T-cell subsets. For CD4 T-cell studies, the Galbraith meta-analysis revealed one study located outside the 95% CI region, and one on the 95% CI borderline (**Figure 6A**). For CD8 T-cell studies, the meta-analysis revealed two studies located outside the 95% CI region (**Figure 6B**). Similarly, using severity, a total of 38 eligible studies were used for pairwise comparison between mild and severe COVID-19 cases for IL-10. The meta-analysis for IL-10 revealed two studies on the 95% CI borderline (**Figure 6C**).

Focusing on mortality, six studies were used for pairwise comparison between survivor and non-survivor COVID-19 cases for T-cell subsets. For CD4 and CD8 T-cell studies, all included studies were located within the 95% CI region (**Figure 6D**) and (**Figure 6E**), respectively. Similarly, a total of 10 eligible studies were used for pairwise comparison between survivor and non-survivor COVID-19 cases for IL-10. The meta-analysis revealed all included studies were located within the 95% CI region (**Figure 6F**).

Assessment of Heterogeneity

The degree of heterogeneity among results from the meta-analysis was assessed using I^2 values. Based on severity, a moderate level of heterogeneity was observed among studies reporting on CD4 T-cells ($P < 0.001$, $I^2 = 73.20\%$) (**Figure 3A**), and CD8 T-cells ($P < 0.001$, $I^2 = 64.19\%$) (**Figure 3B**). Thus, a low level of heterogeneity was observed among studies reporting on IL-10 ($P < 0.001$, $I^2 = 37.43\%$) (**Figure 4**). Similarly, based on mortality, a moderate level of heterogeneity was observed in studies reporting on CD4 T-cells ($P < 0.001$, $I^2 = 51.31\%$) (**Figure 5A**), and CD8 T-cells ($P < 0.001$, $I^2 = 64.08\%$) (**Figure 5B**). However, a high level of heterogeneity was observed for studies reporting on IL-10 ($P < 0.001$, $I^2 = 88.18\%$) (**Figure 5C**).

Subgroup Analysis

A subgroup analysis and meta-regression test were used to assess the source of heterogeneity using study-level covariates stratifying studies based on location (city, country, and continent), study design (retrospective, prospective, or cohort), classification protocol (WHO NCP, CDC, National Health Commission of China, or National/Regional Guidelines), sample acquisition time (at admission or later), population influence (total number of male/female, and mean age of patients), and laboratory influence (test procedure) followed by construction of a bubble plot. Moreover, the covariate of continent was stratified as America, Asia, and Europe. Thus, studies published in America and Europe were sometimes combined due to insufficient studies in each group. The covariate city was stratified as Wuhan or other cities because most studies were based in Wuhan. Similarly, the covariate country was stratified as China or other countries because most studies were based in China. In addition, the total number of male/female patients in each study was indicated as (more or <50), and the mean age of patients was indicated as (more or <50 or 60). We found city, continent, classification protocol, total number of male/female, and mean age of patients were study-level covariates successful in reducing the heterogeneity observed in included studies (in varying degrees based on the parameter being tested).

Based on severity, between-study variability was detected and measured for CD4/CD8 T-cell and IL-10 studies. For CD4

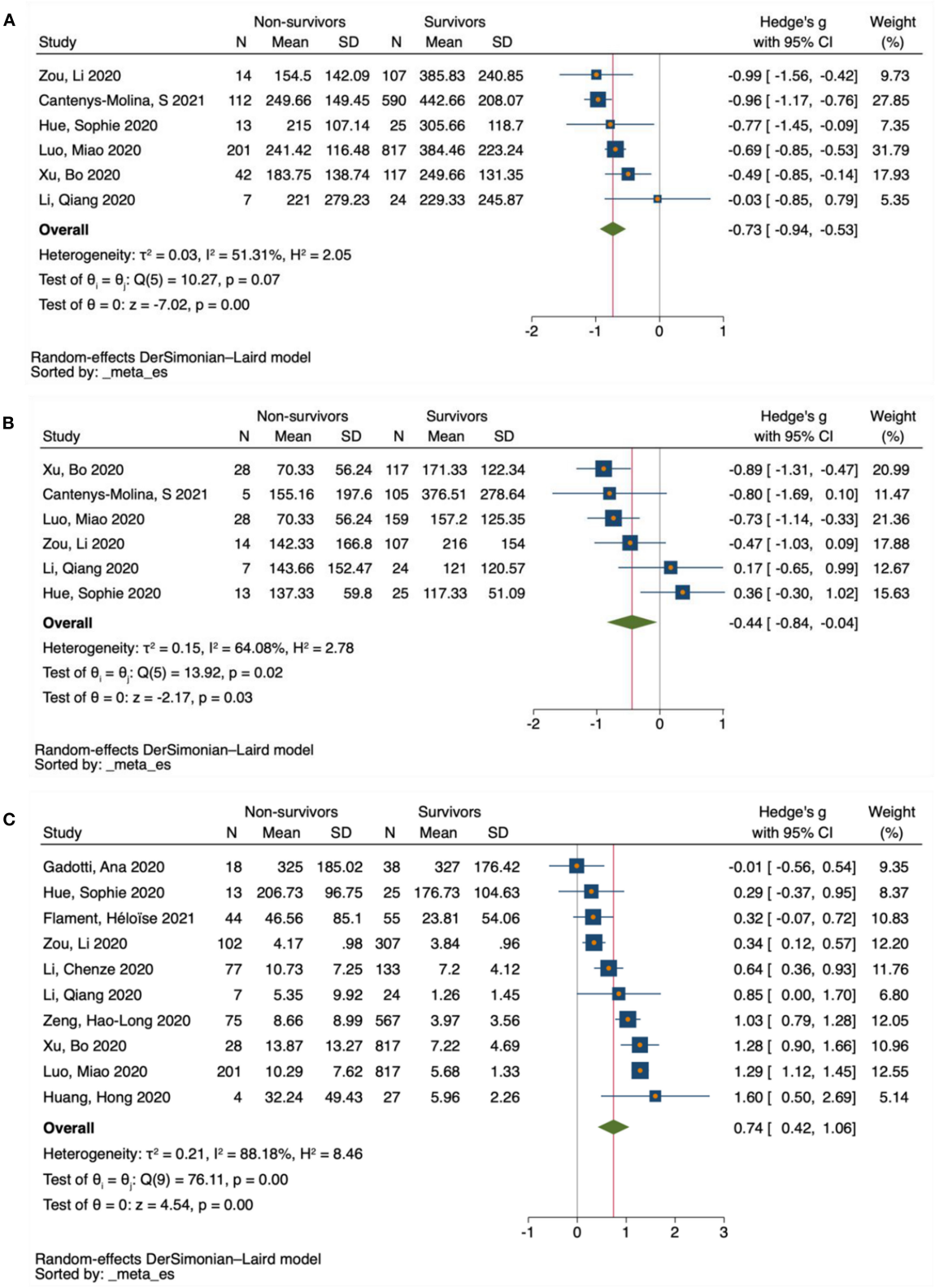

FIGURE 5 | Forest plot of T-cell subsets and IL-10 in COVID-19 mortality studies. **(A)** CD4 T-cells in COVID-19 mortality studies. **(B)** CD8 T-cells in COVID-19 mortality studies. **(C)** IL-10 in COVID-19 mortality studies. The no-effect line is represented at the value of zero. The diamond symbol represents estimated combined effect size.

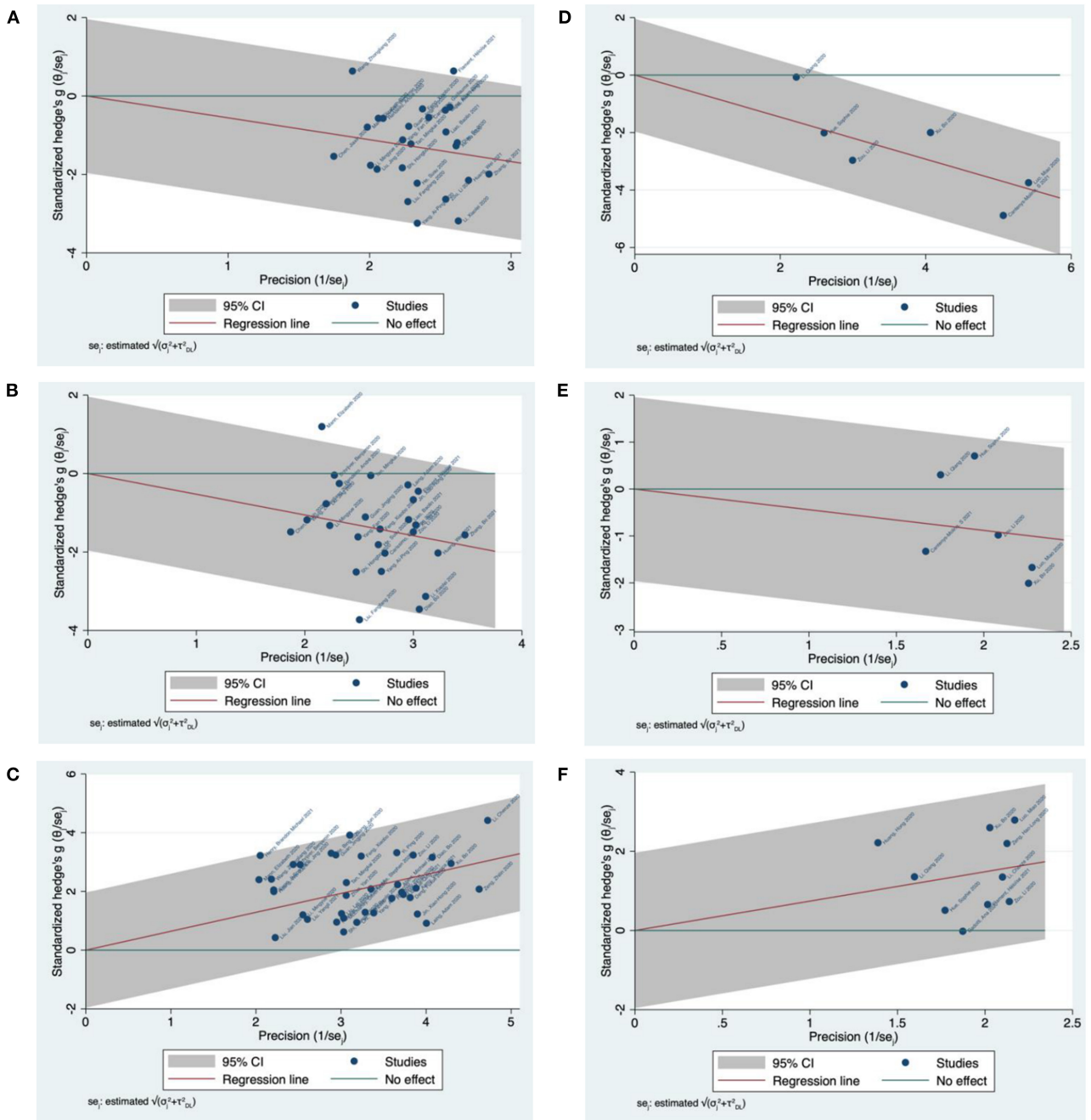

FIGURE 6 | Galbraith plot meta-analysis for CD4/CD8 T-cells and IL-10 in COVID-19 severity and mortality studies. **(A)** CD4 T-cells in COVID-19 severity studies. **(B)** CD8 T-cells in COVID-19 severity studies. **(C)** IL-10 in COVID-19 severity studies. **(D)** CD4 T-cells in COVID-19 mortality studies. **(E)** CD8 T-cells in COVID-19 mortality studies. **(F)** IL-10 in COVID-19 mortality studies.

T-cells, the stratification of studies based on the continent covariate revealed a greater heterogeneity among studies conducted in Asia ($P < 0.001$, $I^2 = 66.76\%$) than for those in Europe and the Americas ($P < 0.001$, $I^2 = 16.79\%$) (**Supplementary Figure 10.3A**). Furthermore, the meta-regression analysis revealed that 25.15% of heterogeneity could be explained by the selected covariate (continent) (**Supplementary Figure 10.3B**) and the effect size increase in studies conducted in Europe or the Americas compared with Asia (**Supplementary Figure 10.3C**). Similarly, the stratification of CD8 T-cell studies based on the continent covariate revealed a higher heterogeneity among studies conducted in Asia ($P < 0.001$, $I^2 = 56.01\%$) than for studies conducted in Europe and the Americas ($P < 0.001$,

I^2 = 0.00%) (**Supplementary Figure 10.13A**). The meta-regression analysis indicated that 42.38% of the heterogeneity could be explained by the selected covariate (continent) (**Supplementary Figure 10.13B**) and the effect size increase in studies conducted in Europe or the Americas compared with Asia (**Supplementary Figure 10.13C**). However, the stratification of IL-10 studies, based on the covariate city, revealed greater heterogeneity among studies conducted in Wuhan ($P < 0.001$, I^2 = 36.10%) compared with other cities ($P < 0.001$, I^2 = 26.39%) (**Supplementary Figure 10.21A**). In addition, the meta-regression analysis showed that 10.91% of heterogeneity could be explained by the selected covariate (city) (**Supplementary Figure 10.21B**) and the effect size increase in studies conducted in Wuhan compared with other cities (**Supplementary Figure 10.21C**).

The total number of included studies was insufficient to perform a subgroup analysis focusing on mortality. However, between-study variability was measured for CD4/CD8 T-cell and IL-10 studies. For CD4 T-cells, the stratification of studies based on the covariate (classification protocol) revealed more heterogeneity among studies conducted following the WHO NCP or CDC guidelines ($P < 0.001$, I^2 = 37.41%) in comparison to those following national or local guidelines ($P < 0.001$, I^2 = 0.00%) (**Supplementary Figure 10.35A**). The analysis revealed that 100% of heterogeneity could be explained by the selected covariate (classification protocol) (**Supplementary Figure 10.35B**) and the effect size increase in studies conducted following WHO NCP or CDC guidelines compared with those following national or local guidelines (**Supplementary Figure 10.35C**). Stratification of CD8 T-cell studies based on the covariate (total number of male/female patients) revealed homogeneity among studies conducted in studies when the total number of male/female patients is (<50) ($P < 0.001$, I^2 = 0.00%) or (>50) ($P < 0.001$, I^2 = 0.00%) (**Supplementary Figures 10.47A**, **10.48A**). Furthermore, the meta-regression analysis revealed that 100% of the heterogeneity was explained by the selected covariate (total number of male/female patients) (**Supplementary Figures 10.47B, 10.48B**), and the effect size decrease in studies when the number of male/female patients is (>50) compared with those (<50) (**Supplementary Figures 10.47C, 10.48C**). Moreover, the stratification of IL-10 studies, based on the covariate (mean age), revealed greater heterogeneity among studies when the mean age of patients is (>60) ($P < 0.001$, I^2 = 82.18%) compared with those (<60) ($P < 0.001$, I^2 = 0.00%) (**Supplementary Figure 10.59A**). The analysis revealed that 44.16% of heterogeneity could be explained by the selected covariate (mean age) (**Supplementary Figure 10.59B**) and the effect size decrease in studies when the mean age of patients is (>60) compared with those (<60) (**Supplementary Figure 10.59C**).

Small Study Effects and Publication Bias

Where heterogeneity was due to small study effects or publication bias, funnel plots were constructed to compare COVID-19 severity and mortality studies. In addition, the regression-based Egger test (using study-level covariates) and the non-parametric rank correlation (Begg) test were performed to statistically evaluate the funnel plot symmetry. Visual inspection of the funnel plot for CD4 T-cell severity studies suggested symmetrical distribution among included studies (**Supplementary Figure 11.1A**). The regression-based Egger's test with study-level covariates showed no evidence of small study effects or publication bias ($P >$ 0.1) (**Supplementary Figure 11.1B**), a finding supported by the non-parametric rank correlation Begg's test ($P > 0.05$) (**Supplementary Figure 11.1C**). Funnel plot symmetry was also confirmed by the non-parametric trim and fill analysis that revealed no missing studies (**Figure 7A**). Similarly, visual inspection of the funnel plot for CD8 T-cell severity studies suggested symmetrical distribution among the studies (**Supplementary Figure 11.2A**). The regression-based Egger's test with study-level covariates indicated no small study effects or publication bias ($P >$ 0.1) (**Supplementary Figure 11.2B**), along with the non-parametric rank correlation Begg's test ($P >$ 0.05) (**Supplementary Figure 11.2C**). Funnel plot symmetry was also confirmed by the non-parametric trim and fill analysis that revealed no missing studies (**Figure 7B**). In contrast, visual inspection of the funnel plot for IL-10 severity studies suggested asymmetrical distribution among included studies (**Supplementary Figure 11.3A**), and the regression-based Egger's test with study-level covariates indicated small study effects or publication bias ($P<.1$) (**Supplementary Figure 11.3B**). Although the non-parametric rank correlation Begg's test revealed no evidence of small study effects or publication bias ($P > 0.05$) (**Supplementary Figure 11.3C**), funnel plot asymmetry was confirmed by the non-parametric trim and fill analysis that revealed four missing studies. However, the overall effect size did not vary greatly with the addition of the four imputed studies (observed SMD = 0.644, 95% CI = 0.547 to 0.741 and observed + imputed SMD = 0.605, 95% = 0.503 to 0.707) (**Figure 7C**).

Visual inspection of the funnel plot for CD4/CD8 T-cell and IL-10 mortality studies suggested symmetrical distribution among included studies (**Supplementary Figures 11.4A, 11.5A, 11.6A**). The regression-based Egger's test with study-level covariates showed no evidence of small study effects or publication bias ($P >$ 0.1) (**Supplementary Figures 11.4B, 11.5B, 11.6B**), a finding supported by the nonparametric rank correlation Begg's test ($P >$ 0.05) (**Supplementary Figures 11.4C, 11.5C, 11.6C**). Funnel plot symmetry for CD4/CD8 T-cell and IL-10 mortality studies was also confirmed by the non-parametric trim and fill analysis that revealed no missing studies (**Figures 8A–C**).

Meta-Analysis Sensitivity Test

We conducted a Leave-One-Out sensitivity analysis to compare mild vs. severe cases and for comparison between survivors vs. non-survivors. Results from each study in the severity group contributed similarly to the overall results for the combined effect size [SMD = −0.52 to −0.58 for CD4 T-cell studies (**Supplementary Figure 12.1**), SMD = −0.50 to −0.56 for CD8 T-cell studies (**Supplementary Figure 12.2**), and SMD = 0.65 to 0.63 for IL-10 studies (**Supplementary Figure 12.3**)].

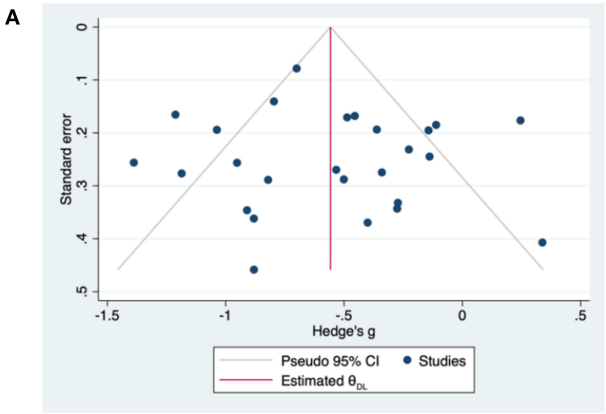

Iteration — Number of studies = 26
Model: Random-effects — observed = 26
Method: DerSimonian-Laird — imputed = 0

Pooling
Model: Random-effects
Method: DerSimonian-Laird

Studies	Hedge's g	[95% conf.	interval]
Observed	-0.557	-0.721	-0.394
Observed + Imputed	-0.557	-0.721	-0.394

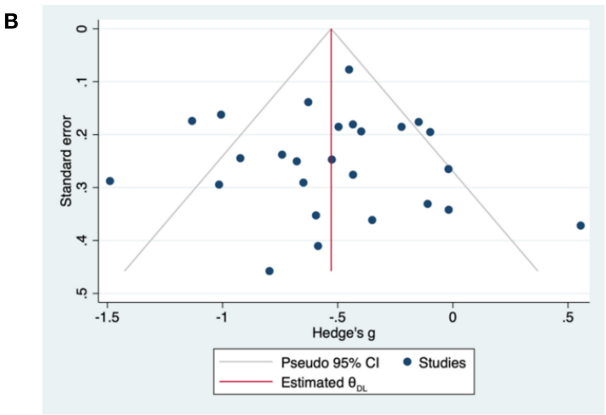

Iteration — Number of studies = 26
Model: Random-effects — observed = 26
Method: DerSimonian-Laird — imputed = 0

Pooling
Model: Random-effects
Method: DerSimonian-Laird

Studies	Hedge's g	[95% conf.	interval]
Observed	-0.528	-0.671	-0.386
Observed + Imputed	-0.528	-0.671	-0.386

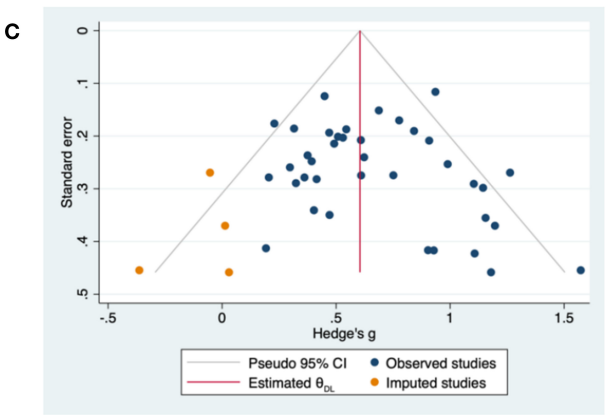

Iteration — Number of studies = 42
Model: Random-effects — observed = 38
Method: DerSimonian-Laird — imputed = 4

Pooling
Model: Random-effects
Method: DerSimonian-Laird

Studies	Hedge's g	[95% conf.	interval]
Observed	0.644	0.547	0.741
Observed + Imputed	0.605	0.503	0.707

FIGURE 7 | Non-parametric trim and fill funnel plot analysis of publication bias for CD4/CD8 T-cells and IL-10 in COVID-19 severity studies. **(A)** CD4 T-cells in COVID-19 severity studies. **(B)** CD8 T-cells in COVID-19 severity studies. **(C)** IL-10 in COVID-19 severity studies. Observed studies (blue). Imputed studies (orange).

Results from each study in the mortality group contributed similarly to the overall result of the combined effect size [SMD = −0.70 to −0.77 for CD4 T-cell studies (**Supplementary Figure 12.4**), (SMD = −0.32 to −0.63 for CD8 T-cell studies (**Supplementary Figure 12.5**), and SMD = 0.82 to 0.69 for IL-10 studies (**Supplementary Figure 12.6**)].

DISCUSSION

The SARS-CoV-2 infection continues to spread globally, with millions of lives lost and many individuals at high risk of developing serious or life-threatening complications. Although vaccines can effectively reduce risks associated with SARS-CoV-2, new variants have been identified worldwide that may challenge the effectiveness of current vaccines (107–109). In addition, vaccination may not be a feasible option for immunocompromised patients or in cases where infection precedes vaccination. Therefore, examining the underlying pathophysiological manifestations of SARS-CoV-2 infection within its human host, as reflected in the resulting clinical picture and laboratory parameters, is paramount to our ability to prevent

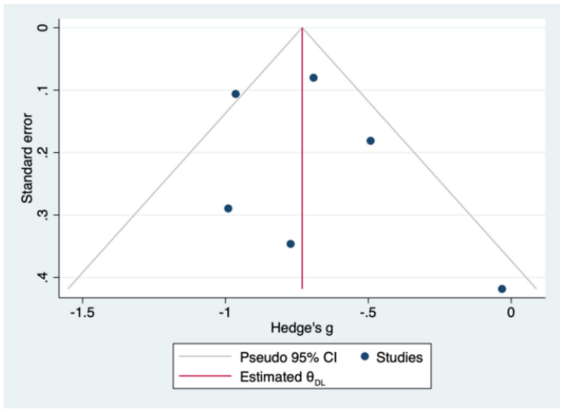


```
Iteration                              Number of studies =      6
  Model: Random-effects                         observed =      6
 Method: DerSimonian-Laird                      imputed  =      0

Pooling
  Model: Random-effects
 Method: DerSimonian-Laird
```

Studies	Hedge's g	[95% conf.	interval]
Observed	-0.731	-0.936	-0.527
Observed + Imputed	-0.731	-0.936	-0.527

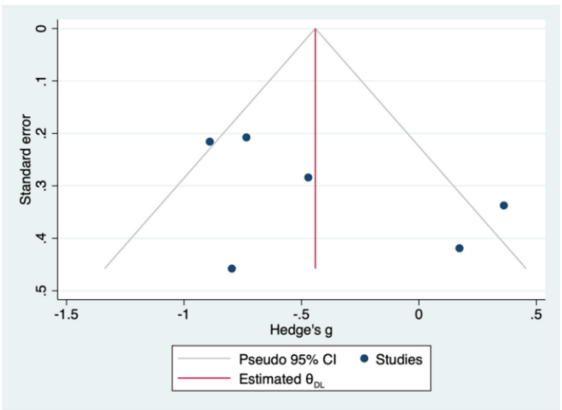


```
Iteration                              Number of studies =      6
  Model: Random-effects                         observed =      6
 Method: DerSimonian-Laird                      imputed  =      0

Pooling
  Model: Random-effects
 Method: DerSimonian-Laird
```

Studies	Hedge's g	[95% conf.	interval]
Observed	-0.441	-0.839	-0.043
Observed + Imputed	-0.441	-0.839	-0.043

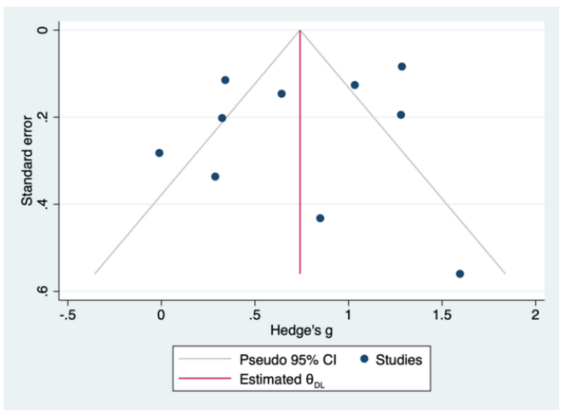


```
Iteration                              Number of studies =     10
  Model: Random-effects                         observed =     10
 Method: DerSimonian-Laird                      imputed  =      0

Pooling
  Model: Random-effects
 Method: DerSimonian-Laird
```

Studies	Hedge's g	[95% conf.	interval]
Observed	0.741	0.421	1.061
Observed + Imputed	0.741	0.421	1.061

FIGURE 8 | Non-parametric trim and fill funnel plot analysis of publication bias for CD4/CD8 T-cells and IL-10 in COVID-19 mortality studies. **(A)** CD4 T-cells in COVID-19 mortality studies. **(B)** CD8 T-cells in COVID-19 mortality studies. **(C)** IL-10 in COVID-19 mortality studies. Observed studies (blue). Imputed studies (orange).

disease progression or mortality in the present time and the future.

Lymphocytopenia is a common outcome among COVID-19 patients, observed mainly as decreased counts of CD4 and CD8 T-cells (26, 96, 110–112). Several studies have shown that patients with recovered T-cell counts experience improvement in their health status, while the condition of patients with non-recovered T-cell counts worsens and sometimes leads to death (110, 113). Thus, the main objective of this review was to assess the magnitude of this immunodepression and its role in enabling the early identification of mild and severe COVID-19 cases and potential survivor and non-survivor cases. Elucidating the influence of SARS-CoV-2 infection on host immunity among COVID-19 cases allows for a better understanding of the disease course and intervention needed during the early phase following infection.

Our meta-analysis shows that COVID-19 alters the status of human host immunity by driving the depression of adaptive immunity, manifesting in the lower counts of CD4 and CD8 T-cells more evident in severe and non-survivor cases. This

observation aligns with recent systematic reviews and meta-analyses in which T-cell subsets were also reduced (114–121). The immune system's ability to overcome the disease by reversing immunosuppression is critical, considering that our systematic review and meta-analysis have shown that mild cases and survivors exhibit a slight depression or possibly recovered T-cell counts compared with severe cases or non-survivors. T-cells play a crucial role in adaptive immunity, essential for fighting infection. Several lines of evidence reveal that in COVID-19, innate immunity is mainly responsible for inducing the inflammation observed following infection with SARS-CoV-2. This translates into a cytokine storm prevalent among patients diagnosed with COVID-19. However, adaptive immunity is essential for virus recognition and immunity against subsequent infection. The fact that this arm of the immune system is paralyzed following infection with SARS-CoV-2 indicates that host ability to produce specific immunity against the virus is compromised. Furthermore, the initiation of the adaptive immune response requires the CD4 T-cells to recognize viral-associated antigens necessary to initiate recognition through antigen-presenting cells (APCs) (122). Similarly, viral clearance through cytotoxic CD8 T-cells is critical following viral infections (123, 124). However, if the very tool that enables antigen recognition and viral clearance is downregulated, the whole arm of adaptive immunity may be affected. This clinical picture is noticed in COVID-19 patients, as described by the cumulative studies in our meta-analysis showing that following infection with SARS-CoV-2, CD4, and CD8 T-cell counts are reduced.

Several mechanisms have been put forward to explain the reduced T-cell counts observed in COVID-19 patients, which may be due to direct infection of T-cells with SARS-CoV-2, impaired T-cell proliferation and activation, T-cell exhaustion and apoptosis, or as a consequence of excessive production of inflammatory cytokines (33, 93, 125–129). Moreover, several cytokines have been found to inversely correlate with T-cell counts in COVID-19, including IL-10, suggesting a possible involvement in T-cell reduction following infection with SARS-CoV-2 (33). This aligns with the fact that during viral infections, the secretion of IL-10 has been found to inhibit the expression of major histocompatibility class II (MHC II) and co-stimulatory molecules CD80 and CD86 on APCs. This restricts CD4 T-cells' ability to recognize viral antigens, and as a consequence CD8 T-cells lose the activation signals initiated by CD4 T-cells (124, 130, 131).

In addition, studies in our meta-analysis revealed that IL-10 concentration is increased following SARS-CoV-2 infection, suggesting that IL-10 may function as a predictor of patients' clinical status and survival. Our meta-analysis results show that IL-10 is increased in severe cases and non-survivors relative to mild or survivor COVID-19 cases. This observation has also been recorded in similar systematic reviews and meta-analysis studies conducted with COVID-19 confirmed patients. Their IL-10 levels were also increased following infection with SARS-CoV-2 (115–117, 119, 120, 132, 133). IL-10 downregulates an exacerbated immune response or excessive inflammation as an anti-inflammatory cytokine (134, 135). However, in COVID-19, IL-10 is associated with severe cases and mortality because the cytokine storm intensifies. Thus, as a counterbalancing cytokine, IL-10 should facilitate the recovery from the cytokine storm initiated primarily through the secretion of IL-6, given that several lines of evidence indicate the involvement of IL-6 in the cytokine storm following SARS-CoV-2 infection (25, 136). Interestingly, IL-6 and IL-10 are increased among severe and non-survivor COVID-19 cases (25). This may indicate that in COVID-19, IL-10 enhances the pro-inflammatory environment. Further, IL-10 inhibits the activation of adaptive immunity by suppressing the function of antigen recognition on APCs, pointing to the possible role of IL-10 as the main driver of the immunosuppression observed in patients with COVID-19. However, more research is needed to verify this hypothesis.

CONCLUSION

Our systematic review and meta-analysis revealed that CD4 and CD8 T-cells are reduced in COVID-19 patients. The studies show that this reduction is more evident in the severe and non-survivor cases than in mild or survivor cases. In addition, our meta-analysis indicated that the IL-10 concentration increases, especially in the severe and non-survivor cases relative to mild or survivor cases. We conclude that the immunodepression observed following infection with SARS-CoV-2 is possibly driven by IL-10. Moreover, evidence demonstrates that the levels of CD4 and CD8 T-cells, and IL-10, are associated with severity and mortality, suggesting the importance of including such critical parameters in the routine diagnostic panel for COVID-19 patients as predictors of severity and mortality following SARS-CoV-2 infection.

Study Limitations

This systematic review and meta-analysis investigated the levels of T-cell subsets and IL-10 in COVID-19 patients. Conclusive data are still emerging because of the relatively short time since the emergence of SARS-CoV-2. Studies that described T-cell subsets together with IL-10 were also scarce, and lymphocyte counts were sometimes reported without dissecting the subsets. These limitations made it challenging to obtain a focused larger study size. In addition, including studies published only in the English language may also have limited our results. However, we believe that the quality of our search and the data obtained could assist in understanding the COVID-19 clinical picture, consistent with the goal of collating reliable sources to aid the scientific community and health care providers in their combat against this novel disease. Nonetheless, further studies are needed to support our conclusions and findings.

DATA AVAILABILITY STATEMENT

The original contributions presented in the study are included in the article/**Supplementary Material**, further inquiries can be directed to the corresponding author.

AUTHOR CONTRIBUTIONS

AA was involved in study conceptualization, literature search, data curation, analysis and interpretation of the data, generation

of the figures, and in drafting and revising the manuscript. JA and HaA were involved in the literature search, data curation, analysis and interpretation of the data, and in revising the manuscript. KA and AA-S were involved in the data curation, analysis and interpretation of the data, and in revising the manuscript. HeA was involved in the data curation, analysis and interpretation of the data, generation of the figures, and in revising the final version of the manuscript. All authors have approved the final version of the manuscript.

FUNDING

The research project was supported by a grant from Research Centre of the Female Scientific and Medical Colleges, Deanship of Scientific Research, King Saud University.

ACKNOWLEDGMENTS

The authors acknowledge the resources and support from the research core facilities at King Saud University and Riyadh Elm University.

SUPPLEMENTARY MATERIAL

The Supplementary Material for this article can be found online at: https://www.frontiersin.org/articles/10.3389/fmed.2022.852749/full#supplementary-material

REFERENCES

1. Li Q, Guan X, Wu P, Wang X, Zhou L, Tong Y, et al. Early transmission dynamics in Wuhan, China, of novel coronavirus-infected pneumonia. *N Engl J Med.* (2020) 382:1199–207. doi: 10.1056/NEJMoa2001316
2. Gorbalenya AE, Baker SC, Baric RS, de Groot RJ, Drosten C, Gulyaeva AA, et al. The species severe acute respiratory syndrome-related coronavirus: classifying 2019-nCoV and naming it SARS-CoV-2. *Nat Microbiol.* (2020) 5:536–44. doi: 10.1038/s41564-020-0695-z
3. Zhou P, Yang XL, Wang XG, Hu B, Zhang L, Zhang W, et al. A pneumonia outbreak associated with a new coronavirus of probable bat origin. *Nature.* (2020) 579:270–3. doi: 10.1038/s41586-020-2012-7
4. CSSE. *Coronavirus COVID-19 Global Cases: The Center for Systems Science and Engineering (CSSE) at Johns Hopkins University (JHU)*. (2021). Available online at: https://gisanddata.maps.arcgis.com/apps/opsdashboard/index.html#/bda7594740fd40299423467b48e9ecf6
5. WHO. *Director-General's Opening Remarks at the Media Briefing on COVID-19*. Geneva: World Health Organization (2020).
6. ENT. *Loss of Sense of Smell as Marker of COVID-19 Infection*. London: Ear, Nose and Throat Surgery at The Royal College of Surgeons of England (2020).
7. Bagheri SH, Asghari A, Farhadi M, Shamshiri AR, Kabir A, Kamrava SK, et al. Coincidence of COVID-19 epidemic and olfactory dysfunction outbreak in Iran. *Med J Islam Repub Iran.* (2020) 34:62. doi: 10.1101/2020.03.23.20041889
8. Kaye R, Chang CWD, Kazahaya K, Brereton J, Denneny JC III. COVID-19 anosmia reporting tool: initial findings. *Otolaryngol Head Neck Surg.* (2020) 163:132–4. doi: 10.1177/0194599820922992
9. Guan W-j, Ni Z-y, Hu Y, Liang W-h, Ou C-q, He J-x, et al. Clinical characteristics of coronavirus disease 2019 in China. *N Engl J Med.* (2020) 382:1708–20. doi: 10.1056/NEJMoa2002032
10. Chen N, Zhou M, Dong X, Qu J, Gong F, Han Y, et al. Epidemiological and clinical characteristics of 99 cases of 2019 novel coronavirus pneumonia in Wuhan, China: a descriptive study. *Lancet.* (2020) 395:507–13. doi: 10.1016/S0140-6736(20)30211-7
11. Zhu N, Zhang D, Wang W, Li X, Yang B, Song J, et al. A novel coronavirus from patients with pneumonia in China, 2019. *N Engl J Med.* (2020) 382:727–33. doi: 10.1056/NEJMoa2001017
12. Hui DS, Azhar EI, Madani TA, Ntoumi F, Kock R, Dar O, et al. The continuing 2019-nCoV epidemic threat of novel coronaviruses to global health - the latest 2019 novel coronavirus outbreak in Wuhan, China. *Int J Infect Dis.* (2020) 91:264–6. doi: 10.1016/j.ijid.2020.01.009
13. Lee PI, Hsueh PR. Emerging threats from zoonotic coronaviruses-from SARS and MERS to 2019-nCoV. *J Microbiol Immunol Infect.* (2020) 53:365–7. doi: 10.1016/j.jmii.2020.02.001
14. Lauer SA, Grantz KH, Bi Q, Jones FK, Zheng Q, Meredith HR, et al. The incubation period of coronavirus disease 2019 (COVID-19) from publicly reported confirmed cases: estimation and application. *Ann Intern Med.* (2020) 172:577–82. doi: 10.7326/M20-0504
15. Wang Y, Wang Y, Chen Y, Qin Q. Unique epidemiological and clinical features of the emerging 2019 novel coronavirus pneumonia (COVID-19) implicate special control measures. *J Med Virol.* (2020) 92:568–76. doi: 10.1002/jmv.25748
16. Liu Y, Gayle AA, Wilder-Smith A, Rocklöv J. The reproductive number of COVID-19 is higher compared to SARS coronavirus. *J Travel Med.* (2020) 27:taaa021. doi: 10.1093/jtm/taaa021
17. Wu JT, Leung K, Bushman M, Kishore N, Niehus R, de Salazar PM, et al. Estimating clinical severity of COVID-19 from the transmission dynamics in Wuhan, China. *Nat Med.* (2020) 26:506–10. doi: 10.1038/s41591-020-0822-7
18. Zhao S, Lin Q, Ran J, Musa SS, Yang G, Wang W, et al. Preliminary estimation of the basic reproduction number of novel coronavirus (2019-nCoV) in China, from 2019 to 2020: A data-driven analysis in the early phase of the outbreak. *Int J Infect Dis.* (2020) 92:214–7. doi: 10.1016/j.ijid.2020.01.050
19. Carissimo G, Xu W, Kwok I, Abdad MY, Chan Y-H, Fong S-W, et al. Whole blood immunophenotyping uncovers immature neutrophil-to-VD2 T-cell ratio as an early marker for severe COVID-19. *Nat Commun.* (2020) 11:5243. doi: 10.1038/s41467-020-19080-6
20. Gao M, Liu Y, Guo M, Wang Q, Wang Y, Fan J, et al. Regulatory CD4(+) and CD8(+) T cells are negatively correlated with CD4(+) /CD8(+) T cell ratios in patients acutely infected with SARS-CoV-2. *J Leukoc Biol.* (2020) 109:91–7. doi: 10.1002/JLB.5COVA0720-421RR
21. Guan J, Wei X, Qin S, Liu X, Jiang Y, Chen Y, et al. Continuous tracking of COVID-19 patients' immune status. *Int Immunopharmacol.* (2020) 89(Pt. A):107034. doi: 10.1016/j.intimp.2020.107034
22. Hue S, Beldi-Ferchiou A, Bendib I, Surenaud M, Fourati S, Frapard T, et al. Uncontrolled innate and impaired adaptive immune responses in patients with COVID-19 ARDS. *Am J Respir Crit Care Med.* (2020) 202:1509–19. doi: 10.1164/rccm.202005-1885OC
23. Liu J, Li S, Liu J, Liang B, Wang X, Wang H, et al. Longitudinal characteristics of lymphocyte responses and cytokine profiles in the peripheral blood of SARS-CoV-2 infected patients. *EBioMedicine.* (2020) 55:102763. doi: 10.1016/j.ebiom.2020.102763
24. Xu B, Fan CY, Wang AL, Zou YL, Yu YH, He C, et al. Suppressed T cell-mediated immunity in patients with COVID-19: a clinical retrospective study in Wuhan, China. *J Infect.* (2020) 81:e51–60. doi: 10.1016/j.jinf.2020.04.012
25. Zou L, Dai L, Zhang Y, Fu W, Gao Y, Zhang Z, et al. Clinical characteristics and risk factors for disease severity and death in patients with coronavirus disease 2019 in Wuhan, China. *Front Med.* (2020) 7:532. doi: 10.3389/fmed.2020.00532
26. Huang C, Wang Y, Li X, Ren L, Zhao J, Hu Y, et al. Clinical features of patients infected with 2019 novel coronavirus in Wuhan, China. *Lancet.* (2020) 395:497–506. doi: 10.1016/S0140-6736(20)30183-5

27. Li X, Liu Y, Li J, Sun L, Yang J, Xu F, et al. Immune characteristics distinguish patients with severe disease associated with SARS-CoV-2. *Immunol Res.* (2020) 68:398–404. doi: 10.1007/s12026-020-09156-2
28. Tang Y, Li Y, Sun J, Pan H, Yao F, Jiao X. Selection of an optimal combination panel to better triage COVID-19 hospitalized patients. *J Inflamm Res.* (2020) 13:773–87. doi: 10.2147/JIR.S273193
29. Gan J, Li J, Li S, Yang C. Leucocyte subsets effectively predict the clinical outcome of patients with COVID-19 pneumonia: a retrospective case-control study. *Front Public Health.* (2020) 8:299. doi: 10.3389/fpubh.2020.00299
30. Chi Y, Ge Y, Wu B, Zhang W, Wu T, Wen T, et al. Serum cytokine and chemokine profile in relation to the severity of coronavirus disease 2019 in China. *J Infect Dis.* (2020) 222:746–54. doi: 10.1093/infdis/jiaa363
31. Keddie S, Ziff O, Chou MKL, Taylor RL, Heslegrave A, Garr E, et al. Laboratory biomarkers associated with COVID-19 severity and management. *Clin Immunol.* (2020) 221:108614. doi: 10.1016/j.clim.2020.108614
32. Zhao Y, Qin L, Zhang P, Li K, Liang L, Sun J, et al. Longitudinal COVID-19 profiling associates IL-1RA and IL-10 with disease severity and RANTES with mild disease. *JCI Insight.* (2020) 5:e139834. doi: 10.1172/jci.insight.139834
33. Diao B, Wang C, Tan Y, Chen X, Liu Y, Ning L, et al. Reduction and functional exhaustion of T cells in patients with coronavirus disease 2019 (COVID-19). *Front Immunol.* (2020) 11:827. doi: 10.3389/fimmu.2020.00827
34. Moher D, Liberati A, Tetzlaff J, Altman DG, The PG. Preferred reporting items for systematic reviews and meta-analyses: the PRISMA statement. *PLoS Med.* (2009) 6:e1000097. doi: 10.1371/journal.pmed.1000097
35. Stroup DF, Berlin JA, Morton SC, Olkin I, Williamson GD, Rennie D, et al. Meta-analysis of observational studies in epidemiology: a proposal for reporting. Meta-analysis Of Observational Studies in Epidemiology (MOOSE) group. *JAMA.* (2000) 283:2008–12. doi: 10.1001/jama.283.15.2008
36. Alshammary H, Alshammary H. T-cell subsets and interleukin-10 levels are predictors of severity and mortality in COVID-19: a systematic review and metananalysis. PROSPERO (2020). Available online at: https://www.crd.york.ac.uk/prospero/display_record.php?ID=CRD42020218918
37. Richardson WS, Wilson MC, Nishikawa J, Hayward RS. The well-built clinical question: a key to evidence-based decisions. *ACP J Club.* (1995) 123:A12–3. doi: 10.7326/ACPJC-1995-123-3-A12
38. Saaiq M, Ashraf B. Modifying "Pico" question into "Picos" model for more robust and reproducible presentation of the methodology employed in a scientific study. *World J Plast Surg.* (2017) 6:390–2.
39. WHO. *Clinical Management of COVID-19*. WHO Headquarters (HQ) (2020).
40. EndNote. *EndNote X9*. Philadelphia, PA: Clarivate (2013).
41. Cheng S, Augustin C, Bethel A, Gill D, Anzaroot S, Brun J, et al. Using machine learning to advance synthesis and use of conservation and environmental evidence. *Conserv Biol.* (2018) 32:762–4. doi: 10.1111/cobi.13117
42. Microsoft. *Microsoft Excel for Mac*. Microsoft Corporation (2020).
43. Rohatgi A. *WebPlotDigitizer. Web Based Tool to Extract Data From Plots, Images, and Maps*. Version 4.4 Released. Pacifica, CA (2020). Available online at: https://automeris.io/WebPlotDigitizer/
44. Peterson J, Welch V, Losos M, Tugwell P. *The Newcastle-Ottawa Scale (NOS) for Assessing the Quality of Nonrandomised Studies in Meta-Analyses*. Ottawa, ON: Ottawa Hospital Research Institute (2011).
45. Wan X, Wang W, Liu J, Tong T. Estimating the sample mean and standard deviation from the sample size, median, range and/or interquartile range. *BMC Med Res Methodol.* (2014) 14:135. doi: 10.1186/1471-2288-14-135
46. Higgins JPT, Chandler J, Cumpston M, Li T, Page M, Welch V. (eds.). *Cochrane Handbook for Systematic Reviews of Interventions* Cochrane (2020). Available online at: www.training.cochrane.org/handbook
47. DerSimonian R, Laird N. Meta-analysis in clinical trials. *Control Clin Trials.* (1986) 7:177–88. doi: 10.1016/0197-2456(86)90046-2
48. Hedges LV, Olkin I. *Statistical Methods for Meta-Analysis*. Orlando, FL: Academic Press (2014).
49. Lakens D. Calculating and reporting effect sizes to facilitate cumulative science: a practical primer for t-tests and ANOVAs. *Front Psychol.* (2013) 4:863. doi: 10.3389/fpsyg.2013.00863
50. STATA. *Stata Statistical Software: Release 17*. College Station, TX: StataCorp LLC (2021).
51. Higgins JP, Thompson SG. Quantifying heterogeneity in a meta-analysis. *Stat Med.* (2002) 21:1539–58. doi: 10.1002/sim.1186
52. Higgins JP, Thompson SG, Deeks JJ, Altman DG. Measuring inconsistency in meta-analyses. *BMJ.* (2003) 327:557–60. doi: 10.1136/bmj.327.7414.557
53. Galbraith RF. A note on graphical presentation of estimated odds ratios from several clinical trials. *Stat Med.* (1988) 7:889–94. doi: 10.1002/sim.4780070807
54. Berkey CS, Hoaglin DC, Mosteller F, Colditz GA. A random-effects regression model for meta-analysis. *Stat Med.* (1995) 14:395–411. doi: 10.1002/sim.4780140406
55. Thompson SG, Higgins JP. How should meta-regression analyses be undertaken and interpreted? *Stat Med.* (2002) 21:1559–73. doi: 10.1002/sim.1187
56. Thompson SG, Sharp SJ. Explaining heterogeneity in meta-analysis: a comparison of methods. *Stat Med.* (1999) 18:2693–708.
57. Light RJ, Pillemer DB. Summing Up: The Science of Reviewing Research Harvard University Press: Cambridge, MA. (1984) xiii+191 pp. *Educ Res.* (1986) 15:16–7.
58. Sterne JAC, Becker BJ, Egger M. *The Funnel Plot. Publication Bias in Meta-Analysis*. New York, NY: Wiley (2005). p. 73–98.
59. Duval S, Tweedie R. Trim and fill: a simple funnel-plot-based method of testing and adjusting for publication bias in meta-analysis. *Biometrics.* (2000) 56:455–63. doi: 10.1111/j.0006-341X.2000.00455.x
60. Duval S, Tweedie R. A nonparametric "Trim and Fill" method of accounting for publication bias in meta-analysis. *J Am Stat Assoc.* (2000) 95:89–98. doi: 10.1080/01621459.2000.10473905
61. Lin L, Chu H. Quantifying publication bias in meta-analysis. *Biometrics.* (2018) 74:785–94. doi: 10.1111/biom.12817
62. Egger M, Davey Smith G, Schneider M, Minder C. Bias in meta-analysis detected by a simple, graphical test. *BMJ.* (1997) 315:629–34. doi: 10.1136/bmj.315.7109.629
63. Begg CB, Mazumdar M. Operating characteristics of a rank correlation test for publication bias. *Biometrics.* (1994) 50:1088–101. doi: 10.2307/2533446
64. Harrer M, Cuijpers P, Furukawa T, Ebert D. *Doing Meta-Analysis with R: A Hands-on Guide*. Boca Raton, FL; London: Chapman & Hall/CRC Press (2019).
65. Abers MS, Delmonte OM, Ricotta EE, Fintzi J, Fink DL, de Jesus AAA, et al. An immune-based biomarker signature is associated with mortality in COVID-19 patients. *JCI Insight.* (2021) 6:e144455. doi: 10.1172/jci.insight.144455
66. Azmy V, Kaman K, Tang D, Zhao H, Dela Cruz C, Topal JE, et al. Cytokine profiles before and after immune modulation in hospitalized patients with COVID-19. *J Clin Immunol.* (2021) 41:738–47. doi: 10.1007/s10875-020-00949-6
67. Cantenys-Molina S, Fernández-Cruz E, Francos P, Lopez Bernaldo de Quirós JC, Muñoz P, Gil-Herrera J. Lymphocyte subsets early predict mortality in a large series of hospitalized COVID-19 patients in Spain. *Clin Exp Immunol.* (2021) 203:424–32. doi: 10.1111/cei.13547
68. Chen J, Han T, Huang M, Yang Y, Shang F, Zheng Y, et al. Clinical characteristics of asymptomatic carriers of novel coronavirus disease 2019: a multi-center study in Jiangsu Province. *Virulence.* (2020) 11:1557–68. doi: 10.1080/21505594.2020.1840122
69. Deng F, Zhang L, Lyu L, Lu Z, Gao D, Ma X, et al. Increased levels of ferritin on admission predicts intensive care unit mortality in patients with COVID-19. *Med Clin.* (2021) 156:324–31. doi: 10.1016/j.medcli.2020.11.030
70. Flament H, Rouland M, Beaudoin L, Toubal A, Bertrand L, Lebourgeois S, et al. Outcome of SARS-CoV-2 infection is linked to MAIT cell activation and cytotoxicity. *Nat Immunol.* (2021) 22:322–35. doi: 10.1038/s41590-021-00870-z
71. Gadotti AC, de Castro Deus M, Telles JP, Wind R, Goes M, Garcia Charello Ossoski R, et al. IFN-gamma is an independent risk factor associated with mortality in patients with moderate and severe COVID-19 infection. *Virus Res.* (2020) 289:198171. doi: 10.1016/j.virusres.2020.198171
72. Han H, Ma Q, Li C, Liu R, Zhao L, Wang W, et al. Profiling serum cytokines in COVID-19 patients reveals IL-6 and IL-10 are

disease severity predictors. *Emerg Microbes Infect.* (2020) 9:1123–30. doi: 10.1080/22221751.2020.1770129
73. He B, Wang J, Wang Y, Zhao J, Huang J, Tian Y, et al. The metabolic changes and immune profiles in patients with COVID-19. *Front Immunol.* (2020) 11:2075. doi: 10.3389/fimmu.2020.02075
74. He S, Zhou C, Lu D, Yang H, Xu H, Wu G, et al. Relationship between chest CT manifestations and immune response in COVID-19 patients. *Int J Infect Dis.* (2020) 98:125–9. doi: 10.1016/j.ijid.2020.06.059
75. Henry BM, Benoit SW, Vikse J, Berger BA, Pulvino C, Hoehn J, et al. The anti-inflammatory cytokine response characterized by elevated interleukin-10 is a stronger predictor of severe disease and poor outcomes than the pro-inflammatory cytokine response in coronavirus disease 2019 (COVID-19). *Clin Chem Lab Med.* (2021) 59:599–607. doi: 10.1515/cclm-2020-1284
76. Huang H, Zhang M, Chen C, Zhang H, Wei Y, Tian J, et al. Clinical characteristics of COVID-19 in patients with preexisting ILD: a retrospective study in a single center in Wuhan, China. *J Med Virol.* (2020) 92:2742–50. doi: 10.1002/jmv.26174
77. Huang W, Li M, Luo G, Wu X, Su B, Zhao L, et al. The inflammatory factors associated with disease severity to predict COVID-19 progression. *J Immunol.* (2021) 206:1597–608. doi: 10.4049/jimmunol.2001327
78. Jin XH, Zhou HL, Chen LL, Wang GF, Han QY, Zhang JG, et al. Peripheral immunological features of COVID-19 patients in Taizhou, China: a retrospective study. *Clin Immunol.* (2021) 222:108642. doi: 10.1016/j.clim.2020.108642
79. Kwon JS, Kim JY, Kim MC, Park SY, Kim BN, Bae S, et al. Factors of severity in patients with COVID-19: cytokine/chemokine concentrations, viral load, and antibody responses. *Am J Trop Med Hyg.* (2020) 103:2412–18. doi: 10.4269/ajtmh.20-1110
80. Laing AG, Lorenc A, Del Molino Del Barrio I, Das A, Fish M, Monin L, et al. A dynamic COVID-19 immune signature includes associations with poor prognosis. *Nat Med.* (2020) 26:1623–35. doi: 10.1038/s41591-020-1038-6
81. Li C, Jiang J, Wang F, Zhou N, Veronese G, Moslehi JJ, et al. Longitudinal correlation of biomarkers of cardiac injury, inflammation, and coagulation to outcome in hospitalized COVID-19 patients. *J Mol Cell Cardiol.* (2020) 147:74–87. doi: 10.1016/j.yjmcc.2020.08.008
82. Li M, Guo W, Dong Y, Wang X, Dai D, Liu X, et al. Elevated exhaustion levels of NK and CD8(+) T cells as indicators for progression and prognosis of COVID-19 disease. *Front Immunol.* (2020) 11:580237. doi: 10.3389/fimmu.2020.580237
83. Li Q, Xu W, Li WX, Huang CL, Chen L. Dynamics of cytokines and lymphocyte subsets associated with the poor prognosis of severe COVID-19. *Eur Rev Med Pharmacol Sci.* (2020) 24:12536–44. doi: 10.26355/eurrev_202012_24051
84. Liao B, Liu Z, Tang L, Li L, Gan Q, Shi H, et al. Longitudinal clinical and radiographic evaluation reveals interleukin-6 as an indicator of persistent pulmonary injury in COVID-19. *Int J Med Sci.* (2021) 18:29–41. doi: 10.7150/ijms.49728
85. Liu F, Ji C, Luo J, Wu W, Zhang J, Zhong Z, et al. Clinical characteristics and corticosteroids application of different clinical types in patients with corona virus disease 2019. *Sci Rep.* (2020) 10:13689. doi: 10.1038/s41598-020-70387-2
86. Liu J, Dong YQ, Yin J, He G, Wu X, Li J, et al. Critically ill patients with COVID-19 with ECMO and artificial liver plasma exchange: a retrospective study. *Medicine.* (2020) 99:e21012. doi: 10.1097/MD.0000000000021012
87. Liu L, Zheng Y, Cai L, Wu W, Tang S, Ding Y, et al. Neutrophil-to-lymphocyte ratio, a critical predictor for assessment of disease severity in patients with COVID-19. *Int J Lab Hematol.* (2020) 43:329–35. doi: 10.1111/ijlh.13374
88. Liu X-Q, Xue S, Xu J-B, Ge H, Mao Q, Xu X-H, et al. Clinical characteristics and related risk factors of disease severity in 101 COVID-19 patients hospitalized in Wuhan, China. *Acta Pharmacol Sin.* (2021) 43:64–75. doi: 10.1038/s41401-021-00627-2
89. Liu Y, Tan W, Chen H, Zhu Y, Wan L, Jiang K, et al. Dynamic changes in lymphocyte subsets and parallel cytokine levels in patients with severe and critical COVID-19. *BMC Infect Dis.* (2021) 21:79. doi: 10.1186/s12879-021-05792-7
90. Luo M, Liu J, Jiang W, Yue S, Liu H, Wei S. IL-6 and CD8+ T cell counts combined are an early predictor of in-hospital mortality of patients with COVID-19. *JCI Insight.* (2020) 5:e139024. doi: 10.1172/jci.insight.139024
91. Mann ER, Menon M, Knight SB, Konkel JE, Jagger C, Shaw TN, et al. Longitudinal immune profiling reveals key myeloid signatures associated with COVID-19. *Sci Immunol.* (2020) 5:eabd6197. doi: 10.1126/sciimmunol.abd6197
92. McElvaney OJ, McEvoy NL, McElvaney OF, Carroll TP, Murphy MP, Dunlea DM, et al. Characterization of the inflammatory response to severe COVID-19 illness. *Am J Respir Crit Care Med.* (2020) 202:812–21. doi: 10.1164/rccm.202005-1583OC
93. Rendeiro AF, Casano J, Vorkas CK, Singh H, Morales A, DeSimone RA, et al. Profiling of immune dysfunction in COVID-19 patients allows early prediction of disease progression. *Life Sci Alliance.* (2021) 4:e202000955. doi: 10.26508/lsa.202000955
94. Schrijver B, Assmann J, van Gammeren AJ, Vermeulen RCH, Portengen L, Heukels P, et al. Extensive longitudinal immune profiling reveals sustained innate immune activation in COVID-19 patients with unfavorable outcome. *Eur Cytok Netw.* (2020) 31:154–67. doi: 10.1684/ecn.2020.0456
95. Shi H, Wang W, Yin J, Ouyang Y, Pang L, Feng Y, et al. The inhibition of IL-2/IL-2R gives rise to CD8(+) T cell and lymphocyte decrease through JAK1-STAT5 in critical patients with COVID-19 pneumonia. *Cell Death Dis.* (2020) 11:429. doi: 10.1038/s41419-020-2636-4
96. Tan M, Liu Y, Zhou R, Deng X, Li F, Liang K, et al. Immunopathological characteristics of coronavirus disease 2019 cases in Guangzhou, China. *Immunology.* (2020) 160:261–8. doi: 10.1111/imm.13223
97. Wang Z, Yang B, Li Q, Wen L, Zhang R. Clinical features of 69 cases with coronavirus disease 2019 in Wuhan, China. *Clin Infect Dis.* (2020) 71:769–77. doi: 10.1093/cid/ciaa272
98. Yang A-P, Li H-M, Tao W-Q, Yang X-J, Wang M, Yang W-J, et al. Infection with SARS-CoV-2 causes abnormal laboratory results of multiple organs in patients. *Aging.* (2020) 12:10059–69. doi: 10.18632/aging.103255
99. Yang F, Shi S, Zhu J, Shi J, Dai K, Chen X. Clinical characteristics and outcomes of cancer patients with COVID-19. *J Med Virol.* (2020) 92:2067–73. doi: 10.1002/jmv.25972
100. Yi P, Yang X, Ding C, Chen Y, Xu K, Ni Q, et al. Risk factors and clinical features of deterioration in COVID-19 patients in Zhejiang, China: a single-centre, retrospective study. *BMC Infect Dis.* (2020) 20:943. doi: 10.1186/s12879-020-05682-4
101. Zeng HL, Lu QB, Yang Q, Wang X, Yue DY, Zhang LK, et al. Longitudinal profile of laboratory parameters and their application in the prediction for fatal outcome among patients infected with SARS-CoV-2: a retrospective cohort study. *Clin Infect Dis.* (2020) 72:626–33. doi: 10.1093/cid/ciaa574
102. Zeng Z, Yu H, Chen H, Qi W, Chen L, Chen G, et al. Longitudinal changes of inflammatory parameters and their correlation with disease severity and outcomes in patients with COVID-19 from Wuhan, China. *Crit Care.* (2020) 24:525. doi: 10.1186/s13054-020-03255-0
103. Zhang B, Yue D, Wang Y, Wang F, Wu S, Hou H. The dynamics of immune response in COVID-19 patients with different illness severity. *J Med Virol.* (2021) 93:1070–7. doi: 10.1002/jmv.26504
104. Zhang J, Yu M, Tong S, Liu LY, Tang LV. Predictive factors for disease progression in hospitalized patients with coronavirus disease 2019 in Wuhan, China. *J Clin Virol.* (2020) 127:104392. doi: 10.1016/j.jcv.2020.104392
105. Feng X, Li P, Ma L, Liang H, Lei J, Li W, et al. Clinical characteristics and short-term outcomes of severe patients with COVID-19 in Wuhan, China. *Front Med.* (2020) 7:491. doi: 10.3389/fmed.2020.00491
106. Durand B. *(Khartis): Interim Administrator of the Institut d'études Politiques de Paris and the Fondation Nationale des Sciences Politiques*. (2021). Available online at: https://www.sciencespo.fr/cartographie/khartis/en/#home (accessed March 15, 2022).
107. Cui J, Li F, Shi ZL. Origin and evolution of pathogenic coronaviruses. *Nat Rev Microbiol.* (2019) 17:181–92. doi: 10.1038/s41579-018-0118-9
108. Woo PC, Lau SK, Yip CC, Huang Y, Tsoi HW, Chan KH, et al. Comparative analysis of 22 coronavirus HKU1 genomes reveals a novel genotype and evidence of natural recombination in coronavirus HKU1. *J Virol.* (2006) 80:7136–45. doi: 10.1128/JVI.00509-06
109. Islam MR, Hoque MN, Rahman MS, Alam ASMRU, Akther M, Puspo JA, et al. Genome-wide analysis of SARS-CoV-2 virus strains circulating worldwide implicates heterogeneity. *Sci Rep.* (2020) 10:14004. doi: 10.1038/s41598-020-70812-6

110. Lippi G, Plebani M. Laboratory abnormalities in patients with COVID-2019 infection. *Clin Chem Lab Med.* (2020) 58:1131–4. doi: 10.1515/cclm-2020-0198
111. Xu Z, Shi L, Wang Y, Zhang J, Huang L, Zhang C, et al. Pathological findings of COVID-19 associated with acute respiratory distress syndrome. *Lancet Respir Med.* (2020) 8:420–2. doi: 10.1016/S2213-2600(20)30076-X
112. Zhong Y, Cao Y, Zhong X, Peng Z, Jiang S, Tang T, et al. Immunity and coagulation/fibrinolytic processes may reduce the risk of severe illness in pregnant women with COVID-19. *Am J Obstet Gynecol.* (2020) 224:393.e1–25. doi: 10.1016/j.ajog.2020.10.032
113. Tan L, Wang Q, Zhang D, Ding J, Huang Q, Tang YQ, et al. Lymphopenia predicts disease severity of COVID-19: a descriptive and predictive study. *Signal Transduct Target Ther.* (2020) 5:33. doi: 10.1038/s41392-020-0159-1
114. Elshazli RM, Toraih EA, Elgaml A, El-Mowafy M, El-Mesery M, Amin MN, et al. Diagnostic and prognostic value of hematological and immunological markers in COVID-19 infection: a meta-analysis of 6320 patients. *PLoS ONE.* (2020) 15:e0238160. doi: 10.1371/journal.pone.0238160
115. Zhang Z, Ai G, Chen L, Liu S, Gong C, Zhu X, et al. Associations of immunological features with COVID-19 severity: a systematic review and meta-analysis. *BMC Infect Dis.* (2021) 21:738. doi: 10.1186/s12879-021-06457-1
116. Qin R, He L, Yang Z, Jia N, Chen R, Xie J, et al. Identification of parameters representative of immune dysfunction in patients with severe and fatal COVID-19 infection: a systematic review and meta-analysis. *Clin Rev Allergy Immunol.* (2022) 18:1–33. doi: 10.1007/s12016-021-08908-8
117. Mulchandani R, Lyngdoh T, Kakkar AK. Deciphering the COVID-19 cytokine storm: systematic review and meta-analysis. *Eur J Clin Invest.* (2021) 51:e13429. doi: 10.1111/eci.13429
118. Moutchia J, Pokharel P, Kerri A, McGaw K, Uchai S, Nji M, et al. Clinical laboratory parameters associated with severe or critical novel coronavirus disease 2019 (COVID-19): a systematic review and meta-analysis. *PloS ONE.* (2020) 15:e0239802. doi: 10.1371/journal.pone.0239802
119. Akbari H, Tabrizi R, Lankarani KB, Aria H, Vakili S, Asadian F, et al. The role of cytokine profile and lymphocyte subsets in the severity of coronavirus disease 2019 (COVID-19): a systematic review and meta-analysis. *Life Sci.* (2020) 258:118167. doi: 10.1016/j.lfs.2020.118167
120. Liu K, Yang T, Peng XF, Lv SM, Ye XL, Zhao TS, et al. A systematic meta-analysis of immune signatures in patients with COVID-19. *Rev Med Virol.* (2021) 31:e2195. doi: 10.1002/rmv.2195
121. Yonas E, Alwi I, Pranata R, Huang I, Lim MA, Yamin M, et al. Elevated interleukin levels are associated with higher severity and mortality in COVID 19 - a systematic review, meta-analysis, and meta-regression. *Diabetes Metab Syndr.* (2020) 14:2219–30. doi: 10.1016/j.dsx.2020.11.011
122. Rogers MC, Lamens KD, Shafagati N, Johnson M, Oury TD, Joyce S, et al. CD4(+) regulatory T cells exert differential functions during early and late stages of the immune response to respiratory viruses. *J Immunol.* (2018) 201:1253–66. doi: 10.4049/jimmunol.1800096
123. Mescher MF, Curtsinger JM, Agarwal P, Casey KA, Gerner M, Hammerbeck CD, et al. Signals required for programming effector and memory development by CD8+ T cells. *Immunol Rev.* (2006) 211:81–92. doi: 10.1111/j.0105-2896.2006.00382.x
124. Zhu J, Yamane H, Paul WE. Differentiation of effector CD4 T cell populations (*). *Ann Rev Immunol.* (2010) 28:445–89. doi: 10.1146/annurev-immunol-030409-101212
125. De Biasi S, Meschiari M, Gibellini L, Bellinazzi C, Borella R, Fidanza L, et al. Marked T cell activation, senescence, exhaustion and skewing towards TH17 in patients with COVID-19 pneumonia. *Nat Commun.* (2020) 11:3434. doi: 10.1038/s41467-020-17292-4
126. Zheng HY, Zhang M, Yang CX, Zhang N, Wang XC, Yang XP, et al. Elevated exhaustion levels and reduced functional diversity of T cells in peripheral blood may predict severe progression in COVID-19 patients. *Cell Mol Immunol.* (2020) 17:541–3. doi: 10.1038/s41423-020-0401-3
127. Alshammary AF, Al-Sulaiman AM. The journey of SARS-CoV-2 in Human Hosts: A Review of Immune Responses, Immunosuppression, and their Consequences. *Virulence.* (2021) 12:1771–94. doi: 10.1080/21505594.2021.1929800
128. Tavakolpour S, Rakhshandehroo T, Wei EX, Rashidian M. Lymphopenia during the COVID-19 infection: what it shows and what can be learned. *Immunol Lett.* (2020) 225:31–2. doi: 10.1016/j.imlet.2020.06.013
129. Tang Y, Liu J, Zhang D, Xu Z, Ji J, Wen C. Cytokine storm in COVID-19: the current evidence and treatment strategies. *Front Immunol.* (2020) 11:1708. doi: 10.3389/fimmu.2020.01708
130. Bogdan C, Vodovotz Y, Nathan C. Macrophage deactivation by interleukin 10. *J Exp Med.* (1991) 174:1549–55. doi: 10.1084/jem.174.6.1549
131. de Waal Malefyt R, Haanen J, Spits H, Roncarolo MG, te Velde A, Figdor C, et al. Interleukin 10 (IL-10) and viral IL-10 strongly reduce antigen-specific human T cell proliferation by diminishing the antigen-presenting capacity of monocytes via downregulation of class II major histocompatibility complex expression. *J Exp Med.* (1991) 174:915–24. doi: 10.1084/jem.174.4.915
132. Udomsinprasert W, Jittikoon J, Sangroongruangsri S, Chaikledkaew U. Circulating levels of interleukin-6 and interleukin-10, but not tumor necrosis factor-alpha, as potential biomarkers of severity and mortality for COVID-19: systematic review with meta-analysis. *J Clin Immunol.* (2021) 41:11–22. doi: 10.1007/s10875-020-00899-z
133. Zawawi A, Naser AY, Alwafi H, Minshawi F. Profile of circulatory cytokines and chemokines in human coronaviruses: a systematic review and meta-analysis. *Front Immunol.* (2021) 12:666223. doi: 10.3389/fimmu.2021.666223
134. Moore KW, de Waal Malefyt R, Coffman RL, O'Garra A. Interleukin-10 and the interleukin-10 receptor. *Annu Rev Immunol.* (2001) 19:683–765. doi: 10.1146/annurev.immunol.19.1.683
135. Fiorentino DF, Zlotnik A, Mosmann TR, Howard M, O'Garra A. IL-10 inhibits cytokine production by activated macrophages. *J Immunol.* (1991) 147:3815–22.
136. Zhou F, Yu T, Du R, Fan G, Liu Y, Liu Z, et al. Clinical course and risk factors for mortality of adult inpatients with COVID-19 in Wuhan, China: a retrospective cohort study. *Lancet.* (2020) 395:1054–62. doi: 10.1016/S0140-6736(20)30566-3

Conflict of Interest: The authors declare that the research was conducted in the absence of any commercial or financial relationships that could be construed as a potential conflict of interest.

Publisher's Note: All claims expressed in this article are solely those of the authors and do not necessarily represent those of their affiliated organizations, or those of the publisher, the editors and the reviewers. Any product that may be evaluated in this article, or claim that may be made by its manufacturer, is not guaranteed or endorsed by the publisher.

frontiers | Frontiers in Medicine

ORIGINAL RESEARCH
published: 21 June 2022
doi: 10.3389/fmed.2022.852973

mTOR Inhibitor Use Is Associated With a Favorable Outcome of COVID-19 in Patients of Kidney Transplant: Results of a Retrospective Study

Biagio Pinchera[1], Lorenzo Spirito[2], Antonio Riccardo Buonomo[1], Maria Foggia[1], Rosa Carrano[3], Fabrizio Salemi[3], Elisa Schettino[3], Fortuna Papa[3], Roberto La Rocca[2], Felice Crocetto[2], Luigi Napolitano[2], Riccardo Villari[1] and Ivan Gentile[1] on behalf of Federico II COVID Team*

[1] Section of Infectious Diseases, Department of Clinical Medicine and Surgery, University of Naples Federico II, Naples, Italy, [2] Section of Urology, Department of Neurosciences, Reproductive and Odontostomatological Sciences, University of Naples Federico II, Naples, Italy, [3] Section of Nephrology, Department of Public Health, University of Naples Federico II, Naples, Italy

OPEN ACCESS

Edited by:
Farid Rahimi,
Australian National University, Australia

Reviewed by:
Manfred Johannes Stangl,
Ludwig Maximilian University of Munich, Germany
Nadim Cassir,
Aix-Marseille Université, France
Nianqiao Gong,
Huazhong University of Science and Technology, China

***Correspondence:**
Biagio Pinchera
biapin89@virgilio.it

Specialty section:
This article was submitted to Infectious Diseases - Surveillance, Prevention and Treatment, a section of the journal Frontiers in Medicine

Received: 11 January 2022
Accepted: 29 April 2022
Published: 21 June 2022

Citation:
Pinchera B, Spirito L, Buonomo AR, Foggia M, Carrano R, Salemi F, Schettino E, Papa F, La Rocca R, Crocetto F, Napolitano L, Villari R and Gentile I (2022) mTOR Inhibitor Use Is Associated With a Favorable Outcome of COVID-19 in Patients of Kidney Transplant: Results of a Retrospective Study. Front. Med. 9:852973. doi: 10.3389/fmed.2022.852973

Introduction: In solid organ transplant recipients, COVID-19 is associated with a poor prognosis because of immunosuppression. Some studies suggest a potential therapeutic role of mammalian Target of Rapamycin (mTOR) inhibitors in SARS-CoV-2 infection. This study aimed to assess the impact of mTOR employment on the evolution and outcome of SARS-CoV-2 infection in solid organ transplant recipients.

Methods: We enrolled kidney transplant patients attending the Azienda Ospedaliera Universitaria Federico II in Naples and followed up on these patients from March 2020 to June 2021. We evaluated the risk of acquiring the SARS-CoV-2 infection, the clinical presentation of the disease, and its outcome together with the type of immunosuppressive therapy. Finally, we assessed the impact of mTOR inhibitors on relevant clinical metrics of SARS-CoV-2 infection.

Results: We enrolled 371 patients, of whom 56 (15.1%) contracted SARS-CoV-2 infection during the period of the study. There were no differences observed among the different immunosuppressive therapies concerning the risk of acquiring SARS-CoV-2 infection. In contrast, the type of immunosuppressive therapy had a significant impact on the outcome of the disease. In detail, patients who received mTOR inhibitors, as part of their immunosuppressive therapy, compared to other regimens had a lower chance of developing a moderate or severe form of the disease (OR = 0.8, 95, CI: (0.21–0.92), $P = 0.041$).

Conclusion: In kidney transplant patients, the use of mTOR inhibitors as part of an immunosuppressive regimen is associated with a better prognosis in the case of COVID-19.

Keywords: kidney transplant, SARS-CoV-2, COVID-19, mTOR inhibitors, immunosuppressive therapy

INTRODUCTION

Immunosuppressive therapy is a crucial aspect in a solid organ transplant patient. It is the mainstay of the prevention of rejection of the allograft, but at the same time, it contributes to determining the patient's susceptibility to several infections (1–3). Different immunosuppressive drugs, such as calcineurin inhibitors (tacrolimus and cyclosporine), corticosteroids, antimetabolite agents (mycophenolate and azathioprine), and the mammalian target Of rapamycin (mTOR) inhibitors (everolimus and sirolimus), are used to prevent rejection (4, 5). In particular, mTOR is a crucial pathway in many physiological processes (such as cell cycle progression, transcription, translation, differentiation, apoptosis, motility, and cell metabolism) and, therefore, plays a central role in the regulation of cell growth and proliferation, at the translational level, and in cell cycle progression. Moreover, as mTOR also modulates protein synthesis at ribosomal and transfer RNA transcription levels, it also plays a fundamental role in viral translation (6). It is already known that several viruses, such as adenovirus, cytomegalovirus, herpes simplex virus, and Middle East respiratory syndrome coronavirus (MERS – CoV), use the mTOR pathway to replicate (7, 8). The mTOR pathway is also involved in the life cycle of SARS-CoV-2 infection (9). The antiviral properties of mTOR have been known and ascribed to a variety of mechanisms (10). This aspect needs to be considered in relation to the pandemic impact (2–4). There are scarce data on the possible role of mTOR inhibitors vs. SARS-CoV-2 and their potential impact on the evolution of the disease; however, some studies support the potential therapeutic role of these drugs (11). Some reviews suggest the therapeutic potential of mTOR inhibitors, such as rapamycin, against COVID-19 both *in vitro* and *in vivo* (12–14).

For these reasons, blocking the mTOR signaling pathway could be a strategy to treat SARS-CoV-2 infection and its evolution. This study aimed to describe and assess the impact of the mTOR inhibitor therapy on the evolution and outcome of SARS-CoV-2 infection in solid organ transplant recipients followed in our center.

MATERIALS AND METHODS

We conducted an observational retrospective cohort study. We enrolled patients with kidney transplants attending the Azienda Ospedaliera Universitaria Federico II in Naples from March 2020 to June 2021. Diagnosis of SARS-CoV-2 infection was obtained by positivity to the rhino-oropharyngeal swab for SARS-CoV-2 RNA research by reverse transcription-polymerase chain reaction (RT-PCR). For patients with COVID-19, we used the Henry Ford Hospital (HFH). COVID-19 severity scoring system to distinguish the disease's mild, moderate, and severe forms (15). In particular, the mild disease was defined as patients who had normal chest radiography and SpO^2 of ≥94% without the need for supplemental oxygen. Patients with moderate disease were those who had abnormal chest radiography, SpO^2 of <94%, and were in need of 1 and 5 L/min supplemental O^2. Patients with severe disease were defined by abnormal chest radiography, SpO2 of <94%, and requiring ≥6 L/min of O^2 (16). For each patient, we evaluated the epidemiological characteristics, the laboratory data, the data of radiological instrumental investigations, clinical characteristics, the time elapsed since the transplant, the type of immunosuppressive treatment, and their changes during SARS-CoV-2 infection, the need for treatment and the type of treatment for SARS infection -CoV-2, and the outcome. In particular, we evaluated the potential relationship between the use of mTOR vs. other immunosuppressive regimens and severity or clinical outcome.

TABLE 1 | Anagraphical and clinical features of patients with kidney transplant with SARS-CoV-2 infection.

Age (median, IQR)	**50 (18–71)**
Gender	
Men	43 (76.7%)
Women	13 (23.3%)
Asymptomatic	**26 (46.4%)**
Men	22 (84.6%)
Women	4 (15.4%)
COVID-19	**30 (53.6%)**
Men	21 (70%)
Women	9 (30%)
Comorbidities:	
Hypertension	53 (94.6%)
Dyslipidemia	31 (55.3%)
Diabetes	10 (17.9%)
Anemia	14 (25%)
Ischemic heart disease	1 (1.78%)
Therapy for COVID-19:	
Modifications of immunosuppressive therapy	30 (100%)
Steroid therapy	22 (73.3%)
Low molecular weight heparin	18 (60%)
Remdesivir	4 (13.4%)

Data were reported as the median and interquartile range (IQR) given their non-parametric distribution. For comparisons between continuous variables, the Mann-Whitney U test was performed. We used the Chi-square test to test if two categorical variables are associated. Covariates significantly associated with death in the univariate analysis were also analyzed in a multivariate model. The *P*-value for statistical significance was set at <0.05 for all the tests.

With respect to the ethical issues, the study was conducted in compliance with the Declaration of Helsinki and the principles of good clinical practice. The authors confirm adherence to the ethical policies of the journal, as noted on the journal's author guidelines page.

RESULTS

We enrolled 371 patients with kidney transplant (229 men, 61.8%) with a median age of 49 (18–86) years and a mean age

TABLE 2 | Immunosuppressive therapy for each patient.

Immunosuppressive therapy	No SARS-CoV-2 infection	SARS-CoV-2 infection		
		Asymptomatic	COVID-19	
			Mild	Moderate/Severe
Tacrolimus + mycophenolate + methylprednisolone	49	6	1	2
Tacrolimus + mycophenolate + prednisone	72	4		2
Tacrolimus + everolimus + methylprednisolone	10	1	1	
Tacrolimus + everolimus + prednisone	4	1		
Tacrolimus + sirolimus + methylprednisolone	1			
Tacrolimus + everolimus + mycophenolate + methylprednisolone	1			
Tacrolimus + everolimus	2	1	1	
Tacrolimus + sirolimus	1			
Cyclosporine + everolimus + methylprednisolone	6			
Cyclosporine + sirolimus + methylprednisolone	1			
Cyclosporine + everolimus + mycophenolate	1			
Cyclosporine + everolimus + prednisone	5		1	
Cyclosporine + everolimus	4		2	
cyclosporine + sirolimus		1		1
Sirolimus + methylprednisolone	10		1	
Everolimus + mycophenolate	1			
Sirolimus + mycophenolate + prednisone	2			
Everolimus + prednisone	4			
Sirolimus + prednisone	1			
Sirolimus	1			
Other immunosuppressive therapies without mTOR inhibitors	137	12	8	10
	315	26	15	15

TABLE 3 | Single vs. double vs. triple immunosuppressive therapy.

Immunosuppressive therapy		No SARS-CoV-2 infection	SARS-CoV-2 infection		
			Asymptomatic	COVID-19	
				Mild	Moderate/Severe
Single	9 (2%)	9 (2.4%)	0	0	0
Double	142 (38%)	112 (30%)	11 (3%)	12 (3.2%)	7 (1.8%)
Triple	220 (60%)	194 (52.6%)	15 (4%)	3 (0.8%)	8 (2.2%)

of 51.4 years. Of these, 56 (15.1%) became infected with SARS-CoV-2 during the period of the study. Of these 56 patients with SARS-CoV-2 infection, 30 (53.6%) showed symptoms of the disease (COVID-19) and 26 had an asymptomatic infection (**Table 1**). Of the 30 patients with COVID-19 symptoms, 15 (50%) had a mild form of the disease, 7 (24%) had a moderate form of the disease, and 8 (26%) had severe form of the disease. Hospitalization was necessary for 12 (21.4%) patients, eight with the severe form of the disease and four with the moderate one. Of the 12 patients admitted, five required oxygen supplementations, five required non-invasive/high flow ventilation, and two required invasive ventilation (**Table 1**). Of the enrolled patients, only 12 patients performed high-resolution lung computed tomography (HRCT); in particular, only hospitalized patients performed HRCT. The severity score index, as proposed by Chung et al. (17) was used for the analysis of each individual HRCT. The 12 patients had a median severity score index equal to 13/20 as proposed by Chung et al. (17). Of the 12 patients, only one was taking mTOR inhibitors, particularly sirolimus, and had a severity score index equal to 10/20, as proposed by Chung et al. (17). Distinguishing the severity score index, proposed by Chung et al. (17) between the group of mTOR inhibitors and the group without mTOR inhibitors (10/20 vs. 13/20), a severity score index, proposed

TABLE 4 | Single vs. dual vs. triple immunosuppressive therapy in patients with SARS-CoV-2 infection.

Immunosuppressive therapy		SARS-CoV-2 infection		
		Asymptomatic	COVID-19	
			Mild	Moderate/Severe
Double	30 (53.6%)	11 (19.6%)	12 (21.4%)	7 (12.5%)
Triple	26 (46.4%)	15 (26.8%)	3 (5.3%)	8 (14.4%)

TABLE 5 | Immunosuppressive therapy evaluation for single immunosuppressant.

Immunosuppressive therapy	No SARS-CoV-2 infection	SARS-CoV-2 infection		
		Asymptomatic	COVID-19	
			Mild	Moderate/Severe
Tacrolimus	247	212	19	9	7
Cyclosporine	92	73	7	4	8
Mycophenolate	209	181	16	3	9
Azathioprine	4	3	0	0	1
Everolimus	48	40	3	5	0
Sirolimus	18	15	1	1	1
Methylprednisolone	182	165	11	9	7
Prednisone	136	120	9	2	5

by Chung et al. (17) was higher among patients without mTOR inhibitors.

All 371 patients underwent immunosuppressive therapy at the time of enrollment. In particular, 220 underwent triple immunosuppressive therapy, 142 dual therapy, and nine single immunosuppressant (**Tables 2**–**4**).

Data concerning the different immunosuppressive regimens also in relation to clinical presentation and outcome are given in **Tables 3**, **6**.

In relation to the different immunosuppressive therapies, 66 patients (17.8%) assumed the immunosuppressive therapy with mTOR inhibitors, 48 with everolimus, and 18 with sirolimus. Of these, 11 (16.6%) (eight treated with everolimus and three with sirolimus) acquired SARS-CoV-2 infection (*OR for SARS-CoV-2 infection acquired vs. no SARS-CoV-2 infection acquired: 1.1, 95, CI: (0.25–2.8) mTOR inhibitors recipients vs. other regimens), p = 0.210*). Of the 11 patients infected, 7 (63.6%) had COVID-19; in particular, six had a mild form of the disease, while 1 had a moderate form of the disease (*OR for moderate/severe form vs. mild:0.8, 95, CI: (0.21–0.92) mTOR inhibitors recipients vs. other regimens; p = 0.041*) (**Tables 2**, **5**, **6**). No patient treated with mTOR inhibitors presented a severe form of the disease.

No significant differences were observed between those patients who received a triple vs. a mono/double immunosuppressive regimen in the risk of acquiring the infection (*OR = 1.1, 95, CI: (0.60–2.5), p = 0.270*) (**Tables 3**, **4**).

All patients with symptoms underwent modifications of the immunosuppressive therapy. Regarding the therapeutic management of the infection, the first step was the reduction of immunosuppressive therapy, providing, in the first instance, the reduction or suspension of antimetabolites. In the case of severe forms of the disease, all immunosuppressive therapy was suspended, except for the steroid therapy, which was increased (*OR for modification/suspension of immunosuppressive therapy vs. non-modification of immunosuppressive therapy in SOT with a moderate-severe form of COVID-19:0.7, 95, CI: (0.44–0.85), p = 0.048*) (18–21). Only one patient experienced acute organ rejection, and two patients died.

We conducted a multivariate analysis of the possible variables that could impact the evolution of the COVID-19 disease, regardless of the presence or absence of mTOR inhibitors. We considered diabetes, BMI, duration of immunosuppressive treatment, duration of renal disease, and concomitant heart disease as variables. The multivariate analysis highlighted the values of diabetes [OR = 0.9, 95, CI: (0.85–1.4), $P = 0.130$], BMI [OR = 1.1, 95, CI: (0.92–1.3), $P = 0.145$], duration of immunosuppressive treatment [OR = 1.2, 95, CI: (0.72-1.8), $P = 0.350$], duration of renal disease [OR = 1.1, 95, CI: (0.52–2.1), $P = 0.420$], and concomitant heart disease [OR = 0.96, 95, CI: (0.88–1.7), $P = 0.290$].

DISCUSSION

Our study first shows that the use of mTOR inhibitors when compared with other immunosuppressive regiments

TABLE 6 | Immunosuppressive therapy evaluation: mTOR inhibitors vs. other types of immunosuppressive therapies.

Immunosuppressive therapy	No SARS-CoV-2 infection	SARS-CoV-2 infection		
		Asymptomatic	COVID-19	
			Mild	Moderate/Severe*
mTOR inhibitors	66 (17.7%)	55 (83%)	4 (6%)	6 (9%)	1 (2%)
Other types of immunosuppressive therapies	305 (82.3%)	260 (85%)	22 (7%)	9 (3%)	14 (5%)

**Moderate/severe vs. asymptomatic/mild P = 0.041.*

was associated with a more favorable outcome of COVID-19 in a cohort of patients. Moreover, none of the patients undergoing immunosuppressive therapy with mTOR inhibitors (everolimus and sirolimus) presented a severe form of the disease.

In contrast, neither the number of immunosuppressive drugs nor their type was associated with the risk of acquiring the infection.

We underline that our data may add knowledge to the management of SARS-CoV-2 infection in patients who underwent solid organ transplant and, in particular, to the management of immunosuppressive therapy during this infection. Moreover, from our study, the role of mTOR inhibitors in COVID-19 treatment could be hypothesized even in a non-transplant setting. However, this hypothesis needs to be deepened and demonstrated with further studies with a different design (i.e., randomized controlled trial).

How can we explain these results? There are at least two possible explanations: an antiviral effect of mTOR inhibitors or an immunomodulant action. With respect to the first hypothesis, we underline that a potential positive impact of mTOR inhibitors in the course of several viral infections is already known in the literature (22, 23). However, to our best knowledge, our study is the first one to show a positive impact of mTOR inhibitors in the course of SARS-CoV-2 infection on the evolution of the disease. The results might be due to the wellknown immunomodulatory effect of these drugs that could reduce the cytokine storm typical of the immune activation phase of the disease. Alternatively, another possible reason could be due to the inhibitory action on the mTOR pathway, which could induce the inhibition of transcriptional processes and consequently induce a reduced viral replication.

By multivariate analysis, it was found that none of the variables considered (diabetes, BMI, duration of immunosuppressive treatment, duration of renal disease, and concomitant heart disease) showed a statistically significant impact regardless of the presence or absence of mTOR inhibitors. Furthermore, as reported in the meta-analysis by Gatti et al. (24) also in our case, there was no increased mortality risk in this category of patients compared to the general population.

We acknowledge that our study presents several limitations, such as the retrospective design, the small sample size, the monocentric cohort, the lack of data on dosages of immunosuppressive therapies, and changes in immunosuppressive therapy during SARS-CoV-2 infection.

CONCLUSION

Our real-life study showed a positive impact of therapy with mTOR inhibitors in SARS-CoV-2 infection occurring in patients who underwent kidney transplant. Due to potential antiviral or immunomodulant properties, this class of drugs might be considered a possible weapon in the fight against COVID-19, both in transplant and non-transplant settings. These hypotheses need to be explored in randomized controlled trials.

FEDERICO II COVID-TEAM

Ametrano Luigi, Amicone Maria, Borrelli Francesco, Buonomo Antonio Riccardo, Cattaneo Letizia, Conte Maria Carmela Domenica, Cotugno Mariarosaria, Di Filippo Giovanni, Di Filippo Isabella, Esposito Nunzia, Festa Lidia, Fusco Ludovica, Foggia Maria, Gallicchio Antonella, Gentile Ivan, Giaccone Agnese, Iuliano Antonio, Lanzardo Amedeo, Licciardi Federica, Mercinelli Simona, Minervini Fulvio, Nobile Mariano, Piccione Amerigo, Pinchera Biagio, Reynaud Laura, Salemi Fabrizio, Sardanelli Alessia, Sarno Marina, Schiano Moriello Nicola, Scordino Fabrizio, Scotto Riccardo, Stagnaro Francesca, Tosone Grazia, Vecchietti Ilaria, Viceconte Giulio, Zappulo Emanuela, and Zotta Irene.

DATA AVAILABILITY STATEMENT

The raw data supporting the conclusions of this article will be made available by the authors, without undue reservation.

ETHICS STATEMENT

The studies involving human participants were reviewed and approved by Ethics Committee Federico II. Written informed consent for participation was not required for this study in accordance with the National Legislation and the Institutional Requirements.

AUTHOR CONTRIBUTIONS

BP: conceptualization, investigation, writing—original draft, writing—review and editing, and project administration. IG: writing—original draft, writing—review and editing, and supervision. RV: resources, data curation, and validation. LN: data curation, software, and project administration. FC: validation, investigation, and writing—review and editing. RL: formal analysis, data curation, and resources. FP: data curation, software, and resources. ES: formal analysis, data curation, and project administration. FS: software, data curation, and investigation. RC: methodology, resources, and supervision. MF: validation, resources, and project administration. AB: methodology, writing—review and editing, and visualization. LS: methodology, formal analysis, and data curation. All authors contributed to the article and approved the submitted version.

REFERENCES

1. Fishman JA. Infection in organ transplantation. *Am J Transplant*. (2017) 17:856–79. doi: 10.1111/ajt.14208
2. Azzi Y, Bartash R, Scalea J, Loarte-Campos P, Akalin E. COVID-19 and solid organ transplantation: a review article. *Transplantation*. (2021) 105:37–55. doi: 10.1097/TP.0000000000003523
3. Nair V, Jandovitz N, Hirsch JS, Nair G, Abate M, Bhaskaran M, et al. COVID-19 in kidney transplant recipients. *Am J Transplant*. (2020) 20:1819–25. doi: 10.1111/ajt.15967
4. Scientific Registry of Transplant Recipients (SRTR) and Organ Procurement and Transplantation Network (OPTN). SRTR/OPTN 2010 annual data report. Department of Health and Human Services, Health Resources and Services Administration, Healthcare Systems Bureau, Division of Transplantation. *Am J Transplant*. (2012) 12(Suppl. 1):553–86. doi: 10.1111/ajt.16983
5. Fishman JA. Infection in solid-organ transplant recipients. *N Engl J Med*. (2007) 357:2601–14. doi: 10.1056/NEJMra064928
6. Castle BT, Dock C, Hemmat M, et al. Biophysical modeling of the SARS-CoV-2 viral cycle reveals ideal antiviral targets. *bioRxiv*. (2020). doi: 10.1101/2020.05.22.111237
7. Le Sage V, Cinti A, Amorim R, Mouland AJ. Adapting the stress response: viral subversion of the mTOR signaling pathway. *Viruses*. (2016) 8:152. doi: 10.3390/v8060152
8. Karam BS, Morris RS, Bramante CT, Puskarich M, Zolfaghari EJ, Lotfi-Emran S, et al. mTOR inhibition in COVID-19: a commentary and review of efficacy in RNA viruses. *J Med Virol*. (2021) 93:1843–46. doi: 10.1002/jmv.26728
9. Terrazzano G, Rubino V, Palatucci AT, Giovazzino A, Carriero F, Ruggiero G. An open question: is it rational to inhibit the mTor-dependent pathway as COVID-19 therapy? *Front Pharmacol*. (2020) 11:e856. doi: 10.3389/fphar.2020.00856
10. Araki K, Turner AP, Shaffer VO, Gangappa S, Keller SA, Bachmann MF, et al. mTOR regulates memory CD8 T-celldifferentiation. *Nature*. (2009) 460:108–12. doi: 10.1038/nature08155
11. Ghasemnejad-Berenji M. mTOR inhibition: a double-edged sword in patients with COVID-19? *Hum Cell*. (2021) 34:698–9. doi: 10.1007/s13577-021-00495-2
12. Husain A, Byrareddy SN. Rapamycin as a potential repurpose drug candidate for the treatment of COVID-19. *Chem Biol Interact*. (2020) 331:109282. doi: 10.1016/j.cbi.2020.109282
13. Omarjee L, Janin A, Perrot F, Laviolle B, Meilhac O, Mahe G. Targeting T-cell senescence and cytokine storm with rapamycin to prevent severe progression in COVID-19. *Clin Immunol*. (2020) 216:108464. doi: 10.1016/j.clim.2020.108464
14. Zheng Y, Li R, Liu S. Immunoregulation with mTOR inhibitors to prevent COVID-19 severity: a novel intervention strategybeyond vaccines and specifc antiviral medicines. *J Med Virol*. (2020) 92:1495–500. doi: 10.1002/jmv.26009
15. Beigel JH, Tomashek KM, Dodd LE, Mehta AK, Zingman BS, Kalil AC, et al. Remdesivir for the treatment of COVID-19 - final report. *N Engl J Med*. (2020) 383:1813-26. doi: 10.1056/NEJMoa2007764
16. Chaudhry ZS,Williams JD, Vahia A, Fadel R, Acosta TP, Prashar R, et al. Clinical characteristics and outcomes of COVID-19 in solid organ transplant recipients: a case-control study. *Am J Transplant*. (2020) 20:3051–60. doi: 10.1111/ajt.16188
17. Chung M, Bernheim A, Mei X, Zhang N, Huang M, Zeng X, et al. CT imaging features of 2019 novel coronavirus (2019-nCoV). *Radiology*. (2020) 295:202–7. doi: 10.1148/radiol.2020200230
18. Di Castelnuovo A, Costanzo S, Antinori A, Berselli N, Blandi L, Bonaccio M, et al. Heparin in COVID-19 patients is associated with reduced in-hospital mortality: the multicenter Italian CORIST Study. *Thromb Haemost*. (2021) 121:1054-65. doi: 10.1055/a-1347-6070
19. COVID-19 RISk and Treatments (CORIST) Collaboration. RAAS inhibitors are not associated with mortality in COVID-19 patients: findings from an observational multicenter study in Italy and a meta-analysis of 19 studies. *Vascul Pharmacol*. (2020) 135:106805. doi: 10.1016/j.vph.2020.106805
20. Sagnelli C, Sica A, Gallo M, Peluso G, Varlese F, D'Alessandro V, et al. Renal involvement in COVID-19: focus on kidney transplant sector. *Infection*. (2021) 49:1265-75. doi: 10.1007/s15010-021-01706-6
21. Desmazes-Dufeu N, Coltey B, Amari L, Gouitaa M, Touzery C, Reynaud-Gaubert M, et al. Discordant courses of COVID-19 in a cohabiting couple of lung transplant recipients. *Case Reports Transpl Infect Dis*. (2021) 23:e13410. doi: 10.1111/tid.13410
22. Bowman LJ, Brueckner AJ, Doligalski CT. The role of mTOR inhibitors in the management of viral infections: a review of current literature. *Transplantation*. (2018) 102(2 Suppl. 1):S50-59. doi: 10.1097/TP.0000000000001777
23. Paoletti E, Citterio F, Corsini A, Potena L, Rigotti P, Sandrini S, et al. Everolimus in kidney transplant recipients at high cardiovascular risk: a narrative review. *J Nephrol*. (2020) 33:69-82. doi: 10.1007/s40620-019-00609-y
24. Gatti M, Rinaldi M, Bussini L, Bonazzetti C, Pascale R, Pasquini Z, et al. Clinical outcome in solid organ transplant recipients affected by COVID-19 compared to general population: a systematic review and meta-analysis. *Clin Microbiol Infect*. (2022). S1198-743X(22)00116-1. doi: 10.1016/j.cmi.2022.02.039

Conflict of Interest: The authors declare that the research was conducted in the absence of any commercial or financial relationships that could be construed as a potential conflict of interest.

frontiers | Frontiers in Immunology

PERSPECTIVE
published: 27 June 2022
doi: 10.3389/fimmu.2022.937667

Anti-MDA5 Antibody Linking COVID-19, Type I Interferon, and Autoimmunity: A Case Report and Systematic Literature Review

Antonio Tonutti[1,2†], *Francesca Motta*[1,3†], *Angela Ceribelli*[1,3], *Natasa Isailovic*[3], *Carlo Selmi*[1,3*] *and Maria De Santis*[1,3]

[1] Department of Biomedical Sciences, Humanitas University, Pieve Emanuele, Italy, [2] Istituto di Ricerca e Cura a Carattere Scientifico (IRCCS) Humanitas Research Hospital, Rozzano, Italy, [3] Division of Rheumatology and Clinical Immunology, Istituto di Ricerca e Cura a Carattere Scientifico (IRCCS) Humanitas Research Hospital, Rozzano, Italy

Introduction: The SARS-CoV-2 infection has been advocated as an environmental trigger for autoimmune diseases, and a paradigmatic example comes from similarities between COVID-19 and the myositis-spectrum disease associated with antibodies against the melanoma differentiation antigen 5 (MDA5) in terms of clinical features, lung involvement, and immune mechanisms, particularly type I interferons (IFN).

Case Report: We report a case of anti-MDA5 syndrome with skin manifestations, constitutional symptoms, and cardiomyopathy following a proven SARS-CoV-2 infection.

Systematic Literature Review: We systematically searched for publications on inflammatory myositis associated with COVID-19. We describe the main clinical, immunological, and demographic features, focusing our attention on the anti-MDA5 syndrome.

Discussion: MDA5 is a pattern recognition receptor essential in the immune response against viruses and this may contribute to explain the production of anti-MDA5 antibodies in some SARS-CoV-2 infected patients. The activation of MDA5 induces the synthesis of type I IFN with an antiviral role, inversely correlated with COVID-19 severity. Conversely, elevated type I IFN levels correlate with disease activity in anti-MDA5 syndrome. While recognizing this ia broad area of uncertainty, we speculate that the strong type I IFN response observed in patients with anti-MDA5 syndrome, might harbor protective effects against viral infections, including COVID-19.

Keywords: COVID-19, type I interferon signature, anti-MDA5 syndrome, inflammatory myositis, immunology, autoimmune disease, cytokines

OPEN ACCESS

Edited by:
Dimitra Dimopoulou, Panagiotis & Aglaia Kyriakou Children's Hospital, Greece

Reviewed by:
Latika Gupta, Royal Wolverhampton Hospitals NHS Trust, United Kingdom
Rossella Talotta, University of Messina, Italy

***Correspondence:**
Carlo Selmi
carlo.selmi@hunimed.eu

†These authors share first authorship

Specialty section:
This article was submitted to Viral Immunology, a section of the journal Frontiers in Immunology

Received: *06 May 2022*
Accepted: *30 May 2022*
Published: *27 June 2022*

Citation:
Tonutti A, Motta F, Ceribelli A, Isailovic N, Selmi C and De Santis M (2022) Anti-MDA5 Antibody Linking COVID-19, Type I Interferon, and Autoimmunity: A Case Report and Systematic Literature Review. Front. Immunol. 13:937667. doi: 10.3389/fimmu.2022.937667

INTRODUCTION

Infections are well known triggers for autoimmune diseases through different proposed mechanisms, including bystander activation, cross-reactivity, epitope spreading, and cryptic antigen unmasking (1–3).

New-onset autoimmune diseases following COVID-19 have been described, including both single-organ (e.g. Guillain-Barré syndrome) (4) and systemic rheumatologic diseases (e.g. inflammatory arthritis, connective tissue diseases, and vasculitis) (5). Anti-melanoma differentiation antigen 5 (anti-MDA5) syndrome is a disease belonging to the spectrum of inflammatory myositis (6); this is a heterogeneous group of systemic autoimmune disorders, characterized by skeletal muscle inflammation (7). Historically, myositis has been classified according to Bohan and Peter's criteria (8). A currently accepted classification divides myositis into clinical-serological categories: dermatomyositis, antisynthetase syndrome, immune-mediated necrotizing myopathies, polymyositis, and inclusion-body myopathy. Concerning muscle pathology, dermatomyositis is characterized by B and CD4 T cell infiltrate with perivascular distribution and complement activation, whereas in polymyositis inflammation appears at endomysial level, with a mononuclear cell infiltrate mainly composed by CD8 T cells and macrophages (7, 9–11). However, since each category might include heterogenous entities, a classification system based on myositis-specific antibodies has been advocated (6). Anti-MDA5 syndrome has usually been classified as dermatomyositis, due to prominent skin manifestations, mild (seldom absent) muscle involvement (clinically amyopathic dermatomyositis), and interstitial pneumonitis (6, 7, 12). The clinical picture of anti-MDA5 syndrome is unique, with digital ulcers, palmar and plantar papules, signs of vasculitis, and severe pulmonary involvement, associated with anti-MDA5 autoantibodies (12). A clinical overlap between COVID-19 and anti-MDA5 syndrome has been described, especially in the terms of rapidly progressive interstitial lung disease (ILD), fever, myalgia, and skin rashes; also, imaging findings show significant similarities, i.e. bilateral ground-glass pneumonitis and peri-bronchovascular consolidations (13, 14). In both conditions, elevated C-reactive protein levels and hyper-ferritinemia have prognostic significance; meanwhile, macrophage activation, endothelial dysfunction, and vasculopathy have been hypothesized as pathogenic factors (15). SARS-CoV-2 infection has been proposed as a human pathogenic model for anti-MDA5 syndrome (16). Furthermore, it has been recently suggested to search for anti-MDA5 antibodies in patients with COVID-19 for prognostic purposes (17).

We observed a case of anti-MDA5 syndrome becoming evident after COVID-19 and then focused on reports of inflammatory myositis occurring in association with SARS-CoV-2 infections *via* a systematic literature review. Ultimately, we aim to hypothesize potential immune pathogenic mechanisms for both conditions.

ANTI-MDA5 SYNDROME FOLLOWING MILD COVID-19: CASE REPORT

In November 2020, a 70-year-old Caucasian woman developed fever, cough, and anosmia. Four months before, she had developed an unexplained skin rash which resolved with glucocorticoids and antihistamines. She had a history of moderate-severity chronic obstructive pulmonary disease (COPD) associated with active smoking. At the time, the woman did not undergo any nasopharyngeal swab, and her symptoms resolved spontaneously in two weeks; meanwhile, her close contacts were diagnosed with COVID-19. One month after the resolution of her flu-like symptoms, she developed arthralgias and skin lesions on her face, chest, and hands; the patient denied any muscle-related symptom or weakness. She sought dermatological evaluation, and a topical treatment was started without any improvement. A SARS-CoV-2 nasopharyngeal swab proved negative and a serum test for immunoglobulin G (IgG) against SARS-CoV-2 spike protein resulted positive (96.1 AU/mL – positive if titer > 15); since the patient was not vaccinated at the time, this result demonstrates previous SARS-CoV-2 infection. For the persistence of skin rash, Gottron-like lesions on her hands (**Figure 1**), and arthralgias, she was admitted to our Department of Rheumatology and Clinical Immunology in March 2021. Blood tests proved normal except for C-reactive protein (2.1 mg/dL – normal value NV < 0.5 mg/dL), aspartate (84 IU/L – NV 5-35 IU/L) and alanine aminotransferase (133 IU/L – NV 5-35 IU/L), polyclonal hyper-gammaglobulinemia (23 g/L – 26.2%), elevated ferritin (595 ng/mL – NV 11-306 ng/mL), troponin I (19 ng/L – NV < 14 ng/L), and type B natriuretic peptide (BNP) (251 pg/mL – NV 5-100 pg/mL); creatine kinase (CK) values were normal (40 IU/L – NV < 135 IU/L), as were complement levels. Serum tests demonstrated previous hepatitis B infection with positive HBs antibody, and IgG antibodies for SARS-CoV-2 spike protein were still positive (96 AU/mL – NV < 15 AU/mL). The patient was tested for serum autoantibodies, including the myositis-associated panel: rheumatoid factor (RF), antinuclear antibodies (ANA), anti-extractable nuclear antigen (ENA) screening, anti-citrullinated protein antibodies (ACPA), antiphospholipid antibodies, and antineutrophil cytoplasm antibodies (ANCA) were negative; anti-MDA5 antibodies proved positive at both immunoblotting and immunoprecipitation analysis. A nailfold video-capillaroscopy showed reduced capillary density, neo-angiogenesis, and giant capillaries (**Figure 1**). She underwent chest CT scan revealing pulmonary emphysema, compatible with her COPD history, but not ILD. Pulmonary function tests demonstrated moderate obstruction and a severe reduction in diffusing capacity for carbon monoxide (DLCO): FVC 1.83 L – 82% of predicted, FEV1 1.12 L – 64% of predicted, and DLCO 37% of predicted. No abnormalities were found on EKG and echocardiography, but cardiac magnetic resonance imaging (MRI) findings were consistent with interstitial fibrosis as mirrored by increased native T1 mapping time (**Figure 1**). A diagnosis of anti-MDA5 syndrome with cutaneous and cardiac

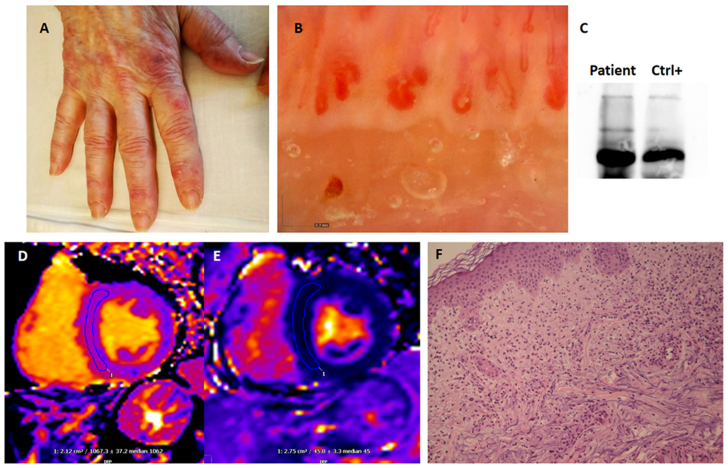

FIGURE 1 | Manifestations of COVID-19-associated anti-MDA5 dermatomyositis. **(A)** Cutaneous manifestations presented as violaceous, maculo-papular lesions on both dorsal and volar sides. **(B)** Nailfold video-capillaroscopy illustrated reduced capillary density, neo-angiogenesis, and tortuous, ectasic and giant capillaries. **(C)** Anti-MDA5 antibodies detected by immunoprecipitation. **(D, E)** T1-weighted cardiac magnetic resonance images presenting increased signal intensity [native T1 = 1067 ± 37msec (NV < 1015)], which, in association with ECV = 30 ± 4% (NV < 29) and normal T2 intensity [native T2 = 46 ± 3 msec (NV < 50 msec)], indicates interstitial myocardial fibrosis and is consistent with previous myocarditis. **(F)** Skin punch biopsy of a Gottron-like lesion on the left hand showing patchy mixed superficial inflammatory infiltrated with leukocytoclastic vasculitis features (Hematoxylin and eosin, 20x magnification).

involvement was made. Screening for malignancy was performed by chest CT scan, neck and abdominal ultrasound, urinary and cervical cytology, fecal occult blood test and resulted negative. Low-dose methylprednisolone (0.25 mg/Kg/die) and azathioprine 100 mg daily were started. Methotrexate was not prescribed due to concomitant non-alcoholic steatohepatitis and according to the patient preferences and disability. After six months, skin lesions improved but did not completely resolve, with a persistent tenuous heliotrope rash and V-neck sign. Furthermore, active myocarditis was retrieved at cardiac MRI, as demonstrated by mild increase in native T2 mapping time. Azathioprine was stopped, and mofetil mycophenolate mofetil 3 grams daily was started (18).

STUDY SEARCH STRATEGY AND SELECTION

The Medline database was accessed from PubMed and systematically searched for articles published in English between January 1st, 2020 and March 31st, 2022. We followed the search strategy and article selection process illustrated in the flowchart in **Supplementary Figure 1**, according to the recommendations of the PRISMA statement (19). Only peer-reviewed articles in English accepted for publication that included case reports and case series were included in this search. Two reviewers (FM and AT) evaluated all potentially relevant articles independently and summarized them. They discussed any area of uncertainty, screened the full text reports, and decided whether these met the inclusion criteria while resolving any disagreement through discussions. Neither of the authors were blind to the journal titles or to the study authors or institutions.

RESULTS

Eleven cases of inflammatory myositis temporally related to COVID-19 have been reported (20–27); the main features are illustrated in **Table 1**. In nine patients, new-onset inflammatory myositis followed SARS-CoV-2 infection; two cases of disease relapse following COVID-19 have been reported: one at pediatric age (22) (in a child who experienced a skin-only relapse of juvenile DM) and one in the adult setting (20) (in a patient positive for both anti-Mi-2 and anti-PM/Scl antibodies). Three out of eleven cases were juvenile DM (22, 26), in the other 8 adult cases the median age was 58 (interquartile range – IQR 50-64) years; a strong female predominance was observed (8/11 cases). In 9/11 reports, the severity of COVID-19 is described: 3/9 patients developed overt pneumonia, one of them succumbing to the infection (20); a flu-like illness was experienced in 4/9 cases, whereas two patients (22, 26) were completely asymptomatic. Apart from the case described by Gokhale (20) et al., none of the patients required specific therapies, oxygen supplementation nor mechanical ventilation for COVID-19. Time from the diagnosis of SARS-CoV-2 infection to the onset of inflammatory myositis was less than two months, and in four patients (20, 24, 26) rheumatologic manifestations were concomitant with the diagnosis of the infection. DM-related skin involvement was present in all the patients, being the only manifestation in one case of relapsed juvenile DM (22). Myopathy was noticed in 10/11 cases, generally in the form of

TABLE 1 | Relevant clinical features of previously reported cases of DM following SARS-CoV-2 infection.

Reference	Patient's characteristics: sex, age, race	Past medical history	Medications	SARS-CoV-2 information (time and severity)	Therapy for COVID-19	Clinical manifestations of DM	Autoimmunity and diagnosis	Therapy for DM	Outcome
Shahidi Dadras, 2021, Clin Case Rep. (21)	F, 58 Asian	Diabetes mellitus Hypothyroidism Coronary artery disease	Losartan Aspirin Metformin Levothyroxine Doxepin	45 days before Flu-like	Home supportive care	Constitutional symptoms Skin manifestations Fever Muscle weakness Pneumonia Cardiomyopathy	Seronegative DM-SLE overlap	PDN 60 mg/d MTX 15 mg/wk HCQ 400 mg/d	Improved
Liquidano-Perez, 2021, Pediatr Neurol. (26)	F, 4 Latino	Negative	N.A.	Concomitant Asymptomatic	N.A.	Muscle weakness Skin manifestations Dyspnea (myogenic)? Esophageal dysmotility	ANA 1:320 Anti-RNP/Sm Anti-Scl70 Anti-Sm Juvenile DM	IVIG 1 g/Kg MPN 0.7 mg/Kg/d, then pulses HCQ MTX CsA	Respiratory deterioration requiring mechanical ventilation. Gradual improvement
Rodero, 2022, J Clin Immunol (22)	F, 15 Unknown	Negative	N.A.	Two weeks before Unknown	No	Constitutional symptoms Arthritis Muscle weakness Skin manifestations and telangiectasias	Seronegative Juvenile DM	IVIG Steroid TOFA 5 mg bid	Remission
Rodero, 2022, J Clin Immunol (22)	F, 12 Unknown	DM, diagnosed eight years before	N.A.	Two weeks before Asymptomatic	No	*8 years before*: Muscle weakness Skin manifestations *Relapse*: Skin manifestations	Seronegative Juvenile DM	First episode: Steroids MTX Relapse: IVIG Steroids	Remission
Keshtkarjahromi, 2021, BMC Rheumatol (23)	F, 65 Caucasian	Psoriasis Hypertension Hyperlipidemia	Amlodipine Atorvastatin Buspirone Pantoprazole	Two months before Unknown	N.A.	Constitutional symptoms Muscle weakness Skin manifestations Dyspnea Arthralgia MAS	ANA Anti-MDA5 Anti-Ro52 DM	PDN 60 mg/d For MAS: MPN boluses, IVIG and mechanical ventilation	Died due to MAS
Gokhale, 2020, J Assoc Physicians India (20)	M, 64 Asian	N.A.	N.A.	Concomitant Pneumonia	IV antibiotic HCQ Ivermectin	Muscle weakness Skin manifestations Fever	ANA 1:320 homogeneous DM	IVIG 2 g/Kg PDN 1 mg/Kg/d MMF 1.5 g/d	Improved
Gokhale, 2020, J Assoc Physicians India (20)	F, 50 Asian	N.A.	N.A.	Concomitant Pneumonia	N.A.	Muscle weakness Skin manifestations OP (COVID-19)? Fever	Anti-MDA5 Anti-SAE-1 DM	MPN CYC 1 g MTX 15 mg/wk	Died due to COVID-19
Gokhale, 2020, J Assoc Physicians India (20)	M, 50 Asian	DM, diagnosed eight years before	PDN 5 mg qd AZA 50 mg bid	Convalescent (positive IgM and IgG antibodies towards SARS-CoV-2 but	N.A.	8 years before: Skin manifestations Muscle weakness Relapse:	Anti-Mi-2 Anti-PM/Scl DM	MTX PDN IVIG	Improved

(Continued)

TABLE 1 | Continued

Reference	Patient's characteristics: sex, age, race	Past medical history	Medications	SARS-CoV-2 information (time and severity)	Therapy for COVID-19	Clinical manifestations of DM	Autoimmunity and diagnosis	Therapy for DM	Outcome
				negative swab) Pneumonia		Muscle weakness Skin manifestations Pneumonia (COVID-19)?			
Borges, 2021, Rheumatology (Oxford) (25)	F, 36 Latino	N.A.	N.A.	Two weeks before Flu-like	N.A.	Skin manifestations Muscle weakness Raynaud's phenomenon	ANA 1:640, fine speckled Anti-Mi-2 DM	MPN	Improved
Okada, 2021, Rheumatology (Oxford) (27)	F, 64 Asian	N.A.	N.A.	One month before Fever	No	Skin manifestations Muscle weakness	Anti-NXP2 DM	MPN 1 g, then oral PDN 60 mg/d AZA 50 mg/d	Improved
Ho, 2021, JAAD Case Rep. (24)	M, 58 Hispanic	Negative	No	Concomitant Flu-like	Supportive care	Constitutional symptoms Muscle weakness Pneumonitis Skin manifestations Pulmonary embolism	Negative serology Biopsy-proven DM	MPN pulses Oral PDN MTX 10 mg/wk	Improved

ANA, antinuclear antibodies; AZA, azathioprine; bid, two times per day; CsA, cyclosporin A; CYC, cyclophosphamide; d, day; DM, dermatomyositis; F, female; HCQ, hydroxychloroquine; IV, intravenous; IVIG, intravenous immunoglobulins; MAS, macrophage activation syndrome; MMF, mofetil mycophenolate; MPN, methylprednisolone; MTX, methotrexate; N.A., not applicable or unknown; OP, organizing pneumonia; PDN, prednisolone; qd, once per day; SLE, systemic lupus erythematosus; TOFA, tofacitinib; wk, week.

a mild/moderate proximal muscle weakness; cardiomyopathy was only detected in one patient with systemic lupus erythematosus-dermatomyositis overlap (21). Pulmonary involvement was present or suspected (based on worsening dyspnea) in five cases (20, 21, 23, 24). There was no report of cancer-related DM.

In terms of autoimmune profiling, 4/11 cases (21, 22, 24) tested negative for serum autoantibodies, including two pediatric cases (22) and a lupus/dermatomyositis overlap syndrome (21). Two patients (20, 23) tested positive for anti-MDA5 antibodies: one of them (also positive for anti-Ro52 antibodies) underwent fatal macrophage activation syndrome (23), the other (also positive for anti-SAE-1 antibodies) died due to pneumonia (20). Two patients were positive for anti-Mi-2 antibodies: one of them was diagnosed new-onset DM (25), the other (also positive for anti-PM/Scl antibodies) experienced disease relapse (20). Moreover, one case of anti-NXP2 DM was described (27). Eight out of eleven patients experienced favorable outcome regarding both inflammatory myositis and COVID-19. One case of juvenile DM required mechanical ventilation due to respiratory deterioration, but gradual improvement followed thereafter (26). As already stated, two deaths were observed: one following macrophage activation syndrome (23), the other attributable to severe SARS-CoV-2 pneumonia (20); both patients had tested positive for anti-MDA5 autoantibodies.

DISCUSSION

SARS-CoV-2 at the Crossroads of Anti-Viral Immunity and Autoimmunity: The Role of MDA5

Viral infections have been hypothesized as environmental triggers in the pathogenesis of autoimmune diseases, including inflammatory myopathies (28), likely through molecular mimicry (1). Three immunogenic linear epitopes with high sequence identity to SARS-CoV-2 proteins have been recently recognized in patients with DM (29) and may explain how SARS-CoV-2 could trigger an autoimmune response in predisposed subjects, leading to autoantibody production. Further, autoantibodies directed towards specific antiviral signaling proteins (i.e., MDA5 and RIG-I) have been recently described by our group in a cohort of patients affected by COVID-19 (28). Notably, SARS-CoV-2 replication occurs through the synthesis of double-stranded RNA intermediates (dsRNA). RIG-I and MDA5 are pattern recognition receptors involved in innate antiviral immunity, and act as major sensors for dsRNA intermediates. While MDA5 recognizes long dsRNAs, RIG-I binds to shorter dsRNA fragments (30, 31). After binding to the viral dsRNA, MDA5/RIG-I activate a Janus kinase (JAK)/Signal Transducer and Activator of Transcription (STAT) signaling pathway leading to type I IFN

production, which is an essential cytokine in antiviral immune response (32). RNA viruses, as well as IFN itself, can upregulate the expression of MDA5 in infected cells, thus amplifying the whole process. After viral-induced cell lysis, dsRNA-MDA5/RIG-I complexes are released in the extracellular space, where they act as cryptic antigens, leading to autoantibody production (14). Through the generation of 'new self' epitopes, SARS-CoV-2 could elicit the synthesis of autoantibodies against antiviral signaling proteins (28). Moreover, apart from inducing type I IFN synthesis, RIG-I seems also to inhibit viral replication in an IFN-independent manner (33). It is unknown whether anti-MDA5 and anti-RIG-I antibodies possess any pathogenic effect, or they just represent the epiphenomenon of an aberrant activation of the immune response.

Type I IFN in the Pathogenesis of COVID-19

The severity of COVID-19 has been reported to be inversely related to the IFN production: if compared with mild-moderate forms, severe and life-threatening infections display an impaired type I IFN activity, a reduced viral clearance, and a delayed hyper-inflammatory response (34). Inborn errors of the type I IFN pathway have been associated with more severe forms of COVID-19, and severe SARS-CoV-2 infection led to new diagnosis of such type of immune deficiencies in a study cohort (35). Moreover, SARS-CoV-2 is able to evade the immune defense by antagonizing various steps involved in type I IFN synthesis (36, 37), including the direct inhibition of RIG-I and MDA5 by specific viral proteins (38). Studies conducted on animal models found that early IFN production would be crucial in producing an effective and protective antiviral response towards SARS-CoV-2, leading to the subsequent development of mild forms of COVID-19 (39). Autoantibodies directed towards type I IFN have been described in patients with severe SARS-CoV-2 pneumonia; by neutralizing IFN molecules, these antibodies would tip the balance in favor of the virus, thereby reducing viral clearance (40). According to these data, low type I IFN activity is associated with more severe COVID-19; vice versa, we could hypothesize that a strong type I IFN signature might be beneficial in orchestrating the antiviral immune response, leading to milder forms of disease.

Type I IFN in the Pathogenesis of Autoimmunity and the Anti-MDA5 Syndrome

Beyond their crucial role in viral clearance, type I IFN levels are elevated in sera of patients with autoimmune diseases, including systemic lupus erythematosus, rheumatoid arthritis, and DM (41, 42). Treatment with IFN-alpha (e.g. for HCV hepatitis or multiple sclerosis) has been associated with the appearance of serum autoantibodies, such as antinuclear antibodies and anti-dsDNA (43). Moreover, cases of new-onset inflammatory myositis following IFN-alpha administration have been described (44). It is worth mentioning that type I IFN levels correlate with disease activity in patients with DM and their downregulation can predict response to therapy (45). Finally, a high type I IFN signature might have a pathogenic role in vasculopathy and interstitial lung damage, which are prominent features of DM (46). If compared with other inflammatory myopathies, anti-MDA5 syndrome shows an even stronger type I IFN signature (46–48). Increased levels of MDA5 expression are found in peripheral mononucleated blood cells of patients with anti-MDA5 syndrome (47), and a possible role for type I IFN in the pathogenesis of the disease has been recently proposed (48). Furthermore, a peculiar population of autoreactive B cells has been recently described in a cohort of patients with severe anti-MDA5 syndrome. These lymphocytes synthetize monoclonal autoantibodies that can stimulate IFN-gamma (a type II IFN) production in peripheral blood mononucleated cells; notably, these antibodies are not directed towards MDA5 (49). The interplay between type I and II IFNs in both antiviral response and autoimmune pathogenesis is currently under investigation. Little is known about the relationship between MDA5 activation, type I IFN signature, autoantibody synthesis, and the immune pathogenic mechanisms that lead to the development of anti-MDA5 syndrome. Moreover, since autoimmune complications have been found in only a minority of patients affected by COVID-19, predisposing factors remain largely unknown.

Case Discussion and Pathogenic Hypothesis

We have recently described autoantibodies directed towards antiviral signaling proteins (e.g., MDA5 and RIG-I) in a cohort of patients affected by mild COVID-19; however, none of the aforementioned patients developed any feature suggestive of systemic autoimmune disease (28).

Through the recognition of viral dsRNA and the activation of a type I IFN response, MDA5 could link SARS-CoV-2 infection and subsequent anti-MDA5 syndrome (50). In our case, overt anti-MDA5 syndrome was preceded by a mild (flu-like) form of SARS-CoV-2 infection. A type I IFN-driven response may have exerted an effective antiviral activity, explaining the mild course of COVID-19 reported by our patient. We may hypothesize that the woman went through a prominent type I IFN response, with subsequent enhanced viral clearance. Besides having antiviral activity, this strong cytokine signature could have triggered the immune mechanisms underlying anti-MDA5 syndrome, which is an IFN-mediated disease (47, 48). Furthermore, COVID-19 could have revealed a pre-existing autoimmune condition/predisposition: the woman might have had previously DM-like skin rash, and SARS-CoV-2 infection could have unveiled overt disease by eliciting a strong IFN signature. There is uncertainty in the patient's past medical history, and no laboratory tests were performed before referral to our clinic: this represents a limitation for any possible conclusion, we must be aware that most cases will remain with some blind spots that need to be recognized.

High type I IFN levels are associated with an increased risk and are predictors of disease activity in some IFN-mediated autoimmune diseases, such is the case of anti-MDA5 syndrome (45, 47). A strong IFN signature might be related to an enhanced

viral clearance and, consequently, to a mild course of SARS-CoV-2 infection. In this view, our patient would be paradigmatic, with mild COVID-19 preceding DM onset/flare. Thus, autoimmunity resulting from an exuberant and dysregulated activation of the immune system could harbor parallel protective effects, due to an increased immune surveillance against viral infections. Notwithstanding, we must be aware that this interpretation is probably simplistic. The presence of anti-MDA5 antibodies has been recently correlated with a severe course of SARS-CoV-2 infection in a Chinese cohort, and it has also been proposed that autoantibody production might occur after the release of the antigen from infected cells (17). As reported in our systematic review, two out of two patients positive for anti-MDA5 antibodies died. In one case (23) anti-Ro52 antibodies, which are associated with rapidly progressive ILD and worse prognosis (51), were also present; the woman succumbed to macrophage activation syndrome, and there's no reason to attribute her death to COVID-19, since anti-MDA5 syndrome appeared two months after recovery from the infection. Meanwhile, the patient described by Gokhale et al. (20) tested positive for anti-SAE1 antibodies, which are associated with ILD and increased cancer risk (52). It is unclear whether the woman died due to SARS-CoV-2 pneumonia or to anti-MDA5 syndrome-associated rapidly progressive-ILD, since both conditions can manifest with organizing pneumonia features at chest CT scan (13). Furthermore, a more severe phenotype of anti-MDA5 syndrome has been described in Asian ancestry (53), such is the case of this patient. Taken together, these demographic, clinical, and serologic differences could partially explain the diversities between previously described cases and our report of anti-MDA5 syndrome following mild SARS-CoV-2 infection.

Similarities between COVID-19 and anti-MDA5 syndrome might implicate changes in treatment strategies in both conditions (16). Further research is required to elucidate the mechanisms that lead to anti-MDA5 autoantibodies synthesis in a subset of SARS-CoV-2 infected patients. Also, there is an urge to understand which predisposing factors (e.g., genetically determined) couple autoantibody production with the development of anti-MDA5 syndrome in only a minority of cases. Furthermore, little is known about if (and how) anti-MDA5 antibodies might influence the outcome of COVID-19. Finally, the balance between immune activation vs. immune tolerance is still extensively unexplored.

CONCLUSIONS

Type I IFN is an essential component of the immune response towards viral infections, and a strong IFN signature has been described in various connective tissue diseases, including anti-MDA5 syndrome. Apart from triggering the synthesis of autoantibodies, SARS-CoV-2 might be able to elicit an autoimmune response involved in inflammatory myositis pathogenesis, associated to the type I IFN-rich molecular *milieu* promoted by the virus itself. Both *de novo* anti-MDA5 syndrome development and disease relapses could occur through such immune mechanisms. Ultimately, clinicians should be aware that autoimmune phenomena, ranging from isolated autoantibody positivity to overt systemic rheumatologic syndromes, are a possible complication of even mild or asymptomatic SARS-CoV-2 infections, and that the dogmatic separation between infections and chronic inflammation should be dynamically reconsidered.

DATA AVAILABILITY STATEMENT

The original contributions presented in the study are included in the article/**Supplementary Material**. Further inquiries can be directed to the corresponding author.

ETHICS STATEMENT

Written informed consent was obtained from the individual(s) for the publication of any potentially identifiable images or data included in this article.

AUTHOR CONTRIBUTIONS

All authors equally contributed to the submitted version of the work, by data achieving, drafting or revising the manuscript.

SUPPLEMENTARY MATERIAL

The Supplementary Material for this article can be found online at: https://www.frontiersin.org/articles/10.3389/fimmu.2022.937667/full#supplementary-material

REFERENCES

1. Ercolini AM, Miller SD. The Role of Infections in Autoimmune Disease. *Clin Exp Immunol* (2009) 155(1):1–15. doi: 10.1111/j.1365-2249.2008.03834.x
2. Smatti MK, Cyprian FS, Nasrallah GK, Al Thani AA, Almishal RO, Yassine HM. Viruses and Autoimmunity: A Review on the Potential Interaction and Molecular Mechanisms. *Viruses* (2019) 11(8):762. doi: 10.3390/V11080762
3. Root-Bernstein R, Fairweather D. Complexities in the Relationship Between Infection and Autoimmunity. *Curr Allergy Asthma Rep* (2014) 14(1):407. doi: 10.1007/s11882-013-0407-3
4. Liu Y, Sawalha AH, Lu Q. COVID-19 and Autoimmune Diseases. *Curr Opin Rheumatol* (2021) 33(2):155–62. doi: 10.1097/BOR.0000000000000776
5. Zacharias H, Dubey S, Koduri G, D'Cruz D. Rheumatological Complications of Covid 19. *Autoimmun Rev* (2021) 20(9):102883. doi: 10.1016/j.autrev.2021.102883
6. Lundberg IE, de Visser M, Werth VP. Classification of Myositis. *Nat Rev Rheumatol* (2018) 14(5):269–78. doi: 10.1038/nrrheum.2018.41
7. Lundberg IE, Fujimoto M, Vencovsky J, Aggarwal R, Holmqvist M, Christopher-Stine L, et al. Idiopathic Inflammatory Myopathies. *Nat Rev Dis Prim* (2021) 7(1):86. doi: 10.1038/s41572-021-00321-x
8. Bohan A, Peter JB. Polymyositis and Dermatomyositis (First of Two Parts). *N Engl J Med* (1975) 292(7):344–7. doi: 10.1056/NEJM197502132920706
9. Selva-O'Callaghan A, Pinal-Fernandez I, Trallero-Araguás E, Milisenda JC, Grau-Junyent JM, Mammen AL. Classification and Management of Adult

Inflammatory Myopathies. *Lancet Neurol* (2018) 17(9):816–28. doi: 10.1016/S1474-4422(18)30254-0
10. Tanboon J, Nishino I. Classification of Idiopathic Inflammatory Myopathies: Pathology Perspectives. *Curr Opin Neurol* (2019) 32(5):704–14. doi: 10.1097/WCO.0000000000000740
11. Barsotti S, Tripoli A, Pollina LE, Mosca M, Neri R. Histopathology of the Muscle in Rheumatic Diseases. *Reumatismo* (2018) 70(3):133–45. doi: 10.4081/reumatismo.2018.1051
12. Nombel A, Fabien N, Coutant F. Dermatomyositis With Anti-MDA5 Antibodies: Bioclinical Features, Pathogenesis and Emerging Therapies. *Front Immunol* (2021) 12:773352. doi: 10.3389/fimmu.2021.773352
13. Wang Y, Du G, Zhang G, Matucci-Cerinic M, Furst DE. Similarities and Differences Between Severe COVID-19 Pneumonia and Anti-MDA-5-Positive Dermatomyositis-Associated Rapidly Progressive Interstitial Lung Diseases: A Challenge for the Future. *Ann Rheum Dis* (2020). doi: 10.1136/ANNRHEUMDIS-2020-218594
14. Mehta P, Machado PM, Gupta L. Understanding and Managing Anti-MDA 5 Dermatomyositis, Including Potential COVID-19 Mimicry. *Rheumatol Int* (2021) 41(6):1021–36. doi: 10.1007/s00296-021-04819-1
15. Kondo Y, Kaneko Y, Takei H, Tamai H, Kabata H, Suhara T, et al. COVID-19 Shares Clinical Features With Anti-Melanoma Differentiation-Associated Protein 5 Positive Dermatomyositis and Adult Still's Disease. *Clin Exp Rheumatol* (2021) 39(3):631–8. doi: 10.1136/annrheumdis-2021-eular.1031
16. Saud A, Naveen R, Aggarwal R, Gupta L. COVID-19 and Myositis: What We Know So Far. *Curr Rheumatol Rep* (2021) 23(8):63. doi: 10.1007/s11926-021-01023-9
17. Wang G, Wang Q, Wang Y, Liu C, Wang L, Chen H, et al. Presence of Anti-MDA5 Antibody and Its Value for the Clinical Assessment in Patients With COVID-19: A Retrospective Cohort Study. *Front Immunol* (2021) 12:791348. doi: 10.3389/fimmu.2021.791348
18. Oddis CV, Aggarwal R. Treatment in Myositis. *Nat Rev Rheumatol* (2018) 14 (5):279–89. doi: 10.1038/nrrheum.2018.42
19. Moher D, Liberati A, Tetzlaff J, Altman DG. Preferred Reporting Items for Systematic Reviews and Meta-Analyses: The PRISMA Statement. *Ann Intern Med* (2009) 151(4):264–69, W64. doi: 10.7326/0003-4819-151-4-200908180-00135
20. Gokhale Y, Patankar A, Holla U, Shilke M, Kalekar L, Karnik ND, et al. Dermatomyositis During COVID-19 Pandemic (A Case Series): Is There a Cause Effect Relationship? *J Assoc Phys India* (2020) 68(11):20–4.
21. Shahidi Dadras M, Rakhshan A, Ahmadzadeh A, Hosseini SA, Diab R, Safari Giv T, et al. Dermatomyositis-Lupus Overlap Syndrome Complicated With Cardiomyopathy After SARS-CoV-2 Infection: A New Potential Trigger for Musculoskeletal Autoimmune Disease Development. *Clin Case Rep* (2021) 9 (10):1–6. doi: 10.1002/ccr3.4931
22. Rodero MP, Pelleau S, Welfringer-Morin A, Study Group FJDM, Duffy D, Melki I, et al. Onset and Relapse of Juvenile Dermatomyositis Following Asymptomatic SARS-CoV-2 Infection. *J Clin Immunol* (2022) 42(1):25–7. doi: 10.1007/s10875-021-01119-y
23. Keshtkarjahromi M, Chhetri S, Balagani A, Tayyab U ul BB, Haas CJ. Macrophage Activation Syndrome in MDA5 Antibody-Positive Dermatomyositis and COVID-19 Infection. *BMC Rheumatol* (2021) 5(1):1–7. doi: 10.1186/s41927-021-00225-z
24. Ho BVK, Seger EW, Kollmann K, Rajpara A. Dermatomyositis in a COVID-19 Positive Patient. *JAAD Case Rep* (2021) 13:97–9. doi: 10.1016/j.jdcr.2021.04.036
25. Borges NH, Godoy TM, Kahlow BS. Onset of Dermatomyositis in Close Association With COVID-19 - A First Case Reported. *Rheumatol* (2021) 60 (SI):SI96. doi: 10.1093/rheumatology/keab290
26. Liquidano-Perez E, García-Romero MT, Yamazaki-Nakashimada M, Maza-Morales M, Rivas-Calderón MK, Bayardo-Gutierrez B, et al. Juvenile Dermatomyositis Triggered by SARS-CoV-2. *Pediatr Neurol* (2021) 121:26–7. doi: 10.1016/j.pediatrneurol.2021.05.011
27. Okada Y, Izumi R, Hosaka T, Watanabe S, Shijo T, Hatchome N, et al. Anti-NXP2 Antibody-Positive Dermatomyositis Developed After COVID-19 Manifesting as Type I Interferonopathy. *Rheumatol (Oxford)* (2022) 61(4): e90-2. doi: 10.1093/rheumatology/keab872
28. De Santis M, Isailovic N, Motta F, Ricordi C, Ceribelli A, Lanza E, et al. Environmental Triggers for Connective Tissue Disease: The Case of COVID-19 Associated With Dermatomyositis-Specific Autoantibodies. *Curr Opin Rheumatol* (2021) 33(6):514-21. doi: 10.1097/BOR.0000000000000844
29. Megremis S, Walker TDJ, He X, Ollier WER, Chinoy H, Hampson L, et al. Antibodies Against Immunogenic Epitopes With High Sequence Identity to SARS-CoV-2 in Patients With Autoimmune Dermatomyositis. *Ann Rheum Dis* (2020) 79(10):1383–6. doi: 10.1136/annrheumdis-2020-217522
30. Sampaio NG, Chauveau L, Hertzog J, Bridgeman A, Fowler G, Moonen JP, et al. The RNA Sensor MDA5 Detects SARS-CoV-2 Infection. *Sci Rep* (2021) 11(1):1–10. doi: 10.1038/s41598-021-92940-3
31. Kouwaki T, Nishimura T, Wang G, Oshiumi H. RIG-I-Like Receptor-Mediated Recognition of Viral Genomic RNA of Severe Acute Respiratory Syndrome Coronavirus-2 and Viral Escape From the Host Innate Immune Responses. *Front Immunol* (2021) 12:700926. doi: 10.3389/fimmu.2021.700926
32. Schreiber G. Type I Interferons in the Pathogenesis and Treatment of Autoimmune Diseases. *Front Immunol* (2020) 11:595739. doi: 10.3389/fimmu.2020.595739
33. Yamada T, Sato S, Sotoyama Y, Orba Y, Sawa H, Yamauchi H, et al. RIG-I Triggers a Signaling-Abortive Anti-SARS-CoV-2 Defense in Human Lung Cells. *Nat Immunol* (2021) 22(7):820–8. doi: 10.1038/s41590-021-00942-0
34. Hadjadj J, Yatim N, Barnabei L, Corneau A, Boussier J. Impaired Type I Interferon Activity and Inflammatory Responses in Severe COVID-19 Patients. *Science* (2020) 369(6504):718–24. doi: 10.1126/science.abc6027
35. Zhang Q, Bastard P, Liu Z, Le Pen J, Moncada-Velez M, Chen J, et al. Inborn Errors of Type I IFN Immunity in Patients With Life-Threatening COVID-19. *Sci.* (2020) 370(6515):eabd4570. doi: 10.1126/science.abd4570
36. Xia H, Cao Z, Xie X, Zhang X, Chen JY, Wang H, et al. Evasion of Type I Interferon by SARS-CoV-2. *Cell Rep* (2020) 33(1):108234. doi: 10.1016/j.celrep.2020.108234
37. Sui L, Zhao Y, Wang W, Wu P, Wang Z, Yu Y, et al. SARS-CoV-2 Membrane Protein Inhibits Type I Interferon Production Through Ubiquitin-Mediated Degradation of TBK1. *Front Immunol* (2021) 12:662989. doi: 10.3389/fimmu.2021.662989
38. Zheng Y, Zhuang MW, Han L, Zhang J, Nan ML, Zhan P, et al. Severe Acute Respiratory Syndrome Coronavirus 2 (SARS-CoV-2) Membrane (M) Protein Inhibits Type I and III Interferon Production by Targeting RIG-I/MDA-5 Signaling. *Signal Transduct Target Ther* (2020) 5(1):299. doi: 10.1038/s41392-020-00438-7
39. Nelson CE, Namasivayam S, Foreman TW, Kauffman KD, Sakai S, Dorosky DE, et al. Mild SARS-CoV-2 Infection in Rhesus Macaques Is Associated With Viral Control Prior To Antigen-Specific T Cell Responses in Tissues. *Sci Immunol* (2022). doi: 10.1126/sciimmunol.abo0535
40. Bastard P, Rosen LB, Zhang Q, Michailidis E, Hoffmann HH, Zhang Y, et al. Autoantibodies Against Type I IFNs in Patients With Life-Threatening COVID-19. *Sci* (2020) 370(6515):eabd4585. doi: 10.1126/science.abd4585
41. Choubey D, Moudgil KD. Interferons in Autoimmune and Inflammatory Diseases: Regulation and Roles. *J Interf Cytokine Res Off J Int Soc Interf Cytokine Res* (2011) 31(12):857–65. doi: 10.1089/jir.2011.0101
42. Qian J, Xu H. COVID-19 Disease and Dermatomyositis: A Mini-Review. *Front Immunol* (2022) 12:747116. doi: 10.3389/fimmu.2021.747116
43. Jiang J, Zhao M, Chang C, Wu H, Lu Q. Type I Interferons in the Pathogenesis and Treatment of Autoimmune Diseases. *Clin Rev Allergy Immunol* (2020) 59 (2):248–72. doi: 10.1007/s12016-020-08798-2
44. Shiba H, Takeuchi T, Isoda K, Kokunai Y, Wada Y, Makino S, et al. Dermatomyositis as a Complication of Interferon-α Therapy: A Case Report and Review of the Literature. *Rheumatol Int* (2014) 34(9):1319–22. doi: 10.1007/s00296-014-2984-4
45. Walsh RJ, Kong SW, Yao Y, Jallal B, Kiener PA, Pinkus JL, et al. Type I Interferon-Inducible Gene Expression in Blood Is Present and Reflects Disease Activity in Dermatomyositis and Polymyositis. *Arthritis Rheumatol* (2007) 56 (11):3784–92. doi: 10.1002/art.22928
46. Ono N, Kai K, Maruyama A, Sakai M, Sadanaga Y, Koarada S, et al. The Relationship Between Type 1 IFN and Vasculopathy in Anti-MDA5 Antibody-Positive Dermatomyositis Patients. *Rheumatol (United Kingdom)* (2019) 58(5):786–91. doi: 10.1093/rheumatology/key386
47. Zhang SH, Zhao Y, Xie QB, Jiang Y, Wu YK, Yan B. Aberrant Activation of the Type I Interferon System may Contribute to the Pathogenesis of Anti-

Melanoma Differentiation-Associated Gene 5 Dermatomyositis. *Br J Dermatol* (2019) 180(5):1090–8. doi: 10.1111/bjd.16917
48. Hu H, Yang H, Liu Y, Yan B. Pathogenesis of Anti-Melanoma Differentiation-Associated Gene 5 Antibody-Positive Dermatomyositis: A Concise Review With an Emphasis on Type I Interferon System. *Front Med* (2022) 8:833114. doi: 10.3389/fmed.2021.833114
49. Coutant F, Bachet R, Pin J-J, Alonzo M, Miossec P. Monoclonal Antibodies From B Cells of Patients With Anti-MDA5 Antibody-Positive Dermatomyositis Directly Stimulate Interferon Gamma Production. *J Autoimmun* (2022) 130:102831. doi: 10.1016/j.jaut.2022.102831
50. Hannah JR, Ali SS, Nagra D, Adas MA, Buazon AD, Galloway JB, et al. Skeletal Muscles and Covid-19: A Systematic Review of Rhabdomyolysis and Myositis In SARS-CoV-2 Infection. *Clin Exp Rheumatol* (2022) 40(2):329–38. doi: 10.55563/clinexprheumatol/mkfmxt
51. Xu A, Ye Y, Fu Q, Lian X, Chen S, Guo Q, et al. Prognostic Values of Anti-Ro52 Antibodies in Anti-MDA5-Positive Clinically Amyopathic Dermatomyositis Associated With Interstitial Lung Disease. *Rheumatol (Oxford)* (2021) 60(7):3343–51. doi: 10.1093/rheumatology/keaa786
52. Matsuo H, Yanaba K, Umezawa Y, Nakagawa H, Muro Y. Anti-SAE Antibody-Positive Dermatomyositis in a Japanese Patient: A Case Report and Review of the Literature. *J Clin Rheumatol Pract Rep Rheum Musculoskelet Dis* (2019) 25(7):e115–6. doi: 10.1097/RHU.0000000000000683
53. Huang K, Vinik O, Shojania K, Yeung J, Shupak R, Nimmo M, et al. Clinical Spectrum and Therapeutics in Canadian Patients With Anti-Melanoma Differentiation-Associated Gene 5 (MDA5)-Positive Dermatomyositis: A Case-Based Review. *Rheumatol Int* (2019) 39(11):1971–81. doi: 10.1007/s00296-019-04398-2

Conflict of Interest: The authors declare that the research was conducted in the absence of any commercial or financial relationships that could be construed as a potential conflict of interest.

Publisher's Note: All claims expressed in this article are solely those of the authors and do not necessarily represent those of their affiliated organizations, or those of the publisher, the editors and the reviewers. Any product that may be evaluated in this article, or claim that may be made by its manufacturer, is not guaranteed or endorsed by the publisher.

frontiers | Frontiers in Immunology

TYPE Original Research
PUBLISHED 26 July 2022
DOI 10.3389/fimmu.2022.938837

OPEN ACCESS

EDITED BY
Giulia Menchinelli,
Catholic University of the Sacred Heart, Rome, Italy

REVIEWED BY
Flavio De Maio,
Fondazione Policlinico Gemelli IRCCS, Institute of Microbiology, Italy
Alberto Antonelli,
University of Florence, Italy

*CORRESPONDENCE
Xia Zhou
zhouxia1977@163.com

SPECIALTY SECTION
This article was submitted to Viral Immunology, a section of the journal Frontiers in Immunology

RECEIVED 08 May 2022
ACCEPTED 01 July 2022
PUBLISHED 26 July 2022

CITATION
Luo H and Zhou X (2022) Bioinformatics analysis of potential common pathogenic mechanisms for COVID-19 infection and primary Sjogren's syndrome.
Front. Immunol. 13:938837.
doi: 10.3389/fimmu.2022.938837

Bioinformatics analysis of potential common pathogenic mechanisms for COVID-19 infection and primary Sjogren's syndrome

Hong Luo[1] and Xia Zhou[1,2,3,4]*

[1]Department of Tuberculosis and Respiratory, Wuhan Jinyintan Hospital, Tongji Medical College, Huazhong University of Science and Technology, Wuhan, China, [2]Hubei Clinical Research Center for Infectious Diseases, Wuhan, China, [3]Wuhan Research Center for Communicable Disease Diagnosis and Treatment, Chinese Academy of Medical Sciences, Wuhan, China, [4]Joint Laboratory of Infectious Diseases and Health, Wuhan Institute of Virology and Wuhan Jinyintan Hospital, Chinese Academy of Sciences, Wuhan, China

Background: Accumulating evidence has revealed that the prevalence of Coronavirus 2019 (COVID-19) was significantly higher in patients with primary Sjogren's syndrome (pSS) compared to the general population. However, the mechanism remains incompletely elucidated. This study aimed to further investigate the molecular mechanisms underlying the development of this complication.

Methods: The gene expression profiles of COVID-19 (GSE157103) and pSS (GSE40611) were downloaded from the Gene Expression Omnibus (GEO) database. After identifying the common differentially expressed genes (DEGs) for pSS and COVID-19, functional annotation, protein-protein interaction (PPI) network, module construction and hub gene identification were performed. Finally, we constructed transcription factor (TF)-gene regulatory network and TF-miRNA regulatory network for hub genes.

Results: A total of 40 common DEGs were selected for subsequent analyses. Functional analyses showed that cellular components and metabolic pathways collectively participated in the development and progression of pSS and COVID-19. Finally, 12 significant hub genes were identified using the cytoHubba plugin, including CMPK2, TYMS, RRM2, HERC5, IFI44L, IFI44, IFIT2, IFIT1, IFIT3, MX1, CDCA2 and TOP2A, which had preferable values as diagnostic markers for COVID-19 and pSS.

Conclusions: Our study reveals common pathogenesis of pSS and COVID-19. These common pathways and pivotal genes may provide new ideas for further mechanistic studies.

KEYWORDS

primary Sjogren's syndrome, COVID-19, differentially expressed genes, hub genes, pathogenesis

Introduction

Primary Sjogren's syndrome (pSS) is one of the most common systemic autoimmune disorders, frequently accompanied by a variety of specific autoantibodies, such as antinuclear antibodies (ANAs), antibodies against Ro/Sjogren's syndrome-related antigen A (SSA) and La/Sjogren's syndrome-related antigen B(SSB), and hypergammaglobulinemia (1, 2). The prevalence of pSS is about 60 cases per 100,000 inhabitants (3) and there is a significant gender distribution difference, with the number of male patients to female patients ratio being about 1:9 (4). It is marked by lymphocytic infiltration of exocrine glands, such as lacrimal glands, salivary glands and other exocrine glands, characterized by oral and ocular dryness. At least one-third of patients with pSS may have multiple organ function impairment, such as severe thrombocytopenic purpura, primary biliary cirrhosis, and interstitial pneumonia, which can seriously compromise the patient's prognosis, and 5% of patients may develop lymphoma (5).

The etiology and pathogenesis of pSS are still not fully elucidated and may be related to various factors such as infection, genetics and sex hormone abnormalities. Among them, viral infections are more closely related to pSS. Epstein-Barr virus (EBV), cytomegalovirus (CMV) and hepatitis C virus (HCV) may play an important role in the pathogenesis of pSS.

EBV, a DNA virus, was the first virus identified in association with pSS. EBV can affect the host immune system by directly infecting lymphocytes and indirectly regulating the expression of viral antigens through immunomodulatory mechanisms (6). The DNA component of EBV has been found to be detectable in the epithelial cells of saliva and lacrimal glands of patients with pSS (7). Studies have reported that EBV can induce autoimmune disorders in pSS through type I interferon, molecular mimicry and ectopic lymphoid-like structures (ELS),a feature of pSS pathogenesis. EBV promotes the development and progression of pSS by inducing TLR to promote IFN-I production by dendritic cells (8, 9). In addition, the molecular mimicry between pSS autoantigens and EBV-associated antigens in the serum of pSS patients suggests that EBV infection may be involved in pathogenesis through molecular mimicry mechanism (10). Moreover, EBV can invade the ELS and thus contribute to the growth and differentiation of self-reactive B cells in pSS patients (11). CMV is a double-stranded DNA virus. It was found that CMV IgG concentrations were higher in the control group than in the pSS patient group, implying that CMV infection may be associated with the development of pSS, however, this needs to be confirmed by further clinical studies (12). HCV is a RNA virus capable of causing chronic hepatitis, cirrhosis and hepatocellular carcinoma. The pSS-characteristic salivary gland lymphocyte infiltration was found in patients with hepatitis C (13). Therefore, it was hypothesized that HCV infection might be associated with the development of SS and further studies are needed to confirm the relationship between HCV and pSS. However, although viruses such as EBV, CMV and HCV have been found to influence the pathogenesis of pSS, there are still relatively few studies focusing on COVID-19 and pSS.

Currently, Coronavirus 2019 (COVID-19), caused by severe acute respiratory syndrome coronavirus 2 (SARS-CoV-2), is ravaging the world, which is posing an ongoing challenge to global health (14). Globally, as of 8 April 2022, there have been 494,587,638 confirmed cases of COVID-19, including 6,170,283 deaths (https://covid19.who.int/). In addition to imposing a severe burden on global healthcare systems, the epidemic is also posing a serious challenge to the management of patients with "inflammatory autoimmune systemic diseases", including primary Sjogren's syndrome (15, 16). Multiple studies have reported that a significantly higher prevalence of COVID-19 has been observed in patients with pSS than in the general population (17, 18). Immune dysfunction, as well as the use of immunosuppressive therapies, have been reported to predispose pSS patients to severe bacterial and viral infections (18), however, the underlying mechanism of this phenomenon is still not fully elucidated.

Exploring the common transcriptional profile of pSS and COVID-19 may provide new insights into common pathogenesis of the two diseases. In this study, we aimed to identify pivotal genes associated with the pathogenesis of pSS complicated with COVID-19. Two datasets downloaded from the GEO database (GSE30999 and GSE28829) were analyzed. Integrated bioinformatics and enrichment analysis were used to identify common DEGs and their functions in COVID-19 and pSS. In addition, a PPI network was constructed using the STRING database and Cytoscape software (version 3.9.1) to analyze the gene modules and identify hub genes. Finally, we identified 12 important hub genes and further constructed TF-gene regulatory network and TF-miRNA regulatory network for these genes. The hub genes identified in this study between COVID-19 and pSS are expected to provide new insights into the biological mechanisms of these two diseases.

Materials and methods

Datasets preparation

GEO (www.ncbi.nlm.nih.gov/geo) is a large database containing gene expression for multiple diseases, which is publicly available and free of charge (19). GSE157103 (20) dataset contains 100 COVID-19 samples and 26 non-COVID-19 samples, which used high throughput sequencing technology based on Illumina NovaSeq 6000 platform. GSE40611 (21) dataset consists of 17 pSS tissues and 18 control tissues, which was based on Affymetrix Human Genome U133 Plus 2.0 Array platform.

Identification of shared DEGs between COVID-19 and primary Sjogren's syndrome

GEO2R (22) (www.ncbi.nlm.nih.gov/geo/geo2r/) is an online web-based tool that can be employed to compare and analyze gene expression between different sample groups. Networkanalyst (23) (www.networkanalyst.ca/) is an online visual analytics platform that enables gene expression differential analysis and enrichment analysis, meta-analysis, protein-protein interaction network analysis, and integrated analysis of multiple datasets. In this study, Networkanalyst was used to identify DEGs for GSE157103 and we employed GEO2R to analyze DEGs for GSE40611. Genes with adjusted P-value < 0.05 and $|\log_2$ fold change $(\log_2 FC)| > 1.0$ were considered DEGs. The R language package VennDiagram (24) was used to obtain shared DEGs between the GSE157103 and GSE40611 datasets.

Gene ontology and KEGG enrichment analysis

KEGG Orthology Based Annotation System (25) (KOBAS; http://bioinfo.org/kobas) is a database developed by Peking University for annotation and identification of enriched pathways and diseases. Gene ontology and KEGG enrichment analysis were performed to analyze the potential function of DEGs by using the KOBAS 3.0 database. Adjusted P-value < 0.05 was considered statistically significant.

Construction of protein–protein interaction network and module analysis

Search Tool for the Retrieval of Interacting Genes (STRING (26); http://string-db.org) (version 11.5) is a database for the study of protein interactions with information on more than 14,000 species, more than 60 million proteins, and more than 20 billion interactions, which include both direct physical interactions as well as indirect functional correlations. The protein-protein interaction (PPI) interaction network of the common DEGs was constructed by STRING with an interaction score > 0.4. Cytoscape software (27) (version 3.9.0) was used to visualize the PPI network and we used the Cytoscape plug-in Molecular Complex Detection (MCODE (28)) to analyze core functional modules. The parameters were set as follows: degree cutoff = 2, max depth = 100, node score cutoff = 0.2 and K-core = 2. Then KOBAS 3.0 was applied to carry out KEGG and GO analysis of the genes in each module.

Identification and analysis of hub genes

The hub genes were selected by a plug-in cytoHubba (29) of Cytoscape and then seven algorithms (Closeness, MCC, Degree, MNC, Radiality, Stress and EPC) were used to confirm the final hub genes, which were visualized by Venn diagram. GeneMANIA (30) (http://genemania.org), an online tool that can predict gene interactions, was utilized to construct a co-expression network of identified hub genes.

Construction of TF-gene regulatory network and TF-miRNA regulatory network

In this study, TF-gene regulatory network and TF-miRNA regulatory network were constructed by utilizing the Networkanalyst platform. In the case of TF-gene regulatory network, the ENCODE (31) (https://www.encodeproject.org/) database, which is included in the Networkanalyst platform, was been used. As for TF-miRNA regulatory network, it was acquired from the RegNetwork (32) (http://www.regnetworkweb.org) database, which is incorporated in the NetworkAnalyst platform.

ROC curves of hub genes

ROC curves were constructed and the area under the ROC curve (AUC) was calculated separately to evaluate the diagnostic performance of the hub genes on COVID-19 and pSS using the R packages "pROC" (33).

Results

Identification of DEGs and shared genes between COVID-19 and primary Sjogren's syndrome

The overall flow chart of this study was shown in Figure 1. For GSE157103 dataset, a total of 1003 DEGs were identified, among which 554 genes were up-regulated and 449 genes were down-regulated (Figure 2A). Based on the GSE40611 dataset, we identified 351 DEGs including 291 upregulated genes and 60 downregulated genes (Figure 2B). Then by taking the intersection of DEGs of GSE157103 dataset and GSE40611 dataset, there were 40 shared DEGs selected, which were visualized by Venn diagrams (Figure 2C).

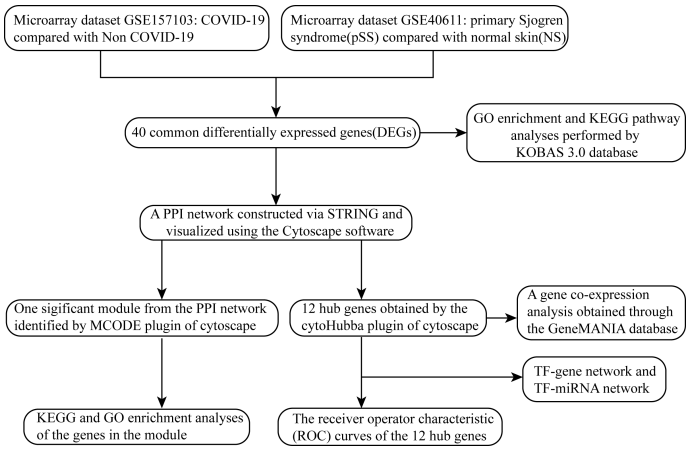

FIGURE 1
Workflow diagram of this study.

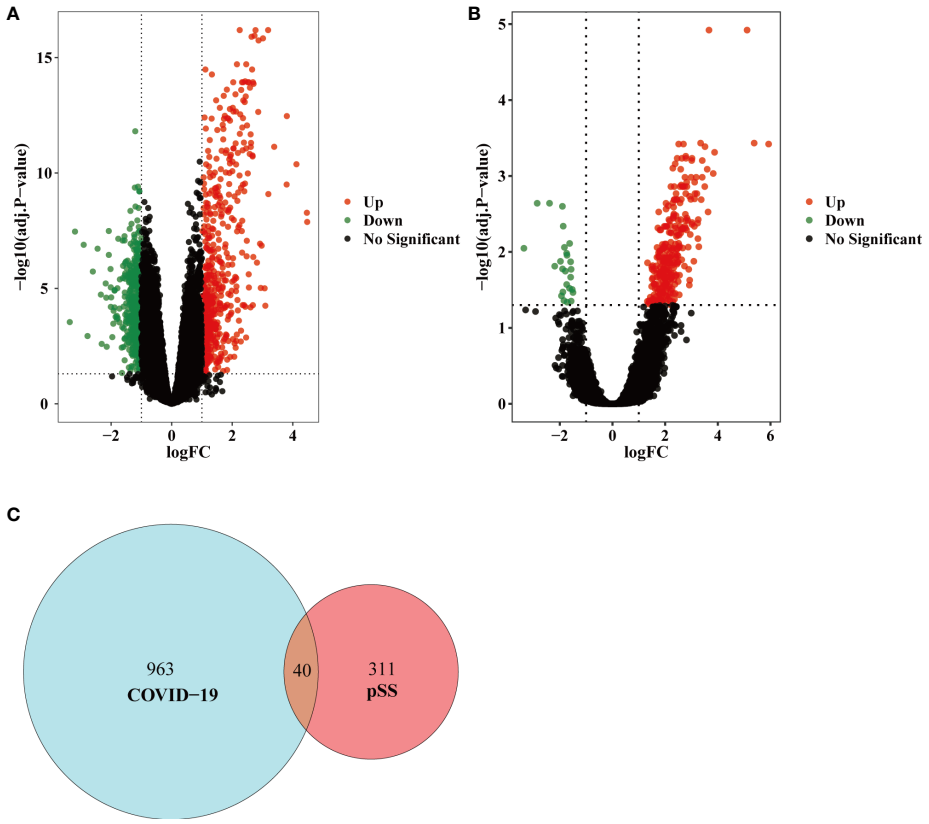

FIGURE 2
Volcano diagram and Venn diagram. **(A)** The volcano map of GSE157103. **(B)** The volcano map of GSE40611. Upregulated genes are colored in red; downregulated genes are colored in green. **(C)** The two datasets showed an overlap of 40 DEGs.

GO and KEGG pathway enrichment analysis

For GO enrichment analysis, the top five significant terms showed that the shared DEGs were mainly involved in protein binding cytoplasm, cytosol, nucleus and nucleoplasm (Figure 3A). In terms of KEGG pathway enrichment analysis, the top five significant terms were metabolic pathways, pyrimidine metabolism, cell cycle, hepatitis C and cytokine-cytokine receptor interaction. These results forcefully indicated that cellular component and metabolic pathways collectively participated in the development and progression of both inflammatory diseases (Figure 3B).

Protein–protein interaction network analysis and submodule analysis

The PPI network included 40 nodes and 149 edges, of which the PPI enrichment P-value was lower than 1.0e − 16 (Figure 4). By visualizing the PPI network using Cytoscape software, the redder the color of the gene in the network, the higher the connectivity of the gene with other genes. A key gene module, including 25 shared DEGs, was obtained by applying the MCODE plug-in of Cytoscape (Figure 5A). GO enrichment analysis of these genes in the module showed that these genes were mainly associated with cytoplasm, defense response to virus, response to virus, cytosol and type I interferon signaling pathway (Figure 5B). KEGG enrichment analysis of these genes in the module indicated that these genes were mainly related to pyrimidine metabolism, cell cycle, p53 signaling pathway, progesterone-mediated oocyte maturation and cellular senescence (Figure 5C).

Identification and functional analysis of hub genes

By applying the seven algorithms of plug-in cytoHubba, we screened the top 20 hub genes. Through the intersection of Venn diagrams, 12 common hub genes were finally identified, including CMPK2, TYMS, RRM2, HERC5, IFI44L, IFI44, IFIT2, IFIT1, IFIT3, MX1, CDCA2 and TOP2A (Figure 6A). According to GeneMANIA database, we constructed a complex gene interaction network to decipher the biological functions of these hub genes, with the co-expression of 60.37%, physical interactions of 33.91%, co-localization of 3.46%, predicted of 2.15% and pathway of 0.10% (Figure 6B). Twenty genes associated with the 12 hub genes were identified, and the results showed that they were mainly linked to response to type I interferon, response to virus, regulation of viral genome replication, regulation of viral life cycle, viral life cycle, deoxyribonucleotide metabolic process and adenylyltransferase activity.

TF-gene interactions and TF-miRNA co-regulatory network

TFs which can interact with the 12 hub genes were predicted by Networkanalyst, and the TF-gene regulatory network was plotted and visualized by Cytoscape (Figure 7). The network contains 124 TFs, 134 nodes and 165 edges. These TFs regulate more than one hub gene in the network, which demonstrated the high interaction of TFs with hub genes. Subsequently, TF-miRNA co-regulatory network was constructed using NetworkAnalyst, which predicted the interaction of miRNA and TF with hub genes (Figure 8). This interaction may be responsible for the regulation of hub gene expression. The network included 65 nodes and 85 edges and 12 miRNAs and 45 TF genes interacted with hub genes.

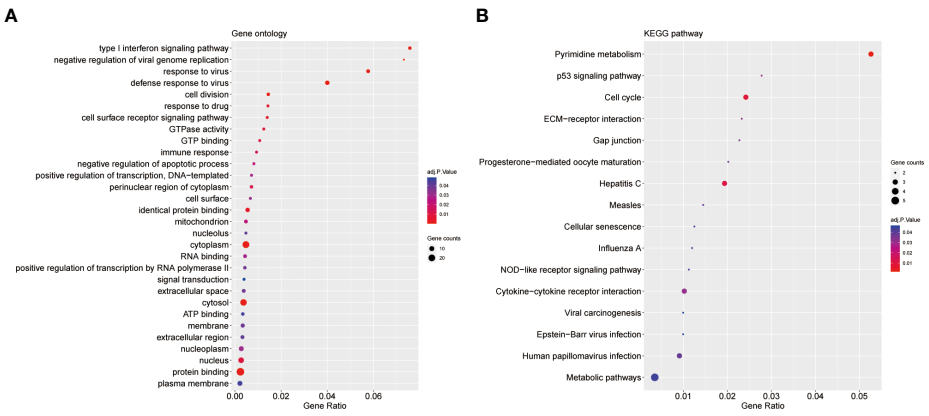

FIGURE 3
GO and KEGG enrichment analysis of common DEGs. **(A)**The enrichment analysis results of GO. **(B)**The enrichment analysis results of KEGG Pathway. Adjusted P-value < 0.05 was considered significant.

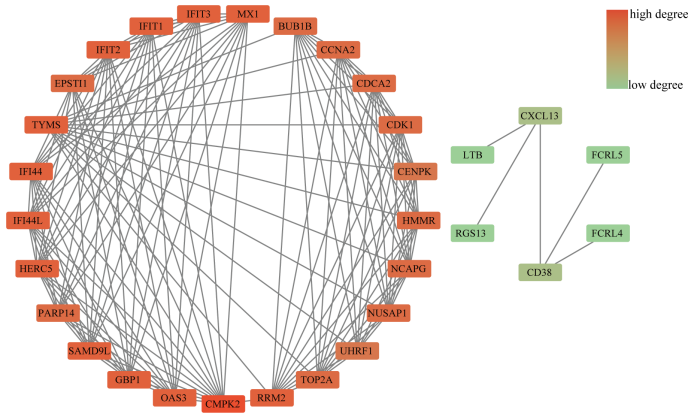

FIGURE 4
PPI network diagram. The redder the color of the gene in the network, the higher the connectivity of the gene with other genes.

ROC curves of hub genes

We assessed the diagnostic efficacy of the 12 hub genes by plotting ROC curves. In the COVID-19 dataset, TYMS (AUC:0.952), RRM2(AUC:0.954), CDCA2(AUC:0.946) and TOP2A(AUC:0.958) exhibited good diagnostic efficiency for differentiating the patients with SARS-CoV-2 from healthy controls (Figure 9A). In the pSS dataset, CMPK2 (AUC:0.922), TYMS (AUC:0.918), IFI44 (AUC:0.925), IFIT1 (AUC:0.948), IFIT3(AUC:0.944) and MX1 (AUC:0.935) exhibited preferable diagnostic performance for differentiating pSS patients from healthy controls (Figure 9B).

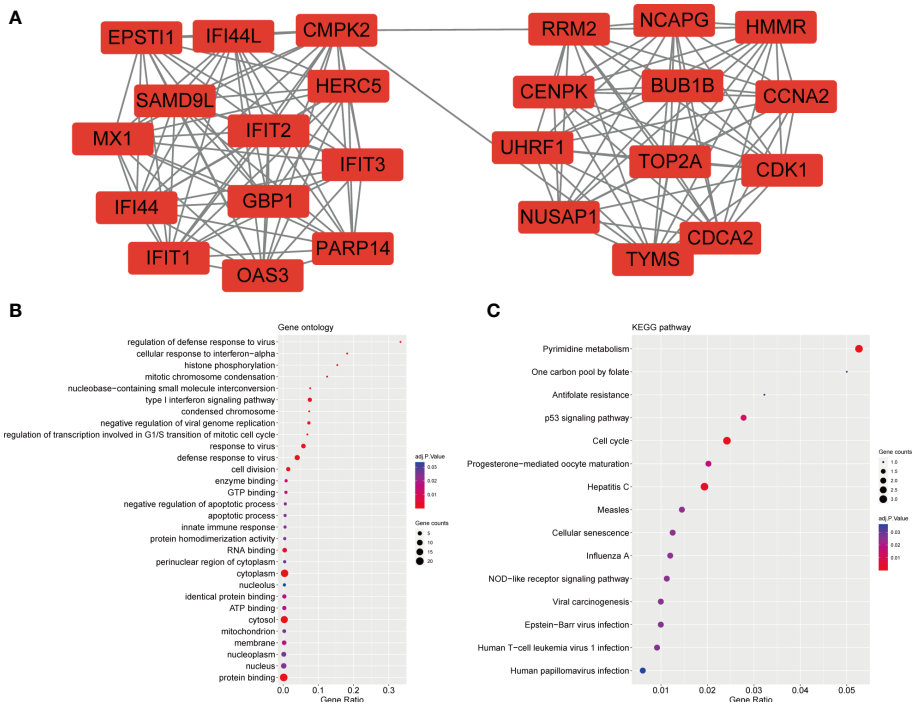

FIGURE 5
Significant gene module and enrichment analysis of the modular genes **(A)** A significant gene clustering module. **(B)** GO enrichment analysis of the modular genes. **(C)** KEGG enrichment analysis of the modular genes.

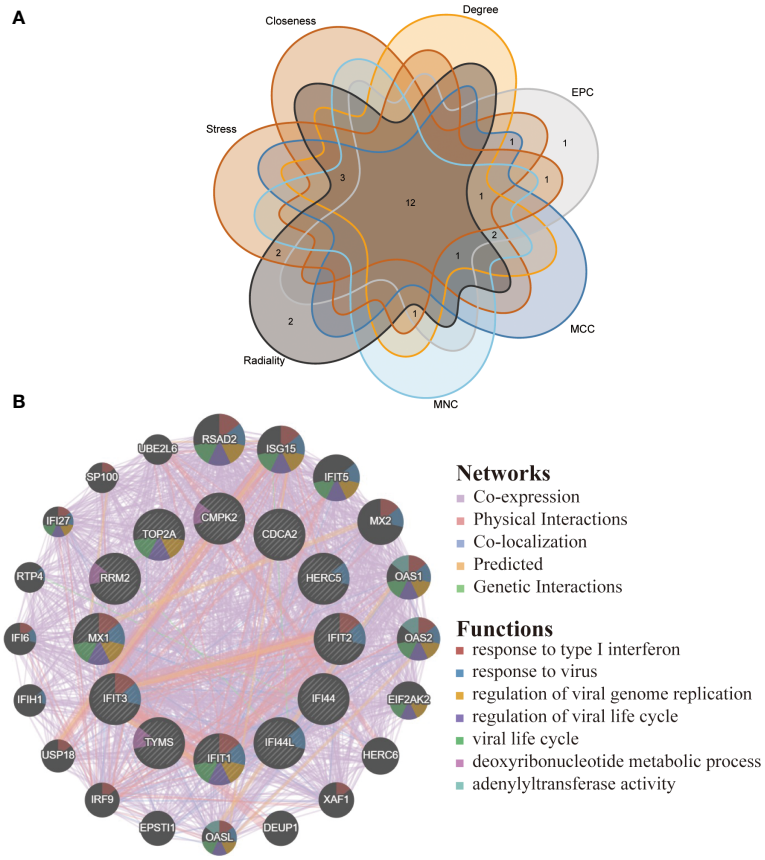

FIGURE 6
Venn diagram and co-expression network of hub genes. **(A)** The Venn diagram showed 12 overlapping hub genes screened by 7 algorithms. **(B)** Hub genes and their co-expression genes were analyzed *via* GeneMANIA.

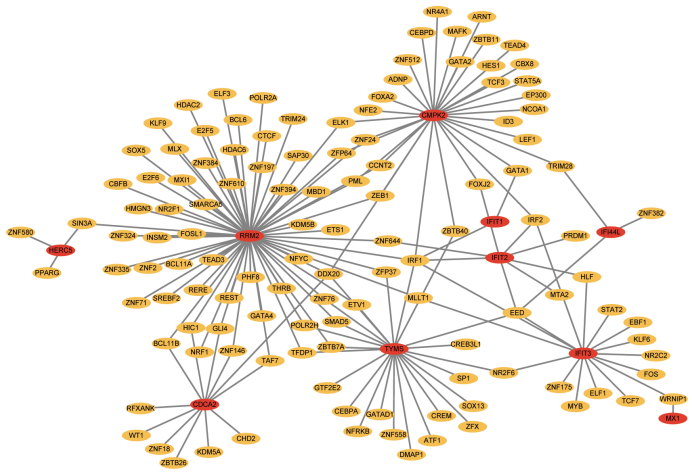

FIGURE 7
Network for TF-gene interaction with hub genes. The highlighted blue color node represents the hub genes and other nodes represent TF-genes.

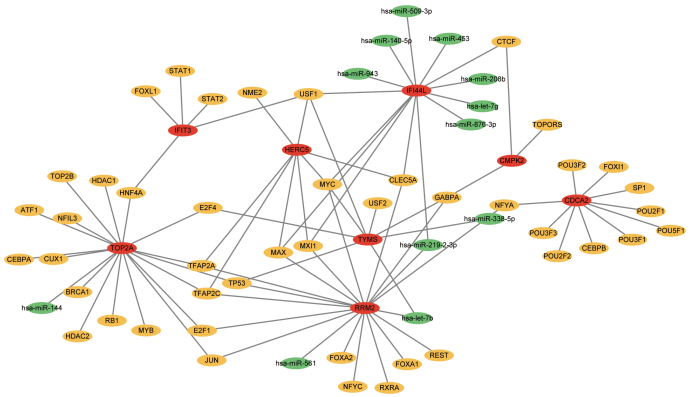

FIGURE 8
The network presents the TF-miRNA coregulatory network. The network consists of 65 nodes and 85 edges including 45 TF-genes, 12 miRNA and 8 hub genes. The nodes in red color are the hub genes, a yellow node represents TF-genes and other nodes indicate miRNAs.

Discussion

Evidence has indicated that the prevalence of COVID-19 was significantly higher in patients with pSS compared to the general population. A variety of viruses (EBV, CMV and HCV) have been found to be closely associated with the development of pSS, but there are still fewer studies on COVID-19 and pSS. Hence, we attempted to explore the shared molecular biological function and pathways between COVID-19 and pSS, and to determine the interrelationship between COVID-19 and pSS.

In this study, 40 shared DEGs of COVID-19 and pSS have been identified. After constructing the PPI network of common DEGs, we identified 12 hub genes (CMPK2, TYMS, RRM2, HERC5, IFI44L, IFI44, IFIT2, IFIT1, IFIT3, MX1, CDCA2 and TOP2A).

Seven genes have been reported to be related to the pathological mechanism of COVID-19 and pSS. CMPK2 (Cytidine/uridine monophosphate kinase 2) is a thymidylate kinase, known to be associated with mitochondrial DNA (mtDNA) synthesis, and may attenuate the severity of acute respiratory distress syndrome (ARDS), a common complication of severe COVID-19, by rate-limiting for mtDNA synthesis (34, 35). In pSS samples, CMPK2 was reported to be upregulated and was linked to the extent of immune cell infiltration, mitochondrial respiratory chain complexes, and

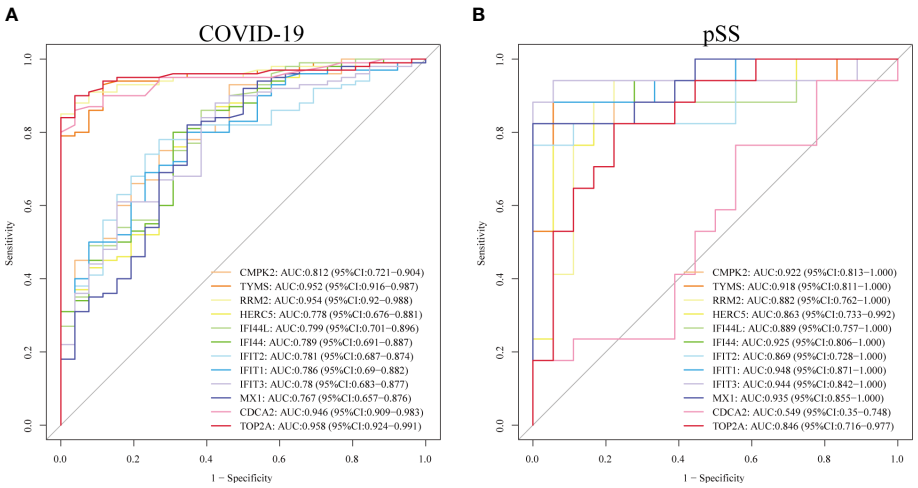

FIGURE 9
Validation of diagnostic shared biomarkers. **(A)** The ROC curve of the diagnostic efficacy verification in GSE157103. **(B)** The ROC curve of the diagnostic efficacy verification in GSE40611.

mitochondrial metabolic pathways (36). HERC5 (HECT and RLD domain containing E3 ubiquitin protein ligase 5) is an antiviral immune protein which is induced by interferon. It can inhibit replication of hepatitis C (HCV), influenza A (IAV), human immunodeficiency virus (HIV), SARS-CoV-2 and other viruses by mediating ISGylation of protein targets induced by type I interferon (37–39). IFI44L (Interferon(IFN) Induced Protein 44 Like) is a type-1 I interferon-stimulated gene, induced by several different viruses. IFI44L expression was significantly higher in pSS patients than in controls and was markedly increased after IFN-α or IFN-β stimulation (40, 41). In addition, this gene was also significantly upregulated in SARS-CoV-2 infected cardiac tissues (42). As a feedback regulator of IFN responses, IFI44L can facilitate virus replication *via* modulating innate immune responses induced after virus infections (43). IFIT (Interferon-induced protein with tetratricopeptide repeats) genes are interferon-stimulated genes and consist of four genes, IFIT1, IFIT2, IFIT3 and IFIT5. The expression of IFIT genes is low in multiple cell types, while viral infection can increase their expression. In pathological conditions, they inhibit viral replication by binding and modulating the function of cellular and viral proteins (44, 45). IFIT1, IFIT2 and IFIT3 have been shown to be upregulated in cells infected with SARS-CoV-2, indicating activation of the interferon innate response, which could be regarded as potential drug targets for the treatment of COVID-19 (46–48). Moreover, they may upregulate the expression of CXCL10 which induces lymphocyte chemotaxis and may inhibit the replication of viruses. These molecules may play a critical role in the innate immune response in response to viruses (49). MX1 (Myxovirus resistance 1) encodes a guanosine triphosphate (GTP) metabolizing protein involved in the cellular antiviral response. The encoded protein is induced by type I and type II interferons and antagonizes the replication process of multiple different RNA and DNA viruses. Through binding to viral nucleoproteins, MX1 can interfere with the transcription of influenza viruses (50–52). Several studies have revealed that MX1 is overexpressed in COVID-19 group compared to control group, due to the activation of MX1 responding to new viruses for which the body has no immune defense (53–55). In addition, the baseline level of MX1 help to identify SARS-CoV-2-positive patients and help to differentiate patients who are inclined to different outcomes (56). Similarly, the expression of MX1 was significantly upregulated in the pSS (57). For the remaining five hub genes (TYMS, CDCA2, TOP2A, RRM2 and IFI44), there are no studies reporting their role in COVID-19 or pSS, which emphasizes its importance in future research.

In this study, GO enrichment analysis indicated that the type I interferon signaling pathway is common pathogenesis of COVID-19 and pSS. Furthermore, based on published publications, we hypothesized that type I interferon might be a shared mechanism of COVID-19 and pSS.

Interferon (IFN) is a class of cytokines with antiviral effects that directly induce anti-pathogenic immune responses by controlling the inflammatory response and coordinating the immune response, thereby resisting invasion and infection by foreign pathogens (58). Interferons induced by viral infections can be produced through different signaling pathways, eventually leading to the transcription and expression of hundreds of IFN-stimulated genes (ISGs), which further exert antiviral effects (59). Interferons are classified into three major classes: type I, II, and III interferons. Type I interferons (IFN-α, IFN-β, IFN-ϵ, IFN-κ, IFN-ω) are secreted by virus-infected cells, type II interferons (IFN-γ) are secreted by activated T cells, and type III IFN (IFN-λ) binds to type III IFN receptors (IFNLR) and is preferentially expressed on epithelial cells and certain bone marrow cells (60). Type I interferon is the main type of interferon that can exert antiviral effects.

Although IFN has anti-multiviral effects, it does not kill viruses directly, but rather inhibits the replication process by producing antiviral proteins (61). Studies have demonstrated that IFN can induce the expression of antiviral proteins upon viral infection (62). IFN-α can significantly enhance cellular susceptibility to microorganisms by upregulating Toll-like receptors (TLRs) expression or the expression of transduction molecules and kinases involved in TLR signaling (63). Moreover, IFN-α strongly increases the differentiation of T cells and enhances cellular immunity (64). In addition to its effect on T cells, IFN can also promote the proliferation of B cells and enhance humoral immune responses (65). In summary, there are two main antiviral mechanisms of IFN: one is acting on viruses, such as interfering with viral replication, and the other is acting on cells to strengthen the immune function of the body.

There is substantial evidence that type I interferon plays an important role in the pathogenesis and progression of pSS due to immune dysregulation (66). For example, it can influence the immune response to pSS, participating in the activation of antiviral responses and controlling immune responses through interactions with the corresponding receptors (67). An important role of type I interferon is to induce immune activation, which affects the production and regulation of pro-inflammatory cytokines and other mediators (68). Monocytes are stimulated by type I interferon to differentiate into dendritic cells and stimulate immature dendritic cells to express chemokines and costimulatory molecules that facilitate their homing to secondary lymphoid organs, thereby activating adaptive immunity (69). In addition, macrophages are stimulated by interferon to enhance phagocytosis. BAFF (B cell activating factor) is known to be involved in the pathogenesis of pSS, as it is upregulated in monocytes in response to type I and type II IFN and promotes B-cell

survival (70). In addition to monocytes, macrophages, dendritic cells and salivary gland epithelial cells also express BAFF in response to IFN stimulation (71, 72). Transgenic mice that overproduce BAFF exhibit increased B cell proliferation, increased germinal center responses, autoantibody production, and increased numbers of immune complexes (73). This suggests that IFN (especially IFN type I) promotes the development of pSS by inducing innate immunity, activating adaptive immunity, and regulating inflammatory cytokines and antibody levels.

Although previous studies have explored the pivotal genes associated with COVID-19 and pSS, respectively. However, few studies have explored the common molecular mechanisms between the two through bioinformatic approaches. In this study, we explored and identified common DEGs, hub genes and TFs of COVID-19 and pSS for the first time, which helped to further elucidate the pathogenesis of both. However, our study also has some limitations. First, this study requires external validation to verify our findings; second, the function of hub genes needs to be further validated in an *in vitro* model, which will be the focus of our future work.

In conclusion, we identified common DEGs for COVID-19 and pSS and performed enrichment and PPI network analysis. We found that COVID-19 and pSS share pathogenic mechanism that may be mediated by specific hub genes. This study provides a potential direction for further investigation of the molecular mechanisms of COVID-19 and pSS.

Data availability statement

The datasets presented in this study can be found in online repositories. The names of the repository/repositories and accession number(s) can be found in the article/supplementary material.

Author contributions

HL performed data analyses and wrote the manuscript draft. XZ revised the manuscript. All authors read and approved the final manuscript. All authors contributed to the article and approved the submitted version.

Funding

This research was supported financially by the Funding of Wuhan Health Planning Commission Program (WX15B21, to XZ).

Acknowledgements

We thank the authors of the GSE157103 and GSE40611 datasets for their contribution.

Conflict of interest

The authors declare that the research was conducted in the absence of any commercial or financial relationships that could be construed as a potential conflict of interest.

Publisher's note

References

1. Mavragani CP. Mechanisms and new strategies for primary sjögren's syndrome. *Annu Rev Med* (2017) 68:331–43. doi: 10.1146/annurev-med-043015-123313

2. Li N, Li L, Wu M, Li Y, Yang J, Wu Y, et al. Integrated bioinformatics and validation reveal potential biomarkers associated with progression of primary sjögren's syndrome. *Front Immunol* (2021) 12:697157. doi: 10.3389/fimmu.2021.697157

3. Qin B, Wang J, Yang Z, Yang M, Ma N, Huang F, et al. Epidemiology of primary sjögren's syndrome: A systematic review and meta-analysis. *Ann Rheum Dis* (2015) 74(11):1983–9. doi: 10.1136/annrheumdis-2014-205375

4. Fox RI. Sjögren's syndrome. *Lancet* (2005) 366(9482):321–31. doi: 10.1016/s0140-6736(05)66990-5

5. Kapsogeorgou EK, Voulgarelis M, Tzioufas AG. Predictive markers of lymphomagenesis in sjögren's syndrome: From clinical data to molecular stratification. *J Autoimmun* (2019) 104:102316. doi: 10.1016/j.jaut.2019.102316

6. Draborg A, Izarzugaza JM, Houen G. How compelling are the data for Epstein-Barr virus being a trigger for systemic lupus and other autoimmune diseases? *Curr Opin Rheumatol* (2016) 28(4):398–404. doi: 10.1097/bor.0000000000000289

7. Saito I, Servenius B, Compton T, Fox RI. Detection of Epstein-barr virus DNA by polymerase chain reaction in blood and tissue biopsies from patients with sjogren's syndrome. *J Exp Med* (1989) 169(6):21941–8. doi: 10.1084/jem.169.6.2191

8. Liu X, Sadaoka T, Krogmann T, Cohen JI. Epstein-Barr Virus (Ebv) tegument protein Bglf2 suppresses type I interferon signaling to promote ebv reactivation. *J Virol* (2020) 94(11):e00258–20. doi: 10.1128/jvi.00258-20

9. Shimizu T, Nakamura H, Takatani A, Umeda M, Horai Y, Kurushima S, et al. Activation of toll-like receptor 7 signaling in labial salivary glands of primary sjögren's syndrome patients. *Clin Exp Immunol* (2019) 196(1):39–51. doi: 10.1111/cei.13242

10. Navone R, Lunardi C, Gerli R, Tinazzi E, Peterlana D, Bason C, et al. Identification of tear lipocalin as a novel autoantigen target in sjögren's syndrome. *J Autoimmun* (2005) 25(3):229–34. doi: 10.1016/j.jaut.2005.09.021

11. Croia C, Astorri E, Murray-Brown W, Willis A, Brokstad KA, Sutcliffe N, et al. Implication of Epstein-Barr virus infection in disease-specific autoreactive b cell activation in ectopic lymphoid structures of sjögren's syndrome. *Arthritis Rheumatol (Hoboken NJ)* (2014) 66(9):2545–57. doi: 10.1002/art.38726

12. Kivity S, Arango MT, Ehrenfeld M, Tehori O, Shoenfeld Y, Anaya JM, et al. Infection and autoimmunity in sjogren's syndrome: A clinical study and

comprehensive review. *J Autoimmun* (2014) 51:17–22. doi: 10.1016/j.jaut.2014.02.008

13. Haddad J, Deny P, Munz-Gotheil C, Ambrosini JC, Trinchet JC, Pateron D, et al. Lymphocytic sialadenitis of sjögren's syndrome associated with chronic hepatitis c virus liver disease. *Lancet* (1992) 339(8789):321–3. doi: 10.1016/0140-6736(92)91645-o

14. Huang C, Wang Y, Li X, Ren L, Zhao J, Hu Y, et al. Clinical features of patients infected with 2019 novel coronavirus in wuhan, China. *Lancet* (2020) 395 (10223):497–506. doi: 10.1016/s0140-6736(20)30183-5

15. Ferri C, Giuggioli D, Raimondo V, L'Andolina M, Tavoni A, Cecchetti R, et al. Covid-19 and rheumatic autoimmune systemic diseases: Report of a Large Italian patients series. *Clin Rheumatol* (2020) 39(11):3195–204. doi: 10.1007/s10067-020-05334-7

16. Chowdhury F, Grigoriadou S, Bombardieri M. Severity of covid-19 infection in primary sjögren's syndrome and the emerging evidence of covid-19-Induced xerostomia. *Clin Exp Rheumatol* (2021) 39 Suppl 133(6):215–22. doi: 10.55563/clinexprheumatol/k7x3ta

17. Akiyama S, Hamdeh S, Micic D, Sakuraba A. Prevalence and clinical outcomes of covid-19 in patients with autoimmune diseases: A systematic review and meta-analysis. *Ann Rheum Dis* (2020) 80(3):384–91. doi: 10.1136/annrheumdis-2020-218946

18. Saadoun D, Vieira M, Vautier M, Baraliakos X, Andreica I, da Silva JAP, et al. Sars-Cov-2 outbreak in immune-mediated inflammatory diseases: The Euro-covimid multicentre cross-sectional study. *Lancet Rheumatol* (2021) 3(7):e481–e8. doi: 10.1016/s2665-9913(21)00112-0

19. Barrett T, Troup DB, Wilhite SE, Ledoux P, Evangelista C, Kim IF, et al. Ncbi geo: Archive for functional genomics data sets–10 years on. *Nucleic Acids Res* (2011) 39(Database issue):D1005–10. doi: 10.1093/nar/gkq1184

20. Overmyer KA, Shishkova E, Miller IJ, Balnis J, Bernstein MN, Peters-Clarke TM, et al. Large-Scale multi-omic analysis of covid-19 severity. *Cell Syst* (2021) 12 (1):23–40.e7. doi: 10.1016/j.cels.2020.10.003

21. Horvath S, Nazmul-Hossain AN, Pollard RP, Kroese FG, Vissink A, Kallenberg CG, et al. Systems analysis of primary sjögren's syndrome pathogenesis in salivary glands identifies shared pathways in human and a mouse model. *Arthritis Res Ther* (2012) 14(6):R238. doi: 10.1186/ar4081

22. Barrett T, Wilhite SE, Ledoux P, Evangelista C, Kim IF, Tomashevsky M, et al. Ncbi geo: Archive for functional genomics data sets–update. *Nucleic Acids Res* (2013) 41(Database issue):D991–5. doi: 10.1093/nar/gks1193

23. Xia J, Benner MJ, Hancock RE. Networkanalyst–integrative approaches for protein-protein interaction network analysis and visual exploration. *Nucleic Acids Res* (2014) 42(Web Server issue):W167–74. doi: 10.1093/nar/gku443

24. Chen H, Boutros PC. Venndiagram: A package for the generation of highly-customizable Venn and Euler diagrams in r. *BMC Bioinf* (2011) 12:35. doi: 10.1186/1471-2105-12-35

25. Bu D, Luo H, Huo P, Wang Z, Zhang S, He Z, et al. Kobas-I: Intelligent prioritization and exploratory visualization of biological functions for gene enrichment analysis. *Nucleic Acids Res* (2021) 49(W1):W317–25. doi: 10.1093/nar/gkab447

26. Szklarczyk D, Gable AL, Lyon D, Junge A, Wyder S, Huerta-Cepas J, et al. String V11: Protein-protein association networks with increased coverage, supporting functional discovery in genome-wide experimental datasets. *Nucleic Acids Res* (2019) 47(D1):D607–13. doi: 10.1093/nar/gky1131

27. Shannon P, Markiel A, Ozier O, Baliga NS, Wang JT, Ramage D, et al. Cytoscape: A software environment for integrated models of biomolecular interaction networks. *Genome Res* (2003) 13(11):2498–504. doi: 10.1101/gr.1239303

28. Bader GD, Hogue CW. An automated method for finding molecular complexes in Large protein interaction networks. *BMC Bioinf* (2003) 4:2. doi: 10.1186/1471-2105-4-2

29. Chin CH, Chen SH, Wu HH, Ho CW, Ko MT, Lin CY. Cytohubba: Identifying hub objects and Sub-networks from complex interactome. *BMC Syst Biol* (2014) 8 Suppl 4(Suppl 4):S11. doi: 10.1186/1752-0509-8-s4-s11

30. Franz M, Rodriguez H, Lopes C, Zuberi K, Montojo J, Bader GD, et al. Genemania update 2018. *Nucleic Acids Res* (2018) 46(W1):W60–4. doi: 10.1093/nar/gky311

31. Davis CA, Hitz BC, Sloan CA, Chan ET, Davidson JM, Gabdank I, et al. The encyclopedia of DNA elements (Encode): Data portal update. *Nucleic Acids Res* (2018) 46(D1):D794–801. doi: 10.1093/nar/gkx1081

32. Liu ZP, Wu C, Miao H, Wu H. Regnetwork: An integrated database of transcriptional and post-transcriptional regulatory networks in human and mouse. *Database (Oxford)* (2015) 2015:bav095. doi: 10.1093/database/bav095

33. Robin X, Turck N, Hainard A, Tiberti N, Lisacek F, Sanchez JC, et al. Proc: An open-source package for r and s+ to analyze and compare roc curves. *BMC Bioinf* (2011) 12:77. doi: 10.1186/1471-2105-12-77

34. Feng C, Tang Y, Liu X, Zhou Z. Cmpk2 of triploid crucian carp is involved in immune defense against bacterial infection. *Dev Comp Immunol* (2021) 116:103924. doi: 10.1016/j.dci.2020.103924

35. Xian H, Liu Y, Rundberg Nilsson A, Gatchalian R, Crother TR, Tourtellotte WG, et al. Metformin inhibition of mitochondrial atp and DNA synthesis abrogates Nlrp3 inflammasome activation and pulmonary inflammation. *Immunity* (2021) 54(7):1463–77.e11. doi: 10.1016/j.immuni.2021.05.004

36. Li N, Li Y, Hu J, Wu Y, Yang J, Fan H, et al. A link between mitochondrial dysfunction and the immune microenvironment of salivary glands in primary sjogren's syndrome. *Front Immunol* (2022) 13:845209. doi: 10.3389/fimmu.2022.845209

37. Xue F, Higgs BW, Huang J, Morehouse C, Zhu W, Yao X, et al. Herc5 is a prognostic biomarker for post-liver transplant recurrent human hepatocellular carcinoma. *J Transl Med* (2015) 13:379. doi: 10.1186/s12967-015-0743-2

38. Paparisto E, Woods MW, Coleman MD, Moghadasi SA, Kochar DS, Tom SK, et al. Evolution-guided structural and functional analyses of the herc family reveal an ancient marine origin and determinants of antiviral activity. *J Virol* (2018) 92(13):e00528–18. doi: 10.1128/jvi.00528-18

39. Mathieu NA, Paparisto E, Barr SD, Spratt DE. Herc5 and the isgylation pathway: Critical modulators of the antiviral immune response. *Viruses* (2021) 13 (6):1102. doi: 10.3390/v13061102

40. Zhao M, Zhou Y, Zhu B, Wan M, Jiang T, Tan Q, et al. Ifi44l promoter methylation as a blood biomarker for systemic lupus erythematosus. *Ann Rheum Dis* (2016) 75(11):1998–2006. doi: 10.1136/annrheumdis-2015-208410

41. Jara D, Carvajal P, Castro I, Barrera MJ, Aguilera S, González S, et al. Type I interferon dependent hsa-Mir-145-5p downregulation modulates Muc1 and Tlr4 overexpression in salivary glands from sjögren's syndrome patients. *Front Immunol* (2021) 12:685837. doi: 10.3389/fimmu.2021.685837

42. Bräuninger H, Stoffers B, Fitzek ADE, Meißner K, Aleshcheva G, Schweizer M, et al. Cardiac sars-Cov-2 infection is associated with pro-inflammatory transcriptomic alterations within the heart. *Cardiovasc Res* (2022) 118(2):542–55. doi: 10.1093/cvr/cvab322

43. DeDiego ML, Martinez-Sobrido L, Topham DJ. Novel functions of Ifi44l as a feedback regulator of host antiviral responses. *J Virol* (2019) 93(21):e01159–19. doi: 10.1128/jvi.01159-19

44. Pidugu VK, Pidugu HB, Wu MM, Liu CJ, Lee TC. Emerging functions of human ifit proteins in cancer. *Front Mol Biosci* (2019) 6:148. doi: 10.3389/fmolb.2019.00148

45. Fensterl V, Sen GC. Interferon-induced ifit proteins: Their role in viral pathogenesis. *J Virol* (2015) 89(5):2462–8. doi: 10.1128/jvi.02744-14

46. Vishnubalaji R, Shaath H, Alajez NM. Protein coding and long noncoding rna (Lncrna) transcriptional landscape in sars-Cov-2 infected bronchial epithelial cells highlight a role for interferon and inflammatory response. *Genes* (2020) 11 (7):760. doi: 10.3390/genes11070760

47. Caldarale F, Giacomelli M, Garrafa E, Tamassia N, Morreale A, Poli P, et al. Plasmacytoid dendritic cells depletion and elevation of ifn-Γ dependent chemokines Cxcl9 and Cxcl10 in children with multisystem inflammatory syndrome. *Front Immunol* (2021) 12:654587. doi: 10.3389/fimmu.2021.654587

48. Prasad K, Khatoon F, Rashid S, Ali N, AlAsmari AF, Ahmed MZ, et al. Targeting hub genes and pathways of innate immune response in covid-19: A network biology perspective. *Int J Biol Macromol* (2020) 163:1–8. doi: 10.1016/j.ijbiomac.2020.06.228

49. Imaizumi T, Hashimoto S, Sato R, Umetsu H, Aizawa T, Watanabe S, et al. Ifit proteins are involved in Cxcl10 expression in human glomerular endothelial cells treated with a toll-like receptor 3 agonist. *Kidney Blood Press Res* (2021) 46 (1):74–83. doi: 10.1159/000511915

50. Aljohani AI, Joseph C, Kurozumi S, Mohammed OJ, Miligy IM, Green AR, et al. Myxovirus resistance 1 (Mx1) is an independent predictor of poor outcome in invasive breast cancer. *Breast Cancer Res Treat* (2020) 181(3):541–51. doi: 10.1007/s10549-020-05646-x

51. Verhelst J, Hulpiau P, Saelens X. Mx proteins: Antiviral gatekeepers that restrain the uninvited. *Microbiol Mol Biol Rev* (2013) 77(4):551–66. doi: 10.1128/mmbr.00024-13

52. Pillai PS, Molony RD, Martinod K, Dong H, Pang IK, Tal MC, et al. Mx1 reveals innate pathways to antiviral resistance and lethal influenza disease. *Science* (2016) 352(6284):463–6. doi: 10.1126/science.aaf3926

53. Haller O, Staeheli P, Schwemmle M, Kochs G. Mx gtpases: Dynamin-like antiviral machines of innate immunity. *Trends Microbiol* (2015) 23(3):154–63. doi: 10.1016/j.tim.2014.12.003

54. Bizzotto J, Sanchis P, Abbate M, Lage-Vickers S, Lavignolle R, Toro A, et al. Sars-Cov-2 infection boosts Mx1 antiviral effector in covid-19 patients. *iScience* (2020) 23(10):101585. doi: 10.1016/j.isci.2020.101585

55. Verhelst J, Parthoens E, Schepens B, Fiers W, Saelens X. Interferon-inducible protein Mx1 inhibits influenza virus by interfering with functional

viral ribonucleoprotein complex assembly. *J Virol* (2012) 86(24):13445–55. doi: 10.1128/jvi.01682-12

56. Maras JS, Sharma S, Bhat A, Rooge S, Aggrawal R, Gupta E, et al. Multi-omics analysis of respiratory specimen characterizes baseline molecular determinants associated with sars-Cov-2 outcome. *iScience* (2021) 24(8):102823. doi: 10.1016/j.isci.2021.102823

57. Papinska J, Bagavant H, Gmyrek GB, Deshmukh US. Pulmonary involvement in a mouse model of sjögren's syndrome induced by sting activation. *Int J Mol Sci* (2020) 21(12):4512. doi: 10.3390/ijms21124512

58. Wang W, Xu L, Su J, Peppelenbosch MP, Pan Q. Transcriptional regulation of antiviral interferon-stimulated genes. *Trends Microbiol* (2017) 25(7):573–84. doi: 10.1016/j.tim.2017.01.001

59. Park A, Iwasaki A. Type I and type iii interferons - induction, signaling, evasion, and application to combat covid-19. *Cell Host Microbe* (2020) 27(6):870–8. doi: 10.1016/j.chom.2020.05.008

60. Kotenko SV, Rivera A, Parker D, Durbin JE. Type iii ifns: Beyond antiviral protection. *Semin Immunol* (2019) 43:101303. doi: 10.1016/j.smim.2019.101303

61. Zhang R, Tang J. Evasion of I interferon-mediated innate immunity by pseudorabies virus. *Front Microbiol* (2021) 12:801257. doi: 10.3389/fmicb.2021.801257

62. Liu SY, Sanchez DJ, Cheng G. New developments in the induction and antiviral effectors of type I interferon. *Curr Opin Immunol* (2011) 23(1):57–64. doi: 10.1016/j.coi.2010.11.003

63. Mitchell D, Chintala S, Dey M. Plasmacytoid dendritic cell in immunity and cancer. *J Neuroimmunol* (2018) 322:63–73. doi: 10.1016/j.jneuroim.2018.06.012

64. Chenna Narendra S, Chalise JP, Biggs S, Kalinke U, Magnusson M. Regulatory T-cells mediate ifn-A-Induced resistance against antigen-induced arthritis. *Front Immunol* (2018) 9:285. doi: 10.3389/fimmu.2018.00285

65. Graalmann T, Borst K, Manchanda H, Vaas L, Bruhn M, Graalmann L, et al. B cell depletion impairs vaccination-induced Cd8(+) T cell responses in a type I interferon-dependent manner. *Ann Rheum Dis* (2021) 80(12):1537–44. doi: 10.1136/annrheumdis-2021-220435

66. Del Papa N, Minniti A, Lorini M, Carbonelli V, Maglione W, Pignataro F, et al. The role of interferons in the pathogenesis of sjögren's syndrome and future therapeutic perspectives. *Biomolecules* (2021) 11(2):251. doi: 10.3390/biom11020251

67. Lee AJ, Ashkar AA. The dual nature of type I and type ii interferons. *Front Immunol* (2018) 9:2061. doi: 10.3389/fimmu.2018.02061

68. Bodewes ILA, Versnel MA. Interferon activation in primary sjögren's syndrome: Recent insights and future perspective as novel treatment target. *Expert Rev Clin Immunol* (2018) 14(10):817–29. doi: 10.1080/1744666x.2018.1519396

69. Luo S, Wu R, Li Q, Zhang G. Epigenetic regulation of Ifi44l expression in monocytes affects the functions of monocyte-derived dendritic cells in systemic lupus erythematosus. *J Immunol Res* (2022) 2022:4053038. doi: 10.1155/2022/4053038

70. Nocturne G, Mariette X. B cells in the pathogenesis of primary sjögren syndrome. *Nat Rev Rheumatol* (2018) 14(3):133–45. doi: 10.1038/nrrheum.2018.1

71. Bron AJ, de Paiva CS, Chauhan SK, Bonini S, Gabison EE, Jain S, et al. Tfos dews ii pathophysiology report. *Ocular Surface* (2017) 15(3):438–510. doi: 10.1016/j.jtos.2017.05.011

72. Kiefer K, Oropallo MA, Cancro MP, Marshak-Rothstein A. Role of type I interferons in the activation of autoreactive b cells. *Immunol Cell Biol* (2012) 90 (5):498–504. doi: 10.1038/icb.2012.10

73. Thompson N, Isenberg DA, Jury EC, Ciurtin C. Exploring baff: Its expression, receptors and contribution to the immunopathogenesis of sjögren's syndrome. *Rheumatol (Oxford)* (2016) 55(9):1548–55. doi: 10.1093/rheumatology/kev420

frontiers | Frontiers in Medicine

TYPE Mini Review
PUBLISHED 23 September 2022
DOI 10.3389/fmed.2022.979373

OPEN ACCESS

EDITED BY
Fabrizio Chiodo,
National Research Council (CNR), Italy

REVIEWED BY
Joke M. M. Den Haan,
VU Medical Center, Netherlands
Alba Silipo,
University of Naples Federico II, Italy

*CORRESPONDENCE
Chrysanthi Skevaki
Chrysanthi.Skevaki@uk-gm.de

SPECIALTY SECTION
This article was submitted to Infectious Diseases – Surveillance, Prevention and Treatment, a section of the journal Frontiers in Medicine

RECEIVED 27 June 2022
ACCEPTED 30 August 2022
PUBLISHED 23 September 2022

CITATION
Herzog S, Fragkou PC, Arneth BM, Mkhlof S and Skevaki C (2022) Myeloid CD169/Siglec1: An immunoregulatory biomarker in viral disease. *Front. Med.* 9:979373. doi: 10.3389/fmed.2022.979373

Myeloid CD169/Siglec1: An immunoregulatory biomarker in viral disease

Silva Herzog[1,2], Paraskevi C. Fragkou[2,3], Borros M. Arneth[1,4], Samr Mkhlof[1,4] and Chrysanthi Skevaki[1,2,4,5]* on behalf of the ESCMID Study Group for Respiratory Viruses (ESGREV)

[1]Institute of Laboratory Medicine and Pathobiochemistry, Molecular Diagnostics, Justus Liebig University Giessen, Giessen, Germany, [2]The European Society of Clinical Microbiology and Infection (ESCMID) Study Group for Respiratory Viruses (ESGREV), Basel, Switzerland, [3]First Department of Critical Care Medicine and Pulmonary Services, School of Medicine, Evangelismos Hospital, National and Kapodistrian University of Athens, Athens, Greece, [4]Institute of Laboratory Medicine and Pathobiochemistry, Molecular Diagnostics, Philipps-University Marburg, Marburg, Germany, [5]Universities of Giessen and Marburg Lung Center, German Center for Lung Research (DZL), Marburg, Germany

CD169, also known as Siglec1 or Sialoadhesin (Sn), is a surface adhesion molecule on human myeloid cells. Being part of the Siglec family, it acts as a receptor for sialylated molecular structures, which are found among various pathogenic and non-pathogenic ligands. Recent data suggest that CD169 may represent a promising new biomarker in acute respiratory and non-respiratory viral infections, such as SARS-CoV-2, Respiratory syncytial virus (RSV) and Human immunodeficiency virus (HIV). Therein lies a great potential to sufficiently differentiate viral from bacterial infection, which has been an incessant challenge in the clinical management of infectious disease. CD169 equips myeloid cells with functions, reaching far beyond pathogen elimination. In fact, CD169 seems to crosslink innate and adaptive immunity by antigen presentation and consecutive pathogen elimination, embodying a substantial pillar of immunoregulation. Yet, our knowledge about the kinetics, mechanisms of induction, signaling pathways and its precise role in host-pathogen interaction remains largely obscure. In this review, we describe the role of CD169 as a potentially novel diagnostic biomarker for respiratory viral infection by evaluating its strengths and weaknesses and considering host factors that are involved in pathogenesis of virus infection. Finally, this brief review aims to point out shortcomings of available evidence, thus, guiding future work revolving the topic.

KEYWORDS

CD169, Siglec1, Sialoadhesin, infection, respiratory infection, immune response, respiratory virus, SARS-CoV-2

Introduction

The correct diagnosis of different infectious diseases in an outpatient or emergency department setting, where rapid decision making and triage are essential for disease management, is constantly being a challenge. Established biomarkers, such as C-reactive protein (CRP), procalcitonin (PCT), erythrocyte sedimentation rate (ESR), and white blood cell counts (WBC) do not provide the needed specificity to precisely differentiate and, thus, diagnose the causative microorganism; oftentimes, these biomarkers are associated with numerous other conditions, such as comorbidities, age, medication, etc. (1), and therefore they show a wide variance of their diagnostic performance (2). Researching new reliable biomarkers in the field of infectious disease would significantly improve the concept of individualized medicine. Differentiating early and accurately viral and bacterial infections will have the great benefit of reducing mortality and morbidity as well as the spread of multi-resistant pathogens due to inappropriate antibiotic use.

CD169 (Siglec1; Sialoadhesin) is featured in several infectious and inflammatory conditions, including autoimmune disease (3, 4) and organ transplant rejection (5). Both protective and pathogenic roles have been attributed to this receptor in several viral infections, e.g., involving HIV, pathogenic murine retrovirus, Zika virus, Dengue virus, and porcine reproductive and respiratory syndrome virus (PRRSV) (6–12). Recent data show that CD169 may be a potential biomarker in respiratory viral diseases, caused by SARS-CoV-2, RSV and Influenza A virus (13–22). This review aims to focus on CD169 and its diagnostic performance in acute viral infection. Potentially involved host factors, that are driving CD169 expression, will be also elaborated.

Molecular characteristics and potential contributions in immunoregulation

CD169 is an inducible and continuously expressed cell surface molecule on mononuclear phagocyte immune cells [macrophages (Mϕ), monocytes (Mo), dendritic cells (DC)], occurring among mammalian species (23, 24), which binds to sialylated ligands [preferentially α (2, 3)-linked sialic acid glycoconjugates] on endogenous and foreign pathogenic membrane surfaces (25, 26). Its level of expression varies among cell subpopulations, depending on the tissue and the niche. (27, 28) CD169+ macrophage subpopulations are strategically situated within the secondary lymphoid organs of lymphnodes [subcapsular sinus macrophages (SSMs) and medullary sinus macrophages (MSMs)] and spleen [marginal metallophilic macrophages (MMMs)]. There, they reside near B- and T-cell populations, serving immunosurveillance. Furthermore, they are distributed extensively among tissue resident macrophage subpopulation (e.g., lung, gut, skin, liver) (29–31) CD169 is characterized by 17-Ig-like domains (23, 32), allowing for pathogen binding, mediating pathogen uptake and cell-cell adhesion between different immune cells. The cytoplasmic residue of CD169, however, is rather short and poorly conserved in length and sequence, which leads to the conclusion, that the predominant function of the receptor is primarily cellular interaction, rather than signaling (23, 24, 33) (**Supplementary Figure 1**).

The roles and functions in immunoregulatory processes seem to be manifold, including pathogen recognition (28), pathogen uptake (28, 34, 35) cross-presentation to CD8α$^+$ DCs (T cell priming) (25, 33, 36, 37), as well as B-cell and invariant natural killer T-cell (iNKT) activation (33, 38).

It has been repeatedly demonstrated, that CD169 plays a crucial role in cases of *trans*-infection in retrovirus invasion (7, 9, 39–43). Thereby, viruses exposing sialylated gangliosides in their outer surface composition are recognized and uptaken by CD169-expressing myeloid cells and subsequently presented to susceptible CD4+ T-cells at the cell-cell interface between antigen presenting cell (APC) and T-cell (39). The ability to *trans* infect has recently been described in the context of SARS-CoV-2 infection as well, extending the results shown in retroviruses (44, 45). In a similar way to what has been described in Ebola-virus infection (46), Perez-Zsolt et al. reported the storage of SARS-CoV-2 particles within virus containing compartments (VCCs) on infected DCs, eventually resulting in *trans*-infection of ACE2-and TMPRSS2-expressing cells *via* DCs (44, 47). Treatment with monoclonal antibodies against the CD169 receptor demonstrated significant decrease of *trans*-infection (40), which shows potential as a therapeutic target.

Pediatric studies are rather scarce. However, Jans et al. investigated the *in vitro* monocytic CD169 expression levels in infants and adults following RSV infection and found comparable upregulation among patient groups. Their research demonstrated, that CD169 induced through RSV infection led to a decrease of interferon-γ (IFN-γ) release by adult CD4+ T-cells, whereas the infant group showed no reduction of IFN-γ, possibly due to the lack of differentiated CD4+ memory T-cells in newborn and infants. Also, lower CD43 expression on naïve T-cells were seen in the pediatric group in comparison to adult T-cell expression (22). CD43 has been proposed as the main counter receptor for CD169 on T-cells and is highly represented on adult memory T-cells (22, 48). Therefore, low CD43 on infants' naïve T-cells is presumably accountable for the lack of inhibitory IFN-γ signaling by CD169 induction (22). An overview of potential immunoregulatory implications of CD169 is depicted in **Figure 1**.

Notably, CD169 is also involved in infection with certain bacteria in diverse peripheral tissues, such as skin, brain, and gut tissue. Encapsulated bacteria like *Escheria coli*, *Campylobacter jejuni*, *Neisseria meningitidis* and group A

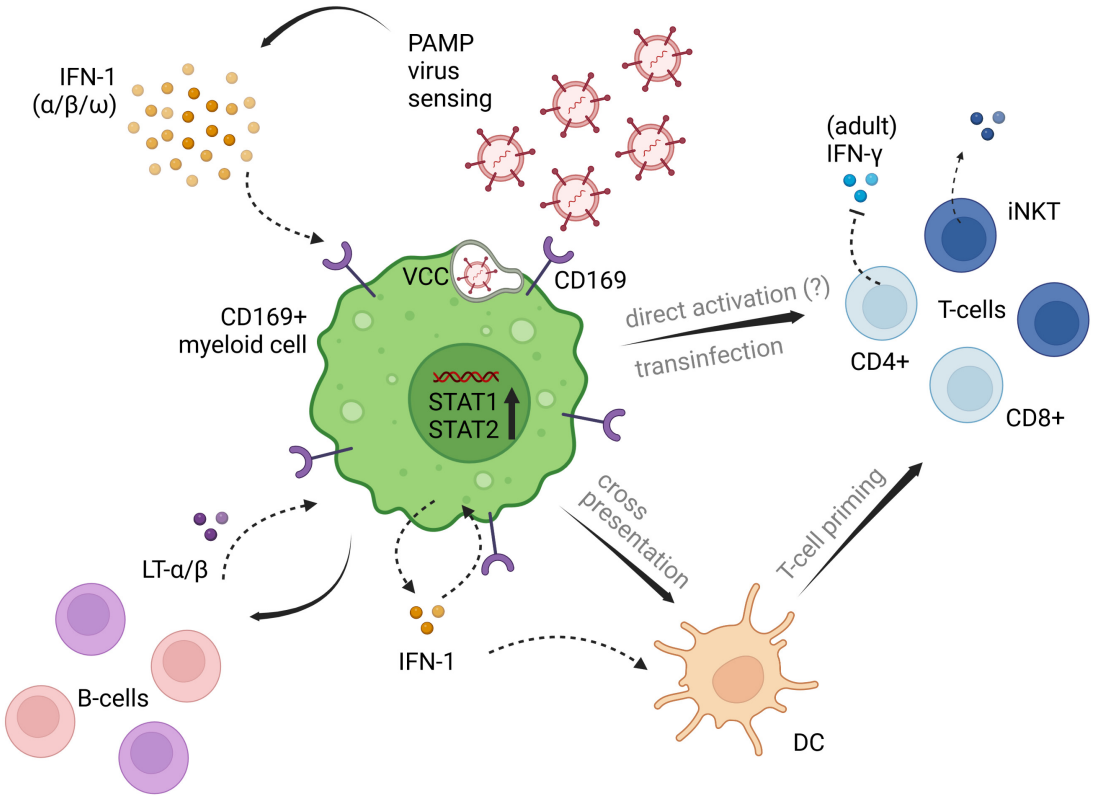

FIGURE 1
Potential implications of CD169+ myeloid cells on different cell subsets of innate and adaptive immunity. CD169+ expression is induced by type I IFN signaling following viral penetration. Downstream IFN pathways are set in motion, promoting virus titer control and adaptive immune cell priming and recruitment. Influencing factors of type I IFN induced CD169, that are contributing to the impairment of antiviral immunity need further clarification. The displayed pathways likely differ between myeloid cell lines, as well as between adults and children, and are depicted in one single figure, solely for illustrating purposes of the processes described in available literature. PAMP, pathogen associated molecular patterns; LT-α/β, lymphotoxin α/β; IFN, interferon; DC, dendritic cell; VCC, virus containing compartment. The figure was created with BioRender.com.

and B *Streptococcus* (GAS, GBS) have evolutionary evolved remarkable escape strategies by mimicking host polysaccharide structures like GM1. These strategies dampen anti-bacterial activities, e.g., by binding to inhibitory members of the Siglec1-family (49, 50). CD169, in contrast, is lacking inhibitory signaling motifs. CD169 is rather capable of recognizing sialylated pathogens, such as GBS, mediating phagocytosis and promoting bactericidal activities (50). In the autoimmune disease Guillain-Barré – Syndrome, *Campylobacter jejuni* expresses lipooligosaccharides structures on its surface, that are structurally similar to gangliosides in humans, allegedly causing auto reactive antibodies *via* CD169-Sia interactions (26). On the other hand, very recent evidence showed, that treatment with *Staphylococcus aureus* on CD169-deficient mice indicated impaired local immune response and adaptive immune cell recruitment of IL-17 producing γδ T-cells in the dermis (51). Additionally, an increase in bacterial burden was observed and the authors proposed a local type I IFN signaling pathway driving CD169 expression, but the source of type I IFN could not be elucidated (51). Lastly, results from knockout experiments on CD169 in *Mycobacterium tuberculosis* infection suggest that the receptor is responsible for the retainment of extracellular vesicles deriving from infected cells resulting in early antiviral immune activation (52).

Summing up, CD169, expressed on myeloid cells comprises fundamental implications on both innate and adaptive immunity. The profound role in pathogen recognition *via* sialylated gangliosides and consecutive virus containment has become evident (27). Beyond that, direct and indirect immunoregulatory influences on adaptive immune cell subsets in an activating, priming, and recruiting fashion are observed. Along with protective antiviral attributions, viral hijacking of CD169+ DCs with subsequent *trans*-infection of susceptible adaptive immune cells have extensively been investigated in retrovirus infection and lately been shown in SARS-CoV-2 infection. The role in enveloped virus transmission *via* CD169 mediated *trans*-infection needs future investigation and holds space for potential therapeutic targeting. Prompt

CD169 upregulation on infant monocytes due to RSV infection suggests an inborne mechanism following evolutionary conserved pathogen recognition receptor (PRR) signaling.

Mechanisms of induction and cell population maintenance

One of the main drivers of CD169 upregulation is through mechanisms that lead to type I interferon (IFN-I) responses. Especially IFN-α plays a major part in CD169 expression (23). The typical involvement of type I interferons are conditions of proinflammatory, immunoregulatory and anti-tumoral nature, which explains the increased expression of myeloid CD169 in this context (53). Furthermore, the capability of detecting and engulfing viruses is critically dependent on the recognition of sialic acid, which has been demonstrated in *in vitro* SARS-CoV-2 experiments, where mutation of CD169 led to impaired viral uptake. Monosialotetrahexosylganglioside (GM1) could be identified as one of the gangliosides interacting with CD169 *in vitro* (44). Although not shown in respiratory viral infection, several studies, found the sialic acid containing monosialodihexosylganglioside (GM3) to be another physiological ligand of CD169 (54–57) *In vivo* analyses revealed a direct and clear upregulation of the receptor upon IFN-I (α/β/ω) stimulation within the physiological ranges of viral infection (58). In addition, significant changes in pSTAT1 and pSTAT2, pathways that are crucially involved in antiviral activity, have been detected (58, 59). Of note, CD169+ macrophages have been found to be one of the main IFN-1 producers upon virus infection, themselves, making a self-enforcing process of IFN-mediated antiviral activity conceivable (27). Supporting that, *in vitro* IFN-α exposure of monocyte-derived macrophages (MDMs) and monocyte-derived dendritic cells (MDDCs) seems to enhance the capacity to uptake SARS-CoV-2 virus particles in contrast to non-stimulated APCs (44).

In mediating immunoregulatory functions, CD169+ cell subpopulations are susceptible toward environmental changes. To date, the evidence on milieu and cell maintenance relationship is obscure. Knockout analyses were able to identify some of the factors, that are creating an environmental niche, which is affecting the differentiation and maintenance of lymphoid tissue CD169+ macrophages: Receptor activator of nuclear factor kappa-B ligand (RANKL), member of the TNF superfamily is a key factor in controlling lymphnode organogenesis and is primarily expressed by marginal reticular cells, a stromal cell subset. RANKL deficiency in *Cd169-cre Rank*$^{fl/fl}$ mice has resulted in quantitative decrease and impaired differentiation in subcapsular sinus macrophages (SSMs) and medullary sinus macrophages (MSMs) (60) Expanding on these results, Camara et al. further revealed in a different work, that deficiency in B-cell derived lymphotoxin α/β (LT α/β) and LTβ receptor (LTβR) also led to decrease in numbers of SSMs and MMMs and to exchange of lymphoid CD169+ macrophages (19, 60, 61) Additionally, Shinde et al. studied the correlation between tumor necrosis factor (TNF), IFN-I expression and CD169 expression in vesicular stomatitis virus (VSV) infection and they demonstrated that, the ablation of TNF receptor (TNF-R) and mucosa-associated lymphoid tissue lymphoma translocation protein 1 (MALT1) led to severe immunopathology (62). They concluded that TNF is contributing to the maintenance of CD169+ cells, resulting in early virus replication, thus promoting early antiviral immune activation. Of note, it's suggested, that the retainment of viral antigen by CD169+ myeloid cells is enabling early antigen presentation, which could be beneficial in amplifying the adaptive immune response in early infection (62).

Host factors in pathogenesis

Given the assumption that CD169 is representing an important immunoregulatory player in the early stages of infection and disease progression, implications of loss-of-function phenotypic variants have demonstrated the course of infection in null individuals; Martinez-Picado et al. investigated a large cohort of HIV-infected individuals comprising of two homozygous and 97 heterozygous individuals expressing a specific stop-codon variant (Glu88Ter) in the CD169 gene (40). This gene is variously found among individuals of different ethnicities (39, 40). Interestingly, no significant differences in terms of virus acquisition, viral plasma load nor disease progression could be seen, despite phenotypical differentially expressed haploinsufficiency or protein absence (40). Yet, the heterozygous subjects revealed lower virus capture abilities than the control group and the results indicated that homozygous loss-of-function variant cannot be compensated. Notably, the identification of two infected null individuals indicate, that functional CD169 is dispensable in terms of HIV acquisition (40). Similarly, another work on PRRSV infection in CD169 knockout pigs showed no significant differences in severity of interstitial pneumonia development or histopathology in CD169 deficient compared to heterozygous and wild type animals, despite the prove of productive PRRSV infection in the piglets (11). However, the ablation of *in vivo* CD169+ alveolar macrophage (AM) population in a transgenic CD-169-DTR mouse strain boosted inflammation and respiratory dysfunction in response to PR8 influenza virus infection, leading the authors to conclude, that CD169+ AMs are thoroughly involved in disease containment, especially early virus titer control, and development of disease severity (27).

Based on the above findings from different animal models and human data, genetic loss of function alterations of CD169 in viral infection provides conflicting results. Impaired virus control and disease aggravation possibly depends on the virus strain, the species

being infected, individual immune status and cell line susceptibility. Future *ex vivo* and *in vivo* research need to shed light on the precise impact of receptor loss-of-function variants.

Regarding the CD169 expression upon IFN-α/β stimulation, impaired or deficient IFN-1 signaling, (as shown in critically ill COVID-19-patients), may also negatively influence the expression of CD169, and, therefore, the viral control in early stages of infection (16, 20, 63). The hypothesis of neutralizing IgG autoantibodies against type I IFN has been tested in SARS-CoV-2 infection and was proven to be a potential underlying factor in the course of critical disease. *In vivo* and *in vitro* studies, published by Bastard et al. demonstrate the presence of neutralizing type I IFN autoantibodies in about 10% of critically ill SARS-CoV-2 patients, that cause decrease in pSTAT1 in the majority of (almost exclusively male) patients (64). Thus, it would be interesting to see, if similar results are reproducible among other viral infections, how they correspond to CD169 expression levels and under which conditions external acquisition of interferonopathy and impairment of downstream CD169 expression is possible. Nevertheless, a connection seems very plausible, since these findings are in accordance with low CD169 levels in severe SARS-CoV-2 infection, as described by Doehn et al. (20). Moreover, Zhang et al. identified inborn type I IFN-associated deficiencies resulting in severe illness in the context of SARS-CoV-2 (64). Moreover, genetic interferonopathies of type I IFN, have been associated with high levels of monocytic CD169 in childhood autoimmune Aicardi Goutière syndrome (AGS) and Singleton-Merten syndrome (SMS) and therefore monocytic CD169 has been proposed as an effective screening marker (65).

CD169: Clinical marker of viral disease

Although, numerous aspects of the positive and negative control mechanisms of CD169 expression in health and disease still need further clarification, its momentous participation in fundamental immunologic processes (such as surveillance, recognition of self and foreign, antigen uptake, containment, and presentation) has been demonstrated. Recently, multiple studies have been testing the capacities of CD169 as a biomarker in viral disease. Clinical trials, performed to date, mainly revolve around SARS-CoV-2 infection (13–16, 19–21, 58). Very few studies have indicated the role in infection by other respiratory viruses, such as RSV, Influenza A virus or Rhinoviruses (15, 22).

The ongoing clinical challenge is how to correctly identify the underlying cause when infection is suspected. The development of reliable host-based biomarkers is necessary to bridge the diagnostic gap in ambiguous clinical cases of infection. High sensitivity (negative test results; "rule-out-approach") values are needed to not miss any patients with bacterial infection in need for antibiotics, whereas a "rule-in-approach" (positive test results), thus high specificity, is necessary in cases of viral infections (14, 66).

CD169 as an early diagnostic marker in SARS-CoV-2 infection

Since the onset of SARS-CoV-2 pandemic in 2019, a series of both retrospective and prospective clinical studies, investigating the diagnostic performance and discriminative ability of (monocytic) CD169 as a host-based biomarker of acute viral disease have been performed.

Monocytic CD169 (mCD169) expression levels reliably detected viral infection and results [measured in mean fluorescence intensity values (MFI) or monocyte/lymphocyte ratio MFI (rMFI)] displayed high sensitivity (≥ 80%) and specificity (≥ 91%) throughout (**Table 1**). Worth mentioning, where data were available, mCD196 expression exceeded the sensitivity and specificity of CRP (14, 16). Moreover, CD169 and viral load (cycle threshold values and time to positive PCR) were directly associated (15, 16, 21). The comparison of mCD169 levels between patients with active SARS-CoV-2 infection and virally suppressed HIV patients under antiretroviral therapy, showed significant differences, substantiating the role of CD169 as a marker of acute viral infection (21). Bedin et al. researched the monocytic CD169 expression at the beginnings of the COVID-19 pandemic (March/April 2020) and several valuable observations were made (16): No association between the onset of symptoms and mCD169 levels on hospital admission could be detected. Interestingly, mCD169 levels were not connected to disease severity or need for ICU treatment. Other observations included positive correlations between mCD169 and IFN-α levels, which both decreased over time of hospitalization. Lastly, the retrospective analysis of anti-SARS-CoV-2-IgG responses, were present in 7 SARS-CoV-2 positive subjects and were accompanied by lower mCD169 expression, suggesting that higher levels are seen before seroconversion (16). These results are in accordance with published evidence by Minutolo et al. who showed positive correlation between the mCD169/lymphocyte ratio (RMFI) and the percentage of marginal naïve B-cells (19). Recently, a study demonstrated the longitudinal CD169 expression in COVID-19 infection, and the results demonstrated higher levels of expression in early stages and mild cases of SARS-CoV-2 infection, in contrast to significantly decreased expression in critically ill patients (20). In mild cases, CD169 expression peaked within the first 3 days post symptom onset and showed slow decrease to normal ranges within 3–4 weeks. In

TABLE 1 Clinical trials indicating the diagnostic performance of monocytic CD169.

Study type	Respiratory virus strain	Variable	Sensitivity %	Specificity %	AUC	Threshold	References
Observational prospective	Influenza A RSV Rhinovirus	rMFI	95	100	0.98	5.34	(15)
Observational retrospective	Parainfluenza	MFI	85.71	100	0.97	1.58	(14)
n.a.	SARS-CoV-2	rMFI	91.7	89.8	0.92	3.3	(21)
n.a.	SARS-CoV-2	rMFI	97	80	0.95	3.51	(16)
n.a.	SARS-CoV-2	rMFI	97	92	0.925	3.01	(19)

The above listed virus strains are referring to respiratory virus strains identified in the trials and are not comprehensive of the overall identified pathogens. rMFI, lymphocyte/monocyte mean fluorescence intensity ratio; AUC, area under the curve; Ref, References; n.a., not available.

addition, as mentioned before, a strong correlation between viral load and CD169 expression in mild cases was seen, which interestingly, was not the case for severe disease (20). Additionally, the assessment of the monocyte landscape by t-distributed stochastic neighbor embedding analysis (t-SNE) showed, that the monocyte subpopulation in mild cases almost exclusively consisted of CD169+ clusters, which were significantly increased in mild disease, decreased in severe disease, and absent in healthy individuals (67). These findings once again are indicative of a protective role of CD169 in viral disease.

In contrast, increased CD169 expression in moderately and severely diseased patients have also been described in untreated patients presenting with severe interstitial pneumonia and SARS-CoV-2 associated multisystem inflammatory syndrome in children (MIS-C), suggesting that CD169 may be a prognostic marker for oxygen need and adverse outcomes (19, 36). Moreover, a significant over-expression of monocytic CD169 has been seen in patients admitted to the ICU due to severe SARS-CoV-2 infection (18).

Comparative immune profiling of patients presenting with or without acute respiratory distress syndrome (ARDS) in SARS-CoV-2 patients revealed a peculiar CD169 associated immune signature, which was not seen in ARDS patients negative for SARS-CoV-2. But no immune signature changes could be seen within the SARS-CoV-2-infected patients (ARDS vs. no ARDS) (68).

In summary, the clinical trials that have been conducted so far, show promising results for the diagnostic potential of CD169 as a screening tool for viral disease. However, not only studies are still scarce but also the "normal" values and limits of CD169 remain non-standardized. Regarding its prognostic and monitoring properties, the evidence is inconsistent. Prospective data should address the host factors, involved in the balancing act of CD169 expression between immune competence and immune deterioration, that are underlying asymptomatic/mild and severe disease progression.

Lastly, another constraint should be addressed: As already indicated, CD169 expression has been shown to be associated not only with respiratory viral disease, but also other (pathogenic) conditions of inflammatory or, infectious nature, e.g., autoimmunity, cancer, organ transplant rejection, bacterial infection, and various non-respiratory viral infections (3–5, 26, 40, 46, 50, 51, 53, 69). It may be assumed, that the diagnostic value of CD169 in patients affected with one or several of the above-mentioned pathologies is of limited significance.

Discussion

The existing evidence clearly indicates the valuable role of CD169 in diverse immunoregulatory functions, particularly in effecting early infection and viral control as well as its impact on adaptive immunity. Being a downstream molecule of type I IFN signaling, various interferonopathies are likely to impair the expression of CD169, as has already been depicted in the literature. Besides, a loss of function variant affecting the CD169 molecule itself has also been described.

The good diagnostic performance of CD169 as a biomarker of acute viral disease so far, seems to be promising in both viral epidemics where high sensitivity is needed ("rule-out-approach"), and in non-epidemic scenarios where high specificity is required ("rule-in approach"). Nonetheless, clinical trials are still limited; moreover, establishing universal laboratory standards and methodological groundwork is crucial for the improvement of comparability of laboratory testing and results among future studies (52). This encompasses pre- and post-analytical issues, as well as prospectively randomized design of clinical studies and patient recruitment strategies. Most of the clinical trials to date, have been conducted among SARS-CoV-2 patients, and only a very small number of studies showed the significance of CD169 as a virus-induced surface marker in other respiratory viral infections, like influenza A virus and RSV. However, large studies focusing on different viral strains are needed to

confirm these preliminary data. Furthermore, future study protocols should take under consideration demographic data including age, gender, ethnical background and comorbidities. Current data regarding CD169 expression in acutely infected patients, almost exclusively focuses on adult patients. Indeed, studying the expression in vulnerable patient groups, e.g., children, elderly, immunocompromised, pregnant, etc., would be particularly interesting, as these groups are commonly affected by severe viral infections, and therefore are more frequently in need for medical care or intervention. Besides viral infections, increased CD169 is seen in autoimmune conditions and anti-tumor immune responses. Hence, the diagnostic performance of CD169 as a biomarker of acute viral disease in these conditions needs further evaluation. What is more, effects of antiviral and anti-inflammatory properties on CD169 expression have not been investigated in depth yet. Finally, more research addressing the positive, but mainly the negative control mechanisms are needed to give a better understanding of origin and fate of these remarkable CD169 expressing myeloid cell subsets.

Finally, it should be mentioned, that this Mini Review has its limitations. Since the literature search has been focused on the implications of CD169 in respiratory viral disease, the connection between CD169 and HIV, respectively autoimmune (e.g., SLE) and cancerous disease have largely remained unconsidered. Moreover, especially with reference to SARS-CoV-2, new evidence emerges constantly. This literature search has been conducted with utmost care; within the common limitations of unsystematic narrative reviews, it aims to serve as a roundup on the available evidence on the role of CD169 within the scope of respiratory viral disease, while also directing future work in a field, that is very much in motion.

Authors contribution

SH wrote the manuscript. SH, BA, and SM contributed to the literature search. BA revised the manuscript. CS and PF critically revised the manuscript and contributed to conceptualization and supervision of the work. All authors contributed to the article and approved the submitted version.

Funding

CS was supported by the Universities Giessen and Marburg Lung Center (UGMLC), German Center for Lung Research (DZL), University Hospital Giessen and Marburg (UKGM) research funding according to article 2, section 3 cooperation agreement, and Deutsche Forschungsgemeinschaft (DFG, German Research Foundation)-SFB 1021 (Project-ID 197785619), KFO 309 (Project-ID 284237345), and SK 317/1-1 (Project-ID 428518790) as well as by the Foundation for Pathobiochemistry and Molecular Diagnostics.

Conflict of interest

CS was supported by Consultancy and Research Funding by Hycor Biomedical, Bencard Allergie, and Thermo Fisher Scientific and Research Funding by Hycor Biomedical and Mead Johnson Nutrition (MJN).

The remaining authors declare that the research was conducted in the absence of any commercial or financial relationships that could be construed as a potential conflict of interest.

Publisher's note

Supplementary material

The Supplementary Material for this article can be found online at: https://www.frontiersin.org/articles/10.3389/fmed.2022.979373/full#supplementary-material

SUPPLEMENTARY FIGURE 1
(a) Domain organization of CD169: CD169 belongs to the Ig-like Siglec superfamily, hence the designation Sialic acid-binding immunoglobulin-type lectins. Siglecs are a group of cell surface molecules, which can roughly be subdivided into highly conserved Siglecs, including CD169, and CD33-related Siglecs (24, 70, 71). CD169, being one of the largests representatives of its family, consists of 17 immunoglobulin domains, that are characteristically protruding in the peripheral extracellular space. This feature distinguishes CD169 from other members of the Siglec family. Consequently, *trans*-binding and cell-cell interaction are the preliminary function of the molecule rather than *cis*-interaction [O'Neill (72), Munday et al. (73)]. Additionally, CD169 has a short cytoplasmic tail. Based on current knowledge it lacks inhibitory or activating signaling motifs. **(b)** N-terminal domain of CD169: The sialic-acid binding domain is situated within a shallow pouch of the V-set domain on the outer extracellular part of the molecule. PDB ID: 1QFP; PDB DOI: http://doi.org/10.2210/pdb1QFP/pdb [Deposition authors: May et al. (74)]. **(c)** Simplified presentation of the representative CD169 ligand GM1. GM1 has been identified as one ligand of CD169 in SARS-CoV-2, binding *via* its single N-acetylneuraminic acid (NANA). Glc, D-Glucose; Gal, D-Galactose; GalNac, D-acetyl-D-galactosamine (75). The figure was created with BioRender.com.

References

1. Dewitt S, Chavez SA, Perkins J, Long B, Koyfman A. Evaluation of fever in the emergency department. *Am J Emerg Med.* (2017) 35:1755–8. doi: 10.1016/j.ajem.2017.08.030

2. Kapasi AJ, Dittrich S, González IJ, Rodwell TC. Host biomarkers for distinguishing bacterial from non-bacterial causes of acute febrile illness: a comprehensive review. *PLoS One.* (2016) 11:e0160278. doi: 10.1371/journal.pone.0160278

3. Von Stuckrad SL, Klotsche J, Biesen R, Lieber M, Thumfart J, Meisel C, et al. SIGLEC1 (CD169) is a sensitive biomarker for the deterioration of the clinical course in childhood systemic lupus erythematosus. *Lupus.* (2020) 29:1914–25. doi: 10.1177/0961203320965699

4. Rose T, Szelinski F, Lisney A, Reiter K, Fleischer SJ, Burmester GR, et al. SIGLEC1 is a biomarker of disease activity and indicates extraglandular manifestation in primary Sjögren's syndrome. *RMD Open.* (2016) 2:e000292. doi: 10.1136/rmdopen-2016-000292

5. Ashokkumar C, Gabriellan A, Ningappa M, Mazariegos G, Sun Q, Sindhi R. Increased monocyte expression of sialoadhesin during acute cellular rejection and other enteritides after intestine transplantation in children. *Transplantation.* (2012) 93:561–4. doi: 10.1097/TP.0b013e3182449189

6. Rempel H, Calosing C, Sun B, Pulliam L. Sialoadhesin expressed on IFN-induced monocytes binds HIV-1 and enhances infectivity. *PLoS One.* (2008) 3:e1967. doi: 10.1371/journal.pone.0001967

7. Gummuluru S, Pina Ramirez NG, Akiyama H. CD169-dependent cell-associated HIV-1 transmission: a driver of virus dissemination. *J Infect Dis.* (2014) 210(Suppl. 3):S641–7. doi: 10.1093/infdis/jiu442

8. Van der Kuyl AC, van den Burg R, Zorgdrager F, Groot F, Berkhout B, Cornelissen M. Sialoadhesin (CD169) expression in CD14+ cells is upregulated early after HIV-1 infection and increases during disease progression. *PLoS One.* (2007) 2:e257. doi: 10.1371/journal.pone.0000257

9. Pino M, Erkizia I, Benet S, Erikson E, Fernández-Figueras MT, Guerrero D, et al. HIV-1 immune activation induces Siglec-1 expression and enhances viral trans-infection in blood and tissue myeloid cells. *Retrovirology.* (2015) 12:37. doi: 10.1186/s12977-015-0160-x

10. Fenutria R, Maringer K, Potla U, Bernal-Rubio D, Evans MJ, Harris E, et al. CyTOF profiling of Zika and dengue virus-infected human peripheral blood mononuclear cells identifies phenotypic signatures of monotype subsets and upregulation of the interferon-inducible protein CD169. *mSphere.* (2021) 6:e0050521. doi: 10.1128/mSphere.00505-21

11. Prather RS, Rowland RRR, Ewen C, Trible B, Kerrigan M, Bawa B, et al. An intact sialoadhesin (Sn/SIGLEC1/CD169) is not required for attachment/internalization of the porcine reproductive and respiratory syndrome virus. *J Virol.* (2013) 87:9538. doi: 10.1128/JVI.00177-13

12. van Gorp H, van Breedam W, Delputte PL, Nauwynck HJ. Sialoadhesin and CD163 join forces during entry of the porcine reproductive and respiratory syndrome virus. *J Gen Virol.* (2008) 89(Pt 12):2943–53. doi: 10.1099/vir.0.2008/005009-0

13. Bourgoin P, Lediagon G, Arnoux I, Bernot D, Morange PE, Michelet P, et al. Flow cytometry evaluation of infection-related biomarkers in febrile subjects in the emergency department. *Future Microbiol.* (2020) 15:189–201. doi: 10.2217/fmb-2019-0256

14. Bourgoin P, Soliveres T, Ahriz D, Arnoux I, Meisel C, Unterwalder N, et al. Clinical research assessment by flow cytometry of biomarkers for infectious stratification in an emergency department. *Biomark Med.* (2019) 13:1373–86. doi: 10.2217/bmm-2019-0214

15. Bourgoin P, Soliveres T, Barbaresi A, Loundou A, Belkacem IA, Arnoux I, et al. CD169 and CD64 could help differentiate bacterial from CoVID-19 or other viral infections in the emergency department. *Cytometry A.* (2021) 99:435–45. doi: 10.1002/cyto.a.24314

16. Bedin AS, Makinson A, Picot MC, Mennechet F, Malergue F, Pisoni A, et al. Monocyte CD169 expression as a biomarker in the early diagnosis of coronavirus disease 2019. *J Infect Dis.* (2021) 223:562–7. doi: 10.1093/infdis/jiaa724

17. Payen D, Cravat M, Maadadi H, Didelot C, Prosic L, Dupuis C, et al. A longitudinal study of immune cells in severe COVID-19 patients. *Front Immunol.* (2020) 11:580250. doi: 10.3389/fimmu.2020.580250

18. Ortillon M, Coudereau R, Cour M, Rimmelé T, Godignon M, Gossez M, et al. Monocyte CD169 expression in COVID-19 patients upon intensive care unit admission. *Cytometry A.* (2021) 99:466–71. doi: 10.1002/cyto.a.24315

19. Minutolo A, Petrone V, Fanelli M, Iannetta M, Giudice M, Ait Belkacem I, et al. High CD169 monocyte/lymphocyte ratio reflects immunophenotype disruption and oxygen need in COVID-19 patients. *Pathogens.* (2021) 10:1639. doi: 10.3390/pathogens10121639

20. Doehn JM, Tabeling C, Biesen R, Saccomanno J, Madlung E, Pappe E, et al. CD169/SIGLEC1 is expressed on circulating monocytes in COVID-19 and expression levels are associated with disease severity. *Infection.* (2021) 49:757–62. doi: 10.1007/s15010-021-01606-9

21. Comins-Boo A, Gutiérrez-Larrañaga M, Roa-Bautista A, Foz SG, García MR, López EG, et al. Validation of a quick flow cytometry-based assay for acute infection based on CD64 and CD169 expression. New tools for early diagnosis in COVID-19 pandemic. *Front Med.* (2021) 8:655785. doi: 10.3389/fmed.2021.655785

22. Jans J, Unger WWJ, Vissers M, Ahout IML, Schreurs I, Wickenhagen A, et al. Siglec-1 inhibits RSV-induced interferon gamma production by adult T cells in contrast to newborn T cells. *Eur J Immunol.* (2018) 48:621–31. doi: 10.1002/eji.201747161

23. Klaas M, Crocker PR. Sialoadhesin in recognition of self and non-self. *Semin Immunopathol.* (2012) 34:353–64. doi: 10.1007/s00281-012-0310-3

24. Crocker PR, Paulson JC, Varki A. Siglecs and their roles in the immune system. *Nat Rev Immunol.* (2007) 7:255–66. doi: 10.1038/nri2056

25. Van Dinther D, Veninga H, Iborra S, Borg EGF, Hoogterp L, Olesek K, et al. Functional CD169 on macrophages mediates interaction with dendritic cells for CD8 + T cell cross-priming. *Cell Rep.* (2018) 22:1484–95. doi: 10.1016/j.celrep.2018.01.021

26. Heikema AP, Bergman MP, Richards H, Crocker PR, Gilbert M, Samsom JN, et al. Characterization of the specific interaction between sialoadhesin and sialylated *Campylobacter jejuni* lipooligosaccharides. *Infect Immun.* (2010) 78:3237–46. doi: 10.1128/IAI.01273-09

27. Purnama C, Ng SL, Tetlak P, Setiagani YA, Kandasamy M, Baalasubramanian S, et al. Transient ablation of alveolar macrophages leads to massive pathology of influenza infection without affecting cellular adaptive immunity. *Eur J Immunol.* (2014) 44:2003–12. doi: 10.1002/eji.201344359

28. Grabowska J, Lopez-Venegas MA, Affandi AJ, den Haan JMM. CD169+ macrophages capture and dendritic cells instruct: the interplay of the gatekeeper and the general of the immune system. *Front Immunol.* (2018) 9:2472. doi: 10.3389/fimmu.2018.02472

29. Hartnell A, Steel J, Turley H, Jones M, Jackson DG, Crocker PR. Characterization of human sialoadhesin, a sialic acid binding receptor expressed by resident and inflammatory macrophage populations. *Blood.* (2001) 97:288–96. doi: 10.1182/blood.v97.1.288

30. Steiniger B, Barth P, Herbst B, Hartnell A, Crocker PR. The species-specific structure of microanatomical compartments in the human spleen: strongly sialoadhesin-positive macrophages occur in the perifollicular zone, but not in the marginal zone. *Immunology.* (1997) 92:307–16. doi: 10.1046/j.1365-2567.1997.00328.x

31. Tacconi C, Commerford CD, Dieterich LC, Schwager S, He Y, Ikenberg K, et al. CD169 + lymph node macrophages have protective functions in mouse breast cancer metastasis. *Cell Rep.* (2021) 35:108993. doi: 10.1016/j.celrep.2021.108993

32. Crocker PR, Mucklow S, Bouckson V, McWilliam A, Willis AC, Gordon S, et al. Sialoadhesin, a macrophage sialic acid binding receptor for haemopoietic cells with 17 immunoglobulin-like domains. *EMBO J.* (1994) 13:4490–503. doi: 10.1002/j.1460-2075.1994.tb06771.x

33. Martinez-Pomares L, Gordon S. CD169+ macrophages at the crossroads of antigen presentation. *Trends Immunol.* (2012) 33:66–70. doi: 10.1016/j.it.2011.11.001

34. Schadee-Eestermans IL, Hoefsmit ECM, van de Ende M, Crocker PR, van den Berg TK. Ultrastructural localisation of sialoadhesin (siglec-1) on macrophages in rodent lymphoid tissues. *Immunobiology.* (2000) 202:309–25. doi: 10.1016/s0171-2985(00)80036-4

35. Junt T, Moseman EA, Iannacone M, Massberg S, Lang PA, Boes M, et al. Subcapsular sinus macrophages in lymph nodes clear lymph-borne viruses and present them to antiviral B cells. *Nature.* (2007) 450:110–4. doi: 10.1038/nature06287

36. Huang JJ, Gaines SB, Amezcua ML, Lubell TR, Dayan PS, Dale M, et al. Upregulation of type 1 conventional dendritic cells implicates antigen cross-presentation in multisystem inflammatory syndrome. *J Allergy Clin Immunol.* (2022) 149:912–22. doi: 10.1016/j.jaci.2021.10.015

37. Affandi AJ, Olesek K, Grabowska J, Nijen Twilhaar MK, Rodríguez E, Saris A, et al. CD169 defines activated CD14+ monocytes with enhanced CD8+ T cell activation capacity. *Front Immunol.* (2021) 12:697840. doi: 10.3389/fimmu.2021.697840

38. Barral P, Polzella P, Bruckbauer A, van Rooijen N, Besra GS, Cerundolo V, et al. CD169(+) macrophages present lipid antigens to mediate early activation of iNKT cells in lymph nodes. *Nat Immunol.* (2010) 11:303–12. doi: 10.1038/ni.1853

39. Martinez-Picado J, McLaren PJ, Telenti A, Izquierdo-Useros N. Retroviruses as myeloid cell riders: what natural human siglec-1 "knockouts" tell us about pathogenesis. *Front Immunol.* (2017) 8:1593. doi: 10.3389/fimmu.2017.01593

40. Martinez-Picado J, McLaren PJ, Erkizia I, Martin MP, Benet S, Rotger M, et al. Identification of siglec-1 null individuals infected with HIV-1. *Nat Commun.* (2016) 7:12412. doi: 10.1038/ncomms12412

41. Sewald X, Ladinsky MS, Uchil PD, Beloor J, Pi R, Herrmann C, et al. Retroviruses use CD169-mediated trans-infection of permissive lymphocytes to establish infection. *Science.* (2015) 350:563–7. doi: 10.1126/science.aab2749

42. Haugh KA, Ladinsky MS, Ullah I, Stone HM, Pi R, Gilardet A, et al. In vivo imaging of retrovirus infection reveals a role for siglec-1/CD169 in multiple routes of transmission. *Elife.* (2021) 10:e64179. doi: 10.7554/eLife.64179

43. Akiyama H, Ramirez NGP, Gudheti M, Gummuluru S. CD169-mediated trafficking of HIV to plasma membrane invaginations in dendritic cells attenuates efficacy of anti-gp120 broadly neutralizing antibodies. *PLoS Pathog.* (2015) 11:e1004751. doi: 10.1371/journal.ppat.1004751

44. Perez-Zsolt D, Muñoz-Basagoiti J, Rodon J, Elosua-Bayes M, Raïch-Regué D, Risco C, et al. SARS-CoV-2 interaction with Siglec-1 mediates trans-infection by dendritic cells. *Cell Mol Immunol.* (2021) 18:2676–8. doi: 10.1038/s41423-021-00794-6

45. Lempp FA, Soriaga LB, Montiel-Ruiz M, Benigni F, Noack J, Park YJ, et al. Lectins enhance SARS-CoV-2 infection and influence neutralizing antibodies. *Nature.* (2021) 598:342–7. doi: 10.1038/s41586-021-03925-1

46. Perez-Zsolt D, Erkizia I, Pino M, García-Gallo M, Martin MT, Benet S, et al. Anti-Siglec-1 antibodies block Ebola viral uptake and decrease cytoplasmic viral entry. *Nat Microbiol.* (2019) 4:1558–70. doi: 10.1038/S41564-019-0453-2

47. Perez-Zsolt D, Raïch-Regué D, Muñoz-Basagoiti J, Aguilar-Gurrieri C, Clotet B, Blanco J, et al. HIV-1 trans-infection mediated by DCs: the tip of the iceberg of cell-to-cell viral transmission. *Pathogens.* (2022) 11:39. doi: 10.3390/pathogens11010039

48. Crocker R, Vestweber D, Fukuda M, van Die I, Timo P, van den Berg K, et al. Cutting edge: CD43 functions as a T Cell counterreceptor for the macrophage adhesion receptor sialoadhesin (Siglec-1). *J Immunol.* (2001) 166:3637–40. doi: 10.4049/jimmunol.166.6.3637

49. Chang YC, Nizet V. Siglecs at the host–pathogen interface. In: Hsieh, SL. *Lectin in Host Defense Against Microbial Infections. Advances in Experimental Medicine and Biology*. Singapore: Springer (2020) p. 197–214. doi: 10.1007/978-981-15-1580-4_8

50. Chang YC, Olson J, Louie A, Crocker PR, Varki A, Nizet V. Role of macrophage sialoadhesin in host defense against the sialylated pathogen group B Streptococcus. *J Mol Med (Berl).* (2014) 92:951–9. doi: 10.1007/s00109-014-1157-y

51. Park YJ, Kang BH, Kim HJ, Oh JE, Lee HK. A microbiota-dependent subset of skin macrophages protects against cutaneous bacterial infection. *Front Immunol.* (2022) 13:799598. doi: 10.3389/fimmu.2022.799598

52. Benet S, Gálvez C, Drobniewski F, Kontsevaya I, Arias L, Monguió-Tortajada M, et al. Dissemination of Mycobacterium tuberculosis is associated to a SIGLEC1 null variant that limits antigen exchange via trafficking extracellular vesicles. *J Extracell Vesicles.* (2021) 10:e12046. doi: 10.1002/jev2.12046

53. Hou X, Chen G, Zhao Y. Research progress on CD169-positive macrophages in tumors. *Am J Transl Res.* (2021) 13:8589–97.

54. Grabowska J, Stolk DA, Nijen Twilhaar MK, Ambrosini M, Storm G, van der Vliet HJ, et al. Liposomal nanovaccine containing α-galactosylceramide and ganglioside GM3 stimulates robust CD8 + T cell responses via CD169 + macrophages and cDC1. *Vaccines.* (2021) 9:1–19. doi: 10.3390/vaccines9010056

55. Jobe O, Kim J, Rao M. The role of siglec-1 in HIV-1/macrophage interaction. *Macrophage.* (2016) 3:e1435. doi: 10.14800/Macrophage.1435

56. Grabowska J, Affandi AJ, van Dinther D, Nijen Twilhaar MK, Olesek K, Hoogterp L, et al. Liposome induction of CD8+ T cell responses depends on CD169+ macrophages and Batf3-dependent dendritic cells and is enhanced by GM3 inclusion. *J Control Release.* (2021) 331:309–20. doi: 10.1016/j.jconrel.2021.01.029

57. Nijen Twilhaar MK, Czentner L, Grabowska J, Affandi AJ, Lau CYJ, Olesek K, et al. Optimization of liposomes for antigen targeting to splenic CD169 + macrophages. *Pharmaceutics.* (2020) 12:1–21. doi: 10.3390/pharmaceutics12121138

58. Bourgoin P, Biéchelé G, Belkacem IA, Morange PE, Malergue F. Role of the interferons in CD64 and CD169 expressions in whole blood: relevance in the balance between viral- or bacterial-oriented immune responses. *Immun Inflamm Dis.* (2020) 8:106–23. doi: 10.1002/iid3.289

59. Rincon-Arevalo H, Aue A, Ritter J, Szelinski F, Khadzhynov D, Zickler D, et al. Altered increase in STAT1 expression and phosphorylation in severe COVID-19. *Eur J Immunol.* (2022) 52:138–48. doi: 10.1002/eji.202149575

60. Camara A, Cordeiro OG, Alloush F, Sponsel J, Chypre M, Onder L, et al. Lymph node mesenchymal and endothelial stromal cells cooperate via the RANK-RANKL cytokine axis to shape the sinusoidal macrophage niche. *Immunity.* (2019) 50:1467–81.e6. doi: 10.1016/j.immuni.2019.05.008

61. Camara A, Lavanant AC, Abe J, Desforges HL, Alexandre YO, Girardi E, et al. CD169+ macrophages in lymph node and spleen critically depend on dual RANK and LTbetaR signaling. *Proc Natl Acad Sci USA.* (2022) 119:e2108540119. doi: 10.1073/pnas.2108540119

62. Shinde P, Xu HC, Maney SK, Kloetgen A, Namineni S, Zhuang Y, et al. Tumor necrosis factor-mediated survival of CD169 + cells promotes immune activation during vesicular stomatitis virus infection. *J Virol.* (2018) 92:e01637-17. doi: 10.1128/jvi.01637-17

63. Hadjadj J, Yatim N, Barnabei L, Corneau A, Boussier J, Smith N, et al. Impaired type I interferon activity and inflammatory responses in severe COVID-19 patients. *Science.* (2020) 369:718–24. doi: 10.1126/science.abc6027

64. Zhang Q, Liu Z, Moncada-Velez M, Chen J, Ogishi M, Bigio B, et al. Inborn errors of type I IFN immunity in patients with life-threatening COVID-19. *Science.* (2020) 370:422. doi: 10.1126/SCIENCE.ABD4570

65. Orak B, Ngoumou G, Ebstein F, Zieba B, Goetzke CC, Knierim E, et al. SIGLEC1 (CD169) as a potential diagnostical screening marker for monogenic interferonopathies. *Pediatr Allergy and Immununol.* (2021) 32:621–5. doi: 10.1111/PAI.13400

66. Plebani M, Zaninotto M, Mion MM. Requirements inside the text of a good biomarker: translation into the clinical laboratory. In: Van Eyk J, Dunn MJ editors. *Clinical Proteomics. From Diagnosis to Therapy*. Weinheim: WILEY-VCH Verlag GmbH & Co (2008). p. 618–29.

67. Chevrier S, Zurbuchen Y, Cervia C, Adamo S, Raeber ME, de Souza N, et al. A distinct innate immune signature marks progression from mild to severe COVID-19. *Cell Rep Med.* (2020) 2:100166. doi: 10.1016/J.XCRM.2020.100166

68. Roussel M, Ferrant J, Reizine F, le Gallou S, Dulong J, Carl S, et al. Comparative immune profiling of acute respiratory distress syndrome patients with or without SARS-CoV-2 infection. *Cell Rep Med.* (2021) 2:100291. doi: 10.1016/j.xcrm.2021.100291

69. Chang YC, Nizet V. Siglecs at the host–pathogen interface. *Adv Exp Med Biol.* (2020) 1204:197–214.

70. Lim J, Sari-Ak D, Bagga T. Siglecs as therapeutic targets in cancer. *Biology.* (2021) 10:1178. doi: 10.3390/biology10111178

71. Bornhöfft KF, Goldammer T, Rebl A, Galuska SP. Siglecs: a journey through the evolution of sialic acid-binding immunoglobulin-type lectins. *Dev Comp Immunol.* (2018) 86:219–31. doi: 10.1016/j.dci.2018.05.008

72. O'Neill AS, van den Berg TK, Mullen GE. Sialoadhesin – A macrophage-restricted marker of immunoregulation and inflammation. Immunology. (2013) 138:198–207. doi: 10.1111/imm.12042

73. Munday J, Floyd H, Crocker PR. Sialic acid binding receptors (siglecs) expressed by macrophages. *J Leukoc Biol.* (1999) 66:705–11. doi: 10.1002/jlb.66.5.705

74. May AP, Robinson RC, Vinson M, Crocker PR, Jones EY. Crystal structure of the N-terminal domain of sialoadhesin in complex with 3′ sialyllactose at 1.85 Å Resolution. *Mol Cell.* (1998) 1:719–28. doi: 10.1016/s1097-2765(00)80071-4

75. Cutillo G, Saariaho AH, Meri S. Physiology of gangliosides and the role of antiganglioside antibodies in human diseases. *Cell Mol Immunol.* (2020) 17:313–22. doi: 10.1038/s41423-020-0388-9

frontiers | Frontiers in Immunology

TYPE Original Research
PUBLISHED 31 October 2022
DOI 10.3389/fimmu.2022.1020624

OPEN ACCESS

EDITED BY
Paraskevi C. Fragkou,
Evaggelismos General Hospital,
Greece

REVIEWED BY
Biagio Pinchera,
University of Naples Federico II, Italy
Elisabeth Mack,
Philipps-University Marburg, Germany

*CORRESPONDENCE
Christos Tsatsanis
tsatsani@med.uoc.gr
Ahmed A. Al-Qahtani
aqahtani@kfshrc.edu.sa
Eleni Vergadi
vergadi@med.uoc.gr

†These authors share first authorship

SPECIALTY SECTION
This article was submitted to
Viral Immunology,
a section of the journal
Frontiers in Immunology

RECEIVED 16 August 2022
ACCEPTED 17 October 2022
PUBLISHED 31 October 2022

CITATION
Al-Qahtani AA, Pantazi I,
Alhamlan FS, Alothaid H,
Matou-Nasri S, Sourvinos G,
Vergadi E and Tsatsanis C (2022)
SARS-CoV-2 modulates inflammatory
responses of alveolar epithelial type II
cells *via* PI3K/AKT pathway.
Front. Immunol. 13:1020624.
doi: 10.3389/fimmu.2022.1020624

SARS-CoV-2 modulates inflammatory responses of alveolar epithelial type II cells *via* PI3K/AKT pathway

Ahmed A. Al-Qahtani[1,2*†], Ioanna Pantazi[3,4†], Fatimah S. Alhamlan[1,2], Hani Alothaid[5], Sabine Matou-Nasri[6], George Sourvinos[7], Eleni Vergadi[4*] and Christos Tsatsanis[3,8*]

[1]Department of Infection and Immunity, Research Center, King Faisal Specialist Hospital and Research Center, Riyadh, Saudi Arabia, [2]Department of Microbiology and Immunology, College of Medicine, Alfaisal University, Riyadh, Saudi Arabia, [3]Laboratory of Clinical Chemistry, Medical School, University of Crete, Heraklion, Greece, [4]Department of Pediatrics, Medical School, University of Crete, Heraklion, Greece, [5]Department of Basic Sciences, Faculty of Applied Medical Sciences, Al-Baha University, Al-Baha, Saudi Arabia, [6]Cell and Gene Therapy Group, Medical Genomics Research Department, King Abdullah International Medical Research Center, King Saud bin Abdulaziz University for Health Sciences, Ministry of National Guard Health Affairs, Riyadh, Saudi Arabia, [7]Laboratory of Virology, Medical School, University of Crete, Heraklion, Greece, [8]Institute of Molecular Biology and Biotechnology, Foundation for Research and Technology (FORTH), Heraklion, Greece

Background: SARS-CoV-2 infects through the respiratory route and triggers inflammatory response by affecting multiple cell types including type II alveolar epithelial cells. SARS-CoV-2 triggers signals *via* its Spike (S) protein, which have been shown to participate in the pathogenesis of COVID19.

Aim: Aim of the present study was to investigate the effect of SARS-CoV2 on type II alveolar epithelial cells, focusing on signals initiated by its S protein and their impact on the expression of inflammatory mediators.

Results: For this purpose A549 alveolar type II epithelial cells were exposed to SARS CoV2 S recombinant protein and the expression of inflammatory mediators was measured. The results showed that SARS-CoV-2 S protein decreased the expression and secretion of IL8, IL6 and TNFα, 6 hours following stimulation, while it had no effect on IFNα, CXCL5 and PAI-1 expression. We further examined whether SARS-CoV-2 S protein, when combined with TLR2 signals, which are also triggered by SARS-CoV2 and its envelope protein, exerts a different effect in type II alveolar epithelial cells. Simultaneous treatment of A549 cells with SARS-CoV-2 S protein and the TLR2 ligand PAM3csk4 decreased secretion of IL8, IL6 and TNFα, while it significantly increased IFNα, CXCL5 and PAI-1 mRNA expression. To investigate the molecular pathway through which SARS-CoV-2 S protein exerted this immunomodulatory action in alveolar epithelial cells, we measured the induction of MAPK/ERK and PI3K/AKT pathways and found that SARS-CoV-2 S protein induced the activation of the serine threonine kinase AKT. Treatment

with the Akt inhibitor MK-2206, abolished the inhibitory effect of SARS-CoV-2 S protein on IL8, IL6 and TNFα expression, suggesting that SARS-CoV-2 S protein mediated its action *via* AKT kinases.

Conclusion: The findings of our study, showed that SARS-CoV-2 S protein suppressed inflammatory responses in alveolar epithelial type II cells at early stages of infection through activation of the PI3K/AKT pathway. Thus, our results suggest that at early stages SARS-CoV-2 S protein signals inhibit immune responses to the virus allowing it to propagate the infection while in combination with TLR2 signals enhances PAI-1 expression, potentially affecting the local coagulation cascade.

KEYWORDS

alveolar epithelial cells, COVID-19, SARS-CoV-2, AKT, inflammation

Introduction

During the last two decades, public health faced several outbreaks of severe respiratory diseases caused by coronaviruses, such as severe acute respiratory syndrome coronavirus (SARS-CoV) and Middle East respiratory syndrome coronavirus (MERS-CoV), which were soon held under control. However, the outbreak of the newer SARS-CoV-2 coronavirus at the end of 2019 in Wuhan City, which causes COVID-19 disease, evolved rapidly to a global pandemic with unprecedented health and economic repercussions. A major complication characterizing COVID-19 pathogenesis, is the presence of microvascular and macrovascular thrombosis which are associated with a high risk of mortality (1, 2). For example, the formation of thrombi in pulmonary vessels can lead to pulmonary embolism and acute respiratory failure observed in patients with COVID-19 (3). Impaired fibrinolysis also raises the thrombotic risk observed in COVID-19 patients. Fibrinolytic activity is regulated by plasminogen activators (tPA, uPA) and plasminogen activator inhibitor-1 (PAI-1), which serve as useful biomarkers of the disease (4).

SARS-CoV-2 cell entry is achieved through binding of its surface spike protein to its main cellular receptor angiotensin converting enzyme 2 (ACE2) (5–7). The spike protein is a homotrimeric class I fusion protein consisting of a receptor-binding subunit S1 and a membrane-fusion subunit S2 (8–10). When SARS-CoV-2 binds to ACE2 with S1 subunit, the spike protein undergoes protease cleavage at the S1/S2 cleavage site by the transmembrane Serine Protease 2 (TMPRSS2), allowing fusion of the viral membrane with the host-cell membrane by the S2 subunit, and the subsequent viral endocytosis (5, 11, 12). In addition to its direct binding to ACE2, the S protein is a potent viral PAMP that is sensed by other cell receptors, such as TLR2 in lung epithelial cells (13). Subsequently, TLR2 forms heterodimers with TLR1 or TLR6, creating a complex containing MyD88 with IRAK kinase family members, leading to activation of NF-κB and MAPK signaling, and ultimately to the production of inflammatory cytokines and chemokines (14). The expression of TLR2 is also increased following SARS-CoV-2 infection and it is positively associated with the severity of COVID-19 (15). In addition to the S protein, TLR2 senses SARS-CoV-2 envelope protein, inducing the production of proinflammatory cytokines independent of viral entry (15).

The initial site of infection and viral replication is the sinonasal airway epithelium, consisting of ciliated and mucus secretory cells (16). As the disease spreads down to the alveolar compartment, the primary cell being infected by SARS-COV-2 is the alveolar type II cell, which is also the main cell type that expresses ACE2 and TMPRSS2 in the lung (17, 18). After SARS-CoV-2 infection, alveolar type II cells release the virus that infects adjacent type II cells, and also secrete interferons and inflammatory cytokines and chemokines to initiate the innate immune response. The inflammatory response includes mobilization of immune cells and tissue damage. The ultimate consequence is diffuse alveolar injury with loss of functional surfactant, damage of type I cells and endothelial cells, alveolar flooding and influx of inflammatory cells (19, 20). Disease severity is associated to a highly dysregulated innate immune response, characterized by this excessive inflammatory response, as well as a relatively delayed interferon (IFN) response against the virus, facilitating robust viral replication and inflammatory damage to tissues (21). In contrast, multiple studies show that critically ill COVID-19 patients are characterized by lymphopenia with loss of CD4+ T, CD8+ T, NK cells and B cells, as well as a decreased number of immune cells producing IFNγ and TNFα (22–24). There are several possible explanations for this, including pulmonary recruitment of lymphocytes from the blood, direct virus killing of lymphocytes, T-cell apoptosis

and exhaustion (25). Furthermore, other studies have also shown an increased release of anti-inflammatory cytokines and mediators, such as IL10 and cytokine growth and differentiation factor 15 (GDF-15) in COVID-19 patients, possibly as a mechanism to downregulate excessive inflammatory responses and restore the balance between pro and anti-inflammatory responses (26–28). Therefore, COVID-19 infection cannot be characterized by a classical cytokine storm syndrome, but rather as a significant inflammatory dysregulation with alternating hyperinflammation and immunosuppression states during the infection. Understanding which immune state predominates at each stage of SARS-CoV-2 infection, as well as the molecular pathways that regulate them, is very crucial in order to enhance our knowledge of disease pathogenesis and develop new therapeutic strategies.

During SARS-CoV-2 infection, several signaling pathways are activated by the interaction of spike protein with its ACE2 receptor. Specifically, it has been shown that SARS-CoV-2 infection can cause multiple intracellular phosphorylation events in the mTOR, ERK and JAK1 pathways (29–31). The PI3K/Akt/mTOR pathway is an important cell signaling pathway that regulates various cell functions and its upregulation has been observed in diseases caused by viruses (32). Following the activation of related receptors by viruses, PI3K generates PIP3, resulting in the activation of PDK1 which further activates protein kinase B (PKB/Akt). The phosphorylated Akt mediates the phosphorylation of mTOR, promoting nuclear translocation of NF-κB, which regulates proinflammatory gene expression. The role of the PI3K/Akt pathway in cytokine production is cell-type specific and depends on the stimulus applied. Therefore, PI3K/Akt might exert proinflammatory or anti-inflammatory properties according to the situation. Several studies have already demonstrated the implication of this pathway in COVID-19 pathogenesis. For example, activation of the PI3K/Akt signaling pathway can be induced by CD147 and furin (involved in SARS-CoV-2 cell entry), while the clathrin-mediated SARS-CoV-2 endocytosis is also regulated by the PI3K/Akt pathway (33). Another proteotranscriptomics study, showed increased levels of phosphorylation of Akt, mTOR and other downstream effectors at 24h post-infection, indicating activation of Akt-mTOR pathway at an early stage of the infection (30).

In the present study, we investigated the impact of SARS-CoV-2 S protein in the production of inflammatory mediators alone or in combination with TLR2 signals from alveolar epithelial type II cell. We further, investigated the possible molecular pathways (MAPK/ERK, PI3K/Akt) implicated in this process, in order to determine how SARS-CoV-2 influences its main entry site at an early stage of the infection.

Materials and methods

Cell culture

The A549 cell line (ATCC: CCL-185) was used in this study as a model of type II alveolar epithelial cells. Cells were cultured in Dulbecco Modified Eagle Medium (DMEM), low glucose (1g/L) (Thermo Fisher Scientific, Waltham, USA) supplemented with 10% fetal bovine serum (FBS) and antibiotics (10,000 U/ml penicillin and 10 mg/ml Streptomycin). Cells were seeded in 24-well plates at a final density of 4×10^5 cells/ml and were stimulated with different concentrations of SARS-CoV-2 Spike-Membrane Recombinant Fusion Protein (10, 20, 50, 100 ng/ml; TP701119, OriGene, Rockville, USA) in the presence or absence of the TLR ligand PAM3csk4 (1μg/ml; Tocris, Bristol, UK) for 6 and 12 hours. In another set of experiments, A549 cells were pre-treated with the selective Akt 1/2/3 inhibitor MK-2206 2HCl (5μM; cat# S1078, SelleckChem, Berlin, Germany) for 24 hours and then stimulated with 50ng/ml SARS-CoV-2 Spike-Membrane Recombinant Fusion Protein for 18 hours to collect cell culture supernatants.

Enzyme-linked immunosorbent assay (ELISA)

A549 cells were stimulated with SARS-CoV-2 Spike-Membrane Recombinant Fusion Protein for 12 hours in the presence or absence of TLR2 ligand, and cell culture supernatants were collected for cytokine quantification. Cytokine production of IL6, IL8 and TNFα was determined using the Elisa Max™ Delux Set (BioLegend, SanDiego USA) as indicated by the manufacturer.

Real-time PCR

For the mRNA level detection of IL6, IL8, TNFα, CXCL5, PAI-1 and IFNα, total RNA was extracted from A549 cells using TRI Reagent (Sigma-Aldrich, St Louis, USA). Eight hundred nanogram of total RNA were used for cDNA synthesis (TAKARA, Primescript RT Reagent kit, Tokyo, Japan). Amplification was performed using KAPA SyBr® Fast Universal qPCR kit (Kapa Biosystems, Cape Town, South Africa). Denaturation was carried out at 95°C for 10 seconds, annealing and extension at 60°C for 30 seconds for 40 cycles in a StepOnePlus™ Real-Time PCR System (Applied Biosystems, Foster City, CA, USA). Data analysis was accomplished using the ΔΔCT method and GAPDH was used as the housekeeping gene. The primer sequences used in this study, were the following: IL6: forward 5' GTCAGGGGTGGTTA TTGCAT 3' and reverse 5' AGTGAGGAACAAGCCAGAGC 3';

10.3389/fimmu.2022.1020624

IL8: forward 5' TGTGAAGGTGCAGTTTTGCC 3' and reverse 5' CACCCAGTTTTCCTTGGGGT 3'; TNFα: forward 5' GCCCA GGCAGTCAGATCAT 3' and reverse 5' TATCTCTCA GCTCCACGCCA 3'; CXCL5: forward 5' ACAGACCACGCAA GGAGTTC 3' and reverse 5' TCTTCAGGGAGGCTACCACT 3'; PAI-1: forward 5' TCACGAGTCTTTCAGACCAAG 3' and reverse 5' CCGGACCACAAAGAGGAAG 3'; IFNα: forward 5' GGAGGAGAGGGTGGGAGAAA 3' and reverse 5' GACAA CCTCCCAGGCACAAG 3'; GAPDH: forward 5' GGAAGGT GAAGGTCGGAGTCA 3' and reverse 5' GTCATTGATGGCAA CAATATCCACT 3'.

Western blot

For Western blot, cell lysates were harvested with RIPA lysis buffer and protein concentration was determined using the Pierce BCA Protein Assay. Protein lysates were resuspended in SDS-containing loading dye, were separated on 10% polyacrylamide gel, and then transferred to nitrocellulose membrane. Briefly, after blocking with 5% Bovine Serum Albumin (BSA) containing 0.1% Tween 20 for an hour at room temperature, the membranes were incubated overnight at 4^0C with primary antibodies (1:1000), washed with PBST and then incubated with peroxidase-conjugated secondary antibodies (1:5000) for 1 hour at room temperature. Membranes were exposed to trans-UV light in a ChemiDoc XRS+ (BioRad Laborato-ries, Inc, Hercules, CA, US) and signals were digitalized and analyzed by densitometry with the embedded software (Image Lab Software, v.6.1). Band intensities of phosphorylated proteins were normalized with total protein intensities as well as with the loading control beta-actin. The antibodies used in this study were the following: p-Akt (cat#9271, Cell Signaling, Massachusetts, USA), Akt (Cell Signaling, #9272, Massachusetts, USA), p-Erk 1/2 (Cell Signaling, #9101, Massachusetts, USA), Erk 1/2 (Cell Signaling, #9102, Massachusetts, USA) and β-actin (Cell Signaling, #3700, Massachusetts, USA).

Statistical analysis

Comparison among groups was performed using t-test for parametric data, or Mann—Whitney and the Kruskal—Wallis test with Dunn's multiple comparison post-test for non-parametric data. Data were depicted in box-and-whiskers or bars and plotted as median with range or mean ± S.D. The GraphPad InStat Software (GraphPad v6.0, San Diego, CA, USA) was used for analysis. P value < 0.05 was considered statistically significant. Results are representative of at least three independent experiments.

Results

SARS-CoV-2 S protein suppresses pro-inflammatory responses in A549 epithelial cells

The inflammatory responses of alveolar epithelial cells driven by the SARS-CoV-2 -Spike/ACE2 interaction were determined by stimulation of A549 cells with different concentrations of SARS-CoV-2 Spike-Membrane recombinant fusion protein and measuring the induction of the inflammatory mediators IL6, TNFα, IL8 at 6 hours following stimulation, since they are induced early in inflammatory responses, and IFNα, CXCL5 and PAI-1 at 12 hours following stimulation, since they are induced at later time points. We utilized a commercially available SARS-CoV-2 S protein raised in HEK293 cells, therefore no bacteria were involved, to avoid potential endotoxin contamination. The results showed that SARS-CoV-2 S protein suppressed the expression and production of IL8, IL6 and TNFα (Figures 1A–C, G–I). At higher doses of the recombinant protein the suppressive effect was abrogated, possibly due to binding of the protein to additional receptors with lower affinity, such as TLRs, through which the effect could be stimulatory. Expression of CXCL5, PAI-1 and IFNα was measured at 6 and 12 hours following stimulation with SARS-CoV-2 S protein but no effect was observed (Figures 1D–F). The results showed that SARS-CoV-2 S protein suppressed the release of pro-inflammatory cytokines at early stages of contact with alveolar epithelial cells.

SARS-CoV-2 S protein modulated TLR2 responses in A549 epithelial cells

To determine the effect of SARS-CoV-2 S protein on alveolar epithelial cells when co-stimulated with TLR2, a signal that can be initiated by SARS CoV2 envelope protein or by bacterial lipoproteins, we exposed A549 cells to the TLR2 ligand PAM3csk4 in the presence of SARS-CoV-2 Spike for 6 and 12 hours. PAM3csk4-stimulated A549 cells demonstrated reduced expression and secretion of IL8 (Figures 2A, G), as well as reduced secretion of IL6 and TNFα (Figures 2H, I), following stimulation with SARS-CoV-2 S protein. At the mRNA level, expression of IL6 and TNFα was not affected (Figures 2B, C), suggesting that regulation of these proteins by SARS-CoV-2 S protein may occur at the post-transcriptional level. On the contrary, PAM3csk4-induced expression of inflammatory mediators CXCL5, PAI-1 and IFNα increased at 12 hours post-stimulation with SARS-CoV-2 S protein (Figures 2D–F). Expression of CXCL5, PAI-1 and IFNα was not affected at 6 hours following stimulation (data not shown). The results showed that SARS-CoV-2 S protein suppressed the induction

10.3389/fimmu.2022.1020624

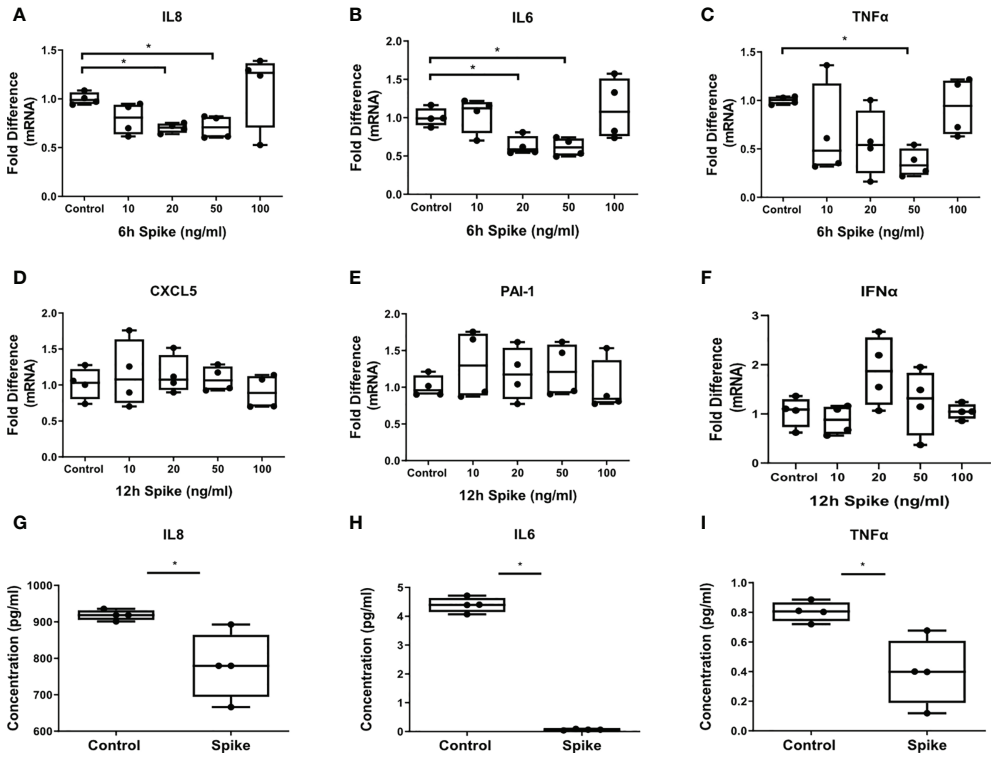

FIGURE 1
SARS-CoV-2 S protein suppressed the expression and production of pro-inflammatory cytokines in A549 cells. A549 cells were treated with different concentrations of SARS-CoV-2 Spike-Membrane recombinant fusion protein (10, 20, 50, 100 ng/ml) for 6 or 12 hours. **(A–C)** mRNA expression of IL6, IL8 and TNFα decreased upon SARS-CoV2 Spike stimulation for 6 hours compared to untreated control cells. **(D–F)** No effect was observed for the expression of CXCL5, PAI-1 and IFNα at 12 hours following stimulation. **(G–I)** Secretion of IL8, IL6 and TNFα decreased upon SARS-CoV2 Spike stimulation (50ng/ml) for 12 hours. Data are illustrated in box-and-whiskers and plotted as median with range (n=4 biological replicates per group). Statistical analysis was performed with Kruskal - Wallis test **(A–F)** and Mann – Whitney U test **(G–I)**. Results are representative of three independent experiments. *p < 0.05.

of pro-inflammatory cytokines in TLR2-stimulated A549 cells at early timepoints, while combination of SARS-CoV-2 S protein and TLR2 induced expression of the anti-viral responses through IFNα, expression of the chemokine CXCL5 potentially leading to recruitment of inflammatory cells.

SARS-CoV-2 S exerted its immunosuppressive action through the PI3K/Akt pathway in A549 cells

To determine which signaling pathway is involved in the early SARS-CoV-2 S immunosuppressive action, we stimulated A549 cells with SARS-CoV-2 S protein, TLR2 ligand PAM3csk4 and the additive effect of both SARS-CoV-2 S protein and PAM3csk4 for 15 and 30 minutes for protein collection and quantification of specific signaling targets in western blot. The signaling pathways investigated were the PI3K/Akt and MAPK/ERK pathway, which were previously associated with COVID19 pathogenesis and progression. While MAPK/ERK is a well characterized pro-inflammatory pathway (34), Akt signals initiate both anti-inflammatory and pro-inflammatory effects (35). The results shown in Figure 3, revealed that SARS-CoV-2 S slightly decreased the phosphorylation and activation of ERK1/2, while it increased the phosphorylation and activation of AKT. The addition of TLR2 stimuli along with SARS-CoV-2 S amplified this effect considerably.

To confirm that suppression of pro-inflammatory cytokines by SARS-CoV-2 S protein was mediated through the PI3K/Akt pathway, we treated A549 cells with the selective AKT inhibitor MK2206 for 24 hours and subsequently stimulated cells with SARS-CoV-2 S protein. Inhibition of Akt with MK2206 was confirmed by western blot (Supplementary Figure 1). In the presence of SARS-CoV-2 S protein, A549 cells secreted reduced IL8, IL6 and TNFα, an effect which was abrogated in MK2206-treated cells (Figure 4). This result confirmed that the initial immunosuppression observed in the presence of SARS-CoV-2 S protein was mediated through the PI3K/Akt pathway.

10.3389/fimmu.2022.1020624

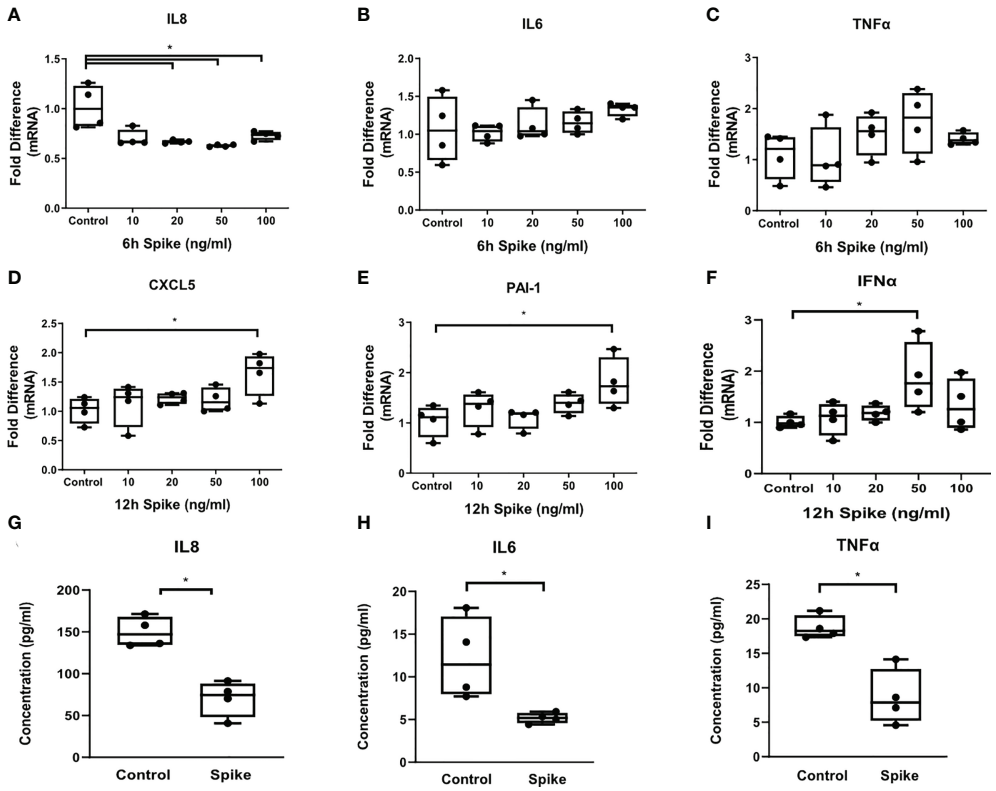

FIGURE 2
SARS-CoV-2 S protein differentially modulated TLR responses in A549 cells. A549 cells were treated with different concentrations of SARS-CoV-2 Spike-Membrane recombinant fusion protein (10, 20, 50, 100 ng/ml) and PAM3csk4 (1μg/ml) for 6 or 12 hours. **(A)** Decreased mRNA expression of IL8 was observed upon co-stimulation with SARS CoV2 S protein and PAM3csk4, compared to cells treated with PAM3csk4-alone (control). **(B, C)** No effect was observed for the expression of IL6 and TNFα. **(D–F)** Increased expression of CXCL5, PAI-1 and IFNα at 12 hours post-stimulation. **(G–I)** Secretion of IL8, IL6 and TNFα decreased in the presence of SARS-CoV-2 S (50ng/ml) after 12 hours. Data are illustrated in box-and-whiskers and plotted as median with range (n=4 biological replicates per group). Statistical analysis was performed with Kruskal - Wallis test **(A–F)** and Mann – Whitney U test **(G–I)**. Results are representative of three independent experiments. *p < 0.05.

Discussion

COVID-19 pandemic continues to pose a major challenge for public health and economy. Severe COVID-19 cases are associated with development of lung injury, vascular damage and ARDS, which is the main cause of high mortality rates (36). SARS-CoV-2 initial sites of infection include the upper and lower respiratory tracts. At the lower respiratory tract, SARS-CoV-2 infects cells of the gas exchange portion of the lung and in particular the alveolar epithelial type II cells. Pathological alterations at this region, include alveolar damage, pneumocyte desquamation and hyaline membrane formation, as well as significant accumulation of monocytes/macrophages, responsible for the robust inflammatory cytokine response observed (37, 38). However, recent studies have shown a dampened innate immune response after SARS-CoV-2 infection of nasal and bronchial epithelial cells (39, 40), as well as an early immunosuppression stage preceding the later hyperinflammation stage that leads to cytokine storm and ARDS (41). Therefore, developing new personalized therapeutic interventions requires a better understanding of the differential immune responses according to the cell type infected, as well as the COVID-19 patient's immune status and how it evolves during the course of the disease.

In the present study, we used A549 cells stimulated with SARS-CoV-2 S protein as a model to investigate the immunomodulatory action of SARS-CoV-2 in alveolar epithelial type II cells. Our findings demonstrated decreased expression and secretion of IL8, IL6 and TNFα, while CXCL5, PAI-1 and IFNα remained unaffected even 12 hours post-infection. This finding implies that alveolar epithelial type II cells may enter an immunosuppressive state at early stages of the infection. Previous studies have already demonstrated reduced expression of pro-inflammatory cytokines in the myeloid cells from patients with COVID-19 (42), as well as reduced production of chemokines (41). A possible explanation for the early decreased inflammatory responses of the airway epithelium could be the result of immune evasion mechanisms employed by

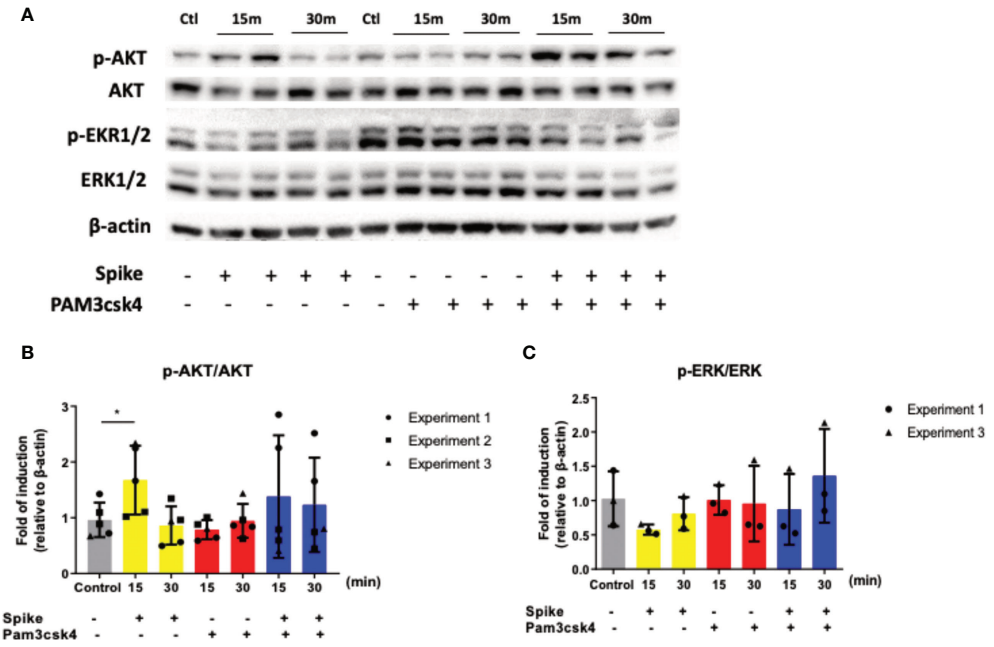

FIGURE 3
SARS-CoV-2 S protein triggered the induction of the PI3K/Akt pathway. A549 cells were treated with 50ng/ml SARS-CoV-2 S protein or PAM3csk4 or SARS-CoV-2 S and PAM3csk4 for 15 and 30 minutes. SARS-CoV-2 S protein slightly decreased the phosphorylation of ERK1/2 **(A, C)**, while significantly increased the phosphorylation of AKT **(A, B)**. Representative western blot **(A)** is presented and densitometry analysis from three **(B)** or two **(C)** independent experiments. Densitometry analysis is illustrated in bar graphs and plotted as mean ± S.D. Individual points indicate the biological replicates from all experiments (experiments 1 and 2 include two biological replicates for each condition and experiment 3 includes one biological replicate per condition). Statistical analysis was performed with t test **(B)**, but it was omitted for ERK due to the small sample size **(C)**. *p < 0.05.

the virus to survive and replicate inside the alveolar epithelial cells avoiding the detection by other immune cells (43). Another potential explanation could be the occurrence of increased cell death and the disruption of tight junction complexes between adjacent epithelial cells observed during SARS-CoV-2 infection (41), leading to the upregulation of homeostatic mechanisms to resolve this situation rather than inflammatory responses. Co-stimulation of SARS-CoV-2 S protein with the TLR2 ligand PAM3csk4, increased significantly the expression of the inflammatory mediators CXCL5, PAI-1 and IFNα at 12 hours following infection, but could not change the decreased production of the pro-inflammatory cytokines IL8, IL6 and

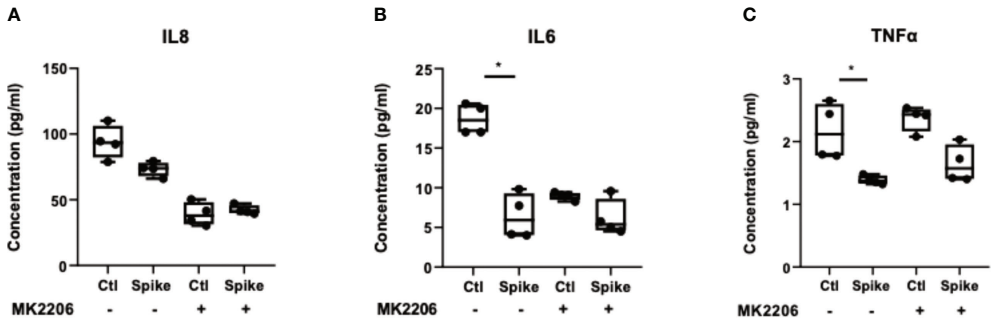

FIGURE 4
Inhibition of AKT abrogated the immunosuppressive action of SARS-CoV-2 S protein. A549 cells were treated with the pan-AKT inhibitor MK2206 (5μM) for 24 hours and then stimulated with SARS-CoV-2 S (50ng/ml) for 12 hours. Secretion of IL8 **(A)**, IL6 **(B)** and TNFα **(C)** decreased in the presence of SARS-CoV-2 S, an effect which was less evident in MK2206-treated cells. Data are illustrated in bars and plotted as median with range (n=4 biological replicates per group). Statistical analysis was performed with Kruskal - Wallis test. *p < 0.05.

TNFα. While it is known that TLR2 signaling induces inflammatory responses via the NF-kB pathway during SARS-CoV-2 infection (14), our findings demonstrate that TLR2-induced cytokine production is not enough to ameliorate the early-stage immunosuppression induced by SARS-CoV-2 in alveolar epithelial type II cells. However, at a later timepoint a potential stimulation of TLR2 by SARS-CoV-2 can induce inflammatory and anti-viral responses (CXCL5, IFNα) and promote disease pathogenesis by enhancing the coagulation mechanism (induction of PAI-1). Several studies have found elevated levels of PAI-1 in hospitalized COVID-19 patients (4, 44, 45). Increased levels of PAI-1 are associated with thrombosis, since inhibition of plasminogen activators results to reduced conversion of plasminogen to plasmin which degrades fibrin clots (46). PAI-1 is expressed in different cell types and its increase can be induced by proinflammatory cytokines, indicating a cross-link between inflammation and thrombosis (47, 48). Moreover, studies have shown that PAI-1 is highly induced in alveolar type II cells in idiopathic pulmonary fibrosis (IPF), regulating alveolar type II cell senescence and secretion of profibrotic mediators (49). Nevertheless, our data show a modest induction of PAI-1 expression in TLR2 activated cells, suggesting that SARS CoV2 S protein signaling may not be the primary signal inducing PAI-1. The simultaneous increase of CXCL5, responsible for neutrophil recruitment, also correlates with the development of immunothrombosis, since neutrophils are known to stabilize microthrombi via the release of neutrophil extracellular traps (NETs) (50).

To decipher the molecular pathway by which SARS-CoV-2 S protein exerts this early immunosuppressive action in alveolar epithelial cells, we treated A549 cells with SARS-CoV-2 S protein, TLR2 ligand PAM3csk4 and their combination for 15 and 30 minutes, in order to investigate their impact to specific molecular pathways, such as PI3K/AKT and MAPK/ERK. Our results demonstrated that SARS-CoV-2 S protein did not affect the MAPK/ERK pathway, but significantly induced the PI3K/AKT pathway, since the induction of AKT phosphorylation was observed upon stimulation with SARS-CoV-2 S protein, particularly when co-stimulated with PAM3csk4. To further verify that the immunosuppressive effects of SARS-CoV-2 were mediated through the activation of PI3K/AKT, we also treated A549 cells with the selective AKT 1/2/3 inhibitor MK2206 and measured the production of IL8, IL6 and TNFα after S protein stimulation compared to mock treated cells. Stimulation with PAM3csk4 was not performed at this instance, since SARS-CoV-2 S protein is the primary cause of the decreased inflammatory responses observed, while PAM3csk4 induces inflammatory responses independently through TLR2 receptor. Indeed, we observed that SARS-CoV-2 S was not able to significantly alter the production of IL8, IL6 and TNFα in MK2206-treated cells compared to mock treated cells. Our findings are in accordance with other studies indicating the possible implication of the PI3K/AKT pathway in the immunosuppressive action of the virus and other diseases. For example, IL-37, a member of the IL-1 family which is stimulated by SARS-CoV-2, has been shown to suppress IL-1β, IL-6, TNFα and CCL2 in rheumatic diseases by acting on mTOR and enhancing the AMPK activity, to maintain mitochondrial membrane potential and limit the toxic effects of ROS (51). Other studies have also shown that PI3K signaling mediates an immunosuppressive phenotype in myeloid cells to prevent excessive innate immunity in chronic infections and inflammation (52). Another possible immunosuppressive activity of SARS-CoV-2 acting through the PI3K/AKT/mTOR pathway is the inhibition of autophagy. Studies have shown that coronaviruses might inhibit the autophagic mechanism by increasing viral replication and through upregulation of AKT/mTOR, since mTORC1 is known to inhibit autophagy (53). For example, the related corona virus MERS-CoV can interfere with host cell autophagy by promoting the degradation of BECN1, after AKT1 activation (54). Hence, Akt/mTOR inhibitors could prove a valuable asset in COVID-19 management. Various studies have shown that blockade of mTOR can inhibit protein synthesis and thus reduce viral replication and inflammation (55–57). Moreover, mTOR inhibitors can limit the proliferation of memory B cells and T cell responses, preventing the production of cross-reactive antibodies for SARS-CoV-2 (58, 59).

Our study has several limitations, since the work was performed in a single cell line A549 and investigated a single molecular pathway (PI3K/AKT). In addition, the implication of the PI3K/AKT pathway could be further investigated with mTOR inhibitors or other downstream AKT targets to delineate the exact mechanism by which PI3K/AKT decreases the pro-inflammatory responses. Even if our study correlates with other studies showing decreased cytokine production in SARS- CoV-2 infection as previously mentioned, there are not many reports for cytokine production at the early stages of the infection and further research should be performed to this direction, before we can reach certain conclusions. However, this study can propose the potential use of AKT/mTOR inhibitors for the regulation of inflammatory responses during SARS-CoV-2 infection.

Data availability statement

The raw data supporting the conclusions of this article will be made available by the authors, without undue reservation.

Author contributions

CT, AA-Q, EV, and GS designed the study, IP performed experiments, IP, EV, FA, and HA, SM-N analyzed data, IP, CT, AA-Q, and EV drafted the manuscript, IP, CT, AA-Q, EV, FA, HA, SM-N, and GS reviewed the manuscript. All authors contributed to the article and approved the submitted version.

Funding

This work has been funded by the Hellenic Foundation for Research and Innovation grant (HFRI, General Secretariat for Research and Technology, GSRT Grant No 1010), the King Abdullah International Medical Research Center under grant number RC17/128/R, and the King Faisal Specialist Hospital and Research Center, Riyadh, Saudi Arabia.

Conflict of interest

The authors declare that the research was conducted in the absence of any commercial or financial relationships that could be construed as a potential conflict of interest.

Publisher's note

Supplementary material

The Supplementary Material for this article can be found online at: https://www.frontiersin.org/articles/10.3389/fimmu.2022.1020624/full#supplementary-material

References

1. Zhou F, Yu T, Du R, Fan G, Liu Y, Liu Z, et al. Clinical course and risk factors for mortality of adult inpatients with COVID-19 in wuhan, China: a retrospective cohort study. *Lancet* (2020) 395:1054–62. doi: 10.1016/S0140-6736(20)30566-3

2. Guo T, Fan Y, Chen M, Wu X, Zhang L, He T, et al. Cardiovascular implications of fatal outcomes of patients with coronavirus disease 2019 (COVID-19). *JAMA Cardiol* (2020) 5:811. doi: 10.1001/jamacardio.2020.1017

3. Lodigiani C, Iapichino G, Carenzo L, Cecconi M, Ferrazzi P, Sebastian T, et al. Venous and arterial thromboembolic complications in COVID-19 patients admitted to an academic hospital in Milan, Italy. *Thromb Res* (2020) 191:9–14. doi: 10.1016/j.thromres.2020.04.0244

4. Zuo Y, Warnock M, Harbaugh A, Yalavarthi S, Gockman K, Zuo M, et al. Plasma tissue plasminogen activator and plasminogen activator inhibitor-1 in hospitalized COVID-19 patients. *Sci Rep* (2021) 11:1580. doi: 10.1038/s41598-020-80010-z5

5. Hoffmann M, Kleine-Weber H, Schroeder S, Krüger N, Herrler T, Erichsen S, et al. SARS-CoV-2 cell entry depends on ACE2 and TMPRSS2 and is blocked by a clinically proven protease inhibitor. *Cell* (2020) 181:271–280.e8. doi: 10.1016/j.cell.2020.02.0526

6. Letko M, Marzi A, Munster V. Functional assessment of cell entry and receptor usage for SARS-CoV-2 and other lineage b betacoronaviruses. *Nat Microbiol* (2020) 5:562–9. doi: 10.1038/s41564-020-0688-y

7. Wan Y, Shang J, Graham R, Baric RS, Li F. Receptor recognition by the novel coronavirus from wuhan: an analysis based on decade-long structural studies of SARS coronavirus. *J Virol* (2020) 94:e00127-20. doi: 10.1128/JVI.00127-20

8. Li F. Structure, function, and evolution of coronavirus spike proteins. *Annu Rev Virol* (2016) 3:237–61. doi: 10.1146/annurev-virology-110615-042301

9. Tang T, Bidon M, Jaimes JA, Whittaker GR, Daniel S. Coronavirus membrane fusion mechanism offers a potential target for antiviral development. *Antiviral Res* (2020) 178:104792. doi: 10.1016/j.antiviral.2020.104792

10. Walls AC, Park Y-J, Tortorici MA, Wall A, McGuire AT, Veesler D. Structure, function, and antigenicity of the SARS-CoV-2 spike glycoprotein. *Cell* (2020) 181:281–292.e6. doi: 10.1016/j.cell.2020.02.058

11. Ou X, Liu Y, Lei X, Li P, Mi D, Ren L, et al. Characterization of spike glycoprotein of SARS-CoV-2 on virus entry and its immune cross-reactivity with SARS-CoV. *Nat Commun* (2020) 11:1620. doi: 10.1038/s41467-020-15562-9

12. Matsuyama S, Nao N, Shirato K, Kawase M, Saito S, Takayama I, et al. Enhanced isolation of SARS-CoV-2 by TMPRSS2-expressing cells. *Proc Natl Acad Sci* (2020) 117:7001–7003. doi: 10.3389/fmicb.2022.948770

13. Dai J, Wang Y, Wang H, Gao Z, Wang Y, Fang M, Shi S, Zhang P, Wang H, Su Y, Yang M, et al. Toll-Like Receptor Signaling in Severe Acute Respiratory Syndrome Coronavirus 2-Induced Innate Immune Responses and the Potential Application Value of Toll-Like Receptor Immunomodulators in Patients With Coronavirus Disease 2019 *Frontiers in Microbiology* (2022) 13:948770. doi: 10.3389/fmicb.2022.948770

14. Khan S, Shafiei MS, Longoria C, Schoggins JW, Savani RC, Zaki H. SARS-CoV-2 spike protein induces inflammation *via* TLR2-dependent activation of the NF-κB pathway. *Elife* (2021) 10:e68563. doi: 10.7554/eLife.68563

15. Zheng M, Karki R, Williams EP, Yang D, Fitzpatrick E, Vogel P, et al. TLR2 senses the SARS-CoV-2 envelope protein to produce inflammatory cytokines. *Nat Immunol* (2021) 22:829–38. doi: 10.1038/s41590-021-00937-x

16. Ravindra NG, Alfajaro MM, Gasque V, Huston NC, Wan H, Szigeti-Buck K, et al. Single-cell longitudinal analysis of SARS-CoV-2 infection in human airway epithelium identifies target cells, alterations in gene expression, and cell state changes. *PloS Biol* (2021) 19:e3001143. doi: 10.1371/journal.pbio.3001143

17. Sungnak W, Huang N, Bécavin C, Berg M, Queen R, Litvinukova M, et al. SARS-CoV-2 entry factors are highly expressed in nasal epithelial cells together with innate immune genes. *Nat Med* (2020) 26:681–7. doi: 10.1038/s41591-020-0868-6

18. Ziegler CGK, Miao VN, Owings AH, Navia AW, Tang Y, Bromley JD, et al. Impaired local intrinsic immunity to SARS-CoV-2 infection in severe COVID-19. *Cell* (2021) 184:4713–4733.e22. doi: 10.1016/j.cell.2021.07.023

19. Martines RB, Ritter JM, Matkovic E, Gary J, Bollweg BC, Bullock H, et al. Pathology and pathogenesis of SARS-CoV-2 associated with fatal coronavirus disease, united states. *Emerg Infect Dis* (2020) 26:2005–15. doi: 10.3201/eid2609.202095

20. Borczuk AC, Salvatore SP, Seshan SV, Patel SS, Bussel JB, Mostyka M, et al. COVID-19 pulmonary pathology: a multi-institutional autopsy cohort from Italy and new York city. *Mod Pathol* (2020) 33:2156–68. doi: 10.1038/s41379-020-00661-1

21. Lowery SA, Sariol A, Perlman S. Innate immune and inflammatory responses to SARS-CoV-2: Implications for COVID-19. *Cell Host Microbe* (2021) 29:1052–62. doi: 10.1016/j.chom.2021.05.004

22. Zheng M, Gao Y, Wang G, Song G, Liu S, Sun D, et al. Functional exhaustion of antiviral lymphocytes in COVID-19 patients. *Cell Mol Immunol* (2020) 17:533–5. doi: 10.1038/s41423-020-0402-2

23. Zheng Y, Huang Z, Yin G, Zhang X, Ye W, Hu Z, et al. Study of the lymphocyte change between COVID-19 and non-COVID-19 pneumonia cases suggesting other factors besides uncontrolled inflammation contributed to multi-organ injury. *SSRN Electron J* (2020). Available at: http://dx.doi.org/10.2139/ssrn.3555267.

24. Remy KE, Mazer M, Striker DA, Ellebedy AH, Walton AH, Unsinger J, et al. Severe immunosuppression and not a cytokine storm characterizes COVID-19 infections. *JCI Insight* (2020) 5:e140329. doi: 10.1172/jci.insight.140329

25. Azzi Y, Bartash R, Scalea J, Loarte-Campos P, Akalin E. COVID-19 and solid organ transplantation: A review article. *Transplantation* (2021) 105:37–55. doi: 10.1097/TP.0000000000003523

26. Notz Q, Schmalzing M, Wedekink F, Schlesinger T, Gernert M, Herrmann J, et al. Pro- and anti-inflammatory responses in severe COVID-19-Induced acute respiratory distress syndrome–an observational pilot study. *Front Immunol* (2020) 11:581338. doi: 10.3389/fimmu.2020.581338

27. Henry BM, Benoit SW, Vikse J, Berger BA, Pulvino C, Hoehn J, et al. The anti-inflammatory cytokine response characterized by elevated interleukin-10 is a

stronger predictor of severe disease and poor outcomes than the pro-inflammatory cytokine response in coronavirus disease 2019 (COVID-19). *Clin Chem Lab Med* (2021) 59:599–607. doi: 10.1515/cclm-2020-1284

28. Neumann J, Prezzemolo T, Vanderbeke L, Roca CP, Gerbaux M, Janssens S, et al. Increased IL-10-producing regulatory T cells are characteristic of severe cases of COVID-19. *Clin Transl Immunol* (2020) 9:e1204. doi: 10.1002/cti2.120429

29. Stukalov A, Girault V, Grass V, Karayel O, Bergant V, Urban C, et al. Multilevel proteomics reveals host perturbations by SARS-CoV-2 and SARS-CoV. *Nature* (2021) 594:246–52. doi: 10.1038/s41586-021-03493-4

30. Appelberg S, Gupta S, Svensson Akusjärvi S, Ambikan AT, Mikaeloff F, Saccon E, et al. Dysregulation in Akt/mTOR/HIF-1 signaling identified by proteo-transcriptomics of SARS-CoV-2 infected cells. *Emerg Microbes Infect* (2020) 9:1748–60. doi: 10.1080/22221751.2020.1799723

31. Mizutani T, Fukushi S, Saijo M, Kurane I, Morikawa S. JNK and PI3k/Akt signaling pathways are required for establishing persistent SARS-CoV infection in vero E6 cells. *Biochim Biophys Acta - Mol Basis Dis* (2005) 1741:4–10. doi: 10.1016/j.bbadis.2005.04.004

32. Sabbah DA, Hajjo R, Bardaweel SK, Zhong HA. Phosphatidylinositol 3-kinase (PI3K) inhibitors: a recent update on inhibitor design and clinical trials (2016–2020). *Expert Opin Ther Pat* (2021) 31:877–92. doi: 10.1080/13543776.2021.1924150

33. Khezri MR. PI3K/AKT signaling pathway: a possible target for adjuvant therapy in COVID-19. *Hum Cell* (2021) 34:700–1. doi: 10.1007/s13577-021-00484-5

34. Moens U, Kostenko S, Sveinbjørnsson B. The role of mitogen-activated protein kinase-activated protein kinases (MAPKAPKs) in inflammation. *Genes (Basel)* (2013) 4:101–33. doi: 10.3390/genes4020101

35. Arranz A, Doxaki C, Vergadi E, Martinez de la Torre Y, Vaporidi K, Lagoudaki ED, et al. Akt1 and Akt2 protein kinases differentially contribute to macrophage polarization. *Proc Natl Acad Sci* (2012) 109:9517–22. doi: 10.1073/pnas.1119038109

36. Goh KJ, Choong MC, Cheong EH, Kalimuddin S, Duu Wen S, Phua GC, et al. Rapid progression to acute respiratory distress syndrome: Review of current understanding of critical illness from coronavirus disease 2019 (COVID-19) infection. *Ann Acad Med Singapore* (2020) 49:108–18. doi: 10.47102/annals-acadmedsg.202057

37. Barton LM, Duval EJ, Stroberg E, Ghosh S, Mukhopadhyay S. COVID-19 autopsies, Oklahoma, USA. *Am J Clin Pathol* (2020) 153:725–33. doi: 10.1093/ajcp/aqaa062

38. Xu Z, Shi L, Wang Y, Zhang J, Huang L, Zhang C, et al. Pathological findings of COVID-19 associated with acute respiratory distress syndrome. *Lancet Respir Med* (2020) 8:420–2. doi: 10.1016/S2213-2600(20)30076-X

39. Pizzorno A, Padey B, Julien T, Trouillet-Assant S, Traversier A, Errazuriz-Cerda E, et al. Characterization and treatment of SARS-CoV-2 in nasal and bronchial human airway epithelia. *Cell Rep Med* (2020) 1:100059. doi: 10.1016/j.xcrm.2020.100059

40. Gamage AM, Sen TK, WOY C, Liu J, CW T, YK O, et al. Infection of human nasal epithelial cells with SARS-CoV-2 and a 382-nt deletion isolate lacking ORF8 reveals similar viral kinetics and host transcriptional profiles. *PloS Pathog* (2020) 16:e1009130. doi: 10.1371/journal.ppat.1009130

41. Tian W, Zhang N, Jin R, Feng Y, Wang S, Gao S, et al. Immune suppression in the early stage of COVID-19 disease. *Nat Commun* (2020) 11:5859. doi: 10.1038/s41467-020-19706-9

42. Arunachalam PS, Wimmers F, Mok CKP, Perera RAPM, Scott M, Hagan T, et al. Systems biological assessment of immunity to mild versus severe COVID-19 infection in humans. *Science* (2020) 369:1210–20. doi: 10.1126/science.abc6261

43. Rouse BT, Sehrawat S. Immunity and immunopathology to viruses: what decides the outcome? *Nat Rev Immunol* (2010) 10:514–26. doi: 10.1038/nri2802

44. Wright FL, Vogler TO, Moore EE, Moore HB, Wohlauer MV, Urban S, et al. Fibrinolysis shutdown correlation with thromboembolic events in severe COVID-19 infection. *J Am Coll Surg* (2020) 231:193–203e1. doi: 10.1016/j.jamcollsurg.2020.05.007

45. Nougier C, Benoit R, Simon M, Desmurs-Clavel H, Marcotte G, Argaud L, et al. Hypofibrinolytic state and high thrombin generation may play a major role in SARS-COV2 associated thrombosis. *J Thromb Haemost* (2020) 18:2215–9. doi: 10.1111/jth.15016

46. Westrick R, Eitzman D. Plasminogen activator inhibitor-1 in vascular thrombosis. *Curr Drug Targets* (2007) 8:996–1002. doi: 10.2174/138945007781662328

47. Meltzer ME, Lisman T, de Groot PG, Meijers JCM, le Cessie S, Doggen CJM, et al. Venous thrombosis risk associated with plasma hypofibrinolysis is explained by elevated plasma levels of TAFI and PAI-1. *Blood* (2010) 116:113–21. doi: 10.1182/blood-2010-02-267740

48. Libby P, Simon DI. Inflammation and thrombosis. *Circulation* (2001) 103:1718–20. doi: 10.1161/01.CIR.103.13.1718

49. Rana T, Jiang C, Liu G, Miyata T, Antony V, Thannickal VJ, et al. PAI-1 regulation of TGF-β1–induced alveolar type II cell senescence, SASP secretion, and SASP-mediated activation of alveolar macrophages. *Am J Respir Cell Mol Biol* (2020) 62:319–30. doi: 10.1165/rcmb.2019-0071OC

50. Zuo Y, Yalavarthi S, Shi H, Gockman K, Zuo M, Madison JA, Blair CN, Weber A, Barnes BJ, Egeblad M, et al. Neutrophil extracellular traps in COVID-19. *JCI Insight* (2020) 5:e138999. doi: 10.1172/jci.insight.138999

51. Maiese K. The mechanistic target of rapamycin (mTOR): Novel considerations as an antiviral treatment. *Curr Neurovasc Res* (2020) 17:332–7. doi: 10.2174/1567202617666200425205122

52. Condliffe AM. Sequential activation of class IB and class IA PI3K is important for the primed respiratory burst of human but not murine neutrophils. *Blood* (2005) 106:1432–40. doi: 10.1182/blood-2005-03-0944

53. Miller K, McGrath ME, Hu Z, Ariannejad S, Weston S, Frieman M, et al. Coronavirus interactions with the cellular autophagy machinery. *Autophagy* (2020) 16:2131–9. doi: 10.1080/15548627.2020.1817280

54. Gassen NC, Niemeyer D, Muth D, Corman VM, Martinelli S, Gassen A, et al. SKP2 attenuates autophagy through Beclin1-ubiquitination and its inhibition reduces MERS-coronavirus infection. *Nat Commun* (2019) 10:5770. doi: 10.1038/s41467-019-13659-4

55. Gates LE, Hamed AA. The anatomy of the SARS-CoV-2 biomedical literature: Introducing the CovidX network algorithm for drug repurposing recommendation. *J Med Internet Res* (2020) 22:e21169. doi: 10.2196/21169

56. Ramaiah MJ. mTOR inhibition and p53 activation, microRNAs: The possible therapy against pandemic COVID-19. *Gene Rep* (2020) 20:100765. doi: 10.1016/j.genrep.2020.100765

57. Kindrachuk J, Ork B, Hart BJ, Mazur S, Holbrook MR, Frieman MB, et al. Antiviral potential of ERK/MAPK and PI3K/AKT/mTOR signaling modulation for middle East respiratory syndrome coronavirus infection as identified by temporal kinome analysis. *Antimicrob Agents Chemother* (2015) 59:1088–99. doi: 10.1128/AAC.03659-14

58. Lin C-Y, Hsu S-C, Lee H-S, Lin S-H, Tsai C-S, Huang S-M, et al. Enhanced expression of glucose transporter-1 in vascular smooth muscle cells *via* the akt/tuberous sclerosis complex subunit 2 (TSC2)/mammalian target of rapamycin (mTOR)/ribosomal S6 protein kinase (S6K) pathway in experimental renal failure. *J Vasc Surg* (2013) 57:475–85. doi: 10.1016/j.jvs.2012.07.037

59. Raybuck AL, Cho SH, Li J, Rogers MC, Lee K, Williams CL, et al. B cell–intrinsic mTORC1 promotes germinal center–defining transcription factor gene expression, somatic hypermutation, and memory b cell generation in humoral immunity. *J Immunol* (2018) 200:2627–39. doi: 10.4049/jimmunol.1701321

frontiers | Frontiers in Immunology

TYPE Original Research
PUBLISHED 31 October 2022
DOI 10.3389/fimmu.2022.1023903

OPEN ACCESS

EDITED BY
Annapurna Vyakarnam,
King's College London,
United Kingdom

REVIEWED BY
Gill Diamond,
University of Louisville, United States
Rob Janssen,
Canisius Wilhelmina Hospital,
Netherlands

*CORRESPONDENCE
Chrysanthi Skevaki
Chrysanthi.Skevaki@uk-gm.de

†These authors have contributed equally to this work and share first authorship

SPECIALTY SECTION
This article was submitted to Viral Immunology, a section of the journal Frontiers in Immunology

RECEIVED 20 August 2022
ACCEPTED 10 October 2022
PUBLISHED 31 October 2022

CITATION
Kümmel LS, Krumbein H, Fragkou PC, Hünerbein BL, Reiter R, Papathanasiou KA, Thölken C, Weiss ST, Renz H and Skevaki C (2022) Vitamin D supplementation for the treatment of COVID-19: A systematic review and meta-analysis of randomized controlled trials. *Front. Immunol.* 13:1023903. doi: 10.3389/fimmu.2022.1023903

Vitamin D supplementation for the treatment of COVID-19: A systematic review and meta-analysis of randomized controlled trials

Lara S. Kümmel[1†], Hanna Krumbein[1†], Paraskevi C. Fragkou[2], Ben L. Hünerbein[1], Rieke Reiter[1], Konstantinos A. Papathanasiou[3], Clemens Thölken[4], Scott T. Weiss[5], Harald Renz[1] and Chrysanthi Skevaki[1*]

[1]Institute of Laboratory Medicine, Universities of Giessen and Marburg Lung Center (UKGMLC), Philipps Universität Marburg, German Center for Lung Research/ Deutsches Zentrum für Lungenforschung (DZL) Marburg, Marburg, Germany, [2]First Department of Critical Care Medicine and Pulmonary Services, Evangelismos Hospital, Medical School of Athens, National and Kapodistrian University of Athens, Athens, Greece, [3]Medical School, National and Kapodistrian University of Athens, Athens, Greece, [4]Institute of Medical Bioinformatics and Biostatistics, Medical Faculty, Philipps University of Marburg, Marburg, Germany, [5]Channing Division of Network Medicine, Department of Medicine, Brigham and Women's Hospital, Harvard Medical School, Boston, MA, United States

Vitamin D supplementation and its impact on immunoregulation are widely investigated. We aimed to assess the prevention and treatment efficiency of vitamin D supplementation in the context of coronavirus disease 2019 (COVID-19) and any disease-related complications. For this systematic review and meta-analysis, we searched databases (PubMed, Embase, Scopus, Web of Science, The Cochrane Library, medRxiv, Cochrane COVID-19 Study Register, and ClinicalTrial.gov) for studies published between 1 November 2019 and 17 September 2021. We considered randomized trials (RCTs) as potentially eligible when patients were tested for SARS-CoV-2 infection and received vitamin D supplementation versus a placebo or standard-of-care control. A random-effects model was implemented to obtain pooled odds ratios for the effect of vitamin D supplementation on the main outcome of mortality as well as clinical outcomes. We identified a total of 5,733 articles, of which eight RCTs (657 patients) met the eligibility criteria. Although no statistically significant effects were reached, the use of vitamin D supplementation showed a trend for reduced mortality [odds ratio (OR) 0.74, 95% confidence interval (CI) 0.32–1.71, p = 0.48] compared with the control group, with even stronger effects, when vitamin D was administered repeatedly (OR 0.33, 95% CI 0.1–1.14). The mean difference for the length of hospitalization was −0.28 (95% CI −0.60 to 0.04), and the ORs were 0.41 (95% CI 0.15–1.12) and 0.52 (95% CI 0.27–1.02) for ICU admission and

10.3389/fimmu.2022.1023903

mechanical ventilation, respectively. In conclusion, vitamin D supplementation did not improve the clinical outcomes in COVID-19 patients, but trends of beneficial effects were observed. Further investigations are required, especially studies focusing on the daily administration of vitamin D.

KEYWORDS

vitamin D, SARS-CoV-2, COVID-19, systematic review, meta-analysis

Introduction

Within a short period of time, the novel coronavirus [severe acute respiratory syndrome-related coronavirus 2 (SARS-CoV-2)] has become a global challenge. The increase in the number of coronavirus disease 2019 (COVID-19) cases dictates the need for low-cost and widely available therapies, to help prevent SARS-COV-2 infections and protect from severe COVID-19.

There is evidence that vitamin D has an important impact on the human immune system and can prevent respiratory tract infections (1), as vitamin D plays a signaling role in the modulation of the innate and adaptive arms of the immune system and immunoregulation. A link has been made between pathogen recognition, cytokine secretion, the expression of nuclear vitamin D receptors, and 1-α-hydroxylase (CYP27B1), which is expressed in several tissues and immune cells (2). The active forms of vitamin D induce the production of antimicrobial peptides and support the differentiation of monocytes, with the enhancement of phagocytic and chemotactic capacity (3). Vitamin D leads to a more tolerogenic immune environment by downregulating the production of proinflammatory cytokines (e.g., IL-12, IFN-γ, IL-6, IL-8, TNF-α, and IL-9) and increasing the anti-inflammatory responses through blocking the NK-κB pathways (e.g., IL-4, IL-5, and IL-10) (4). The indirect and direct effects on T-cell differentiation lead toward a Th2 phenotype, and B-cell proliferation and immunoglobulin secretion are inhibited by vitamin D (3, 5).

The global prevalence of vitamin D deficiency (<20 ng/ml) is high and even higher for partial deficiency (<30 ng/ml). Several studies have reported data on the prevalence of low vitamin D levels in Europe (up to 40%) and in the United States of America, Canada, and India with more than 20% of the general population being deficient, which shows that inadequate vitamin D serum concentrations are a frequent issue around the globe (6). Vitamin D may come from three different sources: endogenous production after exposure to UVB rays, nutritional sources, or exogenous supplementation. Vitamin D has a good safety profile and is associated with a low risk for acute intoxication with commonly recommended doses (2). Therefore, it is a widely available low-cost supplement with the potential to reduce the prevalence of vitamin D deficiency. Recent observational studies have reported heterogeneous results about the association between insufficient vitamin D serum levels and the risk of developing severe COVID-19, requiring further investigations (7).

The aim of this review was to assess the potential effects of vitamin D supplementation on the treatment and prevention of COVID-19 and severity-related complications. In addition, it also aimed to evaluate the impact of different dosing and administration regimens compared with placebo or standard of care in randomized controlled trials (RCTs).

Materials and methods

Search strategy and selection criteria

This systematic review and meta-analysis was conducted according to the Preferred Reporting Items for Systematic Reviews and Meta-Analyses (PRISMA) guidelines (Supplementary Table 6) (8) and followed the "Cochrane Handbook for Systematic Reviews of Interventions" (9). The study protocol was registered with PROSPERO (CRD42021279150).

Two reviewers (LK, HK) independently performed the systematic search of the databases PubMed/MEDLINE, EMBASE, Scopus, Web of Science, The Cochrane Library, and the preprint server medRxiv in addition to the trial registries Cochrane COVID-19 Study Register and ClinicalTrials.gov for clinical trials published between 1 November 2019 and 17 September 2021. This search was performed using the following search terms: "COVID-19 OR SARS-CoV-2" AND "vitamin D." The search strategies are available in Supplementary Table 1. Additionally, a manual search was performed to identify further records by screening gray literature and references of eligible studies.

Studies were included in this meta-analysis when meeting the following inclusion criteria: involving participants with no age, gender, or ethnicity restriction, who were tested for SARS-CoV-2 infections as defined by the World Health Organization

(10); investigating any type of vitamin D supplementation compared with placebo, standard of care, or no treatment; and giving information of relevant clinical outcomes. Furthermore, only RCTs published in English or German language were eligible. We excluded all other types of studies, studies which administered additional or different agents than vitamin D, and studies that did not test for SARS-CoV-2 infections or with missing assessment of the relevant outcomes.

Two independent teams of two reviewers (LK, RR; HK, BH) screened titles and abstracts to identify potentially eligible studies. The same two teams independently screened the full texts of possibly relevant studies. Any disagreements were resolved by consulting an independent fifth reviewer (KP).

Data analysis

The relevant data of all included studies were extracted and independently reviewed by two reviewers (LK, HK). Data were entered into a predefined table for analysis. The criteria for inclusion were strictly adhered to and any discrepancies were resolved by discussion until an agreement was reached. The corresponding authors of the trials were contacted for important missing data. The risk of bias of the included studies was independently assessed by two reviewers (LK, HK) using the Cochrane Risk of Bias tool for RCTs (11). The tool included five domains, which were rated from low to high risk, and then combined to indicate the overall risk of bias. Any disagreements were resolved by consensus.

Statistical analysis was carried out using the meta (v5.0-0) package (12) in the R (v4.1.2) programming language (13). Meta-analysis of proportions was pooled by fitting a random intercept logistic regression model with the metaprop function to logit-transformed proportions in order to include valid estimates for studies with very few or no events. Study estimates are shown with computed Clopper–Pearson 95% confidence intervals. The same pooled estimates were conducted for subgroups and tested by the χ^2 test for significant pairwise differences. Heterogeneity was assessed by estimating the maximum likelihood of τ^2 and quantified with the I^2 index. Comparisons of studies were analyzed using odds ratios between the treatment and control groups with the metabin function by performing a random-effects model for the pooled odds ratio using the Mantel–Haenszel method (14). Heterogeneity was assessed using a restricted maximum-likelihood estimator of τ^2.

Publication bias was evaluated by performing a funnel plot of the logit-transformed prevalence and inverse variance. This was tested using the metabias function with the linear regression test (15) and the rank correlation test (16) for asymmetry. Correlations with vitamin D levels were investigated by linear regression of mean concentration per study, weighted by study size (reflected by circle size and opacity). Squared Pearson correlation coefficient (R^2) is stated per correlation.

The quality of evidence was analyzed by performing the GRADE approach to evaluate the certainty of evidence. Using the GRADE.pro software (17), we created a summary of findings table.

Results

Study selection

The initial search identified a total of 5,733 articles of potential relevance. After the removal of duplicates, 2,483 articles were screened by title and abstract, and 83 potentially eligible records were selected for full-text reading. In total, 44 RCTs were eligible according to the inclusion criteria; an additional trial was identified by manual search. However, no results were available for 37 of the trials, which were excluded as they did not meet the inclusion criteria. Thus, we were able to finally include eight RCTs in this meta-analysis with a combined total of 657 individual patients (Figure 1).

Study characteristics

All trials included adults of both genders (Supplementary Figure 1) (18–25). Two studies were conducted in India, while the remaining six originated from different countries around the world; six studies assessed the data of hospitalized patients and one only included outpatients. The trial by Sabico et al. included both settings. Patients were only included if SARS-CoV-2 infection was confirmed by PCR or other criteria matching the WHO definition. Participants with a vitamin D deficiency were enrolled in three studies; the Murai et al. trial performed an additional *post-hoc* analysis for patients with vitamin D deficiency at baseline. The COVID-19 severity ranged from asymptomatic to severe, although most studies did not report the severity of disease.

Furthermore, three studies compared the effects of vitamin D supplementation with placebo and five with standard of care. The majority of studies used cholecalciferol. However, the dosage and duration of the vitamin D supplementation varied, ranging from 0.5 to 5,000 μg; vitamin D was administered as a single bolus, a daily dose, or using a combination by administrating a high-dose bolus followed by daily doses (trial by Castillo et al.). Relevant data were reported, with mortality in all eight studies, but other outcomes were assessed more infrequently. The timing of follow-up assessments varied across studies, although it was not always specified. Serum vitamin D levels at baseline were measured in five studies only during follow-up, while the others simply reported the baseline serum levels. The baseline characteristics of the participants were heterogeneous, even reporting significant differences of vitamin D serum levels between the intervention and the control groups,

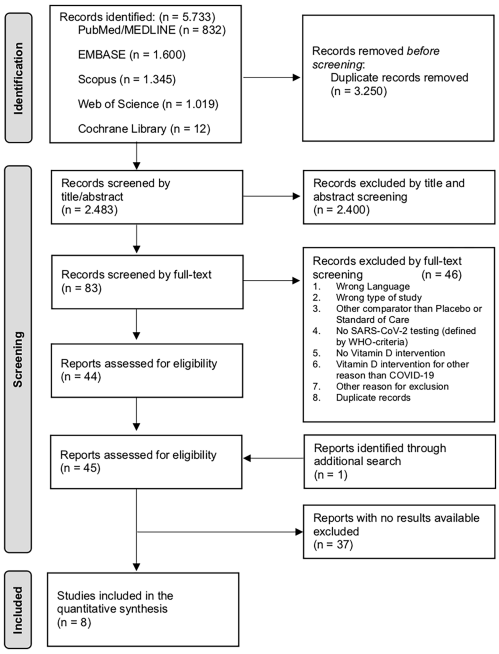

FIGURE 1
PRISMA flowchart showing the study selection process to identify trials on vitamin D supplementation for the treatment and prevention of COVID-19. COVID-19, coronavirus disease 2019; SARS-CoV-2, severe acute respiratory syndrome-related coronavirus 2; WHO, World Health Organization.

when vitamin D concentrations were assessed. Additional characteristics of the included studies are presented in Table 1. No prevention trials were included. The overall risk of bias within the studies was assessed and considered to be low to some concerns (Supplementary Figure 2).

Results of the meta-analyses

The primary analysis of mortality in the vitamin D group compared with the control group was assessed, revealing trends of reduced mortality in the intervention group, although it was not statistically significant [odds ratio (OR) 0.74, 95% confidence interval (CI) 0.32–1.71; Figure 2]. The mortality rate and the count of deaths were reported in all of the eight trials included: no deaths occurred in two trials, while the highest mortality rate was observed in the Soliman et al. trial being 17.86% among all patients; and none of the trials reported a statistically significant effect of vitamin D on mortality themselves.

Subgroup analysis comparing vitamin D supplementation to placebo did not show a beneficial effect on mortality, with an OR of 1.29 (95% CI 0.54–3.07; Figure 3), compared with standard of care in which lower odds were observed (OR 0.33, 95% CI 0.1–1.14), but no significance was reached in either of the subgroups. The subgroup receiving multiple dosages of vitamin D was associated with a trend of lower mortality (OR 0.33, 95% CI 0.1–1.14), by analyzing the same reported events as in the standard-of-care subgroup. Other studies administrating multiple doses of vitamin D did not report any deaths. For the patients receiving a single bolus of vitamin D compared with the control group, no beneficial effect was observed, with the same two studies included as for the placebo subgroup. Furthermore, the vitamin D deficiency subanalysis did not show an effect of vitamin D on mortality (OR 0.95, 95% CI 0.29–3.1) among all patients, with confirmed vitamin D serum levels below 30 or 20 ng/ml at baseline. Overall, subgroup analyses failed to reach statistically significant effects.

By analyzing further clinical outcomes, no statistical significance was observed. However, the length of hospitalization tended to be shorter in the vitamin D group compared with the control group [mean difference (MD) −0.28, 95% CI −0.60 to 0.04; Figure 4]. It should be noted that the Murai et al. study was weighted 82.8% in this analysis. The random-effects model for the need of ICU admission is showing a less frequent admission to ICU in the intervention group (OR 0.41, 95% CI 0.15–1.12), while vitamin D supplementation was associated with lower odds for the need of mechanical ventilation compared with the control group (OR 0.52, 95% CI 0.27–1.02).

For the length of hospitalization and the need for ICU admission, further subgroups were formed, analyzing the trials administering repeated dosages of vitamin D supplementation only. In this process, no statistically significant effects of vitamin D

TABLE 1 Characteristics of the eligible randomized controlled trials and their patients (18–25).

	Trial design	Participants	Vitamin D deficiency	Groups		Vitamin D treatment	Timing of follow-up	Outcomes (relevant for this meta-analysis)
				Intervention	Control			
Castillo et al., 2020 (Spain)	RCT Open label Single center	Inpatients >18 years Total *N* = 76 Female: 31 Mean age: 53 years	No	Calcifediol *N* = 50 Female: 23 Mean age: 53.14 years	Standard of care *N* = 26 Female: 8 Mean age: 52.77 years	Loading dose of 532 μg, followed by 266 μg on days 3, 7, 14, 21, and 28	Until ICU admission, discharge, or death	Mortality Need for ICU admission
Elamir et al., 2021 (Israel)	RCT Open label Multicenter	Inpatients >18 years Total *N* = 50 Female: 25 Mean age: NR	No	Calcitriol *N* = 25 Female: 13 Mean age: 69 years	Standard of care *N* = 25 Female: 12 Mean age: 64 years	Daily dose of 0.5 μg for 14 days or until discharge	Until day 14 or discharge	Mortality Length of hospitalization Need for ICU admission Need for mechanical ventilation
Lakkireddy et al., 2021 (India)	RCT Open label Single center	Inpatients >18 years Total *N* = 87 Female: 22 Mean age: 45 years	Yes, defined as <30 ng/ml	Cholecalciferol *N* = 44 Female: 7 Mean age: 47 years Mean vitamin D level: 16 ng/ml (baseline); 89 ng/ml (follow-up)	Standard of care *N* = 43 Female: 15 Mean age: 44 years Mean vitamin D level: 17 ng/ml (baseline); 16 ng/ml (follow-up)	Daily dose of 1,500 μg for 8 or 10 days	Until day 21	Mortality Length of hospitalization Need for ICU admission
Murai et al., 2021 (Brazil)	RCT Double-blind Multicenter	Inpatients >18 years Total *N* = 237 Female: 104 Mean age: 56.2 years	Subgroup, defined as <20 ng/ml	Cholecalciferol *N* = 119 Female: 49 Mean age: 56.5 years Mean vitamin D level: 21 ng/ml (baseline); 44 ng/ml (follow-up)	Placebo *N* = 118 Female: 55 Mean age: 56 years Mean vitamin D level: 20 ng/ml (baseline); 19 ng/ml (follow-up)	Single dose of 5,000 μg	Until discharge	Mortality Length of hospitalization Need for ICU admission Need for mechanical ventilation
Rastogi et al., 2020 (India)	RCT Double-blind Single center	Inpatients >18 years Total *N* = 40 Female: 20 Median age: NR	Yes, defined as <20 ng/ml	Cholecalciferol *N* = 16 Female: 10 Median age: 50 years Median vitamin D level: 8 ng/ml (baseline); 51 ng/ml (follow-up)	Placebo *N* = 24 Female: 10 Median age: 47.5 years Median vitamin D level: 9 ng/ml (baseline); 15 ng/ml (follow-up)	Daily dose of 1,500 μg for 7 or 14 days	Until day 21	Mortality
Sabico et al., 2021 (Saudi Arabia)	RCT Open label Multicenter	In- and outpatients from 20 to 75 years Total *N* = 69 Female: 35 Mean age: 49.8 years	No	Cholecalciferol *N* = 36 Female: 15 Mean age: 46.3 years Mean vitamin D level: 21 ng/ml (baseline); 25 ng/ml (follow-up)	Standard of care, including 25 μg cholecalciferol *N* = 33 Female: 20 Mean age: 53.5 years Mean vitamin D level: 25 ng/ml (baseline); 23 ng/ml (follow-up)	Daily dose of 125 μg for 14 days	Until discharge	Mortality Length of hospitalization Need for ICU admission
Sanchez-Zuno et al., 2021 (Mexico)	RCT Open label Multicenter	Outpatients >18 years Total *N* = 42 Female: 22 Median age: 43 years	No	Cholecalciferol *N* = 22 Female: 7 Median age: 44 years Median vitamin D level: 20 ng/ml (baseline); 28 ng/ml (follow-up)	Standard of care *N* = 20 Female: 6 Median age: 43 years Median vitamin D level: 23 ng/ml (baseline)	Daily dose of 250 μg for 14 days	Until day 14	Mortality

(Continued)

TABLE 1 Continued

	Trial design	Participants	Vitamin D deficiency	Groups		Vitamin D treatment	Timing of follow-up	Outcomes (relevant for this meta-analysis)
				Intervention	Control			
Soliman et al., 2021 (Egypt)	RCT Double-blind Single center	Inpatients >60 years with DM II Total *N* = 56 Female: 22 Mean age: 70.91 years	Yes, defined as <20 ng/ml	Cholecalciferol *N* = 40 Female: 16 Mean age: 71.3 years Mean vitamin D level: 10 ng/ml (baseline); 20 ng/ml (follow-up)	Placebo *N* = 16 Female: 6 Mean age: 70.19 years Mean vitamin D level: 21 ng/ml (baseline); 21 ng/ml (follow-up)	Single dose of 5,000 µg	Until day 42	Mortality Need for mechanical ventilation

DM, diabetes mellitus; N, number of participants; NR, not reported; RCT, randomized controlled trial.

supplementation compared with the control group were observed, with a trend of shorter hospitalization (MD −0.64, 95% CI −1.42 to 0.13) and less frequent admission to the ICU (OR 0.30, 95% CI 0.07–1.35; Table 2). None of these results were statistically significant.

Significant increases in vitamin D serum levels were assessed by analyzing the five trials reporting on vitamin D levels (Supplementary Figure 3), while three trials did not measure vitamin D serum levels. Thus, it is difficult to relate vitamin D concentrations with reported clinical outcomes.

Publication bias and certainty of evidence

Publication bias was assessed using funnel plots with no significant risk of biases as revealed by Begg's correlation test and Egger's regression (Supplementary Figure 10). The overall quality of evidence was low to moderate, based on the GRADE profile that is available in Supplementary Table 4.

Discussion

To our knowledge, this is the first study specifically focusing on dosing regimens of vitamin D in RCTs in the context of COVID-19 by performing further subgroup analyses. Previously published meta-analyses by Szarpak et al. and Rawat et al. reported similar results to our main outcomes, not reaching a statistical significance for the effect of vitamin D supplementation on abrogating COVID-19-related complications. However, they included quasi-experimental and non-randomized trials, as only three RCTs were available at the time of their final search (26, 27). In contrast, other meta-analyses reported significantly lower rates of adverse outcomes such as the one by Pal et al. (28). They revealed a significantly less frequent admission to the ICU and lower rates of mortality in patients receiving vitamin D supplementation by analyzing RCTs and observational studies. Vitamin D supplementation given before the diagnosis of COVID-19 did not show any benefit. The meta-analysis by Nikniaz et al. reported

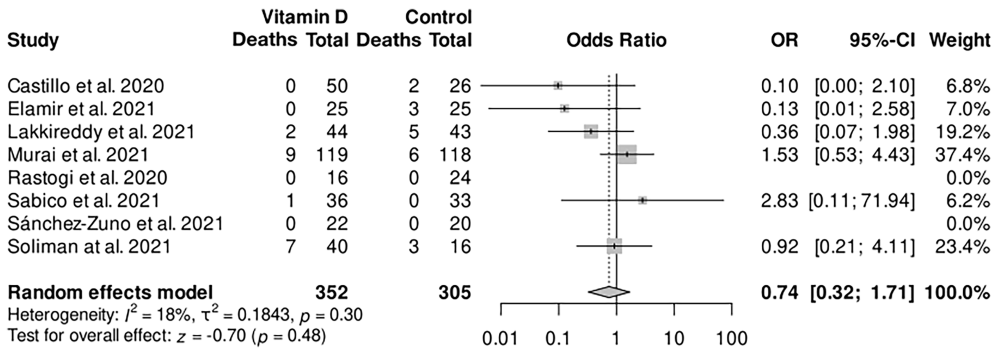

FIGURE 2
Forest plot random-effects model for the association of vitamin D supplementation and the main outcome mortality. CI, confidence interval; OR, odds ratio.

10.3389/fimmu.2022.1023903

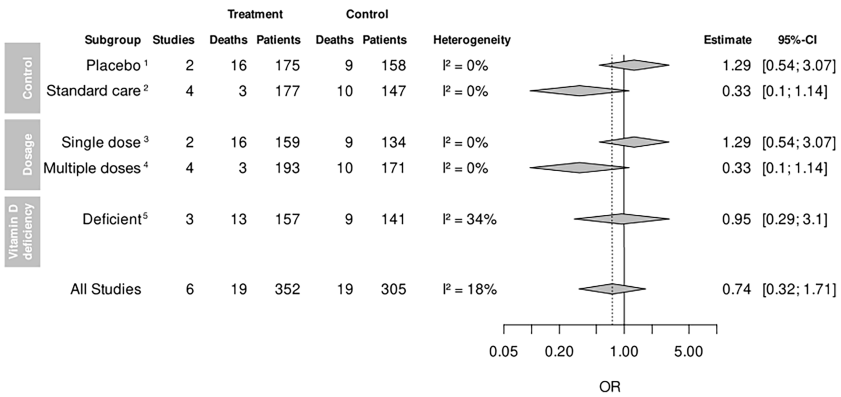

FIGURE 3
Mortality among subgroup analyses. CI, confidence interval; OR, odds ratio. [1]Control group receiving a placebo. [2]Control group receiving standard of care. [3]Patients receiving a single dose of vitamin D once. [4]Patients receiving more than one dose of vitamin D. [5]Patients with confirmed vitamin D deficiency below 30 or 20 ng/ml at baseline.

significantly lower rates of mortality in patients receiving vitamin D supplementation by analyzing two RCTs and one quasi-experimental study, and Shah et al. showed a significantly reduced need for ICU admission by analyzing two RCTs and one observational study (29, 30). Tentolouris et al. and Hosseini et al. also depicted significantly reduced needs for ICU admission, while Beran et al. showed significant effects of vitamin D for the length of hospitalization and the need for mechanical ventilation (29, 31, 32). Overall, these meta-analyses included other types of clinical trials on vitamin D supplementation, while we chose to focus on high-quality studies to limit the risk of bias. Varikasuvu et al. focused on RCTs and were able to show significant effects of vitamin D regarding PCR positivity and COVID-19 severity, but not for COVID-19-related mortality (33). They included

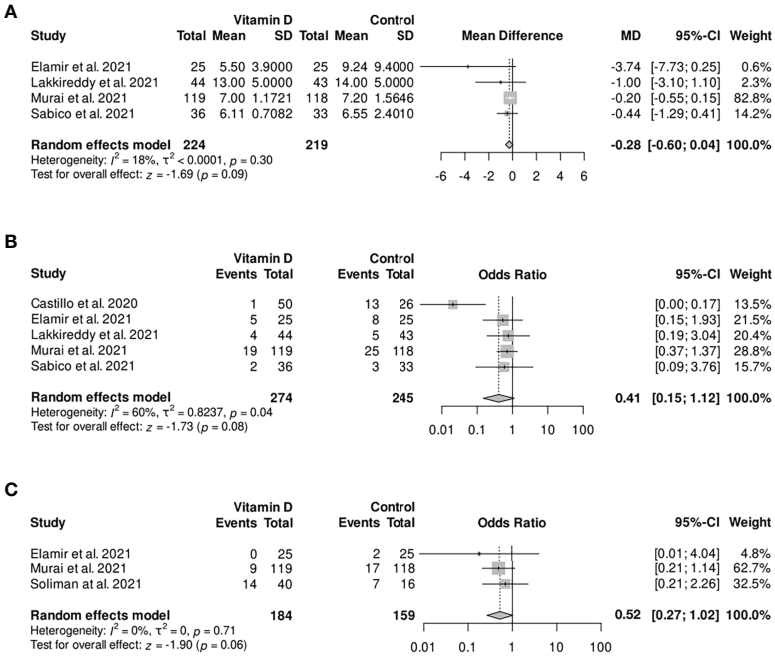

FIGURE 4
Forest plot random-effect model of various outcomes: **(A)** length of hospitalization; **(B)** need for ICU admission; **(C)** need for mechanical ventilation. CI, confidence interval; MD, mean difference; OR, odds ratio; SD, standard deviation.

10.3389/fimmu.2022.1023903

TABLE 2 Outcomes in trials administrating vitamin D repeatedly.

Outcome	Studies	Events/treatment group	Events/control group	Heterogeneity	OR	95% CI
Mortality	6	3/193	10/171	0%	0.33	[0.11–1.14]
ICU admission	4	12/155	29/127	66%	0.30	[0.09–3.76]
Outcome	Studies	Treatment group	Control group	Heterogeneity	MD	95% CI
Length of hospitalization	3	105	101	24%	−0.64	[−1.42 to 0.41]

CI, confidence interval; MD, mean difference; OR, odds ratio.

fewer trials than we did with a total of six RCTs and only two for PCR positivity and assessed COVID-19 severity by analyzing the rate of ICU admission, need for mechanical ventilation, and severity of symptoms as one outcome.

Studies on other respiratory tract infections, conducted before the emergence of SARS-CoV-2, reported lower rates of acute respiratory infections in patients receiving vitamin D supplementation (34–36). One meta-analysis on vitamin D supplementation to prevent acute respiratory tract infections performed subgroup analyses for repeated doses of vitamin D, showing lower rates of respiratory tract infections when vitamin D supplementation was administered on a daily basis (1). In the meta-analysis by D'Ecclesiis, which included all kinds of studies, additional boluses and higher doses had no stronger effects (37).

Overall, previous studies generated heterogeneous results. While some report the protective effects of vitamin D supplementation on mortality and the need for ICU admission, others show no significant association between vitamin D supplementation and COVID-19-related outcomes. However, most studies have several limitations such as the inclusion of low-quality trials, trials offering additional supplementation other than vitamin D (34, 35), non-exclusive focus on COVID-19 (1, 36), missing information on vitamin D serum levels, heterogeneous baseline characteristics of included studies, and varying dosing and administration regimens of vitamin D supplementation. Overall, the quality of trials focusing on vitamin D and COVID-19 is an important issue that obviously affects the quality of published results. Importantly, the *Lancet* recently retracted a preprint article about a trial also investigating the effect of vitamin D treatments on COVID-19 and related outcomes as there was a series of mistakes made by the authors in the qualification of the study and its description (38).

Our analyses revealed no statistically significant findings for our main outcomes and subgroup analyses, but undoubtedly stronger effects were observed when vitamin D supplementation was administered repeatedly. However, it should be considered that the RCTs administrating multiple dosages of vitamin D without a placebo control are of lower quality than RCTs with placebo. The trials comparing vitamin D supplementation with placebo are only weighted in the single-bolus subgroup in this analysis. Therefore, placebo-controlled RCTs are required to draw more robust outcomes on the effect of multiple dosages of vitamin D supplementation in COVID-19 disease.

The main strength of our study is that we included only high-quality studies by limiting the eligible studies to RCTs comparing vitamin D to placebo or standard of care, while previous meta-analyses additionally or only analyzed observational studies. Secondly, we focus on trials investigating vitamin D supplementation in the context of COVID-19 as data from other respiratory infections may not be applicable, compared with meta-analyses assessing the effect of vitamin D supplementation on respiratory tract infections in general (1, 34–36). Thirdly, we augmented our search results by contacting trial investigators for unpublished data. Finally, we conducted an analysis on vitamin D supplementation administered repeatedly to limit the fluctuation of vitamin D serum levels, which is a novel aspect in this context, only investigated by previous meta-analyses performed before the emergence of SARS-CoV-2 (1). Hence, we were able to investigate the effect of a continuous increase of serum concentrations on clinical outcomes.

Our study also has some limitations. Firstly, only a small number of trials passing our inclusion criteria were available. In those trials, only a small number of outcome events were reported, leading to a risk of overestimation of the true intervention effect for assessed outcomes. Secondly, studies were quite heterogeneous using different dosing regimens of vitamin D supplementation. Moreover, the different study locations limit the generalizability of our findings to those settings, while the baseline characteristics of the participants included in individual RCTs were heterogeneous, with no adjustments for vitamin D serum levels. Thirdly, studies were not always evaluating the same primary outcome, or information on clinical outcomes was missing. Data especially on vitamin D serum levels and timing of follow-up measurements were not reported in all trials. Even after contacting trial investigators, not all information was available. Finally, some risk of bias was detected for the included studies (Supplementary Figure 2).

There is an urgent need for further investigation demonstrating the effect of vitamin D supplementation in the context of COVID-19, as sufficient vitamin D serum concentrations may help protect people from severe disease progression all over the world. The major challenge lies in assessing the relationship between vitamin D serum concentrations reached by supplementation and the occurrence of SARS-CoV-2 infection as well as disease-related clinical outcomes. Currently, there are more than 50 ongoing

clinical trials on vitamin D supplementation in COVID-19 patients registered on ClinicalTrials.gov (39). However, when looking at their study protocols, 94% of them (Supplementary Table 5) may have difficulties to prove the beneficial effects of vitamin D serum concentrations reached by supplementation on COVID-19-related outcomes. Consistent monitoring of vitamin D serum levels is necessary, including a run-in period and the adjustment of baseline values between the intervention and the control group in the randomization process. The importance of adjusted vitamin D serum levels can be demonstrated by looking at the trial performed by Soliman et al. with the highest concentrations of vitamin D being measured in the control group at baseline (25), leading to a high risk of misclassification bias and reduced power. Furthermore, the study size must be chosen wisely to be able to show the significant effects of vitamin D supplementation, since participants in the control group can produce vitamin D endogenously as well. The period of investigation, including the duration of vitamin D supplementation and time until the follow-up assessments, needs to be of adequate length to reach sufficient vitamin D serum levels. Since our analysis showed a tendency for a harmful effect of a single bolus of vitamin D, vitamin D supplementation should be administered repeatedly (e.g., daily) rather than once. Considering these suggestions, only three of the ongoing trials, based on their study protocol, could be helpful to assess the effect of vitamin D supplementation for the treatment of COVID-19.

Interestingly, vitamin D supplementation can affect vitamin K levels by influencing vitamin D-dependent proteins and potentially can induce vitamin K deficiency (40, 41). As previous studies have demonstrated that a low vitamin K concentration is associated with higher risks of developing severe COVID-19 and increased IL-6 levels, undoubtedly, further research is needed to investigate the levels of vitamin K in the context of vitamin D insufficiency as well as the role of vitamin D supplementation in vitamin K levels and its related outcomes in the COVID-19 population (42–45).

Overall, a focus on reaching sufficient vitamin D serum levels is crucial, and not only in the context of COVID-19 vitamin D supplementation may be important to help improve immune function globally. With all age groups being affected, the risk of insufficient vitamin D status is prevalent worldwide. Multiple factors such as age, gender, ethnicity, or limited sun exposure influence vitamin D metabolism and can result in insufficient vitamin D serum concentrations. It is important to investigate vitamin D supplementation regimens as a safe and widely available supplement to reduce the prevalence of vitamin D deficiency globally and establish supplementation programs for people of high risk (6, 46, 47). Over the last decade, a successful nutrition policy in Finland resulted in improved vitamin D status in adult people nationally. Finland also reports low rates of SARS-CoV-2 infections and COVID-19-related deaths compared with the United States of America and Europe, even with the lowest rates of SARS-CoV-2 infections in Europe in November 2020. However, if vitamin D sufficiency is one of the multiple factors influencing the prevalence of COVID-19 in Finland and may help improve the global situation, further investigations are required (46, 48).

Conclusion

In conclusion, our findings indicate that vitamin D supplementation is associated with the trend of reducing COVID-19-related mortality and clinical severity, especially in patients receiving repeated vitamin D doses, when vitamin D was given after the diagnosis of COVID-19. Repeated administration of vitamin D supplementation could be helpful to reach sufficient serum levels and improve immune function and, thus, COVID-19-related complications. The available evidence to date is of low quality with heterogeneous findings. Therefore, it is impossible to demonstrate the immunological benefit of vitamin D supplementation in this context yet. Hence, further investigations are required, including updated analyses of ongoing and future RCTs.

Data availability statement

The raw data supporting the conclusions of this article will be made available by the authors, without undue reservation.

Author contributions

LK, HK, CS, and PF conceptualized the study. LK and HK performed the literature search. LK, HK, BH, and RR performed the study screening and selection with the support of KP. LK and HK extracted and verified the study data. CT performed the analysis. LK, HK, CS, and PF wrote the first draft of the manuscript. All authors had access to all data in the study, contributed to the writing process, and approved the published version of the manuscript.

Funding

The authors declare that this study received funding from the Universities Giessen and Marburg Lung Center (UGMLC), German Center for Lung Research (DZL), University Hospital Giessen and Marburg (UKGM) research funding according to article 2, section 3 cooperation agreement, Deutsche Forschungsgemeinschaft (DFG, German Research Foundation) - SFB 1021 (Project-ID 197785619), KFO 309 (P10), and SK 317/1-1 (Project ID 428518790) and from the Foundation for Pathobiochemistry and Molecular Diagnostics. The funders

were not involved in the study design, collection, analysis, interpretation of data, the writing of this article, or the decision to submit it for publication.

Conflict of interest

CS received consultancy fees and research funding from Hycor Biomedical, Bencard Allergie, and Thermo Fisher Scientific and research funding from Mead Johnson Nutrition MJN.

The remaining authors declare that the research was conducted in the absence of any commercial or financial relationships that could be construed as a potential conflict of interest.

Publisher's note

Supplementary material

The Supplementary Material for this article can be found online at: https://www.frontiersin.org/articles/10.3389/fimmu.2022.1023903/full#supplementary-material

References

1. Jolliffe DA, Camargo CA Jr, Sluyter JD, Aglipay M, Aloia JF, Ganmaa D, et al. Vitamin D supplementation to prevent acute respiratory infections: A systematic review and meta-analysis of aggregate data from randomised controlled trials. *Lancet Diabetes Endocrinol* (2021) 9(5):276–92. doi: 10.1016/s2213-8587(21)00051-6

2. Prietl B, Treiber G, Pieber TR, Amrein K. Vitamin d and immune function. *Nutrients* (2013) 5(7):2502–21. doi: 10.3390/nu5072502

3. Greiller CL, Martineau AR. Modulation of the immune response to respiratory viruses by vitamin d. *Nutrients* (2015) 7(6):4240–70. doi: 10.3390/nu7064240

4. Bui L, Zhu Z, Hawkins S, Cortez-Resendiz A, Bellon A. Vitamin d regulation of the immune system and its implications for COVID-19: A mini review. *SAGE Open Med* (2021) 9:20503121211014073. doi: 10.1177/20503121211014073

5. Aranow C. Vitamin d and the immune system. *J Investig Med* (2011) 59 (6):881–6. doi: 10.2310/JIM.0b013e31821b8755

6. Amrein K, Scherkl M, Hoffmann M, Neuwersch-Sommeregger S, Köstenberger M, Tmava Berisha A, et al. Vitamin d deficiency 2.0: An update on the current status worldwide. *Eur J Clin Nutr* (2020) 74(11):1498–513. doi: 10.1038/s41430-020-0558-y

7. Petrelli F, Luciani A, Perego G, Dognini G, Colombelli PL, Ghidini A. Therapeutic and prognostic role of vitamin d for COVID-19 infection: A systematic review and meta-analysis of 43 observational studies. *J Steroid Biochem Mol Biol* (2021) 211:105883. doi: 10.1016/j.jsbmb.2021.105883

8. Page MJ, McKenzie JE, Bossuyt PM, Boutron I, Hoffmann TC, Mulrow CD, et al. The PRISMA 2020 statement: An updated guideline for reporting systematic reviews. *BMJ* (2021) 372:n71. doi: 10.1136/bmj.n71

9. Higgins JPT, Thomas J, Chandler J, Cumpston M, Li T, Page MJ, et al. *Cochrane Handbook for Systematic Reviews of Interventions. 2nd Edition* (Chichester (UK): John Wiley & Sons) (2019).

10. WHO. *COVID-19: Case definitions*. World Health Organization: WHO (2020).

11. Sterne JAC, Savović J, Page MJ, Elbers RG, Blencowe NS, Boutron I, et al. RoB 2: A revised tool for assessing risk of bias in randomised trials. *Bmj*. (2019) 366:14898. doi: 10.1136/bmj.l4898

12. Balduzzi S, Rücker G, Schwarzer G. How to perform a meta-analysis with r: a practical tutorial. *Evid Based Ment Health* (2019) 22(4):153–60. doi: 10.1136/ebmental-2019-300117

13. Team RC. *R: A language and environment for statistical computing*. (Vienna, Austria: R Foundation for Statistical Computing) (2021).

14. Mantel N, Haenszel W. Statistical aspects of the analysis of data from retrospective studies of disease. *J Natl Cancer Inst* (1959) 22(4):719–48. doi: 10.1093/jnci/22.4.719

15. Egger M, Davey Smith G, Schneider M, Minder C. Bias in meta-analysis detected by a simple, graphical test. *Bmj* (1997) 315(7109):629–34. doi: 10.1136/bmj.315.7109.629

16. Begg CB, Mazumdar M. Operating characteristics of a rank correlation test for publication bias. *Biometrics* (1994) 50(4):1088–101. doi: 10.2307/2533446

17. GRADEpro GDT. *GRADEpro guideline development tool*. McMaster University and Evidence Prime (2021).

18. Castillo ME, Costa LME, Barrios JMV, Díaz JFA, Miranda JL, Bouillon R, et al. Effect of calcifediol treatment and best available therapy versus best available therapy on intensive care unit admission and mortality among patients hospitalized for COVID-19: A pilot randomized clinical study. *J Steroid Biochem Mol Biol* (2020) 203:105751. doi: 10.1016/j.jsbmb.2020.105751

19. Elamir YM, Amir H, Lim S, Rana YP, Lopez CG, Feliciano NV, et al. A randomized pilot study using calcitriol in hospitalized COVID-19 patients. *Bone* (2022) 154:116175. doi: 10.1016/j.bone.2021.116175

20. Lakkireddy M, Gadiga SG, Malathi RD, Karra ML, Raju I, Ragini, et al. Impact of daily high dose oral vitamin d therapy on the inflammatory markers in patients with COVID 19 disease. *Sci Rep* (2021) 11(1):10641. doi: 10.1038/s41598-021-90189-4

21. Murai IH, Fernandes AL, Sales LP, Pinto AJ, Goessler KF, Duran CSC, et al. Effect of a single high dose of vitamin D3 on hospital length of stay in patients with moderate to severe COVID-19: A randomized clinical trial. *Jama* (2021) 325 (11):1053–60. doi: 10.1001/jama.2020.26848

22. Rastogi A, Bhansali A, Khare N, Suri V, Yaddanapudi N, Sachdeva N, et al. Short term, high-dose vitamin d supplementation for COVID-19 disease: A randomised, placebo-controlled, study (SHADE study). *Postgrad Med J* (2020) 98(1156):87–90. doi: 10.1136/postgradmedj-2020-139065

23. Sabico S, Enani MA, Sheshah E, Aljohani NJ, Aldisi DA, Alotaibi NH, et al. Effects of a 2-week 5000 IU versus 1000 IU vitamin D3 supplementation on recovery of symptoms in patients with mild to moderate covid-19: A randomized clinical trial. *Nutrients* (2021) 13(7):2170. doi: 10.3390/nu13072170

24. Sánchez-Zuno GA, González-Estevez G, Matuz-Flores MG, Macedo-Ojeda G, Hernández-Bello J, Mora-Mora JC, et al. Vitamin d levels in COVID-19 outpatients from Western Mexico: Clinical correlation and effect of its supplementation. *J Clin Med* (2021) 10(11):2378. doi: 10.3390/jcm10112378

25. Soliman AR, Abdelaziz TS, Fathy A. Impact of vitamin d therapy on the progress COVID-19: Six weeks follow-up study of vitamin d deficient elderly diabetes patients. *Proc Singapore Healthcare* (2021) 0(0):20101058211041405. doi: 10.1177/20101058211041405

26. Szarpak L, Filipiak KJ, Gasecka A, Gawel W, Koziel D, Jaguszewski MJ, et al. Vitamin d supplementation to treat SARS-CoV-2 positive patients. evidence from meta-analysis. *Cardiol J* (2021) 29(2):188–96. doi: 10.5603/CJ.a2021.0122

27. Rawat D, Roy A, Maitra S, Shankar V, Khanna P, Baidya DK. "Vitamin d supplementation and COVID-19 treatment: A systematic review and meta-analysis". *Diabetes Metab Syndr* (2021) 15(4):102189. doi: 10.1016/j.dsx.2021.102189

28. Pal R, Banerjee M, Bhadada SK, Shetty AJ, Singh B, Vyas A. Vitamin d supplementation and clinical outcomes in COVID-19: A systematic review and meta-analysis. *J Endocrinol Invest* (2022) 45(1):53–68. doi: 10.1007/s40618-021-01614-4

29. Nikniaz L, Akbarzadeh MA, Hosseinifard H, Hosseini M-S. The impact of vitamin d supplementation on mortality rate and clinical outcomes of COVID-19

patients: A systematic review and meta-analysis. *Pharm Sci* (2021) 27:S1–12. doi: 10.34172/ps.2021.13

30. Shah K, Saxena D, Mavalankar D. Vitamin d supplementation, COVID-19 and disease severity: A meta-analysis. *Qjm* (2021) 114(3):175–81. doi: 10.1093/qjmed/hcab009

31. Tentolouris N, Samakidou G, Eleftheriadou I, Tentolouris A, Jude EB. The effect of vitamin d supplementation on mortality and intensive care unit admission of COVID-19 patients. A systematic review, meta-analysis and meta-regression. *Diabetes Metab Res Rev* (2022) 38(4):e3517. doi: 10.1002/dmrr.3517

32. Beran A, Mhanna M, Srour O, Ayesh H, Stewart JM, Hjouj M, et al. Clinical significance of micronutrient supplements in patients with coronavirus disease 2019: A comprehensive systematic review and meta-analysis. *Clin Nutr ESPEN* (2022) 48:167–77. doi: 10.1016/j.clnesp.2021.12.033

33. Varikasuvu SR, Thangappazham B, Vykunta A, Duggina P, Manne M, Raj H, et al. COVID-19 and vitamin d (Co-VIVID study): A systematic review and meta-analysis of randomized controlled trials. *Expert Rev Anti Infect Ther* (2022) 20(6):907–13. doi: 10.1080/14787210.2022.2035217

34. Abioye AI, Bromage S, Fawzi W. Effect of micronutrient supplements on influenza and other respiratory tract infections among adults: A systematic review and meta-analysis. *BMJ Glob Health* (2021) 6(1):e003176. doi: 10.1136/bmjgh-2020-003176

35. Vlieg-Boerstra B, de Jong N, Meyer R, Agostoni C, De Cosmi V, Grimshaw K, et al. Nutrient supplementation for prevention of viral respiratory tract infections in healthy subjects: A systematic review and meta-analysis. *Allergy* (2021) 77(5):1373–88. doi: 10.1111/all.15136

36. Martineau AR, Jolliffe DA, Hooper RL, Greenberg L, Aloia JF, Bergman P, et al. Vitamin d supplementation to prevent acute respiratory tract infections: Systematic review and meta-analysis of individual participant data. *Bmj* (2017) 356: i6583. doi: 10.1136/bmj.i6583

37. D'Ecclesiis O, Gavioli C, Martinoli C, Raimondi S, Chiocca S, Miccolo C, et al. Vitamin d and SARS-CoV2 infection, severity and mortality: A systematic review and meta-analysis. *PloS One* (2022) 17(7):e0268396. doi: 10.1371/journal.pone.0268396

38. Nogués X, Ovejero D, Quesada-Gomez JM, Bouillon R, Arenas D, Pascual J, et al. Calcifediol treatment and COVID-19-Related outcomes. *Preprints Lancet* (2021) 106(10):4017–27 doi: 10.1210/clinem/dgab405

39. NIH. U.S. National Library of Medicine. Available at: https://clinicaltrials.gov.

40. Fraser JD, Price PA. Induction of matrix gla protein synthesis during prolonged 1,25-dihydroxyvitamin D3 treatment of osteosarcoma cells. *Calcif Tissue Int* (1990) 46(4):270–9. doi: 10.1007/bf02555007

41. van Ballegooijen AJ, Beulens JWJ, Kieneker LM, de Borst MH, Gansevoort RT, Kema IP, et al. Combined low vitamin d and K status amplifies mortality risk: a prospective study. *Eur J Nutr* (2021) 60(3):1645–54. doi: 10.1007/s00394-020-02352-8

42. Linneberg A, Kampmann FB, Israelsen SB, Andersen LR, Jørgensen HL, Sandholt H, et al. The association of low vitamin K status with mortality in a cohort of 138 hospitalized patients with COVID-19. *Nutrients* (2021) 13(6):1985. doi: 10.3390/nu13061985

43. Desai AP, Dirajlal-Fargo S, Durieux JC, Tribout H, Labbato D, McComsey GA. Vitamin K & d deficiencies are independently associated with COVID-19 disease severity. *Open Forum Infect Dis* (2021) 8(10):ofab408. doi: 10.1093/ofid/ofab408

44. Dofferhoff ASM, Piscaer I, Schurgers LJ, Visser MPJ, van den Ouweland JMW, de Jong PA, et al. Reduced vitamin K status as a potentially modifiable risk factor of severe coronavirus disease 2019. *Clin Infect Dis* (2021) 73(11):e4039–e46. doi: 10.1093/cid/ciaa1258

45. Visser MPJ, Dofferhoff ASM, van den Ouweland JMW, van Daal H, Kramers C, Schurgers LJ, et al. Effects of vitamin d and K on interleukin-6 in COVID-19. *Front Nutr* (2021) 8:761191. doi: 10.3389/fnut.2021.761191

46. Raulio S, Erlund I, Männistö S, Sarlio-Lähteenkorva S, Sundvall J, Tapanainen H, et al. Successful nutrition policy: improvement of vitamin d intake and status in Finnish adults over the last decade. *Eur J Public Health* (2017) 27(2):268–73. doi: 10.1093/eurpub/ckw154

47. Roth DE, Abrams SA, Aloia J, Bergeron G, Bourassa MW, Brown KH, et al. Global prevalence and disease burden of vitamin d deficiency: A roadmap for action in low- and middle-income countries. *Ann N Y Acad Sci* (2018) 1430(1):44–79. doi: 10.1111/nyas.13968

48. Höppner S. *Why is Finland coping so well with the coronavirus crisis?* DW: Deutsche Welle (2020).

frontiers | Frontiers in Immunology

TYPE Original Research
PUBLISHED 23 March 2023
DOI 10.3389/fimmu.2023.1083251

OPEN ACCESS

EDITED BY
Dimitra Dimopoulou,
Panagiotis and Aglaia Kyriakou Children's Hospital, Greece

REVIEWED BY
Amrita Kumar,
Centers for Disease Control and Prevention (CDC), United States
Ria Goswami,
Cornell University, United States

*CORRESPONDENCE
Rong Hai
ronghai@ucr.edu

SPECIALTY SECTION
This article was submitted to Viral Immunology, a section of the journal Frontiers in Immunology

RECEIVED 28 October 2022
ACCEPTED 09 March 2023
PUBLISHED 23 March 2023

CITATION
Chavez JR, Yao W, Dulin H, Castellanos J, Xu D and Hai R (2023) Modeling the effects of cigarette smoke extract on influenza B virus infections in mice.
Front. Immunol. 14:1083251.
doi: 10.3389/fimmu.2023.1083251

Modeling the effects of cigarette smoke extract on influenza B virus infections in mice

Jerald R. Chavez[1,2], Wangyuan Yao[1], Harrison Dulin[1,3], Jasmine Castellanos[1], Duo Xu[1] and Rong Hai[1]*

[1]Department of Microbiology and Plant-pathology, University of California, Riverside, Riverside, CA, United States, [2]Genetics, Genomics and Bioinformatics Graduate Program, University of California, Riverside, Riverside, CA, United States, [3]Cell, Molecular, and Developmental Biology Graduate Program, University of California, Riverside, Riverside, CA, United States

Influenza B virus (IBV) is a major respiratory viral pathogen. Due to a lack of pandemic potential for IBV, there is a lag in research on IBV pathology and immunological responses compared to IAV. Therefore, the impact of various lifestyle and environmental factors on IBV infections, such as cigarette smoking (CS), remains elusive. Despite the increased risk and severity of IAV infections with CS, limited information exists on the impact of CS on IBV infections due to the absence of suitable animal models. To this end, we developed an animal model system by pre-treating mice for two weeks with cigarette smoke extract (CSE), then infected them with IBV and monitored the resulting pathological, immunological, and virological effects. Our results reveal that the CSE treatment decreased IBV specific IgG levels yet did not change viral replication in the upper airway/the lung, and weight recovery post infection. However, higher concentrations of CSE did result in higher mortality post infection. Together, this suggests that CS induced inflammation coupled with IBV infection resulted in exacerbated disease outcome.

KEYWORDS

influenza virus, innate immunity, cigarette smoking, influenza B virus, adaptive immunity

Introduction

Influenza virus infections cause seasonal epidemics that result in significant disease and economic burden (1). Between 2010-2020, estimated yearly symptomatic infections caused by Influenza viruses' range between 9-45 million cases, 140,000-710,000 hospitalizations, and between 12,000-52,000 deaths in the United States (2). Extending out to the global population, 290,000-650,000 die worldwide annually as a result of Influenza virus infections (3). Economically, these infections result in an estimated 2.8-5.0 billion dollars in medical costs in the United States alone as of 2017 (4), representing 0.014-0.03% of the US national GDP for that year (5). Therefore, to better prevent and treat influenza viral infection, it is imperative that we further examine any factors that could exacerbate disease outcomes.

Influenza viruses are negative sense, segmented, RNA enveloped viruses belonging to the Orthomyxoviridae family. There are 4 types: Influenza A virus (IAV), Influenza B virus (IBV), Influenza C virus (ICV), and Influenza D virus (IDV). Type A-C all infect humans, however IAV and IBV are primarily responsible for seasonal epidemics. Between 2000-2020, IAV remained the dominant seasonal influenza virus type in the United States (Table 1) (6–24). Historically, IAV has dominated research efforts and understanding of IBV has lagged behind. This gap in IBV research should be filled since IBV is also a known public health concern. For example, IBV accounted for significant percentages of known cases in the United States, as high as 45% in certain years (Table 1). Of the aforementioned 2.8-5 billion dollar medical cost estimate in 2017, IBV infections accounted for 37% of that total (4). Outside of the United States, IBV has achieved dominant status over IAV in Europe in some years (25). Additionally, IBV can adversely affect specific vulnerable populations. In pediatric cases for example, IBV infection can be more virulent compared to adult cases (26). Despite these sizable economic and disease burdens, IBV remains relatively understudied compared to IAV. With awareness of the impact of IBV, the field has begun to increase efforts for IBV. As evidence, both lineages of IBV have been included in seasonal Flu vaccines, dubbed the quadrivalent Flu vaccine, since 2012 in US. However, it remains largely unknown what is the impact of respiratory related lifestyle factors, such as cigarette smoking, on IBV infection, and its associated co-morbidities.

Cigarette smoking also represents a medical and environmental factor known to damage respiratory tissues. Thus, it is likely to exacerbate IBV infection and disease outcomes. Cigarette smoking (CS) results in an estimated 480,000 deaths in the United States each year, representing approximately 6.8% of the annual cigarette related deaths worldwide (27). CS is known to increase the risk and/or be causative of a number of chronic diseases, including, but not limited to: heart disease, multiple types of cancer, diabetes, and chronic obstructive pulmonary disease (COPD) (28). Smoking is also an established risk factor for infectious disease, including pulmonary bacterial infections like pneumonia (29, 30), Tuberculosis (31–34), acute respiratory tract infections in children exposed to environmental cigarette smoke (dubbed second hand smoke) (35), and viral infections like Human papillomavirus (HPV) infections (36) and Influenza A virus infection (37–39). Similarly, studies have also shown that smoking has detrimental effects on COVID-19 outcomes (40, 41).

Besides the risk, CS is also known to increase the severity of IAV disease in patients (37). Similarly, cigarette smoke has been shown to decrease weight gain (slow recovery) (42–45) and increase both lung remodeling (46) and mortality in animal models of IAV infection (43–45, 47, 48). Interestingly, multiple studies have reported that animal models of cigarette smoking do not exhibit

TABLE 1 Yearly IAV to IBV infection cases in the United States as Reported in the CDC MMWRs.

Flu Season	A/B Case Ratio	% IAV cases	% IBV Cases
2000-2001	5337/4625	54	46.0
2001-2002	13706/1965	87.5	12.5
2002-2003	6180/4768	56.4	43.6
2003-2004	24400/249	99	1.0
2004-2005	17750/5799	75.4	24.6
2005-2006	14355/3642	79.7	20.3
2006-2007	18817/4936	79.2	20.8
2007-2008	28263/11564	71	29.0
2008-2009	18175/9507	66	34.0
2009-2010	155591/2273	99	1.0
2010-2011	40282/13994	74	26.0
2011-2012	19285/3132	86	14.0
2012-2013	51675/21455	71	29.0
2013-2014	46727/6743	87.4	12.6
2014-2015	104,822/20,640	83.5	16.5
2015-2016	62982/28477	68.9	31.1
2016-2017	116590/45361	72	28.0
2017-2018	189716/88187	68.3	31.7
2018-2019	208153/11189	94.9	5.1
2019-2020	27617/19357	58.8	41.2

higher viral titers than non-smoking controls post infection (43, 47–49), suggesting that worse disease outcomes are likely not due to changes in the viral replication. However, CS does appear to alter pro-inflammatory cytokine profile responses to IAV infection. Specifically, CS exposure in mice greater than two weeks appears to result in higher levels of pulmonary pro-inflammatory cytokines including (but not limited to) TNF-α, IFN-γ, IL-6, IL-12, IL-23, IL-1, IL-5, IL-10, KC, MIP-1α, IL-17, and IL-1β (44–46, 48, 50). The favorable explanation is that this increased pro-inflammatory response could give rise to exacerbation of pulmonary inflammation post infection, resulting in greater damage and slower recovery (42, 45, 46, 48, 49, 51).

Surprisingly however, to our knowledge, there is very little information regarding how cigarette smoking affects IBV infections and disease outcomes specifically. Lacking pathological, virological, and immunological profiling of smoking effects on IBV infection could result in severe lag-time between treatment development and deployment, especially in sever epidemics or situations when IBV is of particular concern. To this point, we know second hand smoke has been shown to result in not only higher incidents of infection, but also hospitalization in infants and children (52–54), and because IBV infection can be severe in children, it is critical we further investigate the role of CS in IBV infection. To this end, it is critical to establish an experimental model of how cigarette smoke affects the pathology, virology, immunology, and disease outcomes from IBV infection in mice.

Here, we developed an animal model system to better understand how aspects of CS may affect IBV infections by treating mice for two weeks with liquid cigarette smoke extract (CSE), then infecting them with IBV. Our results showed that exposure to CSE decreased IBV specific antibodies but oddly did not compromise their neutralization potency for IBV. Similar to previous studies in IAV, we also did not observe an impact of CSE on virus replication, and associated disease outcomes. Intriguingly, we observed about a 2-fold increase in IBV specific activated splenocytes from animal exposed to CSE versus the control animals. Additionally, we observed a dose dependent effect of increasing concentrations of CSE on mortality in mice. These data represent the first information regarding the pathological and immunological effects of water-soluble components of CS on IBV infection *in vivo* and suggested that there is a negative impact on IBV disease outcome. Our studies provide an experimental platform to further dissect the impact of CSE on IBV infection.

Materials and Methods

Virus and cells

Influenza B/Victoria/2/87 virus was propagated in pathogen free eggs purchased from Charles River laboratories Inc. and stored at -80°C. A549 and Madin-Darby canine kidney (MDCK) cells were cultured at 37°C in DMEM medium supplemented with 10% FBS, or MEM medium supplemented with 10% FBS, respectively.

Cytotoxicity assay

To evaluate the impact of CSE on cell viability, we used the Cell Counting Kit-8 (CCK-8), Dojindo Inc. Briefly, A549 cells were plated at $2.75x10^5$ cells per well in 96 well plates in DMEM supplemented with 10% FBS for 24 hours (hrs). Cells were subsequently exposed to varying concentrations of CSE, ranging from 40X to 0.16X, with a 3-fold dilution, and maintained at 37°C for an additional 24 hours. CCK-8 solution (10 µL per well) was added, followed by an additional incubation for 2 h. The absorbance was measured at 450 nm.

Multi-step growth curve

To evaluate viral replication under the influence of CSE, A549 cells were plated at $3x10^5$ cells per well in 6 well plates in DMEM supplemented with 10% FBS for 24 hrs. Medium was aspirated, then cells were treated overnight with either PBS, 1x CSE, or 2.5x CSE diluted in DMEM with 10% FBS. The following day, media with CSE or PBS was removed, and cells were infected with a multiplicity of infection (MOI) of 0.05 of Influenza B/Victoria/2/87 virus diluted in PBS/BSA/PS (1x PBS, 0.42% BSA, 100ug/ml Pen-strep, 0.8mM $CaCl_2$-2*H_2O, 1mM $MgCl_2$-6H_2O) and incubated at 33°C for one hour. Then, virus solutions were aspirated and replaced with 1ml of post infection media (1x DMEM, 0.35% BSA, 100U/ml Pen-strep, 2mM L-glutamine, 0.15% sodium bicarbonate, 20mM HEPES pH 7.0, 0.25ug/ml TPCK). Infection samples were collected at 24 and 48 hours post infection. The virus concentrations were evaluated by standard plaque assays.

Plaque assay

MDCK cells were plated in 12 well plates at $5x10^5$ cells/well the night before in MEM supplemented with 10% FBS. Virus was serially diluted in PBS/BSA/PS. MEM media from cells was aspirated and replaced with 200µl of virus dilution for 1hr at 33° C. Plates were rocked every 15 min. Virus was aspirated and replaced with plaque overlay (1x EMEM, 0.21% BSA, 100µg/ml Pen/Strep, 2mM L-Glutamine, 0.22% Sodium Bicarbonate, 10mM HEPEs pH 7.0, 0.1% D-dextrose, 0.7% Avicel, 1µg/ml TPCK). Plates were incubated at 33°C for 72hrs. Cells were fixed with 3.7% Formaldehyde in 1x PBS for 1hr, then stained with 0.08% Crystal Violet.

Mice

6-8 weeks old Female BALB/cJ mice were purchased from the Jackson Laboratory and housed in a pathogen free vivarium facility at the University of California, Riverside. Food and water were available ad libitum.

Cigarette smoke extract exposure

Cigarette smoke extract was prepared as previously described (55, 56). Briefly, cigarette smoke from 40 commercially available Marlboro Class A Cigarettes were filtered through 12.5ml of sterile 1xPBS at a rate of 1 cigarette every 1 minutes in a chemical hood. Cigarettes were smoked until they reached the filter, then replaced. The resulting liquid was filter sterilized through a 0.22uM filter and classified as "40X cigarette smoke extract (CSE)". 40x CSE was aliquoted and frozen at -80°C until use.

6 to 8-week-old BALB/cJ female mice were anesthetized with isoflurane, then intranasally inoculated with 50µl of specified concentration of CSE (diluted in sterile PBS) or PBS as a mock control. Mice were daily treated in the same manner, 6-days per week for two weeks.

Influenza virus infections

After two weeks of CSE exposure, mice were isoflurane anesthetized and intranasally inoculated with 50µl of Influenza B/Victoria/2/87 WT virus diluted in PBS/BSA/PS. Total PFU per mouse given were as specified in figures. Mice were sacrificed on day 0, 3, 6, or 21 post infection depending on the experiment.

Lung pathology

After two weeks of CSE or PBS treatments, mice were infected with 10^5 PFU B/Victoria/2/87 WT virus per mouse. Mice were sacrificed 0 and 3 days post infection, and lungs were extracted, washed in 1x PBS, then fixed in 4% formaldehyde at room temperature. Lungs were dehydrated, embedded in paraffin, and lung sections were subjected to Hematoxylin and Eosin (H&E) staining.

Hematoxylin and eosin staining

Mice were euthanized with CO_2, and lungs were extracted and washed with PBS, the fixed it with 4% formaldehyde for 72 hrs at room temperature. Lungs were subsequently dehydrated with 70%, 80%, 90%, and 95% ethanol for 2, 2, 1, and 1hr respectively, then dehydrated again with 100% ethanol for 1 hr. After xylene treatment, lungs were immersed in liquid paraffin wax. Lungs were sectioned using microtome (Lecia Microsystems, Leica RM2235), at approximately 4µm thickness per slice. The slices were then attached to a glass slide and dried at 45°C for 12 hrs. Last, slides were Hematoxylin-Eosin stained, dried, fixed with neutral resin, then covered with cover slips.

BAL fluid collection

21 days post IBV infection, mice were sacrificed. Tracheas were exposed and incisions were made above the manubrium. One ml of sterile PBS was pushed through the incision and out the nasal cavity for collection. BAL fluid was clarified by centrifugation, aliquoted, and frozen at -80°C until analysis.

Enzyme-linked immunosorbent assay for IgG and IgA

To assess the levels of virus-specific IgG and IgA antibodies present in samples from IBV infected mice, ELISAs were performed on blood sera (for IgG) or lavage fluid (for IgA) samples. In brief, 96 well MaxiSorp ELISA plates (Thermo Fisher Scientific, #442404, Rochester, NY) were coated with 50µl of 10µg/ml purified B/Victoria/2/87 WT virions. Wells were blocked at room temperature with PBS containing 1% dried milk and 0.1% Tween 20 (blocking buffer) for 2hrs, washed with PBS containing 0.1% Tween 20 (wash buffer), and subsequently incubated with blood sera or lavage samples serially diluted in blocking buffer. After 2hr room-temp incubations, plates were washed with wash buffer and incubated with secondary horse radish peroxidase conjugated antibody (Southern Biotech #1040-05 for IgA; Millipore, CAT# AP503P, Temecula, Ca for IgG) for 30min at room temperature. Plates were washed with wash buffer and incubated with colorimetric substrate (o-phenylenediamine dihydrochloride, Invitrogen, Carlsbad, CA) for 30min at room temperature, then read with a plate reader measuring optical density at 450 nm (OD_{450}).

IFN-γ evaluation

Mice were sacrificed 6 days post IBV infection. Spleens were removed and washed in 5ml of R10 media (RPMI media supplemented with 2mM L-glutamine, 100ug/ml Pen-strep, 100mM Hepes pH 7.0, and 10% FBS). Spleens were homogenized through a 40 µM cell strainer, washed with 5 ml of R10 media, centrifuged at 1000g for 5 min, then aspirated. Homogenates were treated with 3ml of Ammonium-Chloride-Potassium (ACK) lysis buffer (NH_4Cl 150mM, $KHCO_3$ 10mM, EDTA 0.1mM, pH to 7.2) for 10min and neutralized with 10ml of R10 media. Homogenates were centrifuged, aspirated, resuspended in 4ml R10 media, then counted. $3x10^5$ cells/well were plated in triplicate per spleen in 96 well plates in R10 media. Boiled B/Victoria/2/87 WT virus was added to a final concentration of 30ug/ml for stimulation, and plates were placed at 37°C for 72 hours. Anti CD3/CD28 antibody at 20ug/ml and R10 media was used as positive and negative controls respectively. Supernatants were harvested, clarified by centrifugation, then frozen at -80°C until ELISA analysis.

We used ELISAs to evaluate IFN-γ content in the supernatant samples. Specifically, Nunc Maxisorp plates were coated with 50µl of 0.5ng/µl Anti-mouse IFN-γ purified antibody (Invitrogen eBioscience #14-7313-85) overnight at 4°C. Wells were washed 3x with wash buffer (PBS with 0.05% Tween 20). 50 µl of supernatant samples were diluted 1:10 in dilutant buffer (PBS with 1% BSA and 0.05% tween 20) and added to wells for 2 hours at 37°C. Wells were washed, then treated with 50µl (0.5 µg/ml) of biotin conjugated anti-mouse IFN-γ antibody (Invitrogen ebioscience #13-7312-85)

for 1hr at 37°C. Wells were washed, then treated with 100 µl (0.5µg/ml) of HRP conjugated streptavidin (Jackson Immunoresearch #016-030-084) for 30min at 37°C. Wells were washed, then incubated with colorimetric substrate (o-phenylenediamine dihydrochloride, Invitrogen, Carlsbad, CA) for 30min and read with plate reader measuring optical density at 450 nm (OD_{450}).

Microneutralization assay

To assess neutralizing potency of antibodies against the challenge virus, we performed microneutralization assays. Briefly, $6x10^4$ MDCK cells were plated in 96 well plates. 24hr after plating, 2000 PFU of B/Victoria/2/87 WT virus was incubated with serum samples serially diluted in PBS containing 0.35% BSA for 1hr at 33°C. Virus-serum mixtures (100µl) were added to MDCK cells (MOI=0.003) and incubated at 33°C for 1hr, then washed with PBS. Cells were then incubated overnight at 33°C in MEM media containing 0.35% BSA, 2mM L-glutamine, 0.15% $NaHCO_3$, and 2 mM HEPES pH 7.0, and 1µg/ml TPCK. 24 hours post infection (hpi), cells were fixed with 100% methanol for 20min at -20°C and washed with PBS. Cells were blocked at room-temp with PBS containing 1% dried milk and 0.1% Tween 20 (blocking buffer) for 1hr, and then incubated with sera from B/Victoria/2/87 infected mice diluted in blocking buffer. After 1hr room-temp incubations, plates were washed with wash buffer and incubated with secondary anti-mouse horse radish peroxidase conjugated antibody HRP (Millipore, Temecula, CA) IgGγ for 30min at room-temp. Plates were washed and then incubated with colorimetric substrate (o-phenylenediamine dihydrochloride, Invitrogen, Carlsbad, CA) for 30min and read with plate reader measuring optical density at 450 nm (OD_{450}).

RNA extraction and qRT-PCR

Mice were euthanized 3 days post infection by CO_2 and lungs were immediately extracted and placed in 1ml of Trizol reagent (Thermo Fisher Scientific). Samples were homogenized, then frozen at -80°C until time of RNA extraction. 250µl of Chloroform was added. Samples were vortexed and centrifuged at 20,000g for 15min at 4°C. The RNA from the aqueous phase was precipitated with isopropyl alcohol at a ratio of 1:1.1 using glycogen as a carrier. The resulting RNA pellet was washed with 70% ethanol, air dried, and resuspended in nuclease-free water.

To remove contaminating genomic DNA, RNA was treated with DNAse I (Ambion #2222, Austin, TX). DNAse was removed by phenol/chloroform extraction and RNA was resuspended in nuclease free water. cDNA was synthesized from 1ug of RNA per sample using Superscript II in 20µl reactions (18064-022, Invitrogen, Carlsbad CA). qRT-PCR reactions used 2µl of a 1:10 dilution of cDNA, 400 nM of each primer, and 10µl of 2x Radiant Green Lo-Rox qPCR mix (QS1005, Alkali Scientific, Fort Lauderdale FL). β-Actin internal control was used to normalize results.

Statistical analysis

The experimental data were analyzed by the student *t*-test or the two-way ANOVA depending on the specific setting using the GraphPad Prism V. 9.0.

Ethics and biosafety statement

Animal studies were approved by University of California, Riverside Institutional Animal Care and Use Committee (IACUC) and performed in the biosafety level 2 facility. All animals were cared for in the Animal Resources Facility under specific-pathogen-free conditions in appliance with the Institute for Laboratory Animal Research Guide for the Care and Use of Laboratory Animals, 8th edition.

Results

CSE suppressed IBV replication in A549 cells

Duffney et al. has previously shown that there was more WSN (A/WS/1933 H1N1) IAV infectivity in human airway epithelial cells exposed to cigarette smoke compared to the control cells (57). To evaluate whether there is a similar impact in human lung cells exposed to the water-soluble components of CS on IBV infection, we treated A549 cells with either PBS (mock), 1x CSE, or 2.5x CSE for 24hr, then infected with Influenza B/Victoria/2/87. We noted that 24 hours post CSE treatment, 1x CSE and mock control cells appeared to have similar morphology (Figure 1A). However, 2.5x CSE treated cells appeared to cease proliferation, likely due to toxicity from high dose CSE. Yet, these cells were still attached to the plate (Figure 1A). To more quantitively evaluate the cytotoxicity of CSE, we measured cell viability using the CCK-8 kit (Figure 1B). The results showed similar readings between cells with or without CSE treatment at 4.44X and below. This suggested that concentrations of CSE at 4.44X and below exhibited no apparent negative impact on cell viability. Post infection, 1x CSE did not appear to increase or decrease virus replication, but 2.5x CSE did appear to significantly decrease viral titers 24 hours post infection (hpi) (Figure 1C).

Low dose of CSE did not exacerbate IBV infection

To examine the pathological effects of cigarette smoke on IBV infection *in vivo*, we intranasally inoculated 6-8 week old female BALB/cJ mice with 1x CSE for two weeks, 6 days/week (Figure 2A). For this period of treatment, 1x CSE exposure did not affect the weights over a two-week period (Figure 2B). Furthermore, 1x CSE exposure did not substantially increase pathological damage in the lungs of mice compared to PBS control mice (Figure 2G, Top). Subsequently, we infected these mice with $1X10^3$, $1X10^4$, or $1X10^5$

10.3389/fimmu.2023.1083251

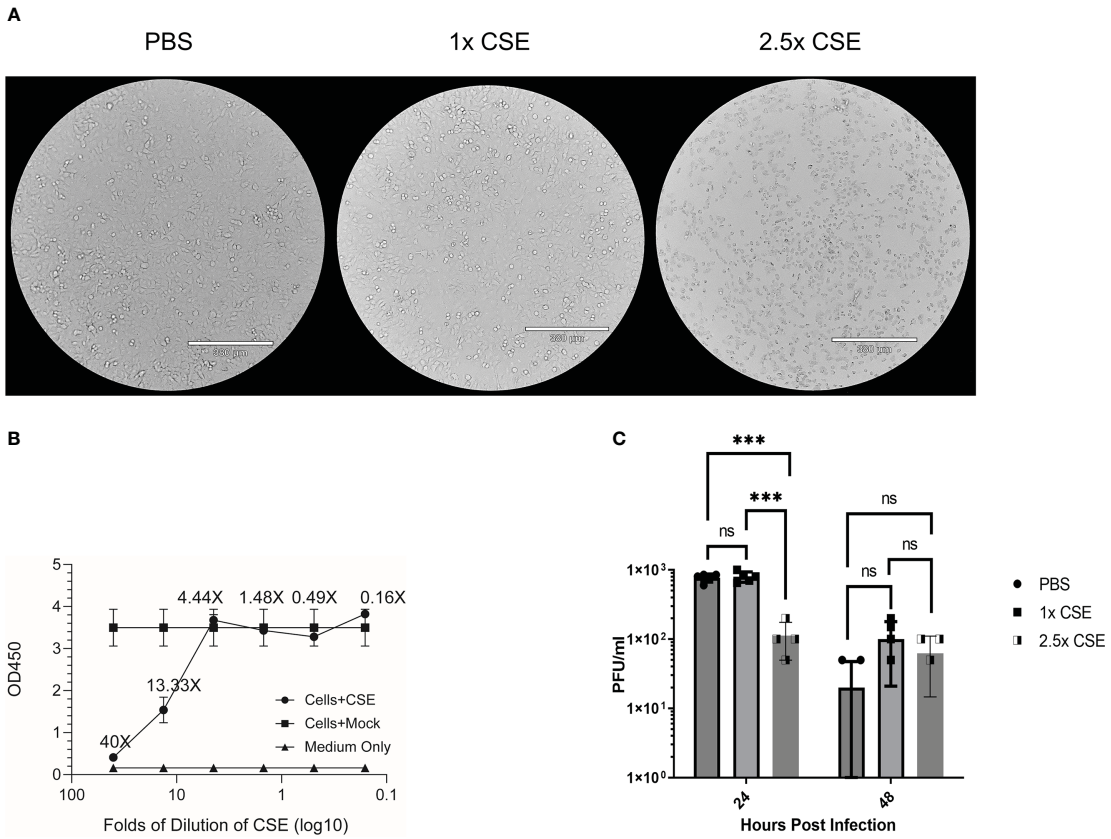

FIGURE 1
CSE suppressed viral replication ex vivo. A549 cells were treated for 24hrs with either PBS (mock), 1x CSE, or 2.5x CSE **(A)**. Cytotoxicity of CSE on A549 cells were further analyzed with CCK-8 kit **(B)**. Cells were infected with Influenza B/Victoria/2/87 at an MOI = 0.05. Supernatant samples were taken at 24 and 48 hpi and tittered by standard plaque assay **(C)**. A standard 2-way ANOVA with multiple comparisons was used for statistical analysis in PRISM software 9.0, *** = p<0.0001. N=4 per treatment group. NS, Not statistically significant.

PFU/mouse of IBV (Influenza B/Victoria/2/87). We observed mice body weight changes for 14 days post infection. We found that 1x CSE exposure did not increase weight loss during this two-week period post infection, regardless of the dose of IBV compared to PBS control mice (Figures 2C, E), nor did 1x CSE exposure have any effect on mortality among different groups of mice (Figures 2D, F). Finally, lung histology on tissue from three days post infection indicated immunocyte infiltration only in infected samples with or without CSE treatment. However, the phenomenon was not observed in samples from CSE treatment alone (Figure 2G, Bottom). This suggests that our current CSE dose is not high enough to exhibit a significant negative impact on disease outcomes.

We next assessed the potential impact of CSE on the viral pulmonary replication and immunological responses post IBV infection. We treated mice with 1x CSE and infected as described in earlier sections (Figure 3A). We observed that with both low and high doses of IBV, 1x CSE exposure did not affect the amount of virus detected in the lungs from mice at 3 and 6 days post infection (dpi) (Figures 3B, C) compared to control PBS groups. Similarly, we did not find any difference between 1x CSE and PBS viral titers in the upper respiratory fluid 3 or 6 dpi (Figure 3D). Also, we found that 1x CSE treatment did not have a significant impact on pro-inflammatory cytokine gene expression 3 dpi (Figure 2H).

Because smoking has been shown to alter innate and adaptive immune responses post IAV infection in some reports (44–46, 58), we went further to determine whether CSE exposure influences the host immune responses after IBV infection. Here, we examined both cellular and humoral responses through evaluating IFN-γ production from the IBV specific splenocytes, IBV specific IgA level from nasal lavage samples, and IBV specific IgG levels from sera samples (Figure 4A). Even though we observed significantly higher IFN-γ production from splenocytes of CSE mice versus those of PBS control animals (Figure 4B), we did not observe a discernable difference in PBS *vs* CSE treated animal in their IgA (Figure 4C) or IgG (Figure 4D) titers at 21dpi. Furthermore, we evaluated the potency of those IBV specific IgGs by microneutralization assays. Similarly, we did not detect significant difference between CSE or PBS treatment groups (Figure 4E). To evaluate whether our observation is independent of IBV dose usage, we repeated the experiments with a higher dose infection at $1x10^5$ PFU/mouse. Similarly, we found that neither IgG (Figure 5A) nor neutralization titers (Figure 5B) differed between CSE or PBS groups. Collectively, our results suggest that early cellular immune responses are elevated in CSE mice, but mucosal and humoral immunity by later stages post infection have equalized. However, this is likely due to the low dose of CSE used here in these studies. At three days post infection,

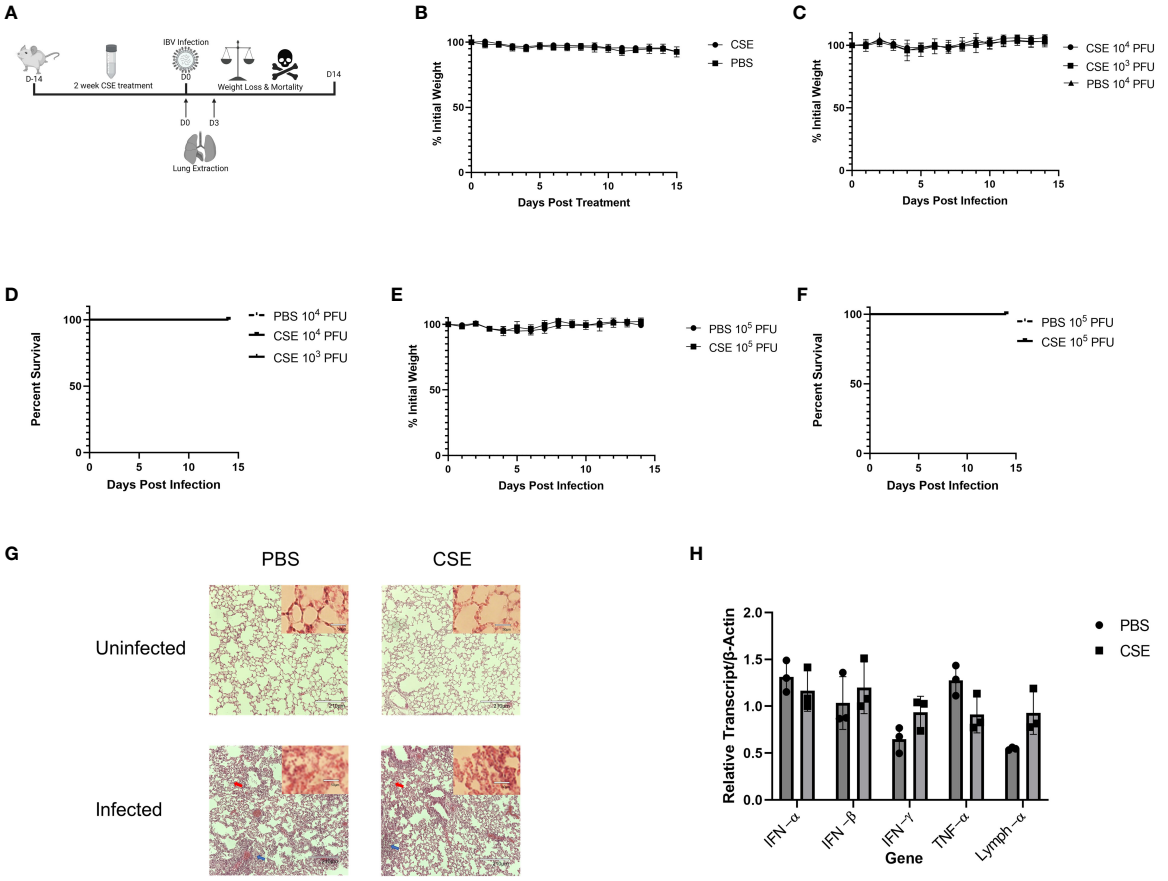

FIGURE 2
1X CSE treatment does not affect mice weight loss or survival before or after IBV infection. **(A)** 6–8-week-old female BALB/cJ mice were treated intranasally with 50µl of 1xCSE daily, six days per week, for two weeks total. Weights of mice were monitored during 1x CSE treatment **(B)** and after infection **(C)** with 10^3, 10^4, or 10^5 **(E)** PFU/mouse. Survival was monitored up to 14 days post infection for **(D)** 10^3/10^4 or 10^5 **(F)** PFU/mouse groups. N=5 for all groups. Lungs were harvested from 1X CSE treated mice at the day of infection, Day 0, or three days post IBV infections. For mice of 3 DPI, half of tissues were fixed for H&E staining analysis **(G)** and the rest were used for qPCR gene expression analysis of pro-inflammatory molecules **(H)**. Larger lung pictures are 10X magnification, while smaller picture in upper right corner of lung histology represents 20x magnification. Red arrows indicated thickening of the alveolar septa with congestion, blue arrows indicate the infiltration of inflammatory cells. With higher resolution at 20X, a large number of neutrophils and lymphocytes were only present in infected samples. Statistical significance for figure were determined by 2-way ANOVA with multiple comparisons.

lung histology indicated cell infiltration only in infected samples regardless of CSE treatment, which was not observed in samples from CSE treatment alone (Figure 2G, Bottom). This suggests a likely caveat that our current CSE dose is not high enough to impact on host immune responses.

Increasing concentration of CSE reduces survival of mice post IBV infection

Smoking commonly varies among people, typically between 1 cigarette to multiple packs a day (https://www.lung.org/research/trends-in-lung-disease/tobacco-trends-brief/overall-tobacco-trends). To better mimic the physiologic condition, but more importantly to mimic the heavy smoking conditions, we further tested higher dose of CSE on IBV pathology, disease outcome, and immune responses. To this end, we first treated mice as described in Figure 6A with increasing amount of CSE. We observed that mice exhibited similar weight changes among different groups during the two-week CSE treatment period. The result suggested that increasing concentrations of CSE did not have an overwhelming impact on mice with up to 14 days treatment resulting in no significant effect of weight changes (Figure 6B). Following the same amount (10^5 PFU) of IBV infection, based on the weight records for surviving animals, we did not find significant differences in weight between our CSE treatment groups and the PBS mock treatment group (Figure 6C). However, from our survival data, we observed that the survival rate was inversely correlated with the amount of CSE used (Figure 6D). To further assess impact of high dose CSE on humoral responses, we tested IgA levels of nasal wash samples (mucosal) and IgG level of sera samples (systematic). Intriguingly, we observed a significant decrease in IBV specific IgA titers only for the undiluted samples (Figure 6E) and a more profound significant decrease in IBV specific IgG titers up to around 900-fold of dilutions of original sera (Figure 6F). On the contrary, we did not observe a difference in IgG neutralizing titers

10.3389/fimmu.2023.1083251

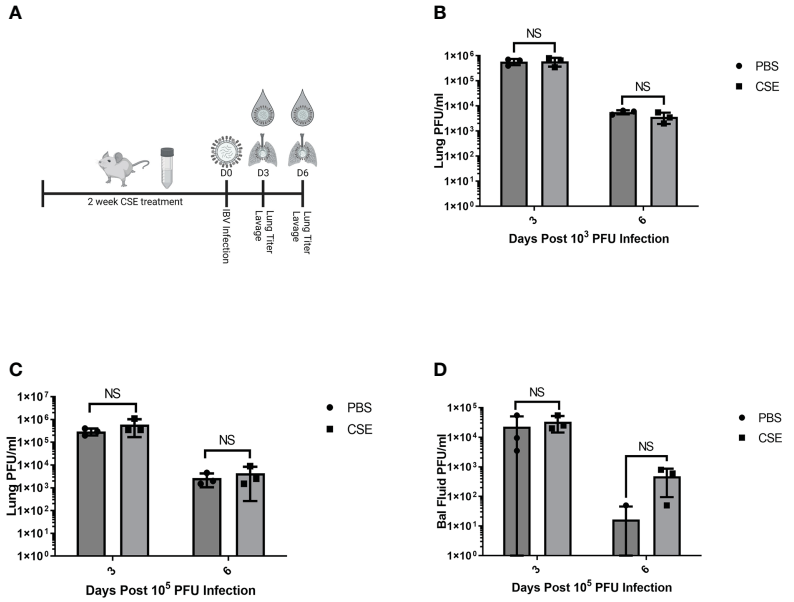

FIGURE 3
1X CSE treatment does not affect respiratory viral replication or pathological responses. **(A)** schematic describing 6–8-week-old female BALB/cJ mice treated with 1X CSE and infected with IBV. Virus lung replication was measured on day 3 and day 6 post $1x10^3$ **(B)** or $1x10^5$ PFU/mouse of IBV infection **(C)**. **(D)** Virus replication was also measured from upper airway lavage fluid collected from $1x10^3$ PFU infected mice by standard plaque assay. Significance was determined by standard students *t*-test. N=3. NS, Not statistically significant.

for IBV (Figure 6G) between CSE treated animals and PBS controlled animals. Furthermore, with increasing amounts of CSE used, we observed a decrease in survival following the subsequent IBV infection. Finally, we treated mice with CSE, subsequently infected them as in Figure 6A and assessed the potential impact of increasing CSE concentrations on the viral pulmonary and upper bal fluid replication 3 DPI (Figures 6H, I). Similar to 1xCSE treatments, increasing concentrations of CSE did not significantly alter viral replication in the lungs or upper bal fluid. Together, these facts revealed the CSE did not have direct negative impact on viral replication outcomes, for both upper and lower respiratory tracts.

Overall, we established a smoking model system for IBV using water-soluble components of CS. We found that the treatment negatively affected IBV infection outcomes and dampened host immune responses. The results validate that our smoking system recapitulated the disease outcomes of natural smoking behavior upon viral infection. Together, we provided a valuable resource to understand the impact of CS on IBV infection.

Discussion

Cigarette smoking increases the risk of IAV infection and exacerbates negative health outcomes, increasing both the time to recover and mortality. However, there is very little data on how cigarette smoking affects IBV infection, disease and to what degree. To this end, we developed an *in vivo* smoking model to study the pathological, immunological, and viral effects cigarette smoking may have on IBV infections. This was accomplished by pre-treating mice for two weeks with various concentrations of CSE, then infecting them with IBV and monitoring morbidity, mortality, lung inflammation, viral pulmonary and upper airway replication, and IBV specific serum and mucosal antibody levels. Ex vivo, IBV viral replication is not altered by 2.5x CSE treatment in A549 cells. *In vivo*, weight loss and mortality post IBV infection were not affected by 1x CSE regardless of the IBV dose compared to PBS control mice. Similarly, IgA, IgG, and neutralizing IgG levels were all similar in 1x CSE and PBS mock controls. However, 1x CSE induced a roughly 2-fold increase in IBV specific spleenocyte IFN-γ levels compared to PBS controls. Finally, increasing concentrations of CSE resulted in increased mortality compared to PBS controls after subsequent IBV infection, a significant decrease in IBV specific IgA or IgG levels but did not impact weight loss. Together, our system established a platform for further study of CS on IBV and provided first *in vivo* data on impact of CS on IBV infection in model systems.

Studying cigarette smoking and determining the specific chemical or compound in CS responsible for certain pathological or immunological responses is difficult for many reasons. Noah et al. measured live IBV vaccine RNA and specific cytokine levels post vaccination in nasal lavage fluid from active young smokers, secondhand smoke exposed, and never smoker groups (59). They noted that smokers had higher levels of IBV vaccine RNA and lower IL-6/IFN-γ levels compared to never smoker controls. Noteworthy, their conclusions were heavily influenced by variation in daily cigarettes consumed, type of cigarettes smoked, age, genetic background, unknown co-morbidities, other environmental factors, and use of attenuated vaccine virus.

To minimize the impact from those factors, it is necessary to perform a similar evaluation in a better controlled experimental

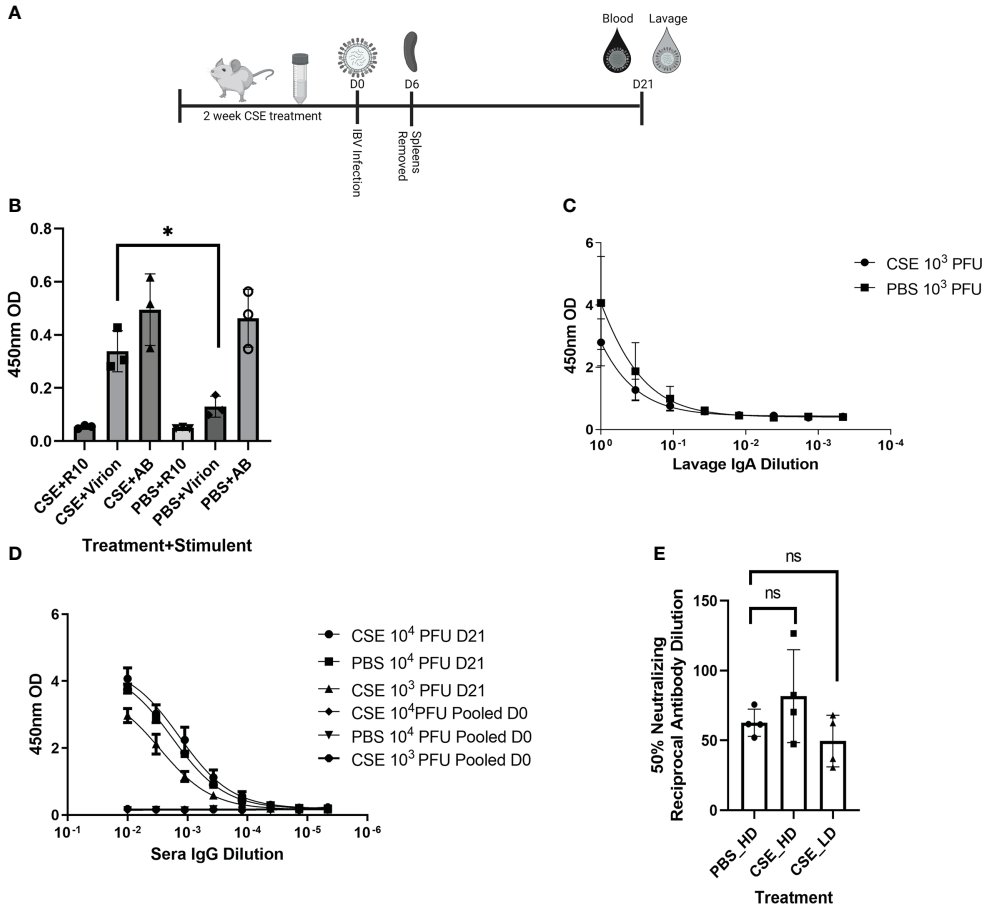

FIGURE 4
1X CSE treated mice do not exhibit altered adaptive immune responses post IBV infection. As shown in schematic **(A)** mice were treated with 1x CSE for two weeks and infected with either 10^3 or 10^4 PFU/mouse of IBV. Spleens from 10^3 PFU infection group were removed 6 DPI, homogenized and stimulated with either IBV virion, R10 media only, or Positive Control Antibody CD3/CD28 (AB). **(B)** IFN-γ expression was measured from stimulated splenocytes by ELISA. N=3. **(C)** Upper airway lavage fluid was used to measure IgA antibody titers 21 DPI by ELISA from mice infected with 10^3 PFU of IBV **(D)** Blood sera was drawn from mice infected with 10^3 or 10^4 PFU of IBV 21 DPI to measure IBV specific IgG responses by ELISA (N=5) or **(E)** neutralizing antibody titers as calculated from the 50% Reciprocal Inhibition Titer. Two-way ANOVA was used to test significant differences with multiple comparisons, * indicating $p<0.5$. NS, Not statistically significant.

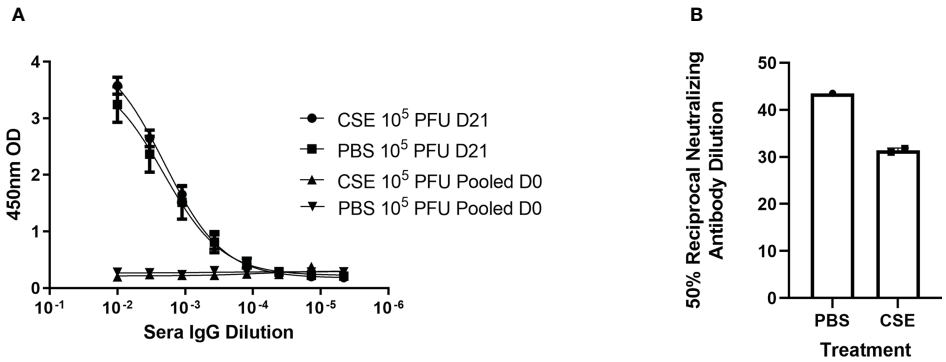

FIGURE 5
1x CSE treatment does not affect IgG or neutralizing titers of mice infected with higher doses of IBV. Mice were treated with 1x CSE as in Figure 4, and infected with 10^5 PFU/mouse of IBV. **(A)** Blood sera was drawn from mice infected with 10^3 PFU (LD) or 10^4 PFU (HD) of IBV 21 DPI to measure IgG responses by ELISA (N=5) or **(B)** neutralizing antibody titers as calculated from the 50% Reciprocal Inhibition Titer. Two-way ANOVA was used to test significant differences.

10.3389/fimmu.2023.1083251

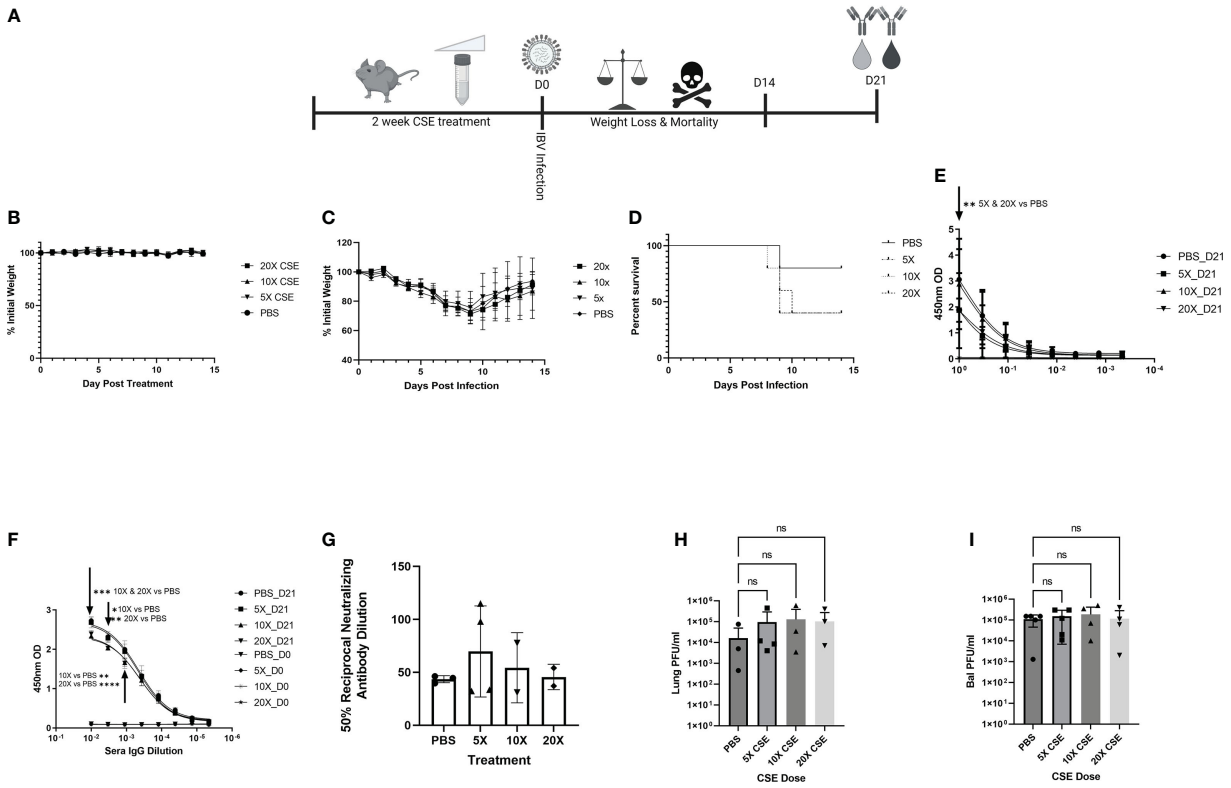

FIGURE 6
Increasing concentrations of CSE reduced survival. **(A)** Schematic showing 6-8-week-old female BALB/cJ mice were treated intranasally with 50µl of CSE, ranging from 5x to 20x, daily for six days per week, for two weeks total. **(B)** Weights of mice were monitored during CSE treatment and **(C)** after infection with 10^5 PFU/mouse of IBV for 14 days. **(D)** Survival was monitored for up to 14 days post infection, N=5 for all groups. **(E)** Lavage IgA or **(F)** Sera IgG specific for IBV from samples collected at 21 DPI was determine by ELISA from surviving mice, and **(G)** neutralizing antibody titers were calculating from microneutralization assays. Two-way ANOVA was used to test significant differences. In a second experiment, 5 mice per group were CSE treated and infected as in schematic 6A, and viral replication for the lungs **(H)** and upper bal fluid **(I)** was measured with standard plaque assay 3 DPI. One-way ANOVA with multiple comparisons was used to test significant differences to PBS group. NS, Not statistically significant. * = p=0.01, ** = p<0.0077, *** = p=0.0001, **** = p<0.0001.

system. Humans are exposed to at least 3 different types of smoke from cigarettes: firsthand, secondhand, and thirdhand smoke. Firsthand smoke comes from a person inhaling smoke through the cigarette directly into their lungs, also known as "mainstream" smoke (60), while secondhand smoke is smoke released into the environment from the lite side of the cigarette or from exhaled smoke and can be unintentionally inhaled by bystanders, a form of "side-stream" smoke (61). Thirdhand smoke come from either first or secondhand smoke that has settled or built up on furniture or surroundings that subsequently come into contact with people interacting with the smoke covered objects (62). Many systems that model cigarette smoking in mice place the mice in plexiglass chambers and expose them to mixtures of air and cigarette smoke pumped into the chamber for a specified time (whole body exposure), simulating side-stream smoke exposure or utilize nose only exposure systems (63), creating difficulty in both replicating CS exposure at relative human mass to cigarette ratios and study to study experiments.

Traditionally, the experimental system is built on the usage of a smoking chamber. Even though it can better mimic natural respiratory conditions, it suffers from the imprecise inoculation amount, let alone the financial requirements necessary for purchase. Here, we established a system based on the usage of water-soluble components from CS. CS is comprised of over 7000 chemicals and compounds. Our system will allow us to quickly distinguish water soluble component effects of cigarette smoke on IBV infection from the non-water soluble effects with fewer confounding factors. Additionally, it is superior in financial cost and prevents research personnel from handling mice that otherwise may be covered in toxic or carcinogenic components of cigarette smoke collected on their fur from side-stream smoke exposure. All these factors make this system a simple yet robust platform for evaluating CSE on respiratory viral infection.

We found that CSE treatment did not affect weight loss at any concentration from 1x to 20x. This is curious as smoking has been shown to result in weight loss in mice (64, 65). At least three factors could partially explain this lack of weight loss: a) the CSE we made contains only the water-soluble components of cigarette smoke, b) the mice were not exposed to CSE long enough to induce physical changes, or c) there were chemical variation in the cigarettes we used compared to previous studies. During the actual act of smoking cigarettes, there would be constant exposure of the lungs to water soluble and insoluble components of CS. To make our CSE, we bubble CS through PBS to capture the water soluble components, but allow the rest of the smoke to escape through the pump. Subsequently, any water insoluble particles that are

trapped on the liquid surface are mostly removed by filter sterilization. As such, it's possible the water insoluble particles or the combination with soluble components are necessary to induce weight loss. For CSE exposure length, previous studies have shown that there is a difference in pro-inflammatory cytokine response profiles depending on CS exposure of less than or greater than 2 weeks (66). It is possible that CSE exposure more than 2 weeks could have yielded a more significant effect on morbidity and mortality. Animal model studies with IAV range from as few as 3 days (67) to as long as 6 months (50). Given that there is huge variation in treatment period and amount of cigarettes used, it is not surprising to observe no significant weight loss from CSE treatment alone. Additionally, the brand of cigarette used in a study may have potential consequences on disease outcomes, including damage to the lungs. For example, Goel et al. found that among 27 brands of US commercially available cigarettes, there was as much as a 12-fold variation in free radicals in the gas phase of the CS (68). These free radicals can cause damage to cellular membranes and DNA (69), resulting in tissue damage to exposed organs. Because cigarette smoke contains over 7000 different chemicals and compounds (70), variation in which cigarettes are used in academic studies are likely going to lead to phenotypic variation post infection. Nevertheless, our CSE treatment did exhibit negative impacts on experimental animals, which resulted in decreased survival after subsequent IBV infection in a CSE dose dependent manner. The difference in weight loss warrants necessity for future studies to further titrate the specific amount, treatment time and types of CS or CSE.

Our data indicates that 1x CSE treatment did not impact IBV viral loads at 3 or 6 dpi with high or low doses of IBV or CSE. Gualano et al. has reported that cigarette smoke exposure in mice can lead to a moderate increase to viral loads (42). However, more reports indicate CS exposure does not impact viral loads of IAV infections, which is in line with our findings (43, 47–49). This would suggest that worse disease outcomes in our smoking model is likely not due to increased viral burden. Our speculation is in line with previous reports, which have correlated the final severity of disease outcome with the elevated inflammatory responses post IAV infection in smoking conditions, rather than with viral replication.

We noted interestingly that 1x CSE treatment resulted in increased IFN-γ production in spleenocytes compared to the PBS controls. IFN-γ promotes differentiation and proliferation of $CD8^+$ T-cells and upregulates antigen presenting cell MHC II expression, aiding in $CD4^+$ T-cell activation (71, 72). Only a specific set of immune cells produce IFN-γ, including $CD8^+$ cytotoxic T-cells, B cells, and antigen presenting cells (APCs) (73). Our data suggests that post infection, CSE treatment may have resulted in either an expansion of IBV specific immune cells or the spleenocyte immune cells are producing more IFN-γ than none CSE treatment under the same IBV specific stimulation. This was also mentioned earlier that there was a time dependent effect of CS on immune cytokine responses to infection (66). It is possible that elevated IFN-γ responses post infection could reflect higher inflammatory responses (attracting more cells) post IBV infection in 1x CSE treated mice. Interestingly, this differs from IAV data, as Feng et al. has shown that there was reduced IFN-γ from the lungs of CS mice, as well as reduced numbers of IFN-γ^+ cells from lungs and spleens of CS treated mice compared to control mice (43). It is possible this represents a potential pathological difference between IAV and IBV models of smoking, but it also may likely reflect experimental parameter differences including 1) exposure time, 6 weeks CS exposure *vs* 2 weeks CSE exposure and 2) exposure materials, CS versus CSE. Additionally, treatments with higher concentrations of CSE led to higher mortality after IBV infection. This suggests that higher concentrations of CSE are resulting in higher levels of inflammation post infection and could be responsible for exacerbating disease outcomes. Indeed, a number of IAV/CS studies have found higher lung and upper airway cell infiltration in CS mice compared to control groups (46, 48, 49).

Together, our results show that our system is a valid, rapid, and safer method to explore the effects of CS on IBV pathology and immune response compared to traditional experimental chamber models. We used the system to provide evidence to validate the negative impact of smoking on IBV infection. Together, we provided a valuable resource to understand the impact of CS on IBV vaccination and coinfections from different respiratory viruses, including IAV and even SARS-CoV-2. Furthermore, our model can serve as a platform for initial testing of the efficacy of anti-viral drugs and treatments under smoking conditions or could be used to examine if or how treatments designed to alleviate smoking consequences like inflammation affect infection outcomes. In result, these studies would provide the ground level animal model data required for further clinical testing in humans. In summary, our system will extend our understanding of other respiratory microbes under smoking conditions or other co-morbidities, such as diabetes, to help guide clinicians to achieve better treatment outcomes.

Data availability statement

The original contributions presented in the study are included in the article/supplementary material, further inquiries can be directed to the corresponding author/s.

Ethics statement

The animal study was reviewed and approved by University of California, Riverside Institutional Animal Care and Use Committee (IACUC).

Author contributions

JRC, WY, HD performed experiments. JRC and HD performed the CSE treatment. WY performed histology analysis. WY and JRC analyzed histology data. JC and DX performed and analysis the cytotoxicity analysis. JRC performed Statistics. JRC and RH wrote the draft of the manuscript and all authors contributed to the revising of the manuscript prior to submission. All authors contributed to the article and approved the submitted version.

Funding

JC was supported by a pre-doctoral fellowship provided by the University of California Office of the President (UCOP), under the Tobacco Related Disease Research Program (TRDRP, T30DT1060). This work was partially supported by NIAID (1R21AI147057 and R01AI153419) to RH.

Acknowledgments

Schematic figures were created with Biorender. We thank Samantha Cordingley for the help with our qRT-PCR analysis.

Conflict of interest

The authors declare that the research was conducted in the absence of any commercial or financial relationships that could be construed as a potential conflict of interest.

Publisher's note

All claims expressed in this article are solely those of the authors and do not necessarily represent those of their affiliated organizations, or those of the publisher, the editors and the reviewers. Any product that may be evaluated in this article, or claim that may be made by its manufacturer, is not guaranteed or endorsed by the publisher.

References

1. Lee VJ, Ho ZJM, Goh EH, Campbell H, Cohen C, Cozza V, et al. Advances in measuring influenza burden of disease. *Influenza Other Respir Viruses* (2018) 12:3–9. doi: 10.1111/irv.12533

2. Anonymous. *CDC Factsheet: Influenza disease burden* (Atlanta, GA: Center for Disease Control and Prevention).

3. Organization WH. *WHO influenza seasonal factsheet 2020.* (2020) (Geneva, Switzerland: World Health Organization).

4. Yan SK, Weycker D, Sokolowski S. US Healthcare costs attributable to type a and type b influenza. *Hum Vaccines Immunotherapeutics* (2017) 13:2041–7. doi: 10.1080/21645515.2017.1345400

5. Bank W. *GDP (current US$).* Available at: https://data.worldbank.org/indicator/NY.GDP.MKTP.CD (Accessed 8/31/22).

6. CDC. *2000-2001 INFLUENZA SEASON SUMMARY* (2001). Available at: https://www.cdc.gov/flu/weekly/weeklyarchives2000-2001/00-01summary.htm (Accessed 8/22/22).

7. CDC. *2001-02 INFLUENZA SEASON SUMMARY* (2002). Available at: https://www.cdc.gov/flu/weekly/weeklyarchives2001-2002/01-02summary.htm (Accessed 8/22/22).

8. CDC. *03 U.S. INFLUENZA SEASON SUMMARY* (2002). Available at: https://www.cdc.gov/flu/weekly/weeklyarchives2002-2003/02-03summary.htm (Accessed 8/22/22).

9. CDC. *2003 - 04 U.S. INFLUENZA SEASON SUMMARY* (2004). Available at: https://www.cdc.gov/flu/weekly/weeklyarchives2003-2004/03-04summary.htm (Accessed 8/22/22).

10. CDC. *2004-05 U.S. INFLUENZA SEASON SUMMARY* (2005). Available at: https://www.cdc.gov/flu/weekly/weeklyarchives2004-2005/04-05summary.htm (Accessed 8/22/22).

11. CDC. *2005-06 U.S. INFLUENZA SEASON SUMMARY* (2006). Available at: https://www.cdc.gov/flu/weekly/weeklyarchives2005-2006/05-06summary.htm.

12. CDC. *2006-07 U.S. INFLUENZA SEASON SUMMARY* (2007). Available at: https://www.cdc.gov/flu/weekly/weeklyarchives2006-2007/06-07summary.htm.

13. CDC. *2007-08 U.S. INFLUENZA SEASON SUMMARY* (2008). Available at: https://www.cdc.gov/flu/weekly/weeklyarchives2007-2008/07-08summary.htm (Accessed 8/22/22).

14. CDC. *2008-2009 influenza season summary* (2009). Available at: https://www.cdc.gov/flu/weekly/weeklyarchives2008-2009/08-09summary.htm (Accessed 8/22/22).

15. CDC. *2009-2010 influenza season summary* (2010). Available at: https://www.cdc.gov/flu/weekly/weeklyarchives2009-2010/09-10Summary.htm (Accessed 8/22/22).

16. CDC. *Update: Influenza activity - united states, 2010-11 season, and composition of the 2011-12 influenza vaccine* (2011). Available at: https://www.cdc.gov/mmwr/preview/mmwrhtml/mm6021a5.htm (Accessed 8/22/22).

17. CDC. *Update: Influenza activity - united states, 2011-12 season and composition of the 2012-13 influenza vaccine* (2012). Available at: https://www.cdc.gov/mmwr/preview/mmwrhtml/mm6122a4.htm (Accessed 8/22/22).

18. CDC. *Influenza activity - united states, 2012-13 season and composition of the 2013-14 influenza vaccine* (2013). Available at: https://www.cdc.gov/mmwr/preview/mmwrhtml/mm6223a5.htm?s_cid=mm6223a5_e (Accessed 8/22/22).

19. CDC. *Influenza activity - united states, 2013-14 season and composition of the 2014-15 influenza vaccines* (2014). Available at: https://www.cdc.gov/mmwr/preview/mmwrhtml/mm6322a2.htm (Accessed 8/22/22).

20. CDC. *Influenza activity - united states, 2014-15 season and composition of the 2015-16 influenza vaccine* (2015). Available at: https://www.cdc.gov/mmwr/preview/mmwrhtml/mm6421a5.htm (Accessed 8/22/22).

21. CDC. *Influenza activity - united states, 2015-16 season and composition of the 2016-17 influenza vaccine* (2016). Available at: https://www.cdc.gov/mmwr/volumes/65/wr/mm6522a3.htm (Accessed 8/22/22).

22. CDC. *Update: Influenza activity in the united states during the 2016–17 season and composition of the 2017–18 influenza vaccine* (2017). Available at: https://www.cdc.gov/mmwr/volumes/66/wr/mm6625a3.htm (Accessed 8/22/22).

23. CDC. *Update: Influenza activity in the united states during the 2017–18 season and composition of the 2018–19 influenza vaccine* (2018). Available at: https://www.cdc.gov/mmwr/volumes/67/wr/mm6722a4.htm?s_cid=mm6722a4_w (Accessed 8/22/22).

24. CDC. *FluView interactive map (2019-2020, weeks 40-26).* Available at: https://gis.cdc.gov/grasp/fluview/fluportaldashboard.html (Accessed 8/22/22).

25. Anonymous. *Influenza in Europe, summary of the season 2017–18* (Solna Municipality, Sweden: European Centre for Disease Prevention and Control) (2018).

26. Bhat YR. Influenza b infections in children: A review. *World J Clin Pediatr* (2020) 9:44–52. doi: 10.5409/wjcp.v9.i3.44

27. Anonymous. *CDC Smoking & tobacco use factsheet.* (2020) (Atlanta, GA: Center for Disease Control and Prevention).

28. Control CfD. *CDC Smoking & tobacco use: Health effects factsheet* (Atlanta, GA: Center for Disease Control and Prevention) (2020).

29. Almirall J, Gonzalez CA, Balanzo X, Bolibar I. Proportion of community-acquired pneumonia cases attributable to tobacco smoking. *Chest* (1999) 116:375–9. doi: 10.1378/chest.116.2.375

30. Almirall J, Bolibar I, Balanzo X, Gonzalez CA. Risk factors for community-acquired pneumonia in adults: a population-based case-control study. *Eur Respir J* (1999) 13:349–55. doi: 10.1183/09031936.99.13234999

31. Aryanpur M, Masjedi MR, Hosseini M, Mortaz E, Tabarsi P, Soori H, et al. Cigarette smoking in patients newly diagnosed with pulmonary tuberculosis in Iran. *Int J Tuberculosis Lung Dis* (2016) 20:679–84. doi: 10.5588/ijtld.15.0662

32. Alcaide J, Altet MN, Plans P, Parron I, Folguera L, Salto E, et al. Cigarette smoking as a risk factor for tuberculosis in young adults: A case-control study. *Tubercle Lung Dis* (1996) 77:112–6. doi: 10.1016/S0962-8479(96)90024-6

33. Smith GS, Van Den Eeden SK, Baxter R, Shan J, Van Rie A, Herring AH, et al. Cigarette smoking and pulmonary tuberculosis in northern California. *J Epidemiol Community Health* (2015) 69:568–73. doi: 10.1136/jech-2014-204292

34. Bonacci RA, Cruz-Hervert LP, Garcia-Garcia L, Reynales-Shigematsu LM, Ferreyra-Reyes L, Bobadilla-del-Valle M, et al. Impact of cigarette smoking on rates and clinical prognosis of pulmonary tuberculosis in southern Mexico. *J Infect* (2013) 66:303–12. doi: 10.1016/j.jinf.2012.09.005

35. Pavic I, Jurkovic M, Pastar Z. Risk factors for acute respiratory tract infections in children. *Collegium Antropologicum* (2012) 36:539–42.

36. Mazarico E, Gomez-Roig MD, Guirado L, Lorente N, Gonzalez-Bosquet E. Relationship between smoking, HPV infection, and risk of cervical cancer. *Eur J Gynaecological Oncol* (2015) 36:677–80. doi: 10.12892/ejgo2713.2015

37. Kark JD, Lebiush M, Rannon L. Cigarette-smoking as a risk factor for epidemic a (H1n1) influenza in young men. *N Engl J Med* (1982) 307:1042–6. doi: 10.1056/NEJM198210213071702

38. Finklea JF, Sandifer SH, Smith DD. Cigarette smoking and epidemic influenza. *Am J Epidemiol* (1969) 90:390. doi: 10.1093/oxfordjournals.aje.a121084

39. Aronson MD, Weiss ST, Ben RL, Komaroff AL. Association between cigarette smoking and acute respiratory tract illness in young adults. *JAMA* (1982) 248:181–3. doi: 10.1001/jama.1982.03330020025023

40. Organization WH. *Smoking and COVID-19* (Geneva, Switzerland: World Health Organization) (2020).

41. Poudel R, Daniels LB, DeFilippis AP, Hamburg NM, Khan Y, Keith RJ, et al. Smoking is associated with increased risk of cardiovascular events, disease severity, and mortality among patients hospitalized for SARS-CoV-2 infections. *PloS One* (2022) 17: e0270763. doi: 10.1371/journal.pone.0270763

42. Gualano RC, Hansen MJ, Vlahos R, Jones JE, Park-Jones RA, Deliyannis G, et al. Cigarette smoke worsens lung inflammation and impairs resolution of influenza infection in mice. *Respir Res* (2008) 9:53. doi: 10.1186/1465-9921-9-53

43. Feng Y, Kong Y, Barnes PF, Huang FF, Klucar P, Wang XS, et al. Exposure to cigarette smoke inhibits the pulmonary T-cell response to influenza virus and mycobacterium tuberculosis. *Infection Immun* (2011) 79:229–37. doi: 10.1128/IAI.00709-10

44. Han Y, Ling MT, Mao HW, Zheng J, Liu M, Lam KT, et al. Influenza virus-induced lung inflammation was modulated by cigarette smoke exposure in mice. *PLoS One* (2014) 9:e86166. doi: 10.1371/journal.pone.0086166

45. Hong MJ, Gu BH, Madison MC, Landers C, Tung HY, Kim M, et al. Protective role of gamma delta T cells in cigarette smoke and influenza infection. *Mucosal Immunol* (2018) 11:894–908. doi: 10.1038/mi.2017.93

46. Kang MJ, Lee CG, Lee JY, Dela Cruz CS, Chen ZJ, Enelow R, et al. Cigarette smoke selectively enhances viral PAMP- and virus-induced pulmonary innate immune and remodeling responses in mice. *J Clin Invest* (2008) 118:2771–84. doi: 10.1172/JCI32709

47. Ferrero MR, Garcia CC, Dutra de Almeida M, Torres Braz da Silva J, Bianchi Reis Insuela D, Teixeira Ferreira TP, et al. CCR5 antagonist maraviroc inhibits acute exacerbation of lung inflammation triggered by influenza virus in cigarette smoke-exposed mice. *Pharm (Basel)* (2021) 14:A4552. doi: 10.3390/ph14070620

48. Robbins CS, Bauer CMT, Vujicic N, Gaschler GJ, Lichty BD, Brown EG, et al. Cigarette smoke impacts immune inflammatory responses to influenza in mice. *Am J Respir Crit Care Med* (2006) 174:1342–51. doi: 10.1164/rccm.200604-561OC

49. Bauer CMT, Zavitz CCJ, Botelho FM, Lambert KN, Brown EG, Mossman KL, et al. Treating viral exacerbations of chronic obstructive pulmonary disease: Insights from a mouse model of cigarette smoke and H1N1 influenza infection. *PloS One* (2010) 5:e13251. doi: 10.1371/journal.pone.0013251

50. Wang JM, Li QH, Xie JG, Xu YJ. Cigarette smoke inhibits BAFF expression and mucosal immunoglobulin a responses in the lung during influenza virus infection. *Respir Res* (2015) 16:37. doi: 10.1186/s12931-015-0201-y

51. Mebratu YA, Smith KR, Agga GE, Tesfaigzi Y. Inflammation and emphysema in cigarette smoke-exposed mice when instilled with poly (I:C) or infected with influenza a or respiratory syncytial viruses. *Respir Res* (2016) 17:75. doi: 10.1186/s12931-016-0392-x

52. Ladomenou F, Kafatos A, Galanakis E. Environmental tobacco smoke exposure as a risk factor for infections in infancy. *Acta Paediatrica* (2009) 98:1137–41. doi: 10.1111/j.1651-2227.2009.01276.x

53. Jedrychowski W, Flak E. Maternal smoking during pregnancy and postnatal exposure to environmental tobacco smoke as predisposition factors to acute respiratory infections. *Environ Health Perspect* (1997) 105:302–6. doi: 10.1289/ehp.97105302

54. Miyahara R, Takahashi K, Anh NTH, Thiem VD, Suzuki M, Yoshino H, et al. Exposure to paternal tobacco smoking increased child hospitalization for lower respiratory infections but not for other diseases in Vietnam. *Sci Rep* (2017) 7:45481. doi: 10.1038/srep45481

55. Aedo G, Miranda M, Chavez MN, Allende ML, Egana JT. A reliable preclinical model to study the impact of cigarette smoke in development and disease. *Curr Protoc Toxicol* (2019) 80:e78. doi: 10.1002/cptx.78

56. Elliott MK, Sisson JH, West WW, Wyatt TA. Differential *in vivo* effects of whole cigarette smoke exposure versus cigarette smoke extract on mouse ciliated tracheal epithelium. *Exp Lung Res* (2006) 32:99–118. doi: 10.1080/01902140600710546

57. Duffney PF, Embong AK, McGuire CC, Thatcher TH, Phipps RP, Sime PJ. Cigarette smoke increases susceptibility to infection in lung epithelial cells by upregulating caveolin-dependent endocytosis. *PLoS One* (2020) 15:e0232102. doi: 10.1371/journal.pone.0232102

58. Jaspers I, Horvath KM, Zhang WL, Brighton LE, Carson JL, Noah TL. Reduced expression of IRF7 in nasal epithelial cells from smokers after infection with influenza. *Am J Respir Cell Mol Biol* (2010) 43:368–75. doi: 10.1165/rcmb.2009-0254OC

59. Noah TL, Zhou HB, Monaco J, Horvath K, Herbst M, Jaspers I. Tobacco smoke exposure and altered nasal responses to live attenuated influenza virus. *Environ Health Perspect* (2011) 119:78–83. doi: 10.1289/ehp.1002258

60. Health NIo. *Dictionary of cancer terms: Mainstream smoke* (Bethesda, Maryland: National Institute of Health).

61. Health NIo. *Secondhand smoke and cancer* (Bethesda, Maryland: National Institute of Health).

62. Jacob P3rd, Benowitz NL, Destaillats H, Gundel L, Hang B, Martins-Green M, et al. Thirdhand smoke: New evidence, challenges, and future directions. *Chem Res Toxicol* (2017) 30:270–94. doi: 10.1021/acs.chemrestox.6b00343

63. Ghorani V, Boskabady MH, Khazdair MR, Kianmeher M. Experimental animal models for COPD: A methodological review. *Tob Induc Dis* (2017) 15:25. doi: 10.1186/s12971-017-0130-2

64. Chen H, Vlahos R, Bozinovski S, Jones J, Anderson GP, Morris MJ. Effect of short-term cigarette smoke exposure on body weight, appetite and brain neuropeptide y in mice. *Neuropsychopharmacology* (2005) 30:713–9. doi: 10.1038/sj.npp.1300597

65. Chen H, Hansen MJ, Jones JE, Vlahos R, Bozinovski S, Anderson GP, et al. Cigarette smoke exposure reprograms the hypothalamic neuropeptide y axis to promote weight loss. *Am J Respir Crit Care Med* (2006) 173:1248–54. doi: 10.1164/rccm.200506-977OC

66. Chavez J, Hai R. Effects of cigarette smoking on influenza Virus/Host interplay. *Pathogens* (2021) 10:1636. doi: 10.3390/pathogens10121636

67. Boehme SA, Franz-Bacon K, Ludka J, DiTirro DN, Ly TW, Bacon KB. MAP3K19 is overexpressed in COPD and is a central mediator of cigarette smoke-induced pulmonary inflammation and lower airway destruction. *PLoS One* (2016) 11: e0167169. doi: 10.1371/journal.pone.0167169

68. Goel R, Bitzer Z, Reilly SM, Trushin N, Foulds J, Muscat J, et al. Variation in free radical yields from US marketed cigarettes. *Chem Res Toxicol* (2017) 30:1038–45. doi: 10.1021/acs.chemrestox.6b00359

69. Machlin LJ, Bendich A. FREE-RADICAL TISSUE-DAMAGE - PROTECTIVE ROLE OF ANTIOXIDANT NUTRIENTS. *FASEB J* (1987) 1:441–5. doi: 10.1096/fasebj.1.6.3315807

70. Anonymous. *National cancer institute: Harms of cigarette smoking and health benefits of quitting factsheet*. Available at: https://www.cancer.gov/about-cancer/causes-prevention/risk/tobacco/cessation-fact-sheet#:~:text=Of%20the%20more%20than%207%2C000,least%2069%20can%20cause%20cancer.

71. Maraskovsky E, Chen WF, Shortman K. IL-2 AND IFN-GAMMA ARE 2 NECESSARY LYMPHOKINES IN THE DEVELOPMENT OF CYTOLYTIC T-CELLS. *J Immunol* (1989) 143:1210–4. doi: 10.4049/jimmunol.143.4.1210

72. Curtsinger JM, Agarwal P, Lins DC, Mescher MF. Autocrine IFN-gamma promotes naive CD8 T cell differentiation and synergizes with IFN-alpha to stimulate strong function. *J Immunol* (2012) 189:659–68. doi: 10.4049/jimmunol.1102727

73. Castro F, Cardoso AP, Goncalves RM, Serre K, Oliveira MJ. Interferon-gamma at the crossroads of tumor immune surveillance or evasion. *Front Immunol* (2018) 9. doi: 10.3389/fimmu.2018.00847

frontiers | Frontiers in Immunology

TYPE Original Research
PUBLISHED 18 April 2023
DOI 10.3389/fimmu.2023.1169968

OPEN ACCESS

EDITED BY
Paraskevi C. Fragkou,
Evaggelismos General Hospital, Greece

REVIEWED BY
Daniel Prantner,
University of Maryland, United States
Charalampos D. Moschopoulos,
University General Hospital Attikon, Greece

*CORRESPONDENCE
Gen Lu
lugen5663330@sina.com
Can Cao
caoc9@mail.sysu.edu.cn
Minhao Wu
wuminhao@mail.sysu.edu.cn

†These authors have contributed equally to this work

SPECIALTY SECTION
This article was submitted to Viral Immunology, a section of the journal Frontiers in Immunology

RECEIVED 20 February 2023
ACCEPTED 03 April 2023
PUBLISHED 18 April 2023

CITATION
Li L, Fan H, Zhou J, Xu X, Yang D, Wu M, Cao C and Lu G (2023) Human adenovirus infection induces pulmonary inflammatory damage by triggering noncanonical inflammasomes activation and macrophage pyroptosis.
Front. Immunol. 14:1169968.
doi: 10.3389/fimmu.2023.1169968

Human adenovirus infection induces pulmonary inflammatory damage by triggering noncanonical inflammasomes activation and macrophage pyroptosis

Lexi Li[1,2†], Huifeng Fan[2†], Jinyu Zhou[3], Xuehua Xu[2], Diyuan Yang[2], Minhao Wu[3*], Can Cao[3*] and Gen Lu[1,2*]

[1]School of Medicine, South China University of Technology, Guangzhou, China, [2]Department of Respiration, Guangzhou Women and Children's Medical Centre, Guangzhou, China, [3]Department of Immunology, Zhongshan School of Medicine, Sun Yat-sen University, Guangzhou, China

Introduction: Human adenovirus (HAdV) is a common respiratory virus, which can lead to severe pneumonia in children and immunocompromised persons, and canonical inflammasomes are reported to be involved in anti-HAdV defense. However, whether HAdV induced noncanonical inflammasome activation has not been explored. This study aims to explore the broad roles of noncanonical inflammasomes during HAdV infection to investigate the regulatory mechanism of HAdV-induced pulmonary inflammatory damage.

Methods: We mined available data on GEO database and collected clinical samples from adenovirus pneumonia pediatric patients to investigate the expression of noncanonical inflammasome and its clinical relevance. An *in vitro* cell model was employed to investigate the roles of noncanonical inflammasomes in macrophages in response to HAdV infection.

Results: Bioinformatics analysis showed that inflammasome-related genes, including caspase-4 and caspase-5, were enriched in adenovirus pneumonia. Moreover, caspase-4 and caspase-5 expression levels were significantly increased in the cells isolated from peripheral blood and broncho-alveolar lavage fluid (BALF) of pediatric patients with adenovirus pneumonia, and positively correlated with clinical parameters of inflammatory damage. *In vitro* experiments revealed that HAdV infection promoted caspase-4/5 expression, activation and pyroptosis in differentiated THP-1 (dTHP-1) human macrophages via NF-κB, rather than STING signaling pathway. Interestingly, silencing of caspase-4 and caspase-5 in dTHP-1 cells suppressed HAdV-induced noncanonical inflammasome activation and macrophage pyroptosis, and dramatically decreased the HAdV titer in cell supernatants, by influencing virus release rather than other stages of virus life cycle.

Discussion: In conclusion, our study demonstrated that HAdV infection induced macrophage pyroptosis by triggering noncanonical inflammasome activation via a NF-kB-dependent manner, which may explore new perspectives on the

pathogenesis of HAdV-induced inflammatory damage. And high expression levels of caspase-4 and caspase-5 may be a biomarker for predicting the severity of adenovirus pneumonia.

KEYWORDS

human adenovirus, inflammasome, caspase-4, caspase-5, pyroptosis

Introduction

Human adenovirus (HAdV), a member of the family Adenoviridae, is a common pathogen of respiratory tract infection in childhood and immunocompromised persons with high morbidity and mortality (1–3). There are seven different HAdV species (A-G), and to date, over 110 genotypes have been identified (1). And HAdV infection in children can cause numerous diseases such as pleural effusions, acute respiratory distress syndrome (ARDS), respiratory failure, myocarditis, and even death (3–6). Epidemiology suggests that among these serotypes, HAdV-3 and -7 are the most common types causing severe respiratory disease in children less than 5 years old worldwide (1–3, 7).

Inflammasomes, a group of cytosolic protein complexes, are formed to mediate host innate immune responses to microbial infection and cellular damage. They recruit inflammatory caspases, cysteine proteases that initiate or execute cellular programs, to trigger inflammation or cell death. Inflammasomes include canonical and noncanonical inflammasomes. Canonical inflammasomes, such as NLRP3, NLRP1, IPAF, and AIM2 inflammasome, activate caspase-1 to cleave pro-interleukin-1 beta (pro-IL-1β) and IL-18 into the secreted bioactive cytokines (8).. However, noncanonical inflammasomes often respond to intracellular lipopolysaccharide (LPS) and activate caspase-4 and caspase-5 in humans and caspase-11 in mice (9). Activated caspase-1/4/5/11 can induce cleavage of the pore-forming protein gasdermin D (GSDMD), leading to an inflammatory lytic type of cell death called pyroptosis.

It has been reported that HAdV DNA can activate inflammasomes to trigger innate immune responses (10). And K^+ efflux, reactive oxygen species (ROS) and lysosomal damages have been brought forward as the exact cellular events involved in HAdV-induced NLRP3 inflammasome activation (11–13). Another study has shown that AIM2 inflammasome activated during HAdV infection to trigger caspase-1-mediated IL-1β/18 processing and GSDMD cleavage (14).

It is commonly believed that noncanonical caspase-4/5/11 directly senses cytosolic LPS *via* their caspase-activating and recruitment domains (CARD), pointing out the importance of noncanonical inflammasomes in anti-bacterial defense (15–17). Recently studies has verified that virus infection induces noncanonical inflammasomes activation during inflammatory responses, including severe acute respiratory syndrome coronavirus 2 (SARS–CoV-2), murine gammaherpesvirus 68 (MHV68) and coxsackievirus B3 (CVB3) (18–20). However, whether HAdV infection induced noncanonical inflammasomes activation in adenovirus pneumonia has not been explored.

Several signaling pathways play an important role in regulating inflammasome activation. For example, the nuclear factor-κB (NF-κB) signaling pathway serves as a prototypical proinflammatory pathway and provides the first signal for NLRP3 inflammasome activation by inducing pro-IL-1β and NLRP3 expression (21). NF-κB activation also promotes noncanonical caspase expression in inflammatory diseases (22, 23). Moreover, cGAS/STING signaling pathway functions as a cytoplasmic DNA sensor to initiate innate immune response against pathogen infection. The second messenger cGAMP catalyzed by cGAS could activate STING to induce downstream activation of TBK1/IRF3 or NF-κB, which respectively results in the production of type I interferons (IFNs) or proinflammatory cytokines (24–26). STING signaling pathway also contributes to both canonical and noncanonical inflammasome activation in *Chlamydia trachomatis* mouse bone marrow derived macrophages (BMDMs) (27). However, whether STING or NF-κB signaling pathway influences noncanonical inflammasome activation during HAdV infection remains unclear.

In the present study, we explored the role of noncanonical inflammasome during HAdV infection. We found that caspase-4 and caspase-5 expression levels were significantly increased in pediatric patients with adenovirus pneumonia and positively correlated with inflammatory damage. And *in vitro* experiments indicated that HAdV infection induced noncanonical inflammasomes activation and macrophage pyroptosis *via* NF-κB signaling pathway, while the STING signaling pathway was not involved in. Interestingly, silencing of caspase-4 and caspase-5 in dTHP-1 cells dramatically decreased the HAdV titer in cell supernatant. Overall, our study explored the broad role of noncanonical inflammasomes in HAdV-induced inflammatory responses, which may provide a potential therapeutic target for pediatric adenovirus pneumonia and a predictive biomarker for the severity.

Material and methods

Materials and reagents

RPMI medium, fetal bone serum (FBS), penicillin-streptomycin, L-glutamine, Opti-MEM and Lipofectamine™ 2000

were products of Invitrogen (Carlsbad, CA, USA). LPS derived from *Pseudomonas aeruginosa*, propidium iodide (PI), PMA and DMSO were purchased from Sigma Aldrich (St. Louis, MO, USA). C-176 (STING inhibitor) was bought from Selleck (Houston, TX, USA) and BAY11-7082 (NF-κB inhibitor) was bought from MedChemExpress (New Jersey, USA). 2', 3'-cGAMP (STING agonist) and CpG ODN 2006 were bought from Invivogen (San Diego, CA, USA). Primary antibodies: anti-caspase-1 (AG-20B-0048) from Adipogen (San Diego, CA, USA); anti-caspase-4 (4450S), anti-GSDMD (97558S), anti-NF-κB p65 (8242S) and anti-P-NF-κB p65 (3033S) from Cell Signaling Technology (Beverly, MA, USA); another anti-caspase-4 (ab22687) from Abcam (Cambridge, MA, USA); anti-caspase-5 (M060-3) from Medical & Biological Laboratories(Nagoya, Japan); anti-β-actin (A1978) and anti-GAPDH(G9295) from Sigma Aldrich (St Louis, MO, USA).

Bioinformatics analysis

We downloaded the series GSE103119 on the Gene Expression Omnibus (GEO) database, whose microarray platform is GPL10558 (Illumina HumanHT-12 V4.0 expression beadchip). And 20 healthy controls and 80 viral pneumonia samples, including 9 adenovirus pneumonia samples, were used in the present study. Based on the annotation information in the platform, the probes were transformed into the corresponding gene symbols. Then the data were normalized using quantile normalization with the lumi package in R software (Version 4.2.1). Differentially expressed genes (DEGs) were estimated by using an online tool GEO2R (http://www.ncbi.nlm.nih.gov/geo/geo2r) with the following condition: adjusted p-value < 0.05 and the absolute value of $\log_2$fold-change ($\log_2$FC)> 2. We then performed Kyoto Encyclopedia of Genes and Genomes (KEGG) pathway and Gene Ontology (GO) enrichment analysis for genes with these DEGs using Metascape (www.metascape.org), which provides automated meta-analysis tools to reveal common and unique pathways from 40 independent knowledge bases. Gene Set Enrichment Analysis (GSEA) software (Version 4.3.0) was also used to explore the potential biological function difference between the two groups. GSEA was run for the "REACTOME_PYROPTOSIS.v2022.1.Hs.gmt" gene sets. Besides this, the correlations between variables were evaluated by a *Pearson* rank correlation test. The heatmaps and the correlation matrices were plotted by Chiplot (https://www.chiplot.online/), a free online platform for data analysis and visualization.

Clinical specimens and data collection

A total of 28 adenovirus pneumonia pediatric patients were enrolled in the present study. They were diagnosed according to the evidence-based guidelines regarding the diagnosis of pneumonia in children published by the World Health Organization (28). And the evidence of HAdV was confirmed by positive multiplex polymerase chain reaction (PCR) from lower respiratory tract samples. 15 pediatric patients were selected as control subjects, who were verified without recent respiratory infection by clinical characteristics and image manifestations. Severe or non-severe pneumonia was classified on the basis of clinical features detailed as previously reported (29). Peripheral blood and/or bronchoalveolar lavage fluid (BALF) samples, as well as clinical examination data from all the participants, were collected. All the pediatric participants were recruited from Guangzhou Women and Children's Medical Center (Guangzhou, China), and written informed consents were obtained from all the participants' guardians. This study was conducted in accordance with the declaration of Helsinki and approved from the Ethics Committee of the School of Medicine in the South China University of Technology and the Ethics Committee of Guangzhou Women and Children's Medical Center. Detailed clinical characteristics and laboratory information are shown in Table 1.

Cell culture and differentiation

Human THP-1 cells were cultured in RPMI medium supplemented with 10% FBS, 1% penicillin-streptomycin and 1% L-glutamine. And cells were incubated at 37°C in a humidified incubator with 5% CO_2. The THP-1 cells were seeded in 12-well plates (8×10^5 cells/well) or 24-well plates (4×10^5 cells/well), and differentiated with PMA (100 nM) overnight. For mock differentiation, no PMA was used in the procedure.

Cell stimulation and transient transfection

In some cases, differentiated THP-1 (dTHP-1) cells were pretreated with the specific inhibitors, such as C-176 (1μM) and BAY11-7082 (10nM) for 1h before the infection and transfection. According to the manual of Lipofectamine™ 2000, dTHP-1 cells were transiently transfected with specific small interfering RNA against caspase-4 and caspase-5 vs scrambled control siRNA (siNC) or siGSDMD vs siNC. All siRNAs were designed and synthesized by Ruibo Biotechnology (Guangzhou, Guangdong, China). Flagellin transfection was performed according to the manual of DOTAP Liposomal Transfect Reagent (Sigma Aldrich, St. Louis, MO, USA). To stimulate TLR9, its respective ligands CpG DNA (10μg/mL) was added directly into the culture media. To stimulate STING, cGAMP (10μg/mL) was delivered into cytoplasm of dTHP-1 cells by using Lipofectamine™ 2000.

Virus infection and titration

The virus used in this study was the HAdV-3 strain GZ1 (GenBank accession number, DQ099432), generously provided by Dr. Qiwei Zhang at the Institute of Medical Microbiology, Jinan University. HAdV was propagated in A549 cells, with which the virus titers were determined using tissue culture infective dose ($TCID_{50}$) assay. The virus was inoculated into dTHP-1 cells at a multiplicity of infection (MOI) of 100. The infection medium was removed 2h post adsorption and then cultured in fresh RPMI

10.3389/fimmu.2023.1169968

TABLE 1 Summary of clinical features and laboratory results of adenovirus pneumonia pediatric patients.

	Control cases (n=15)	Non-severe cases (n=12)	severe cases (n=16)	P value
Age (years)	4.01 ± 3.12	4.51 ± 2.27	2.81 ± 2.01	
Gender (male/female)	8/7	6/6	6/10	
White blood cell counts (× 10^9/L)	6.83 ± 0.30	9.91 ± 1.14	16.07 ± 1.82	0.017
Neutrophil (%)	44.93 ± 2.70	43.25 ± 4.80	63.01 ± 3.00	0.002
Neutrophil (× 10^9/L)	3.04 ± 0.22	5.14 ± 0.92	9.39 ± 1.44	0.032
Monocytes count (× 10^9/L)	0.39 ± 0.02	0.87 ± 0.16	1.34 ± 0.22	0.122
Lymphocyte count (× 10^9/L)	3.23 ± 0.25	3.16 ± 0.39	4.72 ± 0.65	0.075
Platelet count (× 10^9/L)	304.27 ± 19.87	398.50 ± 28.34	400.07 ± 37.51	0.976
Hemoglobin (g/L)	114.36 ± 8.11	124.00 ± 2.74	115.20 ± 4.91	0.171
Hypersensitive-C-reactive protein (mg/L)	0.45 ± 0.47	17.70 ± 7.36	118.47 ± 22.50	0.007
Procalcitonin (ng/mL)		0.33 ± 0.11	2.45 ± 0.56	0.003
Erythrocyte sedimentation rate (mm/h)		16.80 ± 4.61	34.55 ± 9.24	0.257
PH		7.40 ± 0.02	7.38 ± 0.02	0.573
PaO_2(kPa)		9.83 ± 2.40	8.58 ± 0.62	0.295
$PaCO_2$(kPa)		4.94 ± 0.68	5.54 ± 0.49	0.451
Sodium (mmol/L)		136.23 ± 3.18	135.26 ± 0.79	0.524
Potassium (mmol/L)		3.59 ± 0.41	3.75 ± 0.15	0.550
Lactic acid (mmol/L)		1.51 ± 0.18	2.04 ± 0.23	0.156
Alanine aminotransferase (U/L)		16.00 ± 2.96	21.69 ± 8.78	0.670
Aspartate aminotransferase (U/L)		34.38 ± 3.37	35.88 ± 5.45	0.860
Creatine kinase-MB (U/L)		20.00 ± 2.45	17.38 ± 1.91	0.441
Lactate dehydrogenase (U/L)		231.50 ± 20.63	302.50 ± 20.08	0.033
Creatinine (μmol/L)		33.38 ± 5.78	34.13 ± 4.93	0.930
Total bilirubin (μmol/L)		3.71 ± 0.73	5.42 ± 0.62	0.123
Direct bilirubin (μmol/L)		1.38 ± 0.31	1.82 ± 0.23	0.285
Albumin (g/L)		0.006726994	34.61 ± 1.19	0.007
Prothrombin time (s)		0.025106203	14.39 ± 0.26	0.025
Activated partial thromboplastin time (s)		0.115970773	38.58 ± 1.34	0.116
Fibrinogen (g/L)		0.02422345	5.11 ± 0.45	0.024

medium supplied with 10% FBS. The culture supernatants were sampled at indicated times to assess virus titer using $TCID_{50}$.

Virus binding, entry and replication assay

In the virus binding assay, the dTHP-1 cells were incubated with HAdV (MOI=100) in 4° for 1h as a previous study (30). In the virus entry assay, the dTHP-1 cells were incubated with HAdV (MOI=100) in 37° for 0.5h to allow for virus attachment and internalization. In the virus replication assay, the dTHP-1 cells were incubated with HAdV (MOI=100) in 37° for 2h. The infection medium was removed 2h post adsorption and then cultured in fresh RPMI medium supplied with 10% FBS. The supernatants of cells were discarded, followed by washing with PBS buffer for three times. Total cellular DNA was extracted from the infected cells using Hipure Tissue DNA Mini Kit (Magen, Guangzhou, China). Relative HAdV-3 DNA expression fold was quantified by real-time PCR as a previous study (31). HAdV primer sequence was provided in Supplementary Table 1.

Western blot

Cells were lysed with cell lysis buffer containing 1mM phenylmethylsulfonyl fluoride, 1% protease inhibitor cocktail, 1%

phosphorylase inhibitor cocktail, and 1 mM dithiothreitol (all from Sigma Aldrich, St. Louis, MO, USA). Cell lysate samples were boiled, separated on SDS-PAGE, and then transferred to PVDF membranes. Membranes were blocked with 5% (w/v) nonfat milk and incubated with a primary antibody overnight at 4°C, followed by a second incubation at room temperature for 1-2 h with appropriate HRP-conjugated secondary antibodies. After further washing with PBST, blots on the membranes were visualized with ECL reagent (KeyGEN, Nanjing, China) according to the manufacturer's protocol. Equal protein loading was confirmed in all the experiments by using GAPDH or β-actin as loading control.

Real-time PCR

Total RNA was isolated from cell pellets using TRIzol (Invitrogen, Carlsbad, CA, USA) according to the manufacturer's instruction, and quantitated using a NanoDrop 2000C Spectrophotometers (Thermo Scientific, West Palm Beach, FL, USA). One μg of total RNA was reverse-transcribed to produce cDNA by using the Revert Aid First Strand cDNA synthesis kit (Thermo Fisher Scientific, Waltham, MA, USA). Then the cDNA was amplified using SYBR green master mix (TaKaRa, Mountain View, CA, USA) following the manufacturer's protocol. Quantitative real-time PCR were performed using a Bio-Rad CFX96 Real-Time PCR System. Real-time PCR primers sequences are provided in Supplementary Table 1. Relative expression levels were calculated with the $2^{-\Delta Ct}$ method. Relative mRNA levels were calculated after normalization to the level of β-actin.

Enzyme-linked immunosorbent assay

Secreted IL-1β level in culture supernatants was determined by human IL-1β ELISA kits from Dakewe Biotechnology (Shenzhen, Guangdong, China), according to the manufacturer's instructions.

Propidium iodide staining

The dTHP-1 cells were inoculated on a 24-well plate. Following the treatment, PI staining solution was added to each well (0.3μg/ml). Cells were incubated at room temperature for 10-15 min and then observed under a fluorescence microscope. Three non-overlapping fields were randomly taken and photographed with the inverted fluorescent microscope Leica DMI4000B. The proportion of PI^+ cells was calculated as follows: proportion of PI^+ cells (%) = (number of red fluorescent cells/total cells) × 100%. Two wells were set in each group, and the experiment was repeated three times. The fluorescence images were analyzed and processed using ImageJ software to calculate the relative fluorescence density.

Statistical analysis

Statistical analysis was performed using GraphPad Prism (Version 8.0.2). Differences between the two groups were compared by using Student's t-test. Differences with a p value less than 0.05 were considered statistically significant.

Results

Inflammasome-related genes and signaling pathways were enriched among children hospitalized with viral pneumonia

To unravel the immune regulatory mechanisms of viral pneumonia, we first analyzed changes in the gene transcriptome of whole blood from viral pneumonia pediatric patients and healthy controls by performing the enrichment analysis. The GO and KEGG analysis elucidated numerous statistically enriched biological terms and indicated that the most significantly changed gene enrichment pathways in viral pneumonia pediatric patients were the response to virus (GO:0009615) and the leukocyte activation (GO:0045321). Meanwhile, the pyroptosis (GO: 0070269) and the inflammasome complex pathway (GO: 0061702) were implicated as factors likely to be important for host responses to viral infection (p<0.001) (Figure 1A). The correlation between viral pneumonia and the pyroptosis signaling pathway was further confirmed by GSEA (Figure 1B). Furthermore, heatmaps indicated that the levels of inflammasome-related genes, such as NLRP3, AIM2, caspase-1/4/5, and inflammatory cytokines, including IL-1β/18, IFN-β, and tumor necrosis factor (TNF), were increased in adenovirus pneumonia pediatric patients (Figure 1C). Besides this, volcano plot analysis of adenovirus pneumonia pediatric patients also showed that caspase-4 and caspase-5 were remarkably upregulated compared to healthy controls ($|\log_2 FC|>2$) (Figure 1D). As shown in the heatmap profile, IL-1β and GSDMD indicated positive correlation with caspase-4 and caspase-5 in adenovirus pneumonia pediatric patients, respectively (Figure 1E). Above all, we speculated that noncanonical caspase-4/5 inflammasome may be involved in modulating inflammatory responses during adenovirus pneumonia.

Caspase-4 and caspase-5 expression levels were increased and positively correlated with inflammatory damage

To further verify these findings from transcriptome analysis, we collected clinical samples from adenovirus pneumonia pediatric patients, whose detailed clinical characteristics and laboratory information are shown in Table 1, to measure caspase-4 and caspase-5 expression by real-time PCR. As shown, peripheral blood mononuclear cells (PBMCs) from adenovirus pneumonia pediatric patients and healthy volunteers were enrolled, as well as cells of BALF samples from non-severe and severe pneumonia patients. We found that caspase-4 and caspase-5 mRNA levels significantly upregulated in the PBMCs of pneumonia patients with severe phenotype, while they slightly increased in non-severe patients compared to healthy controls, and increased in BALF of severe cases compared with the non-severe group (Figures 2A, B). Next, *Pearson* correlation matrix

10.3389/fimmu.2023.1169968

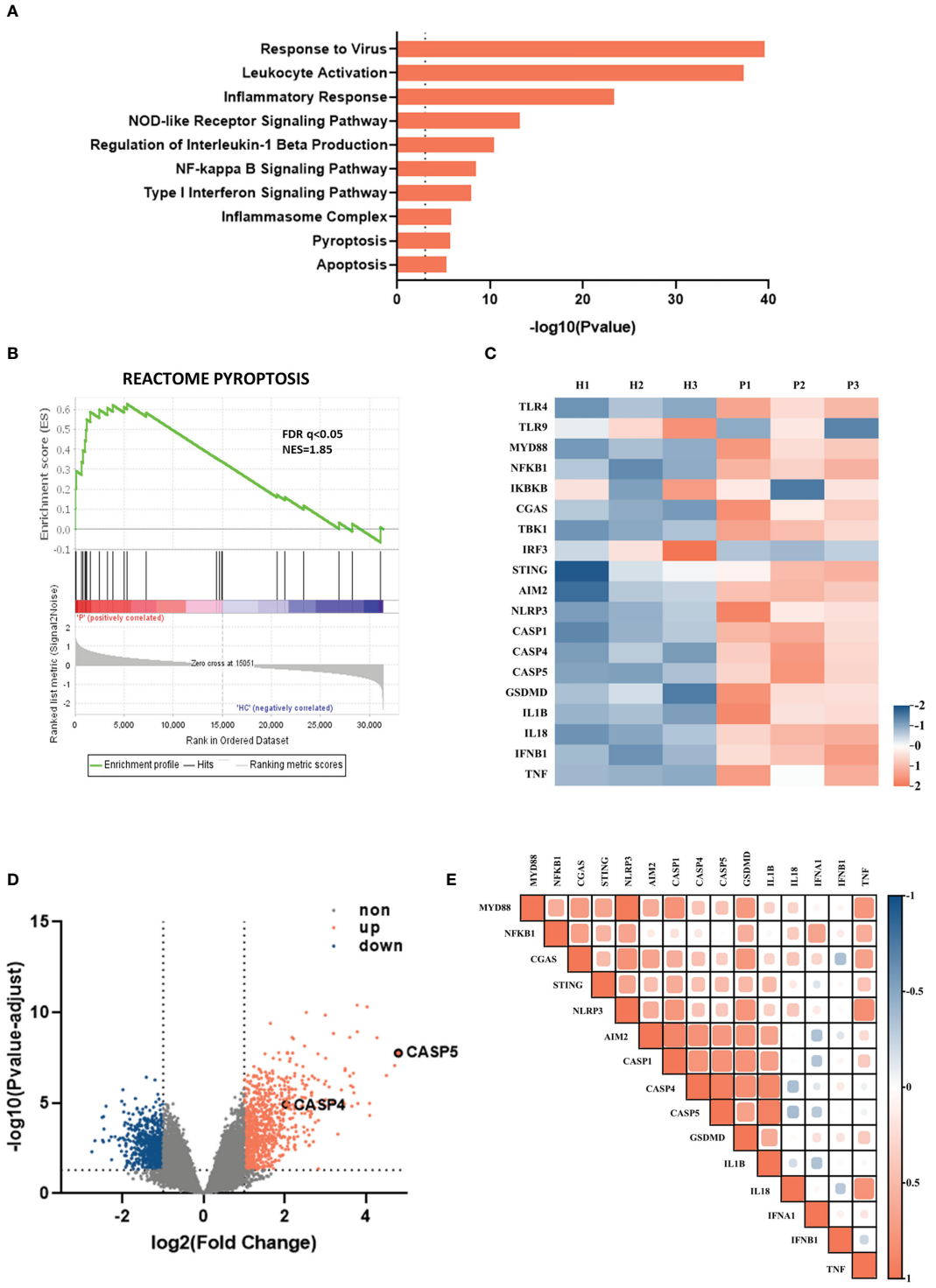

FIGURE 1
Inflammasome-related genes and signaling pathways were enriched among children hospitalized with viral pneumonia. The data, downloaded within the GSE103119 dataset on the GEO database, were normalized using quantile normalization with the lumi package in R. **(A)** Enrichment analysis showing some of significantly enriched signaling pathways in viral pneumonia pediatric patients compared to healthy controls. **(B)** GSEA enrichment plot of the pyroptosis pathway. **(C)** Heatmap depicting the expression profiling of inflammasome-related DEGs in adenovirus pneumonia pediatric patients compare to healthy controls. **(D)** Volcano plot of DEGs in adenovirus pneumonia children and healthy control. **(E)** Heatmap of pairwise correlation of inflammation-related genes expression with caspase-4 and caspase-5.

showed that caspase-4 and caspase-5 levels were positively associated with hypersensitive-C-reactive protein (hsCRP) and lactate dehydrogenase (LDH) concentration in peripheral blood (Figure 2C). As expected, the expression levels of caspase-1/4/5 and IL-1β in PBMCs of pediatric patients were founded to be positively correlated with hsCRP and LDH, respectively (Figures 2D, E).

10.3389/fimmu.2023.1169968

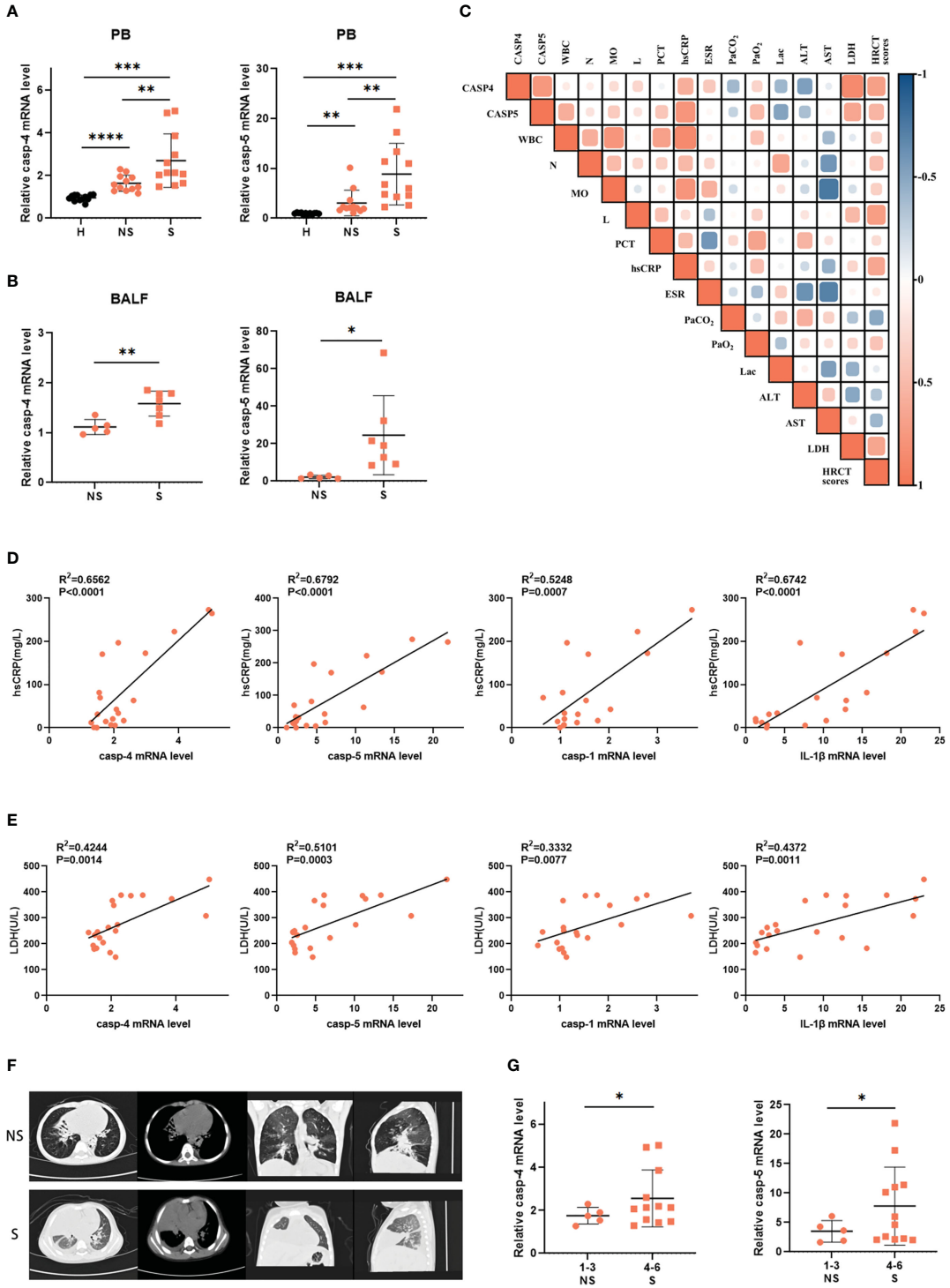

FIGURE 2
Caspase-4 and caspase-5 expression levels were increased and positively correlated with inflammatory damage. **(A)** Expression levels of caspase-4 and caspase-5 in PBMCs isolated from adenovirus pneumonia pediatric patients (12 non-severe vs 12 severe) and healthy volunteers' (n=15) peripheral blood samples or **(B)** in cells isolated from severe (n=7) and non-severe patients (n=5) BALF samples. **(C)** Correlation matrix of caspase-4 and caspase-5 levels of pediatric patients (n=9) and their clinical parameters. **(D, E)** Correlations of indicated clinical inflammatory parameters of pediatric patients (n=20) with inflammation-related genes, respectively. **(F)** The representative lung HRCT images of severe and non-severe adenovirus pneumonia pediatric patients. **(G)** Expression levels of caspase-4/5 in adenovirus pneumonia pediatric patients (n=17) divided into two groups according to the HRCT scores. Data are representative of at least three experiments. Error bars represent the mean ± SEM. *P value<0.05, **P value <0.01, ***P value <0.001, ****P value <0.0001, ns, no significance.

Moreover, we also classified according to the high-resolution computed tomography (HRCT) scores ranging from 1 to 6 as a previous study (32), and divided all patients into two groups to evaluate whether caspase-4/5 expression was correlated with the degree of lung inflammatory damage (Figure 2F). It turned out that expression of caspase-4 and caspase-5 was higher in patients whose HRCT scores were 4-6 than in the 1-3 group (Figure 2G). Taken together, our results showed that caspase-4 and caspase-5 expression was increased in pediatric patients with adenovirus pneumonia and positively correlated with inflammatory damage. Thus, these data highlighted the potential role of noncanonical inflammasome in HAdV-induced inflammatory responses.

HAdV infection induced activation of caspase-4 and caspase-5

Furthermore, we investigated the effects of HAdV infection on expression and activation of caspase-4 and caspase-5 *in vitro*. The dTHP-1 cells were infected with HAdV or transfected with LPS, a positive control inducing noncanonical inflammasome activation. Firstly, increased IFN-β and IL-1β mRNA levels indicated that HAdV successfully infected dTHP-1 cells (Figure 3A). The data also indicated that caspase-4 and caspase-5 mRNA levels were greatly elevated after 4h post-infection (Figure 3A). Western blot data exhibited that HAdV infection induced activation of pro-caspase-1/4/5, as reflected by the appearance of their p20 subunits in a time-dependent manner (Figure 3B). Given caspase-4 and caspase-5 underwent processing, noncanonical inflammasomes seemed to be activated in human macrophages infected with HAdV.

To ascertain the individual roles of noncanonical inflammasomes in HAdV-induced macrophage pyroptosis, we transfected dTHP-1 cells with siRNAs targeting the expression of corresponding caspases or scrambled control siRNA prior to HAdV infection. Compared to the control, caspase-4 and caspase-5 siRNA duplexes effectively suppressed caspase-4 and caspase-5 expression (Figure 3C). And HAdV infection strongly induced the cleavage of GSDMD, which could be attenuated by silencing of caspase-4 and caspase-5 (Figure 3C). We also observed the fraction of PI^+ cells was decreased by silencing of caspase-4 and caspase-5 (Figure 3D). And ELISA data showed that silencing of caspase-4 and caspase-5 decreased secretion of IL-1β, implying that HAdV-induced noncanonical inflammasome activated to promote IL-1β release (Figure 3E). Collectively, caspase-4 and caspase-5 can induce pyroptosis in dTHP-1 cells during HAdV infection.

To identify whether the noncanonical inflammation has any effects on HAdV infection, the supernatants of dTHP-1 cells infected at different timepoints were harvested. The $TCID_{50}$ assay data showed that silencing of caspase-4 and caspase-5 in dTHP-1 cells decreased the virus titer of HAdV when compared to the control group (Figure 3F). As reported, the HAdV life cycle includes five main phases, which are binding, entry, replication, assembly, and release (33, 34). To explore which stage is affected by noncanonical inflammasomes, we constructed HAdV binding and entry models. Real-time PCR data showed that silencing of caspase-4 and caspase-5 did not influence the amount of HAdV bound on the cell surface or entered in the cell (Supplementary Figures 2A, B). Furthermore, intracellular HAdV DNA level in siCASP4+5 vs siNC-transfected and siGSDMD vs siNC-transfected dTHP-1 cells are comparable at different timepoints post-infection (Supplementary Figures 2C, D), indicating that silencing of caspase-4/5 and GSDMD did not affect the HAdV replication. Meanwhile, silencing of GSDMD significantly decreased the HAdV titer in cell culture supernatants compared with the control group (Figure 3G). Based on these results, we speculated that noncanonical caspase-4/5 inflammasome activation and macrophage pyroptosis may promote HAdV release, rather than other virus cycle stages.

NF-κB signal pathway was involved in HAdV infection-induced noncanonical inflammasome activation and macrophage pyroptosis

We next explored the downstream molecules of HAdV infection in modulating caspase-4/5 activation and subsequent macrophage pyroptosis. Given that STING and NF-κB signaling pathway are reported to be involved in inflammasome activation, we used the C-176 (STING inhibitor) or BAY11-7082 (NF-κB inhibitor) to investigate the effects of STING and NF-κB signaling pathways on noncanonical inflammasome activation during HAdV infection. Notably, pyroptosis usually occurred within 12-24h after injury (35, 36), so the duration of infection extended to 12-24h after being pre-treated with indicated inhibitors. Pretreatment of STING inhibitor C-176 dramatically decreased the IFN-β and IL-1β mRNA expression, but slightly reduced NF-κB p65 phosphorylation (Figure 4A and Supplementary Figure 1A). Western blot data showed that C-176 pretreatment also suppressed the cleavages of caspase-1 and GSDMD at indicated times after HAdV infection or LPS transfection (Figure 4B), indicating that inhibition of STING attenuated canonical inflammasome activation and macrophage pyroptosis. Notably, no significant differences in the mRNA and protein levels of caspase-4/5 were observed in the dTHP-1 cells pre-treated with C-176 inhibitor and DMSO, suggesting STING signaling pathway was not involved in noncanonical inflammasome activation during HAdV infection (Figures 4A, B). Real-time PCR data also indicated that mRNA levels of caspase-4 and caspase-5, as well as IFN-β and IL-1β, were downregulated in BAY pre-treated group (Figure 4C). Additionally, western blot further confirmed that BAY pretreatment significantly decreased the expression and cleavage of caspase-4/5, as well as their downstream GSDMD (Figure 4D). To investigate whether NF-κB-mediated caspase-4/5 upregulation *via* TLR9 or STING, dTHP-1 cells were transfected with cGAMP (STING agonist) or stimulated with CpG ODN 2006 (TLR9 agonist). Real-time PCR data showed that CpG ODN 2006 increased the mRNA levels of caspase-4 and caspase-5, while cGAMP had no significant effect on their expression (Supplementary Figures 1B, C). In conclusion, NF-κB, but not STING signaling pathway, may be involved in HAdV-induced noncanonical inflammasome activation and macrophage pyroptosis.

10.3389/fimmu.2023.1169968

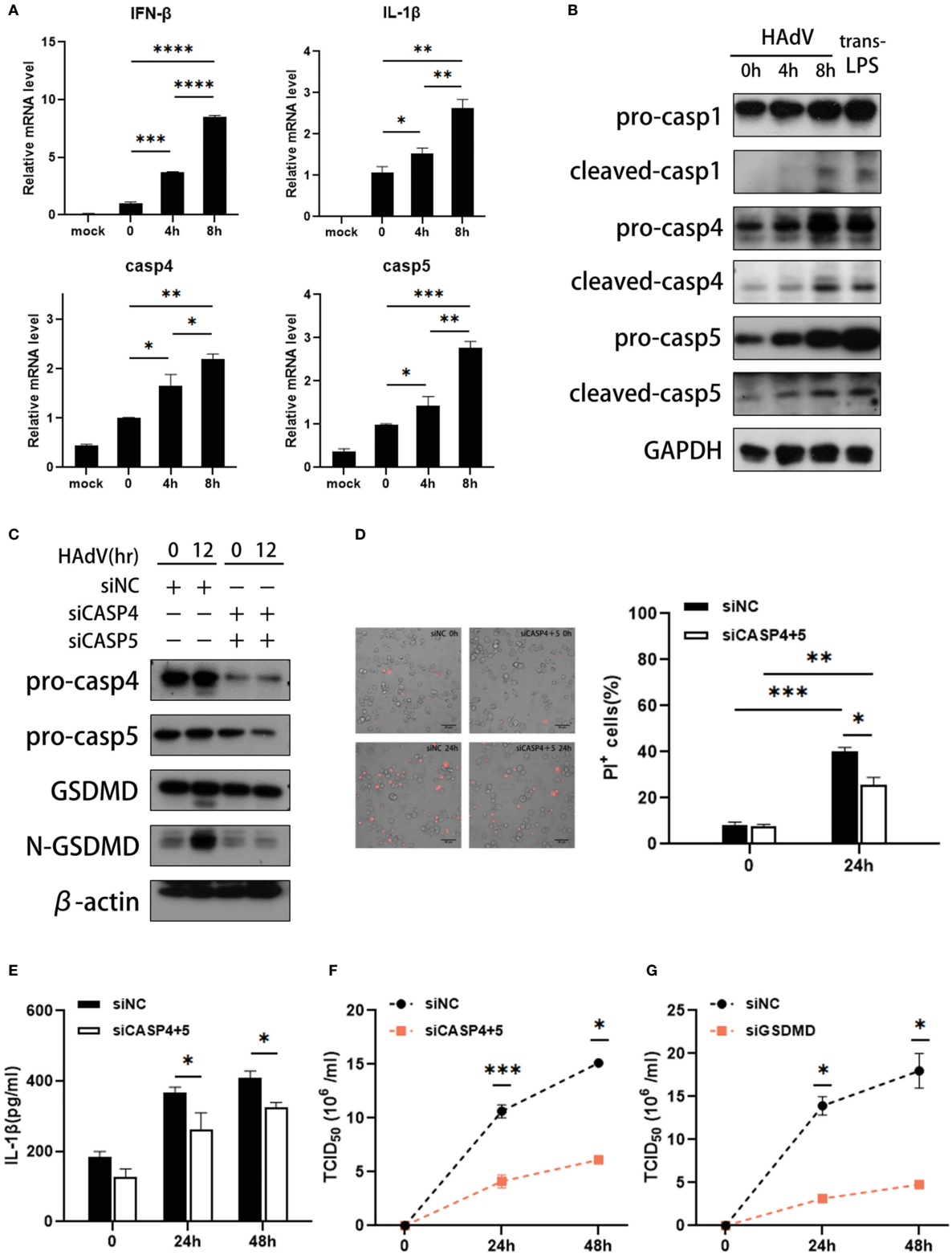

FIGURE 3
HAdV infection induced activation of caspase-4/5. The dTHP-1 cells were infected by HAdV (MOI=100) for indicated times and/or transfected LPS (2.5μg/ml) for 8h. **(A)**The mRNA levels of IFN-β, IL-1β, caspase-4/5 responses to HAdV infection at 0, 4, and 8h were measured by real-time PCR. **(B)** Western blot data showing expression of indicated protein in in dTHP-1 cells infected with HAdV at indicated times. **(C)** Western blot data showing expression of indicated protein in siCASP-4+5-treated dTHP-1 cells infected with HAdV at indicated times. **(D)** Representative images of dead cells stained with PI were observed by fluorescent microscopy (magnification: 20×, scale bar: 100 μm) and quantification of PI^+ cells. **(E)** IL-1β secretion was tested by ELISA at 24h or 48h post-infection. The supernatants of **(F)** siCASP4+5 or **(G)** siGSDMD-treated vs siNC-treated dTHP-1 cells were collected for HAdV titer measured by the $TCID_{50}$. Data are representative of two or three experiments. Error bars represent the mean ± SEM. **P* value<0.05, ***P* value <0.01, ****P* value <0.001, *****P* value <0.0001.

10.3389/fimmu.2023.1169968

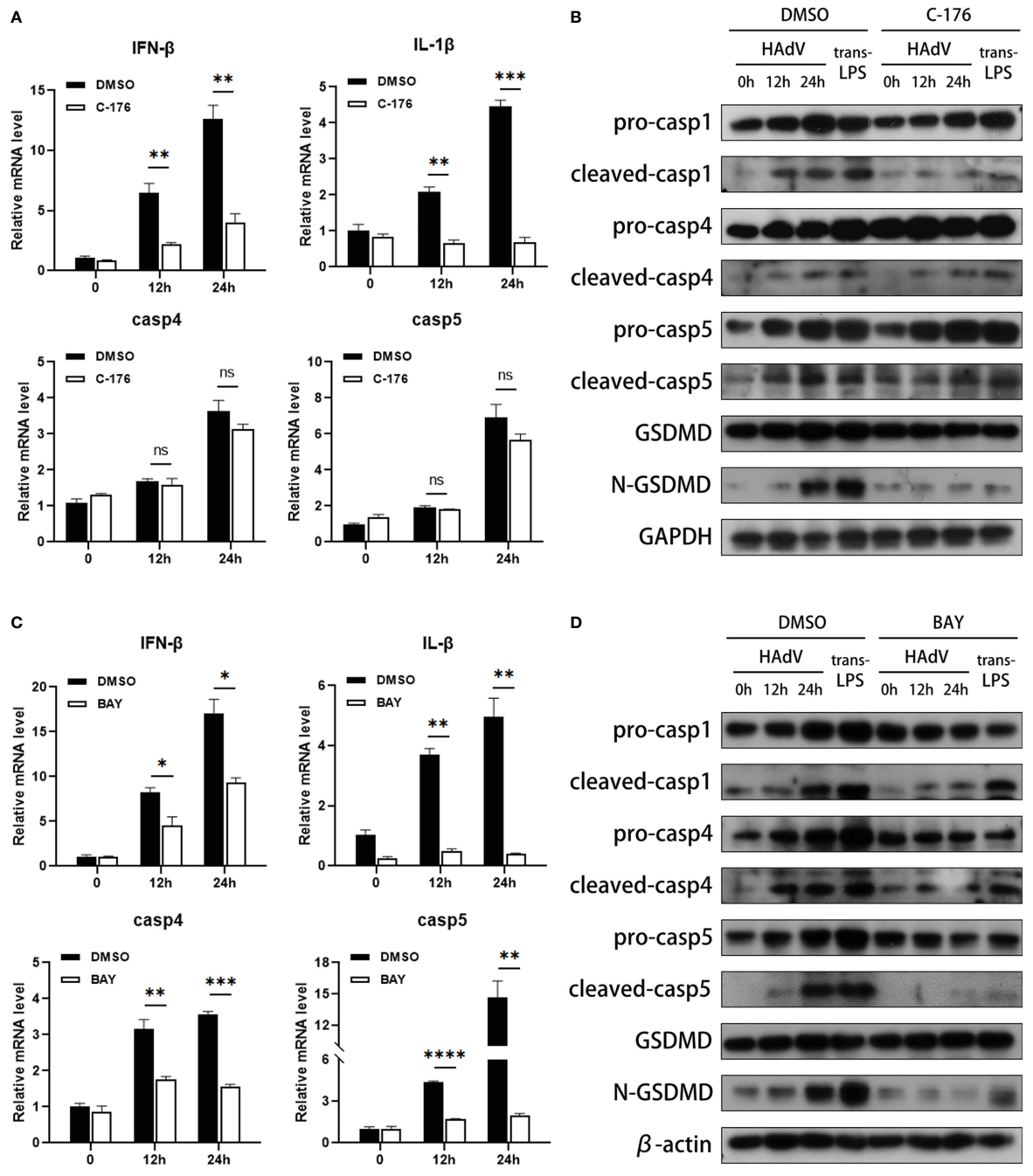

FIGURE 4
NF-κB was involved in noncanonical inflammasome activation and macrophage pyroptosis. The dTHP-1 cells pre-treated by either **(A, B)** C-176 (1μM) or **(C, D)** BAY11-7082 (10nM) vs vehicle control (DMSO) were infected with HAdV (MOI=100) for the indicated times or transfected with LPS (2.5μg/ml) for 8h. **(A, C)** The mRNA levels of IFN-β, IL-1β, and caspase-4/5 were measured by real-time PCR. **(B, D)** Protein levels of indicated molecular in cell lysates were tested by western blot. Data are representative of at least three experiments. Error bars represent the mean ± SEM. *P value<0.05, **P value <0.01, ***P value <0.001, ****P value <0.0001, ns, no significance.

Discussion

Clinical observations have suggested that disease severity and outcomes of HAdV infection are closely associated with release of proinflammatory cytokines (37). Inflammasome-mediated inflammatory responses have been implicated in various microbial infections. However, only canonical inflammasomes, such as NLRP3 and AIM2 inflammasome, have been reported to be activated during HAdV infection (11–14). Here, we utilized wild-type HAdV-3 for the first time, which is one of the most common types causing severe adenovirus pneumonia in children, to investigate whether HAdV infection induces noncanonical inflammasome activation.

We mined available data on GEO database and found that expression of caspase-4 and caspase-5 was elevated in adenovirus pneumonia pediatric patients. Similarly, caspase-4 and caspase-5

expression levels were increased in the cells isolated from peripheral blood plasma and BALF, which collected from adenovirus pneumonia pediatric patients, and positively correlated with the severity of adenovirus pneumonia. HAdV exhibits species-restricted phenotypes, making studying disease progress in animal models particularly problematic (38). Thus, the mechanism and function of noncanonical inflammasomes during HAdV infection were investigated by *in vitro* cell model. Since macrophage is the major immune cell type for inflammasome activation, we stimulated human monocyte cell line THP-1 with PMA, to differentiate them into macrophages (dTHP-1) as previously reported (10–12). In our study, cell experiments identified the intracellular activation of caspase-4 and caspase-5 induced by HAdV infection. Furthermore, treatment with the caspase-4 and caspase-5 siRNAs attenuated HAdV-induced cleavage of GSDMD, confirming that HAdV infection induced macrophage pyroptosis by activating noncanonical inflammasomes.

Pyroptosis is a key function of canonical and noncanonical inflammasomes and usually plays essential roles in eliminating pathogenic infections (39). However, it is still unclear what influences noncanonical inflammasomes have on virus infection. It is reported that caspase-1 silencing enhances chikungunya virus (CHIKV) replication but severely impairs epstein-barr virus (EBV) replication (40, 41). Moreover, other studies find that the absence of canonical and noncanonical inflammasomes has no effect on replication of some viruses (18, 19, 40). The HAdV life cycle includes binding, entry, replication, assembly, and release (33, 34). We found that silencing of caspase-4 and caspase-5 did not affect the HAdV binding, entry, and replication. Meanwhile, silencing of caspase-4/5 and GSDMD in dTHP-1 cells decreased the virus titer of HAdV in cell culture supernatants, respectively. When viral particles are produced and accumulated in the infected cells, canonical and noncanonical inflammasome-induced macrophage pyroptosis will facilitate the viral progeny release (42). In this regard, we speculated that silencing of caspase-4 and caspase-5 suppressed noncanonical inflammasome-induced macrophage pyroptosis, and therefore impeded HAdV release. The effects of noncanonical inflammasomes-mediated pyroptosis have on virus load, inflammatory responses and lung injury would be better to be further investigated *in vivo* once HAdV-infected animal model has been validated.

We next explored the downstream molecules of HAdV infection in modulating caspase-4/5-mediated macrophage pyroptosis. In order to investigate if STING and NF-κB signaling pathway regulate noncanonical inflammasomes activation during HAdV infection, we pretreated dTHP-1 cells with NF-κB inhibitor before infected or transfected. Our results showed that cleavages of caspase-1 and GSDMD were suppressed in STING inhibitor group, confirming that STING signaling pathway was involved in canonical inflammasome activation. But STING inhibitor had no effect on caspase-4 and caspase-5 expression and cleavages, implying that STING signaling pathway was not involved in noncanonical inflammasome activation. We also found that NF-κB inhibitor suppressed HAdV-induced caspase-4 and caspase-5 expression, as well as decreased the cleavages of caspase-4/5 and downstream GSDMD. It is reported that during HAdV infection, both TLR9 and STING can recognize viral DNA and induce NF-κB activation (11, 12, 14). Whereas our *in vitro* data showed that activation of TLR9, but not STING, by using their specific agonists enhanced caspase-4 and caspase-5 expression. Therefore, we speculated that HAdV infection induced caspase-4/5 expression mainly *via* TLR9, rather than STING. Taken together, our current findings indicated that NF-κB, but not STING signaling pathway, may be involved in HAdV-induced noncanonical inflammasome activation and thereafter macrophage pyroptosis.

Canonical and noncanonical inflammasome both can trigger corresponding caspase activation to induce pyroptosis. In this regard, they act independently and in parallel to each other. Notably, they work in concert to protect the host against intracellular pathogens, but the interaction remains unclear. It is reported that activated noncanonical caspases, including caspase-4/5/11, can induce K^+ efflux and then activate canonical NLRP3 inflammasome in some cases (43). And canonical inflammasomes can also act upstream of noncanonical inflammasomes in the host. As another study has reported, caspase-1 induces production of IL-18, which then triggers IFN-γ to prime caspase-11-mediated inflammatory responses during *B. thailandensis* infection (44). In addition, Akhter et al. found that caspase-11 was dispensable for caspase-1 activation in response to *Legionella, Salmonella, Francisella* and *Listeria* (45). Given that more attention has focused on individual impacts that noncanonical inflammasomes have, their interactive and collaborative contributions between canonical and noncanonical inflammasomes were less studied in our present study. Further studies on whether and how they cooperate to defend against HAdV are needed in the future.

In conclusion, our study provided evidence for the first time that HAdV infection induced caspase-4 and caspase-5 activation and thereafter macrophages pyroptosis. And silencing of caspase-4 and caspase-5 in dTHP-1 cells dramatically decreased the HAdV titer in cell supernatants, by influencing virus release. These findings explore new perspectives on the pathogenesis of HAdV-induced inflammatory damage. Moreover, expression of caspase-4 and caspase-5 were increased in pediatric patients with adenovirus pneumonia and positively correlated with severity and other clinical inflammatory parameters. Thus, high expression levels of caspase-4 and caspase-5 may be a biomarker for predicting the severity of adenovirus pneumonia.

Data availability statement

The original contributions presented in the study are included in the article/Supplementary Material. Further inquiries can be directed to the corresponding authors.

Ethics statement

The studies involving human participants were reviewed and approved by the Ethics Committee of the School of Medicine in the South China University of Technology the Ethics Committee of Guangzhou Women and Children's Medical Center. Written

informed consent to participate in this study was provided by the participants' legal guardian/next of kin.

Author contributions

LL, CC and JZ performed the experiments and bioinformatics analyses. HF and XX collected specimens and clinical data of pediatric patients and classified them with HRCT score. GL and DY performed bronchoscopy with BAL. CC, MW, and HF conceived the study. LL and CC drafted the manuscript. GL and MW performed critical revision. All authors contributed to the article and approved the submitted version.

Funding

This study was supported by the Natural Science Foundation of Guangdong Province, China (Grant No. 2021A151510116).

Acknowledgments

We acknowledge the GEO database for providing their platforms and contributors for uploading meaningful datasets. And we thank Dr. Qiwei Zhang at the Institute of Medical Microbiology in Jinan University for generously providing the HAdV-3 strain GZ1.

Conflict of interest

The authors declare that the research was conducted in the absence of any commercial or financial relationships that could be construed as a potential conflict of interest.

Publisher's note

Supplementary material

The Supplementary Material for this article can be found online at: https://www.frontiersin.org/articles/10.3389/fimmu.2023.1169968/full#supplementary-material

References

1. Chen Y, Lin T, Wang CB, Liang WL, Lian GW, Zanin M, et al. Human adenovirus (HAdV) infection in children with acute respiratory tract infections in guangzhou, China, 2010-2021: a molecular epidemiology study. *World J Pediatr* (2022) 18(8):545–52. doi: 10.1007/s12519-022-00590-w

2. Xu D, Chen L, Wu X, Ji L. Molecular typing and epidemiology profiles of human adenovirus infection among hospitalized patients with severe acute respiratory infection in huzhou, China. *PloS One* (2022) 17(4):e0265987. doi: 10.1371/journal.pone.0265987

3. Lai CY, Lee CJ, Lu CY, Lee PI, Shao PL, Wu ET, et al. Adenovirus serotype 3 and 7 infection with acute respiratory failure in children in Taiwan, 2010-2011. *PloS One* (2013) 8(1):e53614. doi: 10.1371/journal.pone.0053614

4. Cho CT, Hiatt WO, Behbehani AM. Pneumonia and massive pleural effusion associated with adenovirus type 7. *Am J Dis Child.* (1973) 126(1):92–4. doi: 10.1001/archpedi.1973.02110190080017

5. Hung KH, Lin LH. Adenovirus pneumonia complicated with acute respiratory distress syndrome: a case report. *Med (Baltimore).* (2015) 94(20):e776. doi: 10.1097/MD.0000000000000776

6. Treacy A, Carr MJ, Dunford L, Palacios G, Cannon GA, O'Grady A, et al. First report of sudden death due to myocarditis caused by adenovirus serotype 3. *J Clin Microbiol* (2010) 48(2):642–5. doi: 10.1128/JCM.00815-09

7. Lee J, Choi EH, Lee HJ. Comprehensive serotyping and epidemiology of human adenovirus isolated from the respiratory tract of Korean children over 17 consecutive years (1991-2007). *J Med Virol* (2010) 82(4):624–31. doi: 10.1002/jmv.21701

8. Schroder K, Tschopp J. The inflammasomes. *Cell.* (2010) 140(6):821–32. doi: 10.1016/j.cell.2010.01.040

9. Downs KP, Nguyen H, Dorfleutner A, Stehlik C. An overview of the non-canonical inflammasome. *Mol Aspects Med* (2020) 76:100924. doi: 10.1016/j.mam.2020.100924

10. Muruve DA, Petrilli V, Zaiss AK, White LR, Clark SA, Ross PJ, et al. The inflammasome recognizes cytosolic microbial and host DNA and triggers an innate immune response. *Nature.* (2008) 452(7183):103–7. doi: 10.1038/nature06664

11. Barlan AU, Griffin TM, McGuire KA, Wiethoff CM. Adenovirus membrane penetration activates the NLRP3 inflammasome. *J Virol* (2011) 85(1):146–55. doi: 10.1128/JVI.01265-10

12. Labzin LI, Bottermann M, Rodriguez-Silvestre P, Foss S, Andersen JT, Vaysburd M, et al. Antibody and DNA sensing pathways converge to activate the inflammasome during primary human macrophage infection. *EMBO J* (2019) 38(21):e101365. doi: 10.15252/embj.2018101365

13. Lee BH, Hwang DM, Palaniyar N, Grinstein S, Philpott DJ, Hu J. Activation of P2X (7) receptor by ATP plays an important role in regulating inflammatory responses during acute viral infection. *PloS One* (2012) 7(4):e35812. doi: 10.1371/journal.pone.0035812

14. Eichholz K, Bru T, Tran TT, Fernandes P, Welles H, Mennechet FJ, et al. Immune-complexed adenovirus induce AIM2-mediated pyroptosis in human dendritic cells. *PloS Pathog* (2016) 12(9):e1005871. doi: 10.1371/journal.ppat.1005871

15. Kayagaki N, Wong MT, Stowe IB, Ramani SR, Gonzalez LC, Akashi-Takamura S, et al. Noncanonical inflammasome activation by intracellular LPS independent of TLR4. *Science.* (2013) 341(6151):1246–9. doi: 10.1126/science.1240248

16. Hagar JA, Powell DA, Aachoui Y, Ernst RK, Miao EA. Cytoplasmic LPS activates caspase-11: implications in TLR4-independent endotoxic shock. *Science.* (2013) 341(6151):1250–3. doi: 10.1126/science.1240988

17. Shi J, Zhao Y, Wang Y, Gao W, Ding J, Li P, et al. Inflammatory caspases are innate immune receptors for intracellular LPS. *Nature.* (2014) 514(7521):187–92. doi: 10.1038/nature13683

18. Eltobgy MM, Zani A, Kenney AD, Estfanous S, Kim E, Badr A, et al. Caspase-4/11 exacerbates disease severity in SARS-CoV-2 infection by promoting inflammation and immunothrombosis. *Proc Natl Acad Sci U S A.* (2022) 119(21):e2202012119. doi: 10.1073/pnas.2202012119

19. Cieniewicz B, Dong Q, Li G, Forrest JC, Mounce BC, Tarakanova VL, et al. Murine gammaherpesvirus 68 pathogenesis is independent of caspase-1 and caspase-11 in mice and impairs interleukin-1beta production upon extrinsic stimulation in culture. *J Virol* (2015) 89(13):6562–74. doi: 10.1128/JVI.00658-15

20. Yu Y, Shi H, Yu Y, Liu M, Li M, Liu X, et al. Inhibition of calpain alleviates coxsackievirus B3-induced myocarditis through suppressing the canonical NLRP3 inflammasome/caspase-1-mediated and noncanonical caspase-11-mediated pyroptosis pathways. *Am J Transl Res* (2020) 12(5):1954–64.

21. Segovia J, Sabbah A, Mgbemena V, Tsai SY, Chang TH, Berton MT, et al. TLR2/MyD88/NF-kappaB pathway, reactive oxygen species, potassium efflux activates NLRP3/ASC inflammasome during respiratory syncytial virus infection. *PloS One* (2012) 7(1):e29695. doi: 10.1371/journal.pone.0029695

22. Du SH, Qiao DF, Chen CX, Chen S, Liu C, Lin Z, et al. Toll-like receptor 4 mediates methamphetamine-induced neuroinflammation through caspase-11 signaling pathway in astrocytes. *Front Mol Neurosci* (2017) 10(1662-5099(1662-5099 (Print):409. doi: 10.3389/fnmol.2017.00409

23. Tian J, An X, Niu L. Correlation between NF-kappaB signal pathway-mediated caspase-4 activation and Kawasaki disease. *Exp Ther Med* (2017) 13(6):3333–6. doi: 10.3892/etm.2017.4409

24. Hopfner KP, Hornung V. Molecular mechanisms and cellular functions of cGAS-STING signalling. *Nat Rev Mol Cell Biol* (2020) 21(9):501–21. doi: 10.1038/s41580-020-0244-x

25. Wu J, Sun L, Chen X, Du F, Shi H, Chen C, et al. Cyclic GMP-AMP is an endogenous second messenger in innate immune signaling by cytosolic DNA. *Science.* (2013) 339(6121):826–30. doi: 10.1126/science.1229963

26. Sun L, Wu J, Du F, Chen X, Chen ZJ. Cyclic GMP-AMP synthase is a cytosolic DNA sensor that activates the type I interferon pathway. *Science.* (2013) 339 (6121):786–91. doi: 10.1126/science.1232458

27. Webster SJ, Brode S, Ellis L, Fitzmaurice TJ, Elder MJ, Gekara NO, et al. Detection of a microbial metabolite by STING regulates inflammasome activation in response to chlamydia trachomatis infection. *PloS Pathog* (2017) 13(6):e1006383. doi: 10.1371/journal.ppat.1006383

28. Li MY, Kelly J, Subhi R, Were W, Duke T. Global use of the WHO pocket book of hospital care for children. *Paediatr Int Child Health* (2013) 33(1):4–17. doi: 10.1179/2046905512Y.0000000017

29. Bradley JS, Byington CL, Shah SS, Alverson B, Carter ER, Harrison C, et al. The management of community-acquired pneumonia in infants and children older than 3 months of age: clinical practice guidelines by the pediatric infectious diseases society and the infectious diseases society of America. *Clin Infect Dis* (2011) 53(7):e25–76. doi: 10.1093/cid/cir531

30. Ma X, Luo X, Zhou S, Huang Y, Chen C, Huang C, et al. Hydroxycarboxylic acid receptor 2 is a zika virus restriction factor that can be induced by zika virus infection through the IRE1-XBP1 pathway. *Front Cell Infect Microbiol* (2019) 9(2235-2988(2235-2988 (Electronic):480. doi: 10.3389/fcimb.2019.00480

31. Fu Y, Tang Z, Ye Z, Mo S, Tian X, Ni K, et al. Human adenovirus type 7 infection causes a more severe disease than type 3. *BMC Infect Dis* (2019) 19(1):36. doi: 10.1186/s12879-018-3651-2

32. Lu B, Liu M, Wang J, Fan H, Yang D, Zhang L, et al. IL-17 production by tissue-resident MAIT cells is locally induced in children with pneumonia. *Mucosal Immunol* (2020) 13(5):824–35. doi: 10.1038/s41385-020-0273-y

33. Greber UF, Flatt JW. Adenovirus entry: From infection to immunity. *Annu Rev Virol* (2019) 6(1):177–97. doi: 10.1146/annurev-virology-092818-015550

34. Pied N, Wodrich H. Imaging the adenovirus infection cycle. *FEBS Lett* (2019) 593(24):3419–48. doi: 10.1002/1873-3468.13690

35. Fu L, Zhang DX, Zhang LM, Song YC, Liu FH, Li Y, et al. Exogenous carbon monoxide protects against mitochondrial DNA–induced hippocampal pyroptosis in a model of hemorrhagic shock and resuscitation. *Int J Mol Med* (2020) 45(4):1176–86. doi: 10.3892/ijmm.2020.4493

36. Zhang LM, Zhang DX, Fu L, Li Y, Wang XP, Qi MM, et al. Carbon monoxide-releasing molecule-3 protects against cortical pyroptosis induced by hemorrhagic shock and resuscitation via mitochondrial regulation. *Free Radic Biol Med* (2019) 141(1873-4596(1873-4596 (Electronic):299–309. doi: 10.1016/j.freeradbiomed.2019.06.031

37. Li J, Wei J, Xu Z, Jiang C, Li M, Chen J, et al. Cytokine/Chemokine expression is closely associated disease severity of human adenovirus infections in immunocompetent adults and predicts disease progression. *Front Immunol* (2021) 12(1664-3224(1664-3224 (Electronic):691879. doi: 10.3389/fimmu.2021.691879

38. Atasheva S, Yao J, Shayakhmetov DM. Innate immunity to adenovirus: lessons from mice. *FEBS Lett* (2019) 593(24):3461–83. doi: 10.1002/1873-3468.13696

39. Man SM, Karki R, Kanneganti TD. Molecular mechanisms and functions of pyroptosis, inflammatory caspases and inflammasomes in infectious diseases. *Immunol Rev* (2017) 277(1):61–75. doi: 10.1111/imr.12534

40. Ekchariyawat P, Hamel R, Bernard E, Wichit S, Surasombatpattana P, Talignani L, et al. Inflammasome signaling pathways exert antiviral effect against chikungunya virus in human dermal fibroblasts. *Infect Genet Evol* (2015) 32(1567-7257(1567-7257 (Electronic):401–8. doi: 10.1016/j.meegid.2015.03.025

41. Gastaldello S, Chen X, Callegari S, Masucci MG. Caspase-1 promotes Epstein-Barr virus replication by targeting the large tegument protein deneddylase to the nucleus of productively infected cells. *PloS Pathog* (2013) 9(10):e1003664. doi: 10.1371/journal.ppat.1003664

42. Verdonck S, Nemegeer J, Vandenabeele P, Maelfait J. Viral manipulation of host cell necroptosis and pyroptosis. *Trends Microbiol* (2022) 30(6):593–605. doi: 10.1016/j.tim.2021.11.011

43. Huang Y, Xu W, Zhou R. NLRP3 inflammasome activation and cell death. *Cell Mol Immunol* (2021) 18(9):2114–27. doi: 10.1038/s41423-021-00740-6

44. Aachoui Y, Kajiwara Y, Leaf IA, Mao D, Ting JP, Coers J, et al. Canonical inflammasomes drive IFN-gamma to prime caspase-11 in defense against a cytosol-invasive bacterium. *Cell Host Microbe* (2015) 18(3):320–32. doi: 10.1016/j.chom.2015.07.016

45. Akhter A, Caution K, Abu Khweek A, Tazi M, Abdulrahman BA, Abdelaziz DH, et al. Caspase-11 promotes the fusion of phagosomes harboring pathogenic bacteria with lysosomes by modulating actin polymerization. *Immunity.* (2012) 37(1):35–47. doi: 10.1016/j.immuni.2012.05.001

frontiers | Frontiers in Medicine

TYPE Original Research
PUBLISHED 24 May 2023
DOI 10.3389/fmed.2023.1176427

OPEN ACCESS

EDITED BY
Carmine Selleri,
University of Salerno, Italy

REVIEWED BY
Georgia Damoraki,
National and Kapodistrian University of Athens, Greece
Valentina Giudice,
University of Salerno, Italy

*CORRESPONDENCE
Chrysanthi Skevaki
✉ Chrysanthi.Skevaki@uk-gm.de
Elisabeth K. M. Mack
✉ elisabeth.mack@staff.uni-marburg.de

†These authors share first authorship

‡These authors share last authorship

RECEIVED 28 February 2023
ACCEPTED 24 April 2023
PUBLISHED 24 May 2023

CITATION
Völkel S, Tarawneh TS, Sacher L, Bhagwat AM, Karim I, Mack HID, Wiesmann T, Beutel B, Hoyer J, Keller C, Renz H, Burchert A, Neubauer A, Graumann J, Skevaki C and Mack EKM (2023) Serum proteomics hint at an early T-cell response and modulation of SARS-CoV-2-related pathogenic pathways in COVID-19-ARDS treated with Ruxolitinib. *Front. Med.* 10:1176427. doi: 10.3389/fmed.2023.1176427

Serum proteomics hint at an early T-cell response and modulation of SARS-CoV-2-related pathogenic pathways in COVID-19-ARDS treated with Ruxolitinib

Sara Völkel[1†], Thomas S. Tarawneh[2†], Laura Sacher[1], Aditya M. Bhagwat[3], Ihab Karim[2], Hildegard I. D. Mack[4], Thomas Wiesmann[5,6], Björn Beutel[7,8], Joachim Hoyer[9], Christian Keller[10], Harald Renz[1,8], Andreas Burchert[2], Andreas Neubauer[2], Johannes Graumann[3,11], Chrysanthi Skevaki[1,8*‡] and Elisabeth K. M. Mack[2*‡]

[1]Institute of Laboratory Medicine, Philipps-University Marburg, Marburg, Germany, [2]Department of Hematology, Oncology and Immunology, University Hospital Gießen and Marburg, Philipps-University Marburg, Marburg, Germany, [3]Institute of Translational Proteomics, Philipps-University Marburg, Marburg, Germany, [4]Institute for Biomedical Aging Research, Leopold-Franzens-Universität Innsbruck, Innsbruck, Austria, [5]Department of Anesthesiology and Intensive Care Medicine, University Hospital Gießen and Marburg, Philipps-University Marburg, Marburg, Germany, [6]Department of Anesthesiology, Intensive Care Medicine and Pain Therapy, Diakonie-Klinikum Schwäbisch Hall, Schwäbisch Hall, Germany, [7]Department of Pulmonary and Critical Care Medicine, University Hospital Gießen and Marburg, Philipps-University Marburg, Marburg, Germany, [8]German Center for Lung Research (DZL), Member of the Universities of Gießen and Marburg Lung Center, Gießen, Germany, [9]Department of Nephrology, University Hospital Gießen and Marburg, Philipps-University Marburg, Marburg, Germany, [10]Institute of Virology, Philipps-University Marburg, Marburg, Germany, [11]Biomolecular Mass Spectrometry, Max Planck Institute for Heart and Lung Research, Bad Nauheim, Germany

Background: Acute respiratory distress syndrome (ARDS) in corona virus disease 19 (COVID-19) is triggered by hyperinflammation, thus providing a rationale for immunosuppressive treatments. The Janus kinase inhibitor Ruxolitinib (Ruxo) has shown efficacy in severe and critical COVID-19. In this study, we hypothesized that Ruxo's mode of action in this condition is reflected by changes in the peripheral blood proteome.

Methods: This study included 11 COVID-19 patients, who were treated at our center's Intensive Care Unit (ICU). All patients received standard-of-care treatment and n = 8 patients with ARDS received Ruxo in addition. Blood samples were collected before (day 0) and on days 1, 6, and 10 of Ruxo treatment or, respectively, ICU admission. Serum proteomes were analyzed by mass spectrometry (MS) and cytometric bead array.

Results: Linear modeling of MS data yielded 27 significantly differentially regulated proteins on day 1, 69 on day 6 and 72 on day 10. Only five factors (IGLV10-54, PSMB1, PGLYRP1, APOA5, WARS1) were regulated both concordantly and significantly over time. Overrepresentation analysis revealed biological processes involving T-cells only on day 1, while a humoral immune response and complement activation were detected at day 6 and day 10. Pathway enrichment

analysis identified the *NRF2-pathway* early under Ruxo treatment and *Network map of SARS-CoV-2 signaling* and *Statin inhibition of cholesterol production* at later time points.

Conclusion: Our results indicate that the mechanism of action of Ruxo in COVID-19-ARDS can be related to both known effects of this drug as a modulator of T-cells and the SARS-CoV-2-infection.

KEYWORDS

acute respiratory distress syndrome, COVID-19, proteomics, Ruxolitinib, SARS-CoV-2

1. Introduction

Severe acute respiratory syndrome corona virus 2 (SARS-CoV-2) was first described as the cause of severe pneumonia in Wuhan, China in December 2019 (1). The clinical presentation of corona virus disease 19 (COVID-19) is highly heterogenous ranging from asymptomatic courses to flu-like symptoms and all the way to lethal pneumonia with acute respiratory distress syndrome (ARDS) (2–4). Due to the rapid spread of the COVID-19 pandemic (5), treatment initially relied on repurposing of already available drugs (6) and standard-of-care management for ARDS including mechanical ventilation and other organ replacement therapies. ARDS associated with SARS-CoV-2 infection is characterized by clinical symptoms and laboratory findings that are consistent with a massive cytokine release syndrome, such as increased plasma levels of proinflammatory cytokines and altered lymphocyte subsets (2, 3). No new medication has been developed specifically for critical SARS-CoV-2 pneumonia (7–12), but based on the understanding of the pathophysiology of ARDS in COVID-19, several immunosuppressive strategies emerge as rational treatment approaches. Indeed, corticosteroids (13), Janus kinase (JAK) inhibitors that block cytokine signaling pathways such as Ruxolitinib (Ruxo) (14–21) or Baricitinib (22–25), the IL-6 antibody Tocilizumab (26–28) or the IL-1 receptor antagonist Anakinra (29, 30) were found to improve outcome in hospitalized COVID-19 patients. Intriguingly, the JAK1/2 inhibitor Baricitinib, which also targets the kinase AAK1, a regulator of endocytosis of the SARS-CoV-2 receptor ACE2, had been predicted as a promising treatment for COVID-19 by artificial intelligence algorithms as early as February 2020 (31).

At the University Hospital Marburg, following the successful individual treatment of a single patient (32), we conducted a non-randomized phase-II trial of the JAK1/2-Inhibitor Ruxolitinib in critically ill COVID-19 patients requiring mechanical ventilation (20). Ruxo was first approved for the treatment of myeloproliferative disorders (33), in which an activating mutation of JAK2 (V617F) is a common genomic finding (34). JAK2 is an intracellular tyrosine kinase that transduces signals from cytokine receptors, which in turn activate proliferative signaling cascades such as the MAP-kinase- or the PI3K/AKT-pathway (35). Beyond its antiproliferative impact on the cellular level, Ruxo also exerts immunosuppressive effects due to the integral function of JAK2 and its paralog JAK1 in cytokine networks, which are exploited clinically for the treatment of *graft-versus-host disease* (GvHD) following allogenic hematopoietic stem cell transplantation (36, 37). In this context, Ruxo not only acts via suppression of T-lymphocytes, but also of neutrophil granulocytes, which are major inducers of tissue damage in GvHD. In COVID-19, quantitative changes in neutrophils and monocytes have also been observed among patients with severe and moderate courses (38) as well as under treatment with Baricitinib (24). Moreover, inflammatory reactions in both GvHD and COVID-19 are at least partially mediated by the same cytokines, which include both proinflammatory mediators such as IL-6 or TNFα, and anti-inflammatory components such as IL-10 or TGFβ (39–41). In this study, we hypothesized that Ruxo's mode of action in COVID-19-associated ARDS is reflected by changes in the peripheral blood proteome. To investigate this hypothesis, we applied mass spectrometry-based (MS) quantitative proteomics and cytometric bead array (CBA) analyses on serum samples from critically ill COVID-19 patients under treatment with Ruxo.

2. Materials and methods

2.1. Patients and samples

This study included 11 adult patients (age $\geq$ 18 years) with severe to critical COVID-19, who were treated at an Intensive Care Unit of the University Hospital Marburg between April 2020 and January 2022. All patients had not been vaccinated against SARS-CoV-2. SARS-CoV-2 infection was confirmed by polymerase chain reaction as described (20), yet, determination of SARS-CoV-2 variants was not included in the diagnostic routine. All patients were treated according to the current standard of care at the time of hospitalization. Eight patients were treated with Ruxo either on an individual basis or on a clinical trial (20). Informed consent to obtain and analyze samples for research purposes was obtained from all patients. Serum samples were stored at −80°C.

2.2. Serum proteomics

Samples were prepared for proteomic analysis by in gel digest (42, 43), as well as in solution digest (44) followed by high pH reversed phase separation (Pierce High pH Reversed-Phase Peptide Fractionation Kit, ThermoFisher Scientific) according to

10.3389/fmed.2023.1176427

TABLE 1 Characteristics of study patients.

	No./Median	Percentage (%) or range	
Total	11		
Ruxolitinib			
Yes	8	66.7%	
No	3	33.3%	
Basic demographics			
	All patients n (%) median (range)	Ruxo patients n (%) median (range)	Control patients n (%) median (range)
Female	4 (36.4%)	3/8 (37.5%)	1/3 (33%)
Male	7 (63.6%)	5/8 (62.5%)	2/3 (67%)
Age	65 (23–82)	61 (23–82)	70 (23–73)
BMI	27.7 (25.4–51)	29 (25.5–51)	27.7 (26.1–3.4)
Comorbidities			
	All patients n (%)	Ruxo patients *n* (%)	Control patients n (%)
Hypertension	8/11 (72.7%)	6/8 (75%)	2/3 (67%)
Obesity	6/11 (54.5%)	5/8 (62.5%)	1/3 (33%)
Cardiovascular (other than Hypertension)	4/11 (36.4%)	2/8 (25%)	2/3 (67%)
GIT diseases	4/11 (36.4%)	3/8 (37.5%)	1/3 (33%)
Diabetes	3/11 (27.3%)	2/8 (25%)	1/3 (33%)
Hyperlipidemia/Hyperlipoproteinemia	2/11 (18.2%)	1/8 (12.5%)	1/3 (33%)
CKD	2/11 (18.2%)	0/8 (0%)	2/3 (67%)
Malignancy	2/11 (18.2%)	1/8 (12.5%)	1/3 (33%)
Neurologic/Neuromuscular	1/11 (9.1%)	0/8 (0%)	1/3 (33%)
Thyroid	1/11 (9.1%)	1/8 (12.5%)	0/3 (0%)
Previous medication			
	All patients n (%)	Ruxo patients n (%)	Control patients n (%)
Betablockers	5/11 (45.5%)	4/8 (50%)	1/3 (33%)
PPIs	4/11 (36.4%)	2/8 (25%)	2/3 (67%)
ACE-inhibitors	3/11 (27.3%)	1/8 (12.5%)	2/3 (67%)
Antidiabetic medication	3/11 (27.3%)	2/8 (25%)	1/3 (33%)
Calcium antagonists	3/11 (27.3%)	2/8 (25%)	1/3 (33%)
Platelet aggregator inhibitors	3/11 (27.3%)	2/8 (25%)	1/3 (33%)
Statins	3/11 (27.3%)	1/8 (12.5%)	2/3 (67%)
Antineoplastic agents	2/11 (18.2%)	1/8 (12.5%)	1/3 (33%)
Immunosuppressive drugs (particularly corticosteroids, CNIs, rituximab)	2/11 (18.2%)	0/8 (0%)	2/3 (67%)
Diuretics	1/11 (9.1%)	1/8 (12.5%)	0/3 (0%)
NSAIDs and other analgesic drugs	1/11 (9.1%)	0/8 (0%)	1/3 (33%)
Psychoactive drugs	1/11 (9.1%)	1/8 (12.5%)	0/3 (0%)
Thyroid medications	1/11 (9.1%)	1/8 (12.5%)	0/3 (0%)
Outcome			
Days of hospitalization – median (range)	29 (21–67)	28.5 (21–65)	40 (23–67)
Alive at day 28	10/11 (91%)	7/8 (87.5%)	3/3 (100%)
Discharged	7/11 (63.6%)	5/8 (62.5%)	2/3 (67%)
Deceased	4/11 (36.4%)	3/8 (37.5%)	1/3 (33%)

ACE, angiotensin-converting enzyme; BMI, body mass index; CKD, chronic kidney disease; CNI, calcineurin inhibitors; GIT, gastro-intestinal tract; NSAIDs, non-steroidal anti-inflammatory drugs; PPIs, proton-pump inhibitors.

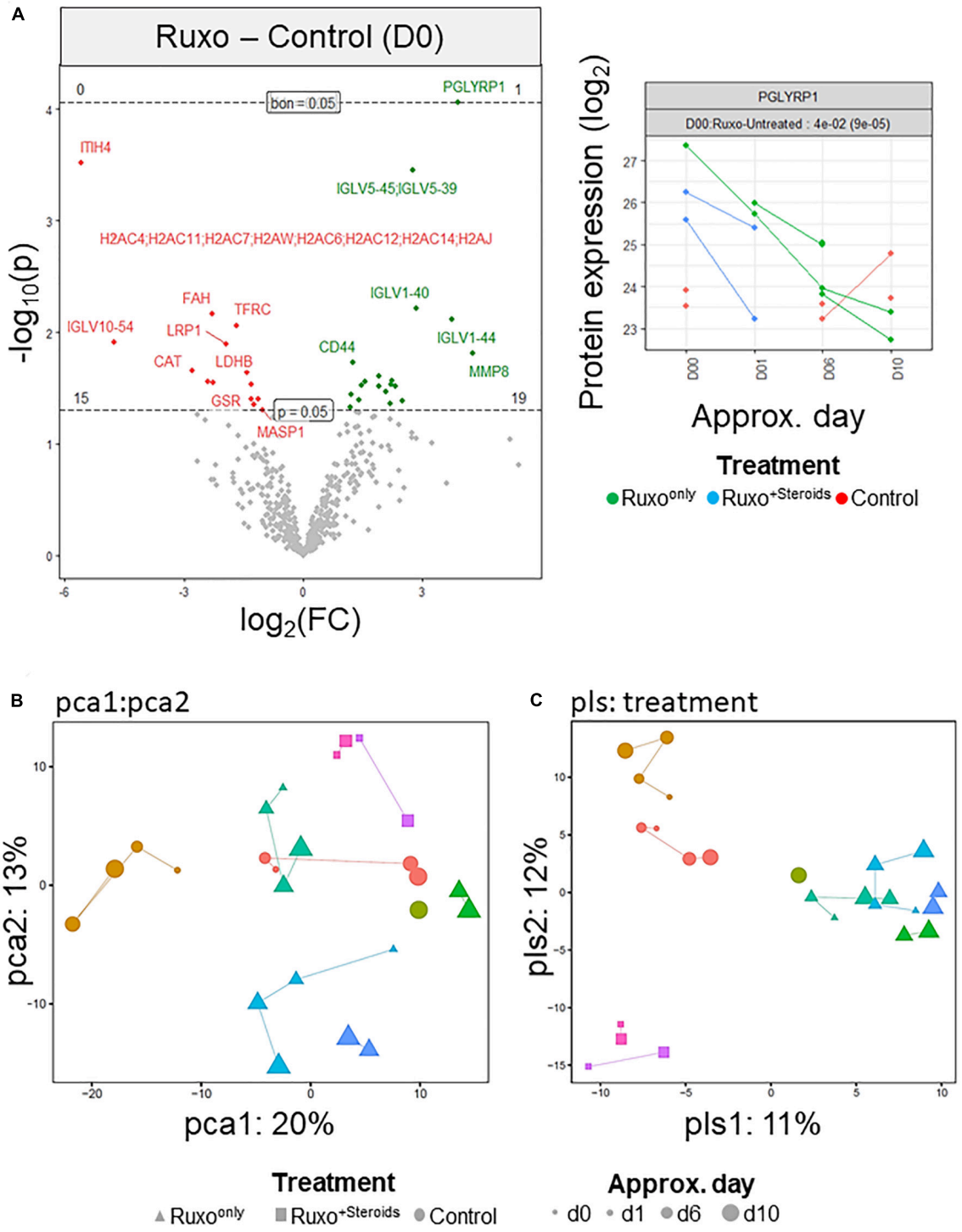

FIGURE 1
Serum proteomes of critically ill COVID-19 patients with and without Ruxo treatment. **(A)** Left panel: Volcano plot of MS data indicating differential protein expression between COVID-19 patients with or without ARDS [Ruxo group (green) vs. control group (red)]. "p" indicates the raw *p*-value, "bon" indicates the Bonferroni-corrected *p*-value. Right panel: Time trajectory from principal component analysis for the protein PGLYRP1. **(B)** Principal component analysis (PCA) score plot derived from mass spectrometry (MS) data of different patients and sampling time points using treatment as a design-factor. Each individual is color-coded. Additionally, for each subject, "Treatment" is coded by symbol shape and "ApproxDay" by size. **(C)** Partial least square regression analysis (PLS) derived from the MS data. Coding as in panel **(B)**.

the manufacturer's protocol, as reported. Briefly, after determining protein concentration of each serum sample by Lowry assay (BioRad Laboratories), 50 μg of total serum protein was separated into ten fractions using the in gel approach. For in solution digest, 150 μg were acetone-precipitated and separated into eight fractions. Liquid chromatography/tandem mass spectrometry was

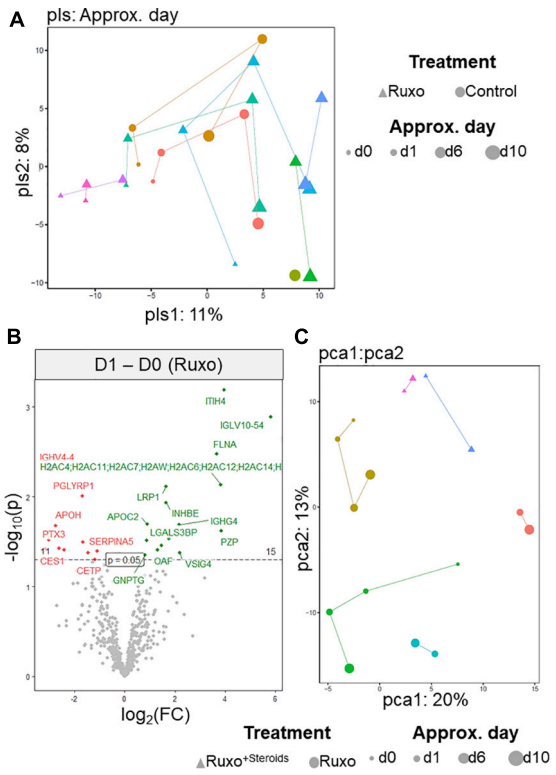

FIGURE 2
Changes in serum proteomes of COVID-19 patients upon Ruxo treatment over time. **(A)** Partial least square regression analysis (PLS) derived from the MS data of different patients and sampling time points using time as a design-factor. Each individual is color-coded. Additionally, for each subject, "Treatment" is coded by symbol shape and "ApproxDay" by size. Samples from the same subject are connected by a line. **(B)** Volcano plot of MS data indicating differential protein expression in COVID-19 patients under treatment with Ruxo at day 1 (green) compared to day 0 (red). "p" indicates the raw *p*-value, "bon" indicates the Bonferroni-corrected *p*-value. **(C)** General linear modeling of protein expression as a function of sampling day.

performed as reported (44). Used parameters were extracted and summarized using MARMoSET (45) and are included in the **Supplementary Material 1**. The mass spectrometry raw data from experiments described here has been deposited in the MassIVE member repository of the ProteomeXchange consortium (46).

2.3. Processing and statistical analysis of proteomics data

MS data were processed using MaxQuant v.2.0.3.0 (47), including label free quantitation against the human Uniprot protein sequence database (08.12.2020 download, canonical only with 75577 protein sequences).[1] Parameters used for MaxQuant are included in the **Supplementary Material 1**. MaxQuant returned a file with 975 protein groups. 16 reverse proteins, 65 contaminant proteins and 194 proteins that were only represented by single peptides were dropped. The remaining 700 proteins were subjected to statistical analyses in R (48). For general linear model analysis we used the *autonomics* version 1.1.7.7 (49) interface fit_limma to the *limma* modeling engine (50). Overlap analyses of significantly regulated proteins identified in the *limma*-model was performed using the R-/Bioconductor package *VennDetail* (51). Functional analyses were performed using the R-/Bioconductor packages *clusterProfiler* (52) and *dbtORA* (53) and results were visualized using the package *enrichplot* (54).

2.4. Cytometric bead array assay

Fifty microliters of 1:4 diluted serum from each patient and time point was analyzed with human cytokine Grp I panel 17-plex cytometric bead array set (M5000031YV; Bio-Rad Laboratories), according to the manufacturer's instructions and as described before (55) to quantify serum cytokines.

3. Results

3.1. Patient characteristics

This study included 11 COVID-19 patients, who were treated during the first to fourth wave of the pandemic (April 2020 - January 2022) at the University Hospital Marburg, Germany. All patients required intensive care treatment including mechanical ventilation (mean duration 26 days ± 10 days). Eight patients with ARDS were treated with Ruxo in a clinical trial (20) or on an individual basis ($Ruxo^{only}$ group), and two of these additionally received steroids ($Ruxo^{+Steroids}$ subgroup) according to the standard of care at the time of hospitalization. One of three control patients (no ARDS, no Ruxo treatment) was treated with steroids. Baseline characteristics of the Ruxo and Control patients are summarized in **Table 1**. Blood samples for the analyses described in this work were collected before (day 0) and on days one (day 1), five to seven or nine to eleven days after initiation of Ruxo treatment. The latter time points were merged to day 6 and day 10, respectively, for statistical analyses. In the control group, different sampling time points are indicated relative to the day of ICU admission, which we considered the clinical peak of critical illness in these patients. All patients except for one in the Ruxo group who died on day 21, survived until day 28, which corresponds to the primary end point in several clinical trials investigating Ruxo in COVID-19-associated ARDS (20, 56) (**Table 1**).

3.2. Serum proteomes of critically ill COVID-19 patients with or without Ruxo-treatment

To explore the serum proteomes of patients with severe COVID-19-associated pneumonia or ARDS and the impact of Ruxo in the latter condition, we performed MS in the absence of any depletion protocol against high-abundant serum proteins on serum samples collected at different time points

1 https://www.uniprot.org/

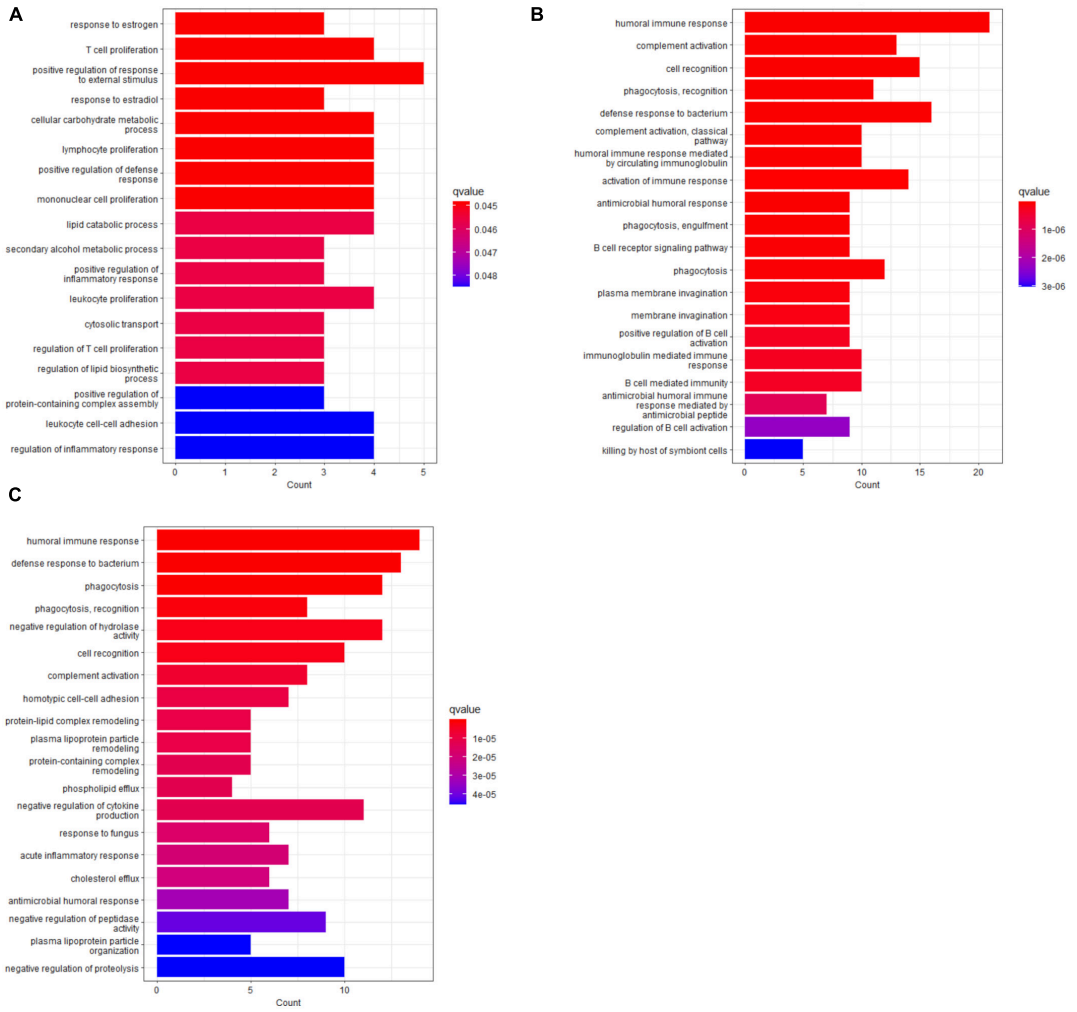

FIGURE 3
Overrepresentation analysis of differentially regulated serum proteins in COVID-19 patients under Ruxo treatment. ORA was performed on differentially regulated proteins (raw p-value < 0.05) as detected by MS on **(A)** day 1, **(B)** day 6, and **(C)** day 10. The top 20 GO terms of the category biological process from analyses using the *clusterProfiler* package were plotted. Note that direction of regulation (up or down) was not considered in this analysis. The barplots indicate the level of significance and the number of included genes for each term. See Supplementary Tables 6–8 in Supplementary Material 2 for complete ORA results.

after initiation of treatment. In total 25 samples from nine patients were investigated including three control, four Ruxo^{only} and two Ruxo$^{+Steroids}$ patients. We observed differential protein expression between Ruxo-treated and untreated patients at day 0 with Peptidoglycan recognition protein 1 (PGLYRP1 as the most significant upregulated factor in the treatment group (Figure 1A). However, principal component analysis (PCA) revealed clear patient-specific effects and time trajectories, which, did not generalize across patients. Subtle treatment effects were only recognizable for the Ruxo$^{+Steroids}$ subgroup (Figure 1B). Thus, the main PCA drivers appeared to be factors unrelated to the study-design. Particularly in the control group, covariates associated with preexisting conditions and/or patients' permanent medications such as chronic kidney disease, diabetes, immunosuppression or antihypertensive drugs, confirmed, that the largest variability in the dataset was not caused by different treatments for COVID-19 (Supplementary Figure 1A in Supplementary Material 3). To further investigate potential effects of our experimental design, we performed partial least square (PLS) regression analysis. In line with the PCA results, examination of "treatment" as a design-factor revealed no clear separation of groups, (Figure 1C). These calculations underlined considerable heterogeneity of individual patients in all treatment groups in our limited dataset.

3.3. Changes in serum proteomes of COVID-19 patients under Ruxo treatment over time

Given that "treatment" did not allow to distinguish patients treated with Ruxo from untreated patients, we next investigated "time" as a relevant design-factor in our experimental setting by PLS. Indeed, we detected some generalizable time effects, which were most pronounced (i.e., displayed the highest PLS1 loadings) for the proteins Afamin (AFM), Apolipoprotein C3 (APOC3), Lipopolysaccharide binding protein (LBP), and Serpin family A

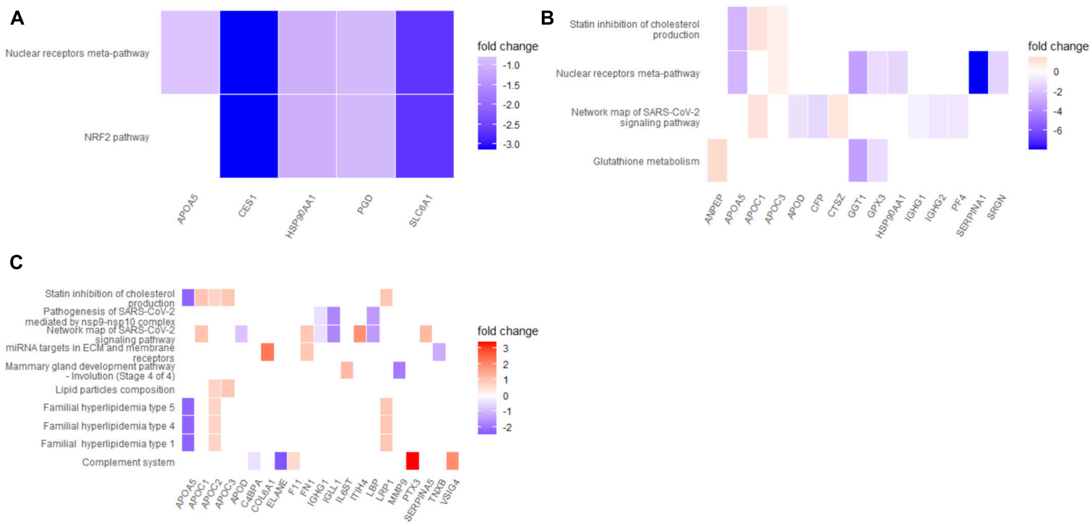

FIGURE 4
Pathway enrichment analysis of differentially regulated serum proteins in COVID-19 patients under Ruxo treatment. Wiki-Pathway enrichment analysis was performed on differentially regulated proteins (raw p-value < 0.05) as detected by MS on **(A)** day 1, **(B)** day 6 and **(C)** day 10. Heatmap-like plots indicate expression of individual genes involved in each pathway.

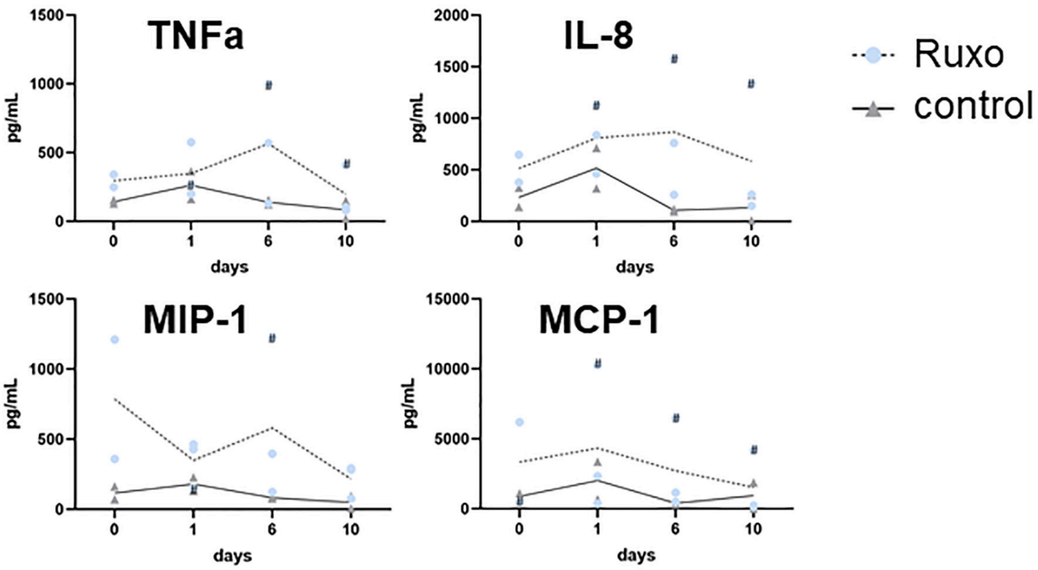

FIGURE 5
Serum cytokine levels in treated and untreated COVID-19 patients. Cytometric bead array assay performed with serum samples collected at different time points (day 0, day 1, day 6, and day 10) from three COVID-19 patients under Ruxo treatment and two control patients, without Ruxo treatment. One patient in the Ruxo group also received steroids (marked by #).

member 5 (SERPINA5) (Figure 2A and Supplementary Figure 1B in Supplementary Material 3). Yet, these exploratory analyses still revealed considerable heterogeneity within the three non-Ruxo patients, precluding to use them as an appropriate control group. Thus, these patients were excluded from subsequent analyses.

Considering only Ruxo-treated patients ($Ruxo^{only}$ and $Ruxo^{+Steroids}$), we next investigated differential protein expression at different time points. Inter-Alpha-Trypsin Inhibitor Heavy Chain 4 (ITH4) was most significantly upregulated while, PGLYRP1 was expressed at lower levels under treatment (Figure 2B). This latter observation was consistent with our initial finding that PGLYRP1 was less abundant in the less severely ill patients. Subsequently, we extended our time-course analyses and performed general linear modeling of protein expression as a function of collection day, including subject as a random effect. This analysis revealed four proteins which changed systematically (FDR < 0.05) across patients, although these were not measured in all patients and/or at all time points: Apolipoprotein A5 (APOA5), N-Acetylglucosamine-1-phosphate transferase subunit gamma (GNPTG), PGLYRP1 and Serpin family A member 1 (SERPINA1) (Figure 2C, Supplementary Figure 1C in Supplementary Material 3, and Supplementary

Table 1 in Supplementary Material 2). Modifying this analysis by calculating Helmert contrasts, i.e., comparing each day against the average of the previous time points confirmed systematic time-effects on APOA5 and SERPINA1 and added one more protein, Immunoglobulin Heavy Variable 3/OR16-12 (IGHV3OR16-12), a poorly characterized immunoglobulin complex component (Supplementary Figure 1C in Supplementary Material 3). The statistically significant time-effect observed for SERPINA1 attracted our particular attention, as this protein was detected in the two Ruxo$^{+Steroids}$ patients at d0 and d1 at approximately identical levels, but appeared completely absent at later time points. Moreover, when we compared the proteomes of critically ill COVID-19 patients who eventually deceased due to the infection to those who could be discharged from hospital, we found SERPINA1 among the factors that were higher expressed in the survivors. This observation was also remarkable because most of the factors that differentiated between final outcomes were largely unchanged over time (Supplementary Figure 2 in Supplementary Material 3). Due to the heterogeneity of our dataset, we could not confirm the time-effect of SERPINA1 as a true switch-like response, as a global analysis of presence/absence schematics in our dataset exhibited a random pattern (data not shown). In addition, since we had also collected peripheral blood mononuclear cells (PBMCs) from some patients at day 0, day 1 and day 6, we applied qPCR to examine whether changes in serum protein levels were paralleled by mRNA expression changes in these cells. However, this seemed not to be the case, which we attribute to differential expression of candidate genes (GNPTG, HP, C4B, PGLYRP1, WARS1, and SERPINA1) in various PBMC-subsets as well as expression in other tissues which contribute to serum levels of these proteins, such as liver (data not shown). Taken together, these results suggested that a mode of action for Ruxo in a small cohort of critically ill COVID-19 patients is potentially more reliably deduced from longitudinal in-patient effects rather than from comparisons between treatment groups.

3.4. Functional analysis of differentially regulated proteins under Ruxo treatment compared to baseline

To further characterize the response to Ruxo in COVID-19-ARDS patients on a functional level, we performed gene ontology (GO) and pathway enrichment analyses on the proteins that were differentially regulated at different time points according to our linear model. Each treatment day was compared to day 0 separately since the time trajectories from PLS analyses indicated opposite effects on several proteins over time. Focusing on significant proteins (raw p-value < 0.05) we identified ten proteins that were upregulated upon Ruxo treatment at day 1 and 17 proteins that were downregulated. At day 6 and 10, 22 and 47, or, respectively, 32 and 40 proteins were up- or downregulated (Supplementary Tables 2–4 in Supplementary Material 2). Overlap analyses of affected proteins at day 1, 6, and 10 confirmed opposite regulation of several factors as indicated by PLS. We identified only five factors that were regulated both concordantly and significantly over time (up: IGLV10-54, PSMB1, down: PGLYRP1, APOA5, WARS1, Supplementary Table 5 in Supplementary Material 2). Overrepresentation analysis (ORA) of GO terms (52) including all significant proteins (raw p-value < 0.05) at any individual time point revealed enrichment of biological processes that implicated a T-cell response only on day 1, but not on days 6 and 10 (Figure 3 and Supplementary Tables 6–8 in Supplementary Material 2). The highest fold change of T-cell-proliferation-related proteins was observed for VSIG4, a negative regulator of this process (57), which was upregulated approximately 2-fold (Supplementary Figure 3 in Supplementary Material 3). On the later time points, we found significant enrichment of the humoral immune response with a marked focus on B-cell-dependent processes on day 6, as well as complement activation. Notably, most proteins relating to these terms were downregulated (Figures 3B, C and Supplementary Tables 6–8 in Supplementary Material 2). Similar results were obtained applying a different implementation of ORA (dbtORA (53), Supplementary Tables 9–11 in Supplementary Material 2). Pathway enrichment analysis using the curated Wiki pathway database (52) yielded only two gene sets, the *Nuclear receptors meta-pathway* and the *NRF2-pathway* at day 1. The first one was also enriched on day 6, together with additional pathways including *Network map of SARS-CoV-2 signaling* and *Statin inhibition of cholesterol production*. These SARS-CoV-2- and Cholesterol-gene sets in turn were shared by enrichment results for day 6 and day 10 (Figure 4). Of note, most of the affected pathways included APOA5, which was downregulated under Ruxo treatment at all time points. Although enrichment analyses are less robust for the day 1 time point due to a very short list of only 27 significantly regulated proteins (compared to 69 on day 6 and 72 on day 10), these results suggest that Ruxo exerts immediate, but transient effects in COVID-19-ARDS patients, that during the course of several days clearly connect to the underlying condition, namely SARS-CoV-2-infection.

3.5. Serum cytokine levels in COVID-19-ARDS and effects of Ruxo treatment

Cytokines and chemokines are generally difficult to capture by MS because of very low serum concentrations compared to other serum proteins. We therefore investigated these mediators in COVID-19-ARDS compared to COVID-19-pneumonia and their potential regulation by Ruxo separately using a cytometric bead array (CBA) assay. This analysis was restricted to three Ruxo and two control patients from whom sufficient sample material was available. COVID-19 patients with ARDS exhibited higher serum levels of all cytokines and chemokines measured (IFNy, TNFa, IL-4, IL-6, IL-7, IL-8, IL-10, IL-13, MIP-1b, and MCP-1) compared to patients with COVID-19 pneumonia without ARDS (data not shown). Moreover, serum cytokines and chemokines clearly showed patient-specific time courses, as observed in our proteomics experiments. However, despite heterogenous time-patterns, several mediators in Ruxo patients tended to approximate control levels after 10 days of treatment, such as TNFa, IL-8, MIP-1b, and MCP-1 (Figure 5). This observation presumably reflects attenuation of the cytokine storm, consistent with the expected clinical effects of Ruxo, although with slower kinetics than expected based on our initial clinical experience with Ruxo (32) and even transient increase of proinflammatory cytokines (58).

4. Discussion

Ruxo has been repurposed for the treatment of SARS-CoV-2 infection in different clinical settings inside and outside of clinical trials, but the clinical significance of this drug in COVID-19 pneumonia and ARDS remains to be firmly established (18, 20, 21, 32, 56, 59–62). The work presented here adds to previous work on the mechanisms of action of Ruxo in hyperinflammation and respiratory distress (63, 64). Specifically, we aimed to gain deeper insights into systemic effects of Ruxo in critical COVID-19 by studying serum proteomes by MS and cytokine array analyses at different time points after initiation of treatment. Based on our early clinical experience with Ruxo for ARDS associated with SARS-CoV-2 infection (32), we expected rapid and profound changes of circulating factors. We therefore analyzed samples from only eight COVID-19-ARDS patients treated with Ruxo and three controls and did not stratify the patients/samples investigated here for outcome.

Firstly, we found time trajectories in the proteomics data that generalized for all patients, which included factors that have been mentioned in the literature in the context of COVID-19 such Afamin (65), APOC3 (66), or SERPINA5 (67). On the other hand, time patterns for a set of different proteins including APOA5, GNPTG or PGLYRP1 only became detectable after excluding the extremely heterogenous control group from further analyses. Only 5 factors were regulated both concordantly and significantly over time, including Immunoglobulin Lambda Variable 10–54 (IGLV10-54) and Proteasome 20S Subunit Beta 1 (PSMB1), which were upregulated and, respectively, PGLYRP1, APOA5 and Tryptophanyl-tRNA Synthetase 1 (WARS1), which were downregulated. IGLV10-54 has been identified as one of the top upregulated genes in SARS-CoV-2 infected individuals compared to healthy controls and also as component of an immune-response related gene cluster that distinguishes Long-COVID-patients from individuals who had recovered from the disease (68, 69). PSMB1, along with other proteasomal subunits has been described to be induced by hypoxia in the context of SARS-CoV-2-infection (70). In addition, certain PGLYRP1-derived peptides have been described to inhibit proinflammatory cytokine-production in a mouse model of acute lung injury with diffuse alveolar damage (71). We have not examined individual peptides on a sub-protein level in our analysis, but in view of these previous results, decrease of PGLYRP1 under Ruxo treatment might not necessarily point out PGLYRP1 as a direct target of Ruxo, but rather indicate resolution of the ARDS-causing cytokine storm within several days. APOA5 has been described to be differentially regulated in severe COVID-19 compared to healthy controls and also during recovery from this condition (72). Finally, WARS1, which has been reported to boost the innate immune response as a ligand of toll-like receptors TLR2 and TLR4 (73), has been identified as a factor involved in several biological processes associated with COVID-19 severity and has been described to be downregulated on the mRNA-level upon SARS-CoV-2-infection (74, 75).

On the functional level, i.e., with regard to biological processes or cellular pathways we found two phases of the response to Ruxo. The early phase on day 1 following treatment initiation was characterized by a T-cell response and repression of the NRF2-pathway, reflecting well established actions of Ruxo as a mediator of T-cells (76) and a previously identified SARS-Cov-2 key pathogenic pathway (77). At later time points, however, we observed enrichment of other SARS-CoV-2-related pathways, which involved, for example, ITIH4. This protein, which acts as a protease inhibitor upon proteolytic cleavage (78), has been detected at increased levels in plasma or serum samples of COVID-19 patients in previous proteomics studies reported in the literature (79, 80) and has also been proposed as a potential predictor for disease mortality (81). These observations support the clinical experience that Ruxo exerts prompt effects in COVID-19-associated ARDS, which only transiently overlay more sustained immune responses or pathomechanisms.

Thus, our careful and detailed analyses of our dataset revealed several lines of evidence that the mechanism of action of Ruxo in COVID-19-ARDS can be related to both known effects of this drug and the clinical condition studied, i.e., SARS-CoV-2-infection. However, interpretation of our experiments is clearly compromised by the very limited number of Ruxo- and control patients that were included in this study, which resulted in extensive variability within our cohort with regard to clinical covariates, and thus, of our proteomics dataset. Moreover, given that we included patients with critical COVID-19 from the first to fourth wave of the pandemic, variant-specific proinflammatory effects of different SARS-CoV-2-mutants may also have contributed to the heterogeneity observed in our dataset (82).

In summary, the results presented here further strengthen the concept of Ruxo constituting a rational treatment for COVID-19-related ARDS that warrants further preclinical and clinical investigation.

Data availability statement

The mass spectrometry proteomics data presented in this study have been deposited to the ProteomeXchange Consortium (http://proteomecentral.proteomexchange.org) via the MassIVE partner repository with the data set identifier PXD041909 and http://doi.org/10.25345/C5000094G.

Ethics statement

The studies involving human participants were reviewed and approved by the Clinical Ethics Committee of the Faculty of Medicine, Philipps-University Marburg (No. 57/20). The patients/participants provided their written informed consent to participate in this study.

Author contributions

AN, HR, JG, CS, and EM conceptualized the study. TT, IK, TW, BB, JH, CK, and AB contributed to the sample acquisition. SV, TT, LS, and HM designed and performed the experiments. AMB, JG, SV, and EM analyzed the mass spectrometry data. SV and EM wrote the first draft of the manuscript with contributions from AMB and TT. All authors contributed to the manuscript revision, read, and approved the submitted version.

Funding

CS was supported by the Universities of Gießen and Marburg Lung Center (UGMLC), the German Center for Lung Research (DZL), University Hospital Gießen and Marburg (UKGM) research funding according to article 2, section 3 cooperation agreement, and the Deutsche Forschungsgemeinschaft (DFG, German Research Foundation)-Project-ID 197785619 – SFB 1021, KFO 309 (Project Number: 284237345), and SK 317/1-1 (Project Number: 428518790) as well as by the Foundation for Pathobiochemistry and Molecular Diagnostics. EM was supported by the Clinician Scientist Program and the Research Foundation of the Faculty of Medicine, Philipps-University Marburg. SV received an early career support grant from the German Research Foundation (KFO 309). HM was supported by Foundation Daniel Swarovski. AN was funded by the Deutsche José-Carreras Leukämie-Stiftung (Grant Number: AH 06-01) and also received funding for the RuXoCoil trial from Novartis pharma. Open access funding was provided by the Open Acess Publishing Fund of Philipps-University Marburg with support of the Deutsche Forschungsgemeinschaft (DFG, German Research Foundation). Novartis pharma was not involved in the study design, collection, analysis, interpretation of data, the writing of this article, or the decision to submit it for publication.

Acknowledgments

We thank Kathleen Stabla and Jennifer Kremer for help with PBMC isolation, Sylvia Jeratsch and Alicia Klaus for performing proteomic analysis, and Alfred Ultsch for helpful discussion of ORA.

Conflict of interest

CS: Consultancy and Research Funding from Hycor Biomedical, Bencard Allergie and Thermo Fisher Scientific; Research Funding from Mead Johnson Nutrition.

The remaining authors declare that the research was conducted in the absence of any commercial or financial relationships that could be construed as a potential conflict of interest.

Publisher's note

All claims expressed in this article are solely those of the authors and do not necessarily represent those of their affiliated organizations, or those of the publisher, the editors and the reviewers. Any product that may be evaluated in this article, or claim that may be made by its manufacturer, is not guaranteed or endorsed by the publisher.

Supplementary material

The Supplementary Material for this article can be found online at: https://www.frontiersin.org/articles/10.3389/fmed.2023.1176427/full#supplementary-material

References

1. Wu F, Zhao S, Yu B, Chen Y, Wang W, Song Z, et al. A new coronavirus associated with human respiratory disease in China. *Nature.* (2020) 579:265–9. doi: 10.1038/s41586-020-2008-3

2. Yang X, Yu Y, Xu J, Shu H, Xia J, Liu H, et al. Clinical course and outcomes of critically ill patients with SARS-CoV-2 pneumonia in Wuhan, China: a single-centered, retrospective, observational study. *Lancet Respir Med.* (2020) 8:475–81. doi: 10.1016/S2213-2600(20)30079-5

3. Del Sole F, Farcomeni A, Loffredo L, Carnevale R, Menichelli D, Vicario T, et al. Features of severe COVID-19: a systematic review and meta-analysis. *Eur J Clin Invest.* (2020) 50:e13378. doi: 10.1111/eci.13378

4. Guan W, Ni Z, Hu Y, Liang W, Ou C, He J, et al. Clinical characteristics of coronavirus disease 2019 in China. *N Engl J Med.* (2020) 382:1708–20. doi: 10.1056/NEJMoa2002032

5. World Health Organization [WHO]. *WHO Director-General's Opening Remarks at the Media Briefing on COVID-19-11 March 2020.* Geneva: World Health Organization (2020).

6. WHO Solidarity Trial Consortium, Pan H, Peto R, Henao-Restrepo AM, Preziosi MP, Sathiyamoorthy V, Abdool Karim Q, Alejandria MM. Repurposed antiviral drugs for Covid-19 — interim WHO solidarity trial results. *N Engl J Med.* (2021) 384:497–511. doi: 10.1056/NEJMoa2023184

7. Beigel J, Tomashek K, Dodd L, Mehta A, Zingman B, Kalil A, et al. Remdesivir for the treatment of Covid-19 — final report. *N Engl J Med.* (2020) 383:1813–26. doi: 10.1056/NEJMoa2007764

8. Weinreich D, Sivapalasingam S, Norton T, Ali S, Gao H, Bhore R, et al. REGEN-COV antibody combination and outcomes in outpatients with Covid-19. *N Engl J Med.* (2021) 385:e81. doi: 10.1056/NEJMoa2108163

9. Gupta A, Gonzalez-Rojas Y, Juarez E, Crespo Casal M, Moya J, Rodrigues Falci D, et al. Effect of sotrovimab on hospitalization or death among high-risk patients with mild to moderate COVID-19: a randomized clinical trial. *JAMA.* (2022) 327:1236–46. doi: 10.1001/jama.2022.2832

10. Montgomery H, Hobbs F, Padilla F, Arbetter D, Templeton A, Seegobin S, et al. Efficacy and safety of intramuscular administration of tixagevimab-cilgavimab for early outpatient treatment of COVID-19 (TACKLE): a phase 3, randomised, double-blind, placebo-controlled trial. *Lancet Respir Med.* (2022) 10:985–96. doi: 10.1016/S2213-2600(22)00180-1

11. Jayk Bernal A, Gomes da Silva M, Musungaie D, Kovalchuk E, Gonzalez A, Delos Reyes V, et al. Molnupiravir for oral treatment of Covid-19 in nonhospitalized patients. *N Engl J Med.* (2021) 386:509–20. doi: 10.1056/NEJMoa2116044

12. Hammond J, Leister-Tebbe H, Gardner A, Abreu P, Bao W, Wisemandle W, et al. Oral nirmatrelvir for high-risk, nonhospitalized adults with Covid-19. *N Engl J Med.* (2022) 386:1397–408. doi: 10.1056/NEJMoa2118542

13. The R Collaborative Group. Dexamethasone in hospitalized patients with Covid-19. *N Engl J Med.* (2020) 384:693–704. doi: 10.1056/NEJMoa2021436

14. Mortara A, Mazzetti S, Margonato D, Delfino P, Bersano C, Catagnano F, et al. Compassionate use of ruxolitinib in patients with SARS-Cov-2 infection not on mechanical ventilation: short-term effects on inflammation and ventilation. *Clin Transl Sci.* (2021) 14:1062–8. doi: 10.1111/cts.12971

15. Cao Y, Wei J, Zou L, Jiang T, Wang G, Chen L, et al. Ruxolitinib in treatment of severe coronavirus disease 2019 (COVID-19): a multicenter, single-blind, randomized controlled trial. *J Allergy Clin Immunol.* (2020) 146:137–146.e3. doi: 10.1016/j.jaci.2020.05.019.

16. Sarmiento M, Rojas P, Jerez J, Bertín P, Campbell J, García M, et al. Ruxolitinib for severe COVID-19-related hyperinflammation in nonresponders to steroids. *Acta Haematol.* (2021) 144:620–6. doi: 10.1159/000516464

17. Stanevich OV, Fomina D, Bakulin I, Galeev S, Bakin E, Belash V, et al. Ruxolitinib versus dexamethasone in hospitalized adults with COVID-19: multicenter matched cohort study. *BMC Infect Dis.* (2021) 21:1277. doi: 10.1186/s12879-021-06982-z

18. Vannucchi A, Mortara A, D'Alessio A, Morelli M, Tedeschi A, Festuccia M, et al. JAK inhibition with ruxolitinib in patients with COVID-19 and severe pneumonia: multicenter clinical experience from a compassionate use program in Italy. *J Clin Med.* (2021) 10:3752.

19. D'Alessio A, Del Poggio P, Bracchi F, Cesana G, Sertori N, Di Mauro D, et al. Low-dose ruxolitinib plus steroid in severe SARS-CoV-2 pneumonia. *Leukemia.* (2021) 35:635–8. doi: 10.1038/s41375-020-01087-z

20. Neubauer A, Johow J, Mack E, Burchert A, Meyn D, Kadlubiec A, et al. The janus-kinase inhibitor ruxolitinib in SARS-CoV-2 induced acute respiratory distress syndrome (ARDS). *Leukemia.* (2021) 35:2917–23. doi: 10.1038/s41375-021-01374-3

21. La Rosée F, Bremer H, Gehrke I, Kehr A, Hochhaus A, Birndt S, et al. The Janus kinase 1/2 inhibitor ruxolitinib in COVID-19 with severe systemic hyperinflammation. *Leukemia.* (2020) 34:1805–15.

22. Marconi V, Ramanan AV, de Bono S, Kartman C, Krishnan V, Liao R, et al. Efficacy and safety of baricitinib for the treatment of hospitalised adults with COVID-19 (COV-BARRIER): a randomised, double-blind, parallel-group, placebo-controlled phase 3 trial. *Lancet Respir Med.* (2021) 9:1407–18. doi: 10.1016/S2213-2600(21)00331-3

23. Cantini F, Niccoli L, Nannini C, Matarrese D, Di Natale M, Lotti P, et al. Beneficial impact of Baricitinib in COVID-19 moderate pneumonia; multicentre study. *J Infect.* (2020) 81:647–79. doi: 10.1016/j.jinf.2020.06.052

24. Bronte V, Ugel S, Tinazzi E, Vella A, De Sanctis F, Canè S, et al. Baricitinib restrains the immune dysregulation in severe COVID-19 patients. *J Clin Invest* (2020) 130:6409–16. doi: 10.1172/JCI141772

25. Kalil A, Patterson T, Mehta A, Tomashek K, Wolfe C, Ghazaryan V, et al. Baricitinib plus remdesivir for hospitalized adults with Covid-19. *N Engl J Med.* (2020) 384:795–807. doi: 10.1056/NEJMoa2031994

26. The R Investigators. Interleukin-6 receptor antagonists in critically Ill patients with Covid-19. *N Engl J Med.* (2021) 384:1491–502. doi: 10.1056/NEJMoa2100433

27. Abani O, Abbas A, Abbas F, Abbas M, Abbasi S, Abbass H, et al. Tocilizumab in patients admitted to hospital with COVID-19 (RECOVERY): a randomised, controlled, open-label, platform trial. *Lancet.* (2021) 397:1637–45. doi: 10.1016/S0140-6736(21)00676-0

28. Rodríguez-Baño J, Pachón J, Carratalà J, Ryan P, Jarrín I, Yllescas M, et al. Treatment with tocilizumab or corticosteroids for COVID-19 patients with hyperinflammatory state: a multicentre cohort study (SAM-COVID-19). *Clin Microbiol Infect.* (2020) 27:244–52. doi: 10.1016/j.cmi.2020.08.010

29. Huet T, Beaussier H, Voisin O, Jouveshomme S, Dauriat G, Lazareth I, et al. Anakinra for severe forms of COVID-19: a cohort study. *Lancet Rheumatol.* (2020) 2:e393–400. doi: 10.1016/S2665-9913(20)30164-8

30. Pontali E, Volpi S, Signori A, Antonucci G, Castellaneta M, Buzzi D, et al. Efficacy of early anti-inflammatory treatment with high doses of intravenous anakinra with or without glucocorticoids in patients with severe COVID-19 pneumonia. *J Allergy Clin Immunol.* (2021) 147:1217–25. doi: 10.1016/j.jaci.2021.01.024

31. Richardson P, Griffin I, Tucker C, Smith D, Oechsle O, Phelan A, et al. Baricitinib as potential treatment for 2019-nCoV acute respiratory disease. *Lancet.* (2020) 395:e30–1.

32. Neubauer A, Wiesmann T, Vogelmeier C, Mack E, Skevaki C, Gaik C, et al. Ruxolitinib for the treatment of SARS-CoV-2 induced acute respiratory distress syndrome (ARDS). *Leukemia.* (2020) 34:2276–8.

33. Verstovsek S, Mesa R, Gotlib J, Levy R, Gupta V, DiPersio J, et al. A double-blind, placebo-controlled trial of ruxolitinib for myelofibrosis. *N Engl J Med.* (2012) 366:799–807. doi: 10.1056/NEJMoa1110557

34. Kralovics R, Passamonti F, Buser A, Teo S, Tiedt R, Passweg J, et al. A gain-of-function mutation of JAK2 in myeloproliferative disorders. *N Engl J Med.* (2005) 352:1779–90. doi: 10.1056/NEJMoa051113

35. Mascarenhas J, Mughal T, Verstovsek S. Biology and clinical management of myeloproliferative neoplasms and development of the JAK inhibitor ruxolitinib. *Curr Med Chem.* (2012) 19:4399–413.

36. Zeiser R, Burchert A, Lengerke C, Verbeek M, Maas-Bauer K, Metzelder S, et al. Ruxolitinib in corticosteroid-refractory graft-versus-host disease after allogeneic stem cell transplantation: a multicenter survey. *Leukemia.* (2015) 29:2062–8. doi: 10.1038/leu.2015.212

37. Zeiser R, von Bubnoff N, Butler J, Mohty M, Niederwieser D, Or R, et al. Ruxolitinib for glucocorticoid-refractory acute graft-versus-host disease. *N Engl J Med.* (2020) 382:1800–10. doi: 10.1056/NEJMoa1917635

38. Schulte-Schrepping J, Reusch N, Paclik D, Baßler K, Schlickeiser S, Zhang B, et al. Severe COVID-19 is marked by a dysregulated myeloid cell compartment. *Cell.* (2020) 182:1419–40.e23. doi: 10.1016/j.cell.2020.08.001

39. Copaescu A, Smibert O, Gibson A, Phillips E, Trubiano J. The role of IL-6 and other mediators in the cytokine storm associated with SARS-CoV-2 infection. *J Allergy Clin Immunol.* (2020) 146:518–534.e1. doi: 10.1016/j.jaci.2020.07.001

40. Zhou T, Su T, Mudianto T, Wang J. Immune asynchrony in COVID-19 pathogenesis and potential immunotherapies. *J Exp Med.* (2020) 217:e20200674. doi: 10.1084/jem.20200674

41. Chen S, Zeiser R. Novel biomarkers for outcome after allogeneic hematopoietic stem cell transplantation. *Front Immunol.* (2020) 11:1854. doi: 10.3389/fimmu.2020.01854

42. Shevchenko A, Tomas H, Havli J, Olsen JV, Mann M. In-gel digestion for mass spectrometric characterization of proteins and proteomes. *Nat Protoc.* (2006) 1:2856–60. doi: 10.1038/nprot.2006.468

43. Elsemüller A, Tomalla V, Gärtner U, Troidl K, Jeratsch S, Graumann J, et al. Characterization of mast cell-derived rRNA-containing microvesicles and their inflammatory impact on endothelial cells. *FASEB J.* (2019) 33:5457–67. doi: 10.1096/fj.201801853RR

44. Wu C, Jeratsch S, Graumann J, Stainier D. Modulation of mammalian cardiomyocyte cytokinesis by the extracellular matrix. *Circ Res.* (2020) 127:896–907. doi: 10.1161/CIRCRESAHA.119.316303

45. Kiweler M, Looso M, Graumann J. MARMoSET – extracting publication-ready mass spectrometry metadata from RAW files. *Mol Cell Proteomics.* (2019) 18:1700–2. doi: 10.1074/mcp.TIR119.001505

46. Deutsch, E, Bandeira N, Perez-Riverol Y, Sharma V, Carver J, Mendoza L, et al. The ProteomeXchange consortium at 10 years: 2023 update. *Nucleic Acids Res.* (2023) 51:D1539–48. doi: 10.1093/nar/gkac1040

47. Cox J, Mann M. MaxQuant enables high peptide identification rates, individualized p.p.b.-range mass accuracies and proteome-wide protein quantification. *Nat Biotechnol.* (2008) 26:1367–72. doi: 10.1038/nbt.1511

48. R Core Team. *R: A Language and Environment for Statistical Computing*. Vienna: R Foundation for Statistical Computing (2022).

49. Bhagwat, A, Hayat S, Graumann J. Bhagwataditya/A*utonomics: Generifying and Intuifying Cross-Platform Omics Analysis. R package version 1.6.0. 2022. (2022). Available from: https://github.com/bhagwataditya/autonomics.

50. Ritchie M, Phipson B, Wu D, Hu Y, Law C, Shi W, et al. limma powers differential expression analyses for RNA-sequencing and microarray studies. *Nucleic Acids Res.* (2015) 43:e47–47. doi: 10.1093/nar/gkv007

51. Guo K, McGregor B. *VennDetail: A Package for Visualization and Extract Details. R package version 1.14.0. 2022.* (2021). Available online at: from: https://github.com/guokai8/VennDetail (accessed July 28, 2021).

52. Wu T, Hu E, Xu S, Chen M, Guo P, Dai Z, et al. Clusterprofiler 4.0: a universal enrichment tool for interpreting omics data. *Innovation.* (2021) 2:100141. doi: 10.1016/j.xinn.2021.100141

53. Lippmann C, Kringel D, Ultsch A, Lötsch J. Computational functional genomics-based approaches in analgesic drug discovery and repurposing. *Pharmacogenomics.* (2018) 19:783–97. doi: 10.2217/pgs-2018-0036

54. Yu G. *E*nrichplot: Visualization of Functional Enrichment Result. R package version 1.18.3. 2022.* (2022). Available from: https://yulab-smu.top/biomedical-knowledge-mining-book/ (accessed January 31, 2023).

55. Skevaki C, Hudemann C, Matrosovich M, Möbs C, Paul S, Wachtendorf A, et al. Influenza-derived peptides cross-react with allergens and provide asthma protection. *J Allergy Clin Immunol.* (2018) 142:804–14. doi: 10.1016/j.jaci.2017.07.056

56. Rein L, Calero K, Shah R, Ojielo C, Hudock K, Lodhi S, et al. Randomized phase 3 trial of ruxolitinib for COVID-19–associated acute respiratory distress syndrome. *Crit Care Med.* (2022) 50:1701–13.

57. Vogt L, Schmitz N, Kurrer M, Bauer M, Hinton H, Behnke S, et al. VSIG4, a B7 family–related protein, is a negative regulator of T cell activation. *J Clin Invest.* (2006) 116:2817–26. doi: 10.1172/JCI25673

58. Hu B, Huang S, Yin L. The cytokine storm and COVID-19. *J Med Virol.* (2021) 93:250–6. doi: 10.1002/jmv.26232

59. Han M, Antila M, Ficker J, Gordeev I, Guerreros A, Bernus A, et al. Ruxolitinib in addition to standard of care for the treatment of patients admitted to hospital with COVID-19 (RUXCOVID): a randomised, double-blind, placebo-controlled, phase 3 trial. *Lancet Rheumatol.* (2022) 4:e351–61. doi: 10.1016/S2665-9913(22)00044-3

60. Quiros J, Ross-Comptis J, Hathaway D, Sarfraz A, Sarfraz Z, Grigoryan Z, et al. Ruxolitinib and the mitigation of severe COVID-19: a systematic review and meta-analysis. *Infect Chemother.* (2021) 53:436–48. doi: 10.3947/ic.2020.0126

61. Niu J, Lin Z, He Z, Yang X, Qin L, Feng S, et al. Janus kinases inhibitors for coronavirus disease-2019: a pairwise and Bayesian network meta-analysis. *Front. Med.* (2022) 9:973688. doi: 10.3389/fmed.2022.973688

62. Kramer A, Prinz C, Fichtner F, Fischer A, Thieme V, Grundeis F, et al. Janus kinase inhibitors for the treatment of COVID-19. *Cochrane Database Syst Rev.* (2022) 6:CD015209.

63. Mantov N, Zrounba M, Brollo M, Grassin-Delyle S, Glorion M, David M, et al. Ruxolitinib inhibits cytokine production by human lung macrophages without impairing phagocytic ability. *Front Pharmacol.* (2022) 13:896167. doi: 10.3389/fphar.2022.896167

64. Huarte E, Peel M, Verbist K, Fay B, Bassett R, Albeituni S, et al. Ruxolitinib, a JAK1/2 inhibitor, ameliorates cytokine storm in experimental models of hyperinflammation syndrome. *Front Pharmacol.* (2021) 12:650295. doi: 10.3389/fphar.2021.650295

65. Arthur L, Esaulova E, Mogilenko D, Tsurinov P, Burdess S, Laha A, et al. Cellular and plasma proteomic determinants of COVID-19 and non-COVID-19 pulmonary diseases relative to healthy aging. *Nat Aging.* (2021) 1:535–49. doi: 10.1038/s43587-021-00067-x

66. Ciccosanti F, Antonioli M, Sacchi A, Notari S, Farina A, Beccacece A, et al. Proteomic analysis identifies a signature of disease severity in the plasma of COVID-19 pneumonia patients associated to neutrophil, platelet and complement activation. *Clin Proteomics.* (2022) 19:38. doi: 10.1186/s12014-022-09377-7

67. McLaughlin K, Bechtel M, Bojkova D, Münch C, Ciesek S, Wass M, et al. COVID-19-related coagulopathy—is transferrin a missing link? *Diagnostics.* (2020) 10:539. doi: 10.3390/diagnostics10080539

68. Yin K, Peluso M, Thomas R, Shin M, Neidleman J, Luo X, et al. Long COVID manifests with T cell dysregulation, inflammation, and an uncoordinated adaptive immune response to SARS-CoV-2. *bioRxiv [Preprint].* (2023)

69. Khalid Z, Huan M, Sohail Raza M, Abbas M, Naz Z, Kombe Kombe A, et al. Identification of novel therapeutic candidates against SARS-CoV-2 infections: an application of RNA sequencing toward mRNA based nanotherapeutics. *Front Microbiol.* (2022) 13:901848. doi: 10.3389/fmicb.2022.901848

70. Alfaro E, Díaz-García E, García-Tovar S, Zamarrón E, Mangas A, Galera R, et al. Upregulated proteasome subunits in COVID-19 patients: a link with hypoxemia, lymphopenia and inflammation. *Biomolecules.* (2022) 12:442.

71. Sharapova T, Romanova E, Chernov A, Minakov A, Kazakov V, Kudriaeva A, et al. Protein PGLYRP1/Tag7 peptides decrease the proinflammatory response in human blood cells and mouse model of diffuse alveolar damage of lung through blockage of the TREM-1 and TNFR1 receptors. *Int J Mol Sci.* (2021) 22:11213. doi: 10.3390/ijms222011213

72. Chen Y, Yao H, Zhang N, Wu J, Gao S, Guo J, et al. Proteomic analysis identifies prolonged disturbances in pathways related to cholesterol metabolism and myocardium function in the COVID-19 recovery stage. *J Proteome Res.* (2021) 20:3463–74. doi: 10.1021/acs.jproteome.1c00054

73. Nguyen T, Yoon H, Kim Y, Choi Y, Lee W, Jin M. Tryptophanyl-tRNA synthetase 1 signals activate TREM-1 via TLR2 and TLR4. *Biomolecules.* (2020) 10:1283. doi: 10.3390/biom10091283

74. Lipman D, Safo S, Chekouo T. Multi-omic analysis reveals enriched pathways associated with COVID-19 and COVID-19 severity. *PLoS One.* (2022) 17:e0267047. doi: 10.1371/journal.pone.0267047

75. Feng Y, Tang K, Lai Q, Liang J, Feng M, Zhou Z, et al. The landscape of aminoacyl-tRNA synthetases involved in severe acute respiratory syndrome Coronavirus 2 infection. *Front Physiol.* (2022) 12:818297. doi: 10.3389/fphys.2021.818297

76. Braun L, Zeiser R. Kinase inhibition as treatment for acute and chronic graft-versus-host disease. *Front Immunol.* (2021) 12:760199. doi: 10.3389/fimmu.2021.760199

77. Olagnier D, Farahani E, Thyrsted J, Blay-Cadanet J, Herengt A, Idorn M, et al. SARS-CoV2-mediated suppression of NRF2-signaling reveals potent antiviral and anti-inflammatory activity of 4-octyl-itaconate and dimethyl fumarate. *Nat Commun.* (2020) 11:4938. doi: 10.1038/s41467-020-18k764-3

78. Pihl R, Jensen R, Poulsen E, Jensen L, Hansen A, Thøgersen I, et al. ITIH4 acts as a protease inhibitor by a novel inhibitory mechanism. *Sci Adv.* (2023) 7:eaba7381. doi: 10.1126/sciadv.aba7381

79. Park J, Kim H, Kim S, Kim Y, Lee J, Dan K, et al. In-depth blood proteome profiling analysis revealed distinct functional characteristics of plasma proteins between severe and non-severe COVID-19 patients. *Sci Rep.* (2020) 10:22418. doi: 10.1038/s41598-020-80120-8

80. Geyer P, Arend F, Doll S, Louiset M, Virreira Winter S, Müller-Reif J, et al. High-resolution serum proteome trajectories in COVID-19 reveal patient-specific seroconversion. *EMBO Mol Med.* (2021) 13:e14167. doi: 10.15252/emmm.202114167

81. Völlmy F, van den Toorn H, Zenezini Chiozzi R, Zucchetti O, Papi A, Volta C, et al. A serum proteome signature to predict mortality in severe COVID-19 patients. *Life Sci Alliance.* (2021) 4:e202101099.

82. Tyrkalska S, Martínez-López A, Arroyo A, Martínez-Morcillo F, Candel S, García-Moreno D, et al. Differential proinflammatory activities of Spike proteins of SARS-CoV-2 variants of concern. *Sci Adv.* (2023) 8:eabo0732. doi: 10.1126/sciadv.abo0732

frontiers | Frontiers in Immunology

TYPE Original Research
PUBLISHED 03 July 2023
DOI 10.3389/fimmu.2023.1117102

OPEN ACCESS

EDITED BY
Chrysanthi Skevaki,
Universities of Giessen and Marburg Lung Center, Germany

REVIEWED BY
Demba Sarr,
University of Georgia, United States
Wendy Watford,
University of Georgia, United States

*CORRESPONDENCE
Haruki Kitazawa
haruki.kitazawa.c7@tohoku.ac.jp
Julio Villena
jcvillena@cerela.org.ar

†These authors have contributed equally to this work

‡JSPS Research Fellow

RECEIVED 06 December 2022
ACCEPTED 14 June 2023
PUBLISHED 03 July 2023

CITATION
Fukuyama K, Zhuang T, Toyoshi E, Raya Tonetti F, Saha S, Zhou B, Ikeda-Ohtsubo W, Nishiyama K, Aso H, Villena J and Kitazawa H (2023) Establishment of a porcine bronchial epithelial cell line and its application to study innate immunity in the respiratory epithelium. *Front. Immunol.* 14:1117102. doi: 10.3389/fimmu.2023.1117102

Establishment of a porcine bronchial epithelial cell line and its application to study innate immunity in the respiratory epithelium

Kohtaro Fukuyama[1,2†], Tao Zhuang[3†], Eita Toyoshi[1†], Fernanda Raya Tonetti[4†], Sudeb Saha[1,2,5‡], Binghui Zhou[1,2], Wakako Ikeda-Ohtsubo[1,2], Keita Nishiyama[1,2], Hisashi Aso[2,3], Julio Villena[1,4*] and Haruki Kitazawa[1,2*]

[1]Food and Feed Immunology Group, Laboratory of Animal Food Function, Graduate School of Agricultural Science, Tohoku University, Sendai, Japan, [2]Livestock Immunology Unit, International Education and Research Center for Food and Agricultural Immunology (CFAI), Graduate School of Agricultural Science, Tohoku University, Sendai, Japan, [3]Laboratory of Animal Health Science, Graduate School of Agricultural Science, Tohoku University, Sendai, Japan, [4]Laboratory of Immunobiotechnology, Reference Centre for Lactobacilli (CERELA-CONICET), Tucuman, Argentina, [5]Department of Dairy Science, Sylhet Agricultural University, Sylhet, Bangladesh

In vitro culture models that precisely mirror the porcine respiratory epithelium are needed to gain insight into how pathogens and host interact. In this study, a new porcine bronchial epithelial cell line, designated as PBE cells, was established from the respiratory tract of a neonatal pig. PBE cells assumed a cobblestone-epithelial like morphology with close contacts between the cells when they reached confluence. The PBE cell line was characterized in terms of its expression of pattern recognition receptors (PRRs) and its ability to respond to the activation of the Toll-like receptor 3 (TLR3) and TLR4 signaling pathways, which are key PRRs involved in the defense of the respiratory epithelium against pathogens. PBE cells stimulated with poly(I:C) were able to up-regulate the expression of *IFN-β*, *IFN-λ1* (*IL-29*), *IFN-λ3* (*IL-28B*), the antiviral factors *Mx1*, *OAS1*, and *PKR*, as well as the viral PRRs *RIG-1* and *MDA5*. The expression kinetics studies of immune factors in PBE cells allow us to speculate that this cell line can be a useful *in vitro* tool to investigate treatments that help to potentiate antiviral immunity in the respiratory epithelium of the porcine host. In addition, poly(I:C) and LPS treatments increased the expression of the inflammatory cytokines *TNF-α*, *IL-6*, *IL-8*, and *MCP-1/CCL2* and differentially modulated the expression of negative regulators of the TLR signaling pathways. Then, PBE cells may also allow the evaluation of treatments that can regulate TLR3- and TLR4-mediated inflammatory injury in the porcine airway, thereby protecting the host against harmful overresponses.

KEYWORDS

respiratory epithelium, epithelial cells, TLR3, viral immunity, TLR4, porcine respiratory epithelial cell line

Introduction

Respiratory tract infections (RTIs) have been a major cause of morbidity and mortality in humans and animals historically. The improved sanitation, the greater access to health care, the research and development in antimicrobials, and the implementation of vaccines have helped to significantly diminish the incidence and severity of RTIs in humans (1). However, these advances have not been paralleled in the prevention of RTIs in animals of economic importance. The large-scale intensified animal production systems with high-density of individuals in confined spaces and the use of genetically homogenous populations in farms have been major drivers of pathogen spread (1). The prevention of RTIs in livestock is of great importance, not only because of the economic impact associated with the loss of animals, weight loss and reduced weight gain (2), but also because of its direct effect on human health. The modern systems for animal production often serve as the interface between wild and human populations, and multiple viral spillover events have occurred at this nexus (1). In addition, animal trade has contributed to multiple outbreaks globally, particularly RTIs. Perhaps the best example is the swine influenza virus (SIV) that has become endemic in pigs worldwide and was able to cross species barrier to infect humans causing the influenza pandemic in 2009 (3).

Pigs are relevant as livestock and RTIs are one of the main causes of economic losses in the swine industry (2). Both, bacterial and viral pathogens can colonize and infect the porcine respiratory tract causing from mild symptoms to severe lung diseases. Furthermore, it was reported that bacterial and viral pathogens can be detected in various combinations in porcine RTIs, indicating that these infectious diseases are often polymicrobial (2, 4). It was suggested that the onset of porcine RTIs is generally related to a primary viral infection that produce alterations in the respiratory mucosa promoting the secondary bacterial colonization (2, 4), as it has been described for humans (5, 6). Primary viral pathogens such as porcine reproductive and respiratory syndrome virus (PRRSV), porcine respiratory coronavirus (PRCV) and SIV are endemic in pig farms (2), and in addition to being a cause of morbidity, they can favor secondary bacterial infections through the damage of the respiratory epithelium and the impairment of mucosal immunity. The efficient prevention of respiratory viral infections in the porcine host could not only help to mitigate their consequences but also to reduce the incidence and severity of secondary bacterial infections.

Pathogens infecting the porcine respiratory mucosa via aerosols and/or droplets often initiate their replication in respiratory epithelial cells (RECs) in the upper tract (7). After this first replication, pathogens can disseminate and infect RECs from the lower respiratory tract inducing more severe diseases such as pneumonia or bronchitis. As seen in other mucosal surfaces, the RECs are at the interface with the environment and therefore they are of key importance in host defense. RECs facilitate mucociliary clearance and produce antimicrobial compounds to avoid the colonization of infectious pathogens (7). In addition, RECs express pattern recognition receptors (PRRs) that recognize structural components of microbes designated as microbial-associated molecular patterns (MAMPs). The recognition of MAMPs by RECs generates immunological changes in these cells that contribute to limit infections and help to coordinate the response of immune cells. In fact, complex interactions exist between RECs and mucosal immune cells that modulate their response to pathogens in a bidirectional way (7). Considering the important role of RECs in the defense of the respiratory mucosa, *in vitro* systems based on these cells have been proposed to advance in the knowledge of pathogen-host interaction as well as to investigate preventive and therapeutic alternatives that help to mitigate the impact of RTIs.

Primary RECs cultures and cell lines of human origins have been successfully used to investigate host-microbe interaction (reviewed in (8). These *in vitro* tools, which accurately represents the host biology because of the expression of relevant host factors and have less ethical concern than animal models, are of value to explore respiratory infections and characterize potential therapeutics for human RTIs (8). On the other hand, RECs of porcine origin have been studied only to a limited extent. In fact, porcine RECs cultures have been used mainly to study the replication, cytopathic effects, and immune responses of influenza virus (IFV) (9–12). Species-specific differences in the response of cells to viral challenges were observed. The Nipah virus (NiV) infects the respiratory tract of both humans and pigs. However, while NiV-infected pigs develop an acute and often severe inflammatory-mediated respiratory disease, symptoms are seen only in few NiV-infected human patients (13). Comparative studies using primary cultures of human and porcine bronchial epithelial cells infected with NiV revealed that both RECs responded to NiV infection by producing IFN-λ and antiviral factors (*OAS* and *ISG-56*). Human cells were more efficient than porcine cells to up-regulate *IFN-λ* and antiviral factors, which correlated with lower viral RNA content (13). Of note, while porcine bronchial epithelial cells had a reduced capacity to produce IFN-λ, they were capable to strongly express the proinflammatory cytokines *IL-6* and *IL-8*, which were suggested to contribute to inflammatory-pathology. Similar results were described for IFV. Human RECs express significantly higher levels of *IFN-β*, *IFN-λ*, *ISG15*, *Mx1*, and *OAS1* after the challenge with IFV than porcine cells. Furthermore, porcine RECs not only mounted an innate immune response that was lower in magnitude, but it was also delayed compared to human cells (14). Altogether, these results highlight the differences in the immune response of human and porcine RECs, indicating that species-specific cells are needed to investigate treatments that have true therapeutic value *in vivo*. Thus, reproducible *in vitro* culture models that precisely mirror the porcine respiratory epithelium are needed to gain insight into how pathogens and host interact. Investigating the expression of PRRs in porcine RECs, the activation and regulation of the related signaling pathways, their detailed immune response to PAMPs, and the influence of respiratory commensal bacteria in such responses are examples of the knowledge that should be generated to better design strategies to protect the porcine host from RTIs.

In the present study, we established a new porcine bronchial epithelial cell line designated as PBE cells from the respiratory tract of a neonatal pig. We characterized the PBE cell line in terms of its

expression of PRRs and its ability to respond to the activation of the TLR3 and TLR4 signaling pathways, which are key PRRs involved in the defense of the respiratory epithelium against viral and bacterial pathogens, respectively.

Materials and methods

Animals and experimental tissues

Bronchial tissues were obtained from a neonatal LWD pig (Hiruzu Co., Ltd., Miyagi, Japan). The piglet for the bronchial tissue sampling was clinically healthy and free of infectious diseases as assessed by examination of a veterinarian. The piglet was slaughtered by electroshock and bloodletting according to the approved procedures. All procedures were conducted in accordance with the Guidelines for Animal Experimentation of Tohoku University, Japan, under the protocol number 2019 Noudou-038-02.

Isolation and cloning of PBE cells

Tissue pieces of the bronchus were collected from a 7-day piglet. The epithelial layer of the bronchus was scraped with a razor blade, and then transferred to 15 ml tubes containing serum free Dulbecco's modified Eagle medium (DMEM, GIBCO, NY, USA), supplemented with penicillin (10 U/ml) and streptomycin (10 μg/ml). The tube was centrifuged at 1,500 rpm for 10 min at 4°C, and then the supernatant was removed. After washing three times with DMEM, the tissue pieces were transferred to collagen coated flasks (Sumilon, Tokyo, Japan) containing 10% FBS-DMEM, and then incubated at 37°C with 5% CO_2.

In order to establish the PBE cell line, the epithelial cells of the primary cultures were cloned using the limiting dilution method after several passages of the primary culture. The cells were treated with a sucrose/EDTA buffer (pH 7.5; 0.45 M sucrose, 0.36% EDTA in PBS) for 3 min at 37°C, detached using 0.04% trypsin/PBS (GIBCO, NY, USA), and then diluted to 50 cells/ml in 10% FBS-DMEM. The cells were seeded on a collagen-coated 96-well plate (Sumilon, Tokyo, Japan). Each well was checked for cell growth and monoclonal expansion at day 4 after plating by microscopic analysis. A single colony of rapidly growing cells with epithelial-like morphology was found. Then the cells were passaged for the immortalization and the immunocytochemical analysis.

Immortalization

The porcine bronchial epithelial cells were used for transfection with pSV3-neo (ATCC, MA, USA). This plasmid codes for the oncogene SV40 large T antigen and a neomycin (G418)-resistance gene. For transfection, 1×10^6 cells were electroporated and treated with 1μg of SV40 large t antigen DNA per tip in 10 μl in the Neon™ Transfection System (Invitrogen, CA, USA) with. The cells were seeded in a collagen-coated 6 well plate containing 10% FBS-DMEM with 200 μg/ml G418 for the selection of transfected cells. After 5 days culture, the cells were collected and transferred to flasks for further characterization and maintained in culture.

Immunocytochemical staining

The PBE cells were seeded on a collagen-coated 8-well culture-slide at a cell density of 2×10^4 cells/cm^2 for several days, washed with cold PBS once and then fixed with methanol and acetone (vol/vol) for 15 min at -20°C. After washing three times with PBS, the cells were treated with bovine serum albumin containing PBS for 20 min at room temperature. After washing three times with PBS, the cells were incubated with mouse monoclonal anti-SV40 T-antigen antibody (1/50 dilution, Abcam, CA, UK) or mouse monoclonal anti-cytokeratin, pan (mixture) antibody (1/50 dilution, Sigma-Aldrich, MA, USA). The cells were also incubated with rabbit polyclonal anti-ZO-1 antibody (1/2000 dilution, 21773-1-AP, Proteintech, IL, USA), mouse monoclonal anti-occludin antibody (1/3000 dilution, 66378-1-lg, Proteintech, IL, USA), rabbit anti-alpha-tubulin antibody (1/100 dilution, Proteintech, IL, USA), rabbit anti-E-cadherin antibody (1/200 dilution, Proteintech, IL, USA), rabbit anti-muc5B antibody (1/100 dilution, Proteintech, IL, USA), rabbit polyclonal anti-TLR3 antibody (1/100 dilution, GTX113022, Genetex, CA, USA), rabbit polyclonal anti-TLR4 antibody (1/100 dilution, BS-1021R, Bioss Antibodies, MA, USA) or rabbit polyclonal anti-TLR7 antibody (1/100 dilution, BS-6601R, Bioss Antibodies, MA, USA) overnight at 4°C in the dark. The PBE cells were washed three times with PBS, treated with secondary Alexa Fluor 488 conjugated Goat anti-rabbit IgG antibody (1/500 dilution, A-11008, Thermo Fisher Scientific, MA, USA), or Alexa Fluor 488 conjugated Goat anti-mouse IgG antibody (1/500 dilution, A-11001, Thermo Fisher Scientific, MA, USA) for 1h at 4°C in the dark. The PBE cells were washed three times with PBS, treated with secondary Alexa Fluor 488 conjugated donkey anti mouse IgG antibody (1/200 dilution, Jackson Immuno Research, PA, USA), or Alexa Fluor 488 conjugated donkey anti rabbit IgG antibody (1/200 dilution, Jackson Immuno Research, PA, USA) for 1h at -4°C in the dark. After three times washing by PBS, the cells were counterstained with 40,6-diamidino-2-phenylindole (DAPI) for 5 min at room temperature in the dark, and then washed three times with PBS. Cells treated only with secondary antibodies but not with the primary antibodies were used as controls. Slide images were viewed using a Laser Scanning Microscope BZ-9000 (Keyence, Tokyo, Japan), and photographed at 200× with software BZ II Viewer, Version 1.4.0.0.

Cell viability

PBE cells were seeded on a collagen-coated 24 well plate (MS0024, Sumitomo Bakelite, Tokyo, Japan) at an initial

10.3389/fimmu.2023.1117102

concentration of 0.5×104 cells/cm^2 or 1×10^4 cells/cm^2. Cells were collected by Accutase (12679-54, NACALAI TESQUE, Kyoto, Japan) after washing with PBS and mixed cell suspension and Trypan blue stain 1:1. Cell counts were determined by a blood cell counting board every day for 6 days.

Transepithelial electrical resistance analysis

PBE cells were seeded on a collagen-coated inserts 24-well plate (0.4 µm pore size, 354444, Corning, AZ, USA) at an initial concentration of 1×10^5, 1.5×10^5 or 2.0×10^5 cells/well. Transepithelial electrical resistance (TEER) was measured every 2 days of cultivation of PBE cells in transwell inserts using an epithelial volt–ohm meter with a chopstick electrode (Millicell ERS-2, MERS00002, EMD Millipore, Billerica, MA). Triplicate measurements were recorded for each monolayer.

Quantitative expression analysis by real-time PCR

PBE cells were seeded at an initial concentration of 1.0 x 10^4 cells/cm^2. At day 6, PBE cells were stimulated with the TLR3 synthetic agonist poly(I:C) (100 ng/ml) or the TLR4 agonist LPS (1000 ng/ml). The expressions of immune factors were evaluated at several points after the treatments by quantitative real time PCR. The total RNA of PBE cells was isolated by using the TRIzol reagent (Invitrogen, Carlsbad, CA, USA) according to the manufacturer's instructions. The concentration and purity of isolated RNA was determined with NanoDrop® ND-1000 Spectrophotometer. Reverse transcription was performed with the PrimeScript RT reagent Kit (Takara Bio, Shiga, Japan) following the manufactures instructions. The quantitative real time PCR was conducted on a CFX Connect Real-time PCR System (Bio-rad, Hercules, CA, USA) using TB Green Premix Ex Taq (Takara Bio, Shiga, Japan) according to the manufacturer's recommendations. The thermal cycling conditions were 95°C for 30 followed by 40 cycles at 95°C for 5 s and 60°C for 30 s. The primers used were listed in Supplementary Table 1. The β-actin, which is stably expressed in various tissues of pigs, was used as a housekeeping gene (15, 16). The expression level of mRNA was calculated using the calibration curve obtained from serially diluted plasmids, which was normalized by the expression level of β-actin in each sample, and then expressed as relative with the control set as 1.

Statistical analysis

Experiments were performed in triplicate and results were expressed as mean ± standard deviation (SD). After verification of the normal distribution of data, 2-way ANOVA was used. Tukey's test (for pairwise comparisons of the means) was used to test for differences between the groups. Differences were considered significant at $p<0.05$.

Results

Establishment of PBE cells

The PBE cell line was developed using the simian virus 40 large T antigen (SV40). Primary culture cells were transfected with SV40 to create an immortalized cell line (Supplementary Figure 1). Although primary cells only survive between 3-4 passages, the immortalized PBE cells were successfully passaged more than 20 times.

In order to evaluate the growth kinetics of the PBE cells, two initial concentrations (0.5 x 10^4 or 1.0 x 10^4 cells/cm^2) were used, and cells were evaluated until they reached confluence (Figure 1). The cells grew continuously until day 5, reaching confluence between days 5 and 6. The different initial concentration was reflected in different cell densities up to day 4. However, no significant differences in cell densities were observed between days 5 and 6 for the different initial concentrations. Microscopic analysis demonstrated that the PBE cells assumed a cobblestone-epithelial like morphology with close contacts between the cells when they reached confluence (Figure 1). The initial seeding concentration of 1.0 x 10^4 cells/cm^2 was selected for further experiments.

SEM microscopic analysis was performed to characterize the surface of PBE cells at days 2, 10 and 20 (Figure 2). SEM study revealed the formation of cilia on the apical surface of PBE cells, which increased in size over time. This feature is a characteristic of respiratory epithelial cells. To further evaluate the epithelial nature of PBE cells, we performed immunohistochemical analysis to determine the expression of cytokeratin. PBE cells uniformly expressed cytokeratin as shown in Figure 3, confirming that PBE cells possess an epithelial phenotype. Tubulin was also evaluated in PBE cells and results demonstrated a strong expression of this protein (Figure 3). In addition, we studied the expression of proteins involved in cell-to-cell contact in the PBE cell line. It is well known that tight junctions or zona occludens (ZO) allow close contact between epithelial cells contributing to the maintenance of cell polarity and blocking the movement of transmembrane proteins between the apical and the basolateral cell surfaces. The ZO-1 function as an adaptor protein that link junctional transmembrane proteins, such as occludin and claudin, to the actin cytoskeleton. Thus, we studied the expression of ZO-1, occludin and E-cadherin in PBE cells (Figure 3). The expression of the three proteins was clearly observed in the PBE cells, particularly in the cell-to-cell contact regions. To measure the integrity of tight junction dynamics in PBE cells cultures the TEER analysis was applied. It was observed that the electrical resistance of the cellular monolayer gradually increased during a 11-days period (Supplementary Figure 2), confirming the establishment of a barrier. A low production of mucus was detected in PBE cells (data not shown). In order to confirm the production of mucus by the new cell line, we evaluated the expression of muc5B protein (Figure 3). The immunofluorescence study demonstrated a low expression of muc5B in the PBE cells.

Our results indicate that PBE cells reach a 100% confluent monolayer by 6 days of culture. Then, confluent PBE cells that have

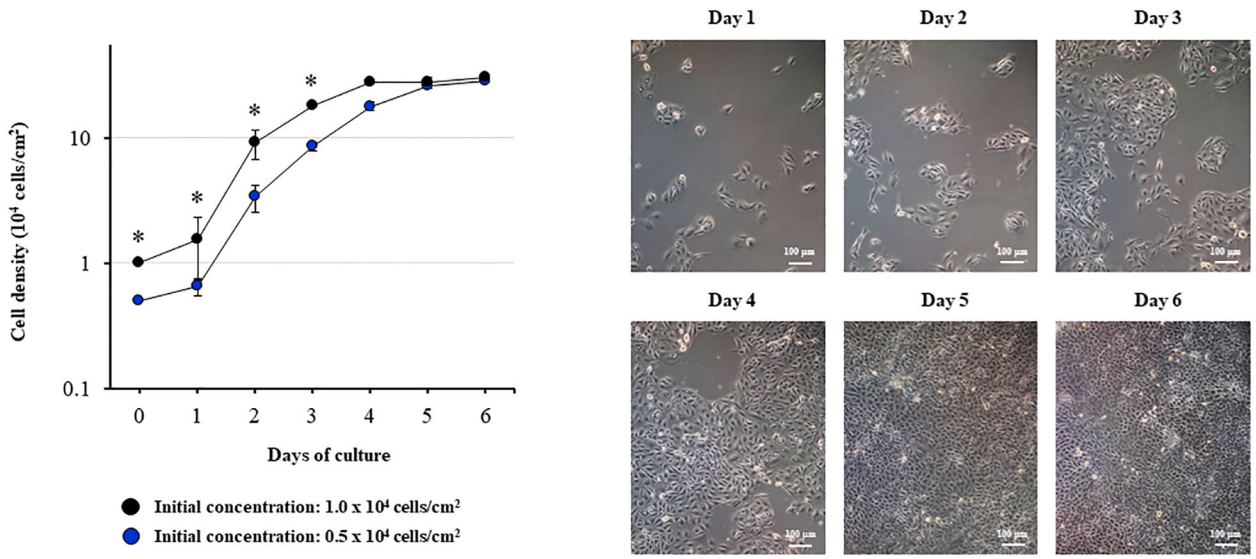

FIGURE 1
Growth kinetics of the originally established porcine bronchial epithelial (PBE) cell line. PBE cells were seeded at an initial concentration of 0.5 x 10^4 or 1.0 x 10^4 cells/cm^2 and evaluated during six days to determine cell density. Microscope photographs show the growth of cells seeded at an initial concentration of 0.5 x 10^4 cells/cm^2 from day 1 to day 6, in which the cells assumed a cobblestone-epithelial like morphology with close contacts between the cells. Results represent data from three independent experiments. Asterisks indicate significant differences in cell densities between the curves with distinct initial concentrations. * ($P < 0.05$).

separated the apical and basolateral compartments were used for further experiments.

Expression of PRRs in PBE cells

We next aimed to evaluate whether the PBE cell line expressed relevant genes of the PRRs families that are involved in the recognition of microorganisms in the respiratory epithelium. We focused our studies in the expressions of PRRs from the Toll-like receptor (TLR) and the nucleotide-binding oligomerization domain-containing protein (NOD) families. The qPCR analysis revealed that PBE cells express *TLR1-9*, being *TLR3*, *TLR4* and *TLR7* the ones more highly expressed in this cell line (Figure 4). We also detected the expression of *NOD1* and *NOD2* in PBE cells (Figure 4). In order to confirm the expression of TLR3, TLR4 and TLR7 and to evaluate their cellular location, we performed immunohistochemical analysis (Figure 4). Both TLR3 and TLR7 were detected in a granular pattern in areas close to the cell nucleus, indicating their expression in endosomes. As expected, TLR4 was detected near the nucleus of cells but also in the cellular membrane (Figure 4).

Response of PBE cells to the activation of TLR3 signaling pathway

Considering the strong expression of TLR3 in PBE cells and the relevant role of this PRR in the defense of the respiratory epithelium against viral pathogens, we next aimed to characterize their response to the TLR3 signaling pathway activation. PBE cells were stimulated with the synthetic TLR3 agonist poly(I:C) and

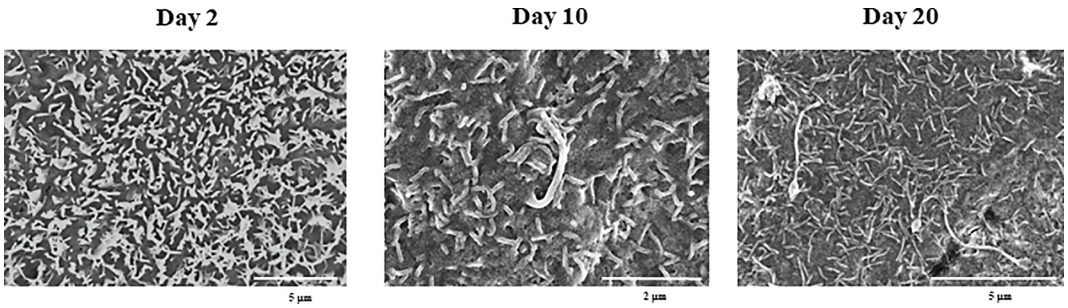

FIGURE 2
Scanning electron microscopy (SEM) characterization of the originally established porcine bronchial epithelial (PBE) cell line. PBE cells were seeded at an initial concentration of 1.0 x 10^4 cells/cm^2 and evaluated at days 2, 10 and 20 by SEM analysis. SEM photographs show the surface of PBE cells in which the formation of cilia that increase in size over time can be distinguished. Results represent data from two independent experiments.

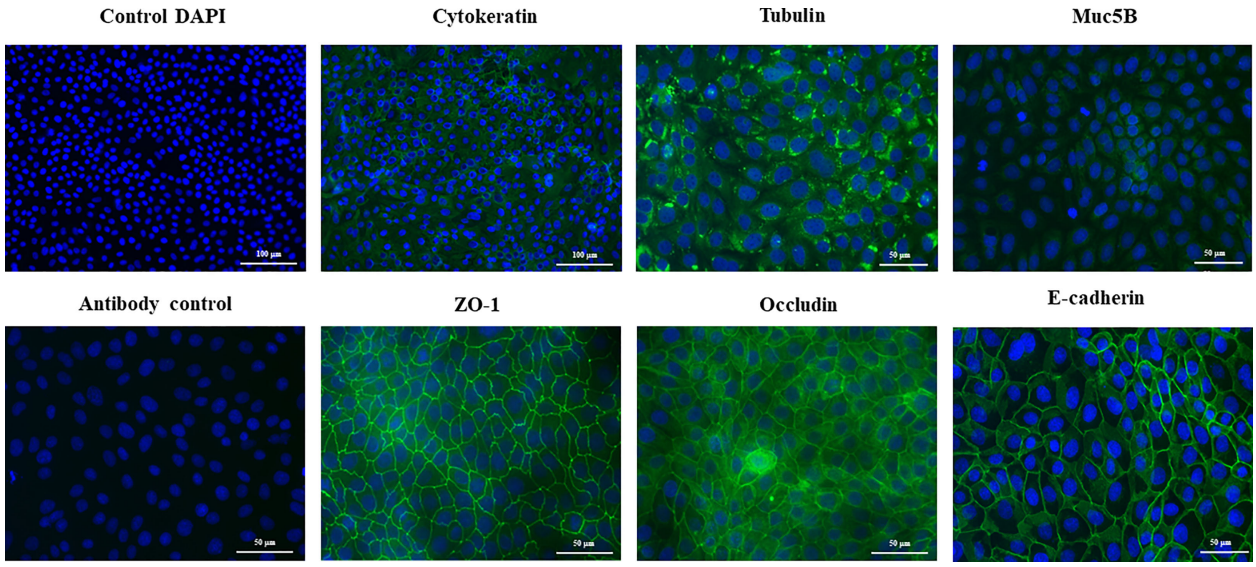

FIGURE 3
Immunohistochemical characterization of the originally established porcine bronchial epithelial (PBE) cell line. PBE cells were seeded at an initial concentration of 1.0 x 10^4 cells/cm^2 and evaluated at day 6. Photographs show the PBE cells stained with fluorescent antibodies directed to cytokeratin, tubulin, muc5B protein, the peripheral membrane phosphoprotein zona occludens 1 (ZO-1), occludin or E-cadherin. Cell nuclei were stained with DAPI. Antibody controls were performed by incubating cells with secondary antibodies without the addition of primary antibodies. The photographs show antibody control for ZO-1. Results represent data from two independent experiments.

the expressions of *IFN-β*, *IFN-λ1* (*IL-29*), *IFN-λ3* (*IL-28B*) and the antiviral factors *Mx1*, *OAS1*, and *PKR* were evaluated by qPCR at several time points (Figure 5). Poly(I:C) stimulation increased the expression of *IFN-β*, *IFN-λ1*, and *IFN-λ3* in PBE cells. A peak at hour 6 was observed for *IFN-β*, which then started to decrease until hour 24. For *IFN-λ1* and *IFN-λ3* the peak was detected later at hour 12 (Figure 5). Consistent with the peak of *IFN-β* at hour 6, the IFN-induced genes *Mx1*, *OAS1*, and *PKR* were significantly increased from hour 12 and remained elevated until hour 24 (Figure 5). The changes in the expression of the viral PRRs *RIG-1* and *MDA5* were also evaluated (Figure 6). *MDA5* was significantly increased in PBE cells stimulated with poly(I:C) from hour 6, reaching a peak at hour 12. On the other hand, *RIG-I* was enhanced from hour 12 (Figure 6).

We also evaluated the changes in the expressions of inflammatory cytokines and chemokines in PBE cells stimulated with poly(I:C) (Figure 7). The activation of the TLR3 signaling pathway in PBE cells triggered the up-regulation of *TNF-α, IL-6, IL-8*, and *MCP-1/CCL2. TNF-α* and *IL-8* showed a peak at hour 6 and then decreased gradually until hour 24. The peak for the expression of *IL-6* and *MCP-1* was observed at hour 12 (Figure 7).

We assessed whether poly(I:C) treatment modified the expression of negative regulators of the TLR signaling pathway in PBE cells (Figure 8, Supplementary Figure 3). The expressions of the TLR negative regulators *A20, Bcl-3, IRAK-M*, *SIGIRR*, *MKP-1*, and *Tollip* were evaluated at several time points after TLR3 activation. No significant changes were detected for the expression of *SIGIRR*, *IRAK-M*, *Tollip* and *MKP-1* when poly(I:C)-stimulated PBE cells were compared to unstimulated controls (Supplementary Figure 3). Slight but statistically significant increase of *Bcl-3* were observed at hour 12 (Figure 8). The most notable change in the expression of the TLR negative regulators was observed for *A20*. An increase of more than 4-fold expression was detected for *A20* at hour 6, which then decreased until hour 24 (Figure 8).

Response of PBE cells to the activation of TLR4 signaling pathway

Our studies showed a strong expression of TLR4 in PBE cells (Figure 4). Considering the important role of this PRR in the inflammatory response triggered by LPS in the respiratory epithelium, we next aimed to characterize the response of PBE cells to the TLR4 signaling pathway activation. PBE cells were stimulated with the TLR4 agonist LPS and the expressions of *TNF-α, IL-6, IL-8*, and *MCP-1* were evaluated at several time points (Figure 9). *TNF-α* and *MCP-1* showed a peak at hour 6 and then decreased gradually until hour 24. The peak for the expression of *IL-8* was observed between hours 6 and 12; while *IL-6* elevated its expression from hour 3 and was maintained at those levels until the end of the studied period (Figure 9). When we evaluated the expressions of the TLR negative regulators in PBE cells after TLR4 activation, it was observed that *SIGIRR*, *MKP-1*, and *Tollip* were not modified (Supplementary Figure 4). In contrast, LPS stimulation significantly augmented the expression of *A20, Bcl-3*, and *IRAK-M* in PBE cells (Figure 10). An increase of *Bcl-3* was observed at hour 3, which then decreased until hour 24 while the expression of *IRAK-M* showed a peak at hour 12 (Figure 10). An increase of more than 4-fold expression was detected for *A20* between hours 3 and 12, which then decreased at hour 24 (Figure 10).

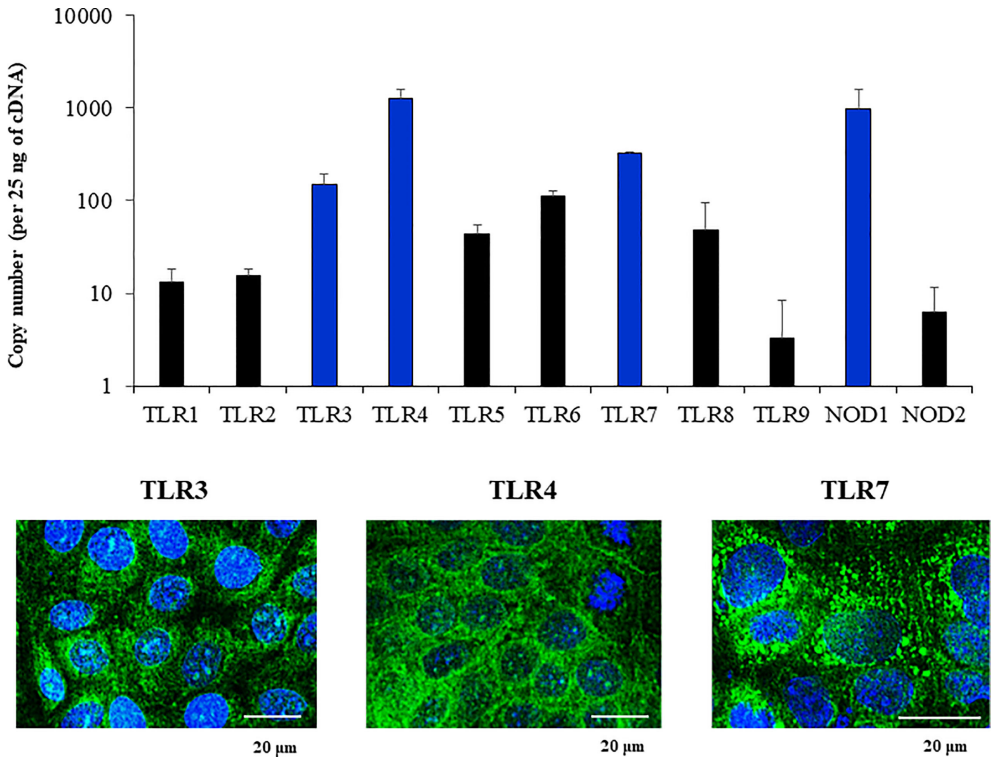

FIGURE 4
Expression of Pattern Recognition Receptors (PRRs) in the originally established porcine bronchial epithelial (PBE) cell line. PBE cells were seeded at an initial concentration of 1.0 x 10^4 cells/cm^2 and evaluated at day 6. The expressions of PRRs from the Toll-like receptor (TLR) and the nucleotide-binding oligomerization domain-containing protein (NOD) families were evaluated by qPCR. Results are expressed as copy numbers of the PRRS genes per 25 ng of cDNA. Photographs show the PBE cells stained with fluorescent antibodies directed to TLR3, TLR4, or TLR7. Cell nuclei were stained with DAPI. Results represent data from three independent experiments.

Discussion

The RECs lining the airway mucosa are key actors in host defense because of their capacity to interact with cells of the immune system (7, 17). Epithelial cells of the respiratory mucosa recognize pathogens via PRRs leading to the production of IFNs, cytokines and chemokines that render them and their neighboring cells in an alert state and cooperate to recruit and activate immune cells (18). Then, besides a barrier role, RECs have inherent innate immunity functions and for that reason they are of great interest in the study of immunity to infections. Both, primary RECs cultures and cell lines of human and porcine origins have been successfully used to investigate host-microbe interactions.

The use of primary RECs cultures has some limitations. The comparison of studies using primary cultures of RECs is not easy, because of the differences in the anatomic source of the cells, the use of undifferentiated versus differentiated cells, the culture methods as well as the donor variability (reviewed in (8). In addition, it was shown that primary RECs cultures are often contaminated with fibroblasts and can be passaged a limited number of times before the loss of epithelial integrity and senescence occurs (10), which is frequently accompanied by an altered gene expression (19). These facts significantly limit the number of experiments that can be performed with primary cultures. To avoid these disadvantages, models based on immortalized cell lines were developed, which were proved to be useful in the study of infections and immune responses at a cellular and molecular levels (8). Although there are several cell lines of human origin, there are less examples of porcine RECs lines (10, 20). A porcine lung epithelial cell line designated St. Jude porcine lung cells (SJPL) was established and proposed as a useful *in vitro* tool to investigate IFV replication (21) and immunity (22). However, it was demonstrated later that the SJPL cell line is not of porcine origin but of monkey origin (23). A porcine cell line designated as newborn pig trachea (NPTr) was developed by serial culture of primary cells (20). The work demonstrated that several types of porcine virus were capable to replicate in this cell line although no detailed studies of the immune responses were performed. Immortalized porcine bronchial epithelial cells (PBECs) were established by Xie et al. (24), by transfecting primary cells with human telomerase reverse transcriptase. Authors demonstrated that immortalized PBECs retained the morphological and functional features of primary RECs as indicated by proliferation and cytokeratin expression assays. The work also reported that this cell line is susceptible to SIV and porcine circovirus (24). Porcine nasal and tracheal respiratory epithelial cells were also immortalized to develop the siNEC and siTEC cell lines, respectively. Both cell lines were capable to form tight junctions and cilia as well as to support IFV replication (10). Similarly, the porcine airway cell line (MK1-OSU) derived from the distal trachea of a 5-week-old piglet has been useful for the

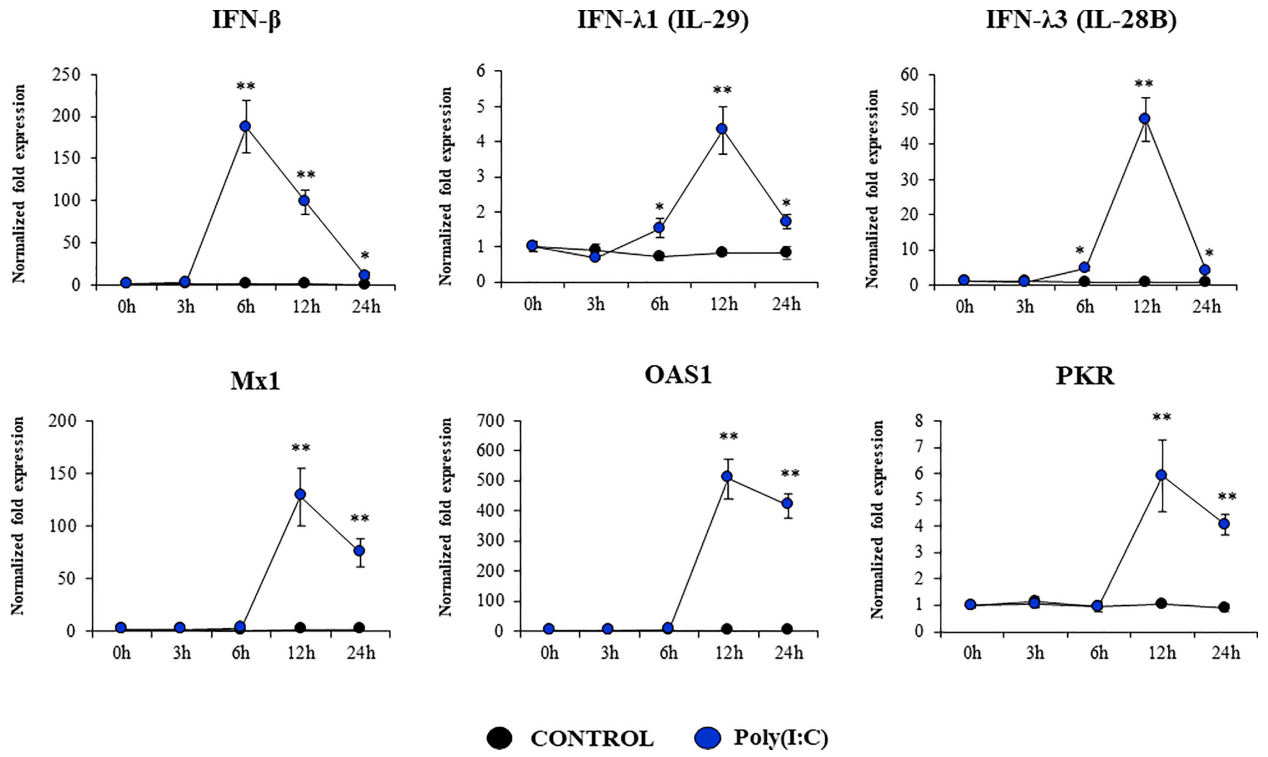

FIGURE 5
Expression of interferons (IFNs) and antiviral factors in the originally established porcine bronchial epithelial (PBE) cell line in response to the activation of the Toll-like receptor 3 (TLR3) signaling pathway. PBE cells were seeded at an initial concentration of 1.0 x 10^4 cells/cm^2. At day 6, PBE cells were stimulated with the TLR3 synthetic agonist poly(I:C) (100 ng/ml) and the expressions of *IFN-β*, *IFN-λ1* (*IL-29*), *IFN-λ3* (*IL-28B*) and the antiviral factors *Mx1*, *OAS1*, and *PKR* were evaluated by qPCR at the indicated time points. Results represent data from three independent experiments. Asterisks indicate significant differences between the control and the poly(I:C)-treated PBE cells. * ($P < 0.05$), ** ($P < 0.01$).

evaluation of IFV infection (12). Then, porcine RECs lines have been used to a limited extent and mainly to research in IFV infection. Here, we developed a PBE cell line from the bronchial epithelium of a neonatal pig and demonstrated that these cells are able to grow in laboratory conditions, reach confluence and express tight junction proteins and cilia. Furthermore, we showed that PBE cells express PRRs and respond to both TLR3 and TLR4 signaling pathways activation.

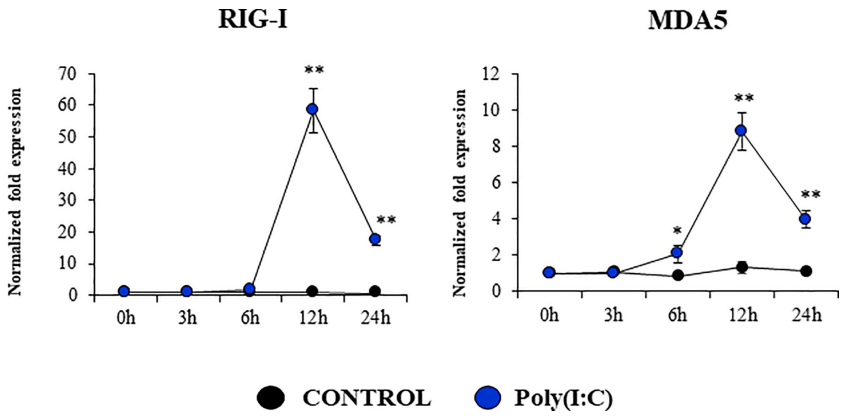

FIGURE 6
Expression of antiviral Pattern Recognition Receptors (PRRs) in the originally established porcine bronchial epithelial (PBE) cell line in response to the activation of the Toll-like receptor 3 (TLR3) signaling pathway. PBE cells were seeded at an initial concentration of 1.0 x 10^4 cells/cm^2. At day 6, PBE cells were stimulated with the TLR3 synthetic agonist poly(I:C) (100 ng/ml) and the expressions of the PRRs *RIG-1*, and *MDA5* were evaluated by qPCR at the indicated time points. Results represent data from three independent experiments. Asterisks indicate significant differences between the control and the poly(I:C)-treated PBE cells. * ($P < 0.05$), ** ($P < 0.01$).

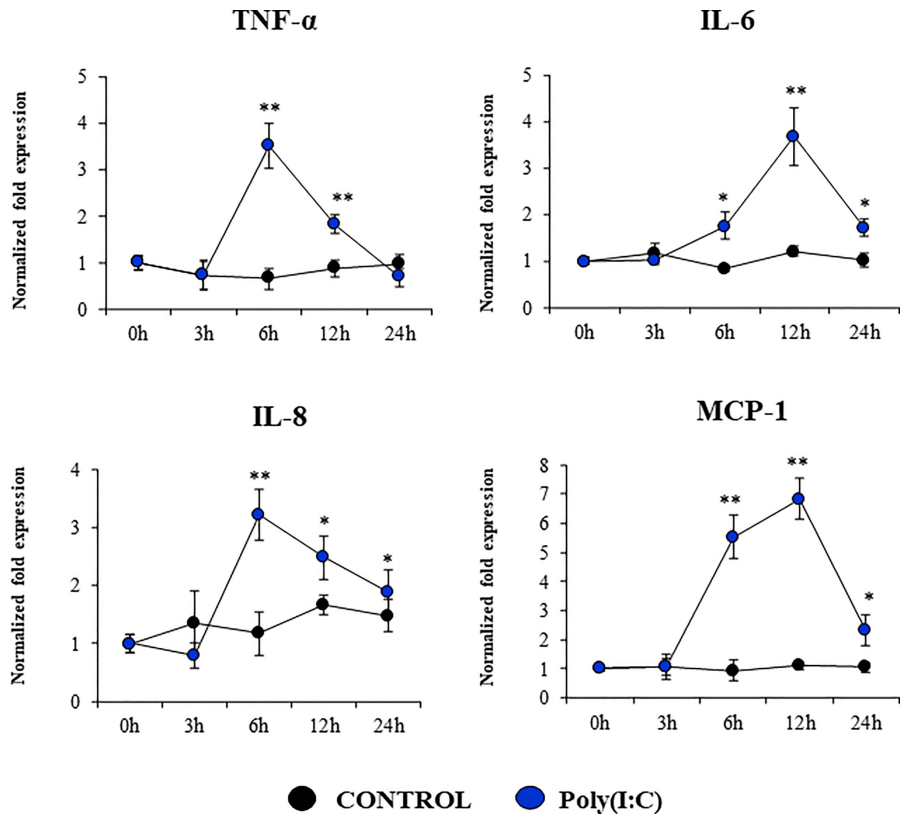

FIGURE 7
Expression of inflammatory cytokines and chemokines in the originally established porcine bronchial epithelial (PBE) cell line in response to the activation of the Toll-like receptor 3 (TLR3) signaling pathway. PBE cells were seeded at an initial concentration of 1.0 x 10^4 cells/cm^2. At day 6, PBE cells were stimulated with the TLR3 synthetic agonist poly(I:C) (100 ng/ml) and the expressions of the inflammatory factors *TNF-α, IL-6, IL-8*, and *MCP-1* were evaluated by qPCR at the indicated time points. Results represent data from three independent experiments. Asterisks indicate significant differences between the control and the poly(I:C)-treated PBE cells. * ($P < 0.05$), ** ($P < 0.01$).

Tight junctions and adherent junctions help to selectively regulate the paracellular diffusion of molecules and form a barrier against invading pathogens in the respiratory epithelium (25). This characteristic is of key importance in REC lines that should be preserved despite immortalization. It was shown that porcine respiratory cell lines like siTEC cells retained the abilities to form tight junctions and to form cilia (10). Similarly, we observed that the new PBE cell line reached confluence, expressed ZO-1, occludin and

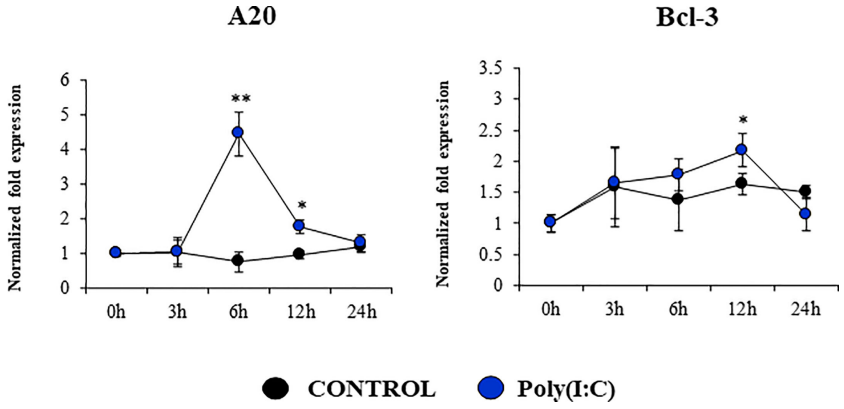

FIGURE 8
Expression of negative regulators of the Toll-like receptor (TLR) signaling pathway in the originally established porcine bronchial epithelial (PBE) cell line in response to the activation of TLR3. PBE cells were seeded at an initial concentration of 1.0 x 10^4 cells/cm^2. At day 6, PBE cells were stimulated with the TLR3 synthetic agonist poly(I:C) (100 ng/ml) and the expressions of the TLR negative regulators *A20* and *Bcl-3* were evaluated by qPCR at the indicated time points. Results represent data from three independent experiments. Asterisks indicate significant differences between the control and the poly(I:C)-treated PBE cells. * ($P < 0.05$), ** ($P < 0.01$).

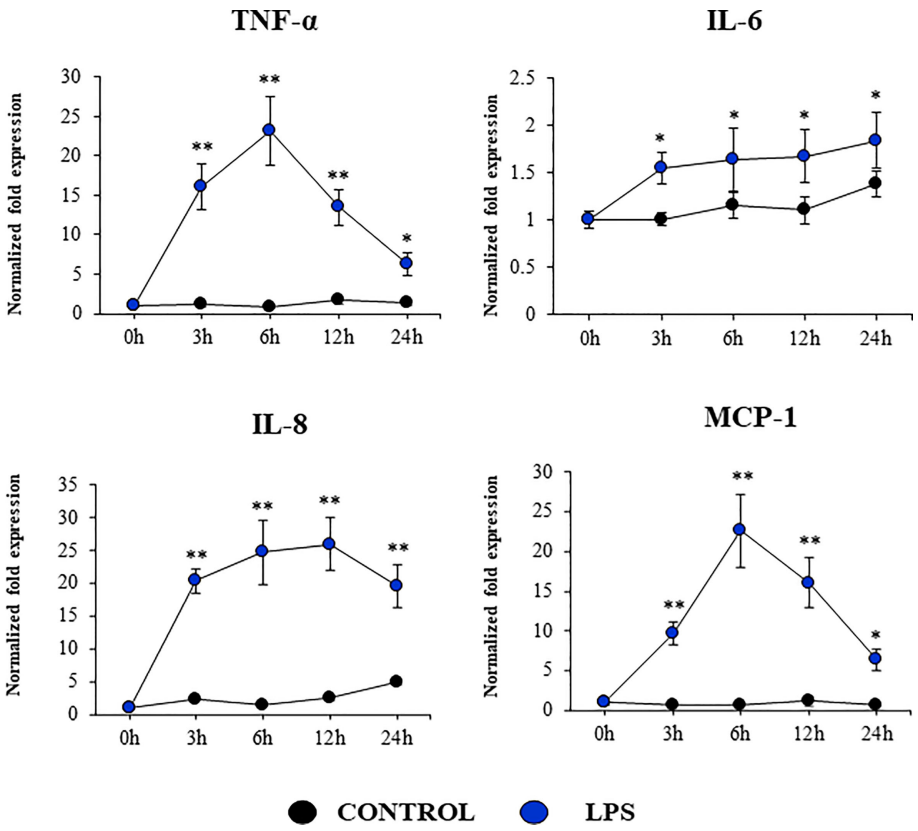

FIGURE 9
Expression of inflammatory cytokines and chemokines in the originally established porcine bronchial epithelial (PBE) cell line in response to the activation of the Toll-like receptor 4 (TLR4) signaling pathway. PBE cells were seeded at an initial concentration of 1.0 x 10^4 cells/cm^2. At day 6, PBE cells were stimulated with the TLR4 agonist LPS (1000 ng/ml) and the expressions of the inflammatory factors *TNF-α, IL-6, IL-8*, and *MCP-1* were evaluated by qPCR at the indicated time points. Results represent data from three independent experiments. Asterisks indicate significant differences between the control and the poly(I:C)-treated PBE cells. * ($P < 0.05$), ** ($P < 0.01$).

E-cadherin, and developed cilia. In addition, it was demonstrated that bronchial epithelial cells express functional TLR1-6 and TLR9 (26). Thus, RECs are equipped with PRRs, such as TLRs and NODs, which rapidly sense pathogens and initiate immune responses in the respiratory tract (27). The expression of functional PRRs is also an important characteristic of cell lines aimed to evaluate immunity in the respiratory epithelium. In this regard, it was shown that MK1-OSU cells expressed TLRs-2, -4, -9, RIG-I, and MDA5 (12). TLR-3

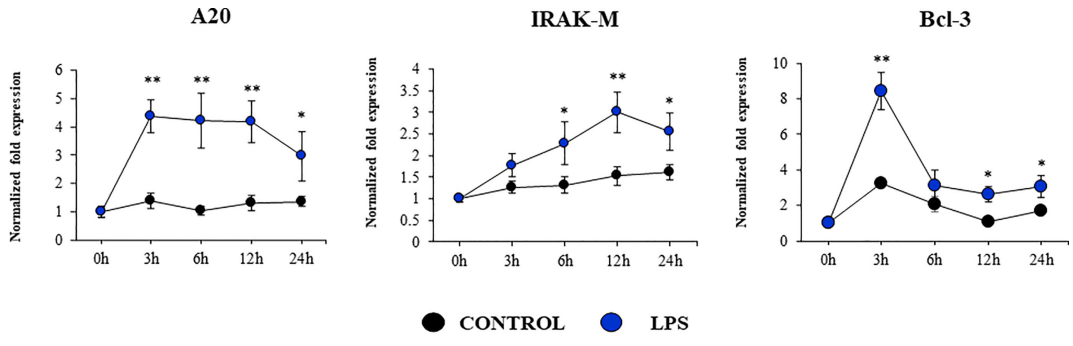

FIGURE 10
Expression of negative regulators of the Toll-like receptor (TLR) signaling pathway in the originally established porcine bronchial epithelial (PBE) cell line in response to the activation of TLR4. PBE cells were seeded at an initial concentration of 1.0 x 10^4 cells/cm^2. At day 6, PBE cells were stimulated with the TLR4 agonist LPS (1000 ng/ml) and the expressions of the TLR negative regulators *A20, IRAK-M* and *Bcl-3* were evaluated by qPCR at the indicated time points. Results represent data from three independent experiments. Asterisks indicate significant differences between the control and the poly(I:C)-treated PBE cells. * ($P < 0.05$), ** ($P < 0.01$).

was not detected in this cell line and authors proposed that this fact was related to the lack of cross-reactivity of human detection antibodies with swine antigens. The expression of TLR3 mRNA levels was not investigated. In this work, we demonstrated that PBE cells express TLR1-9, NOD1 and NOD2. Furthermore, we showed that TLR3 is one of the most strongly expressed PRRs and we characterized the response of PBE cells to the activation of this signaling pathway by up-regulating antiviral factors as well as inflammatory cytokines and chemokines.

Type I and III IFN induction is a potent mechanism of protection against viral infections. It was reported that primary porcine bronchial epithelial cells responded to synthetic dsRNA stimulation upregulating the expression of *IFN-β* and *IFN-λ* (14). Furthermore, porcine RECs pretreated with poly(I:C) and then challenged with IFV had viral titers that were significantly lower than cells infected only with IFV (14). In line with these results, primary cultures of RECs from the trachea and bronchus of pigs have been shown to significantly up-regulate the expression of the antiviral factors *Mx1* and *ISG15* in response to both poly(I:C) and IFV challenges (11). The work also demonstrated that the inhibition of the JAK/STAT signaling pathway significantly increased the IFV replication. Furthermore, the challenge of porcine RECs with the avian IFV H1N1/06 induced a reduced expression of antiviral factors allowing the virus to replicate efficiently and to cause detrimental effects on cells. Interestingly, the pretreatment of porcine RECs with poly(I:C) diminished IFV replication via the paracrine IFN-β stimulation (11). The expression kinetics studies of *IFN-β*, *IFN-λ1*, *IFN-λ3* and antiviral factors in PBE cells allow us to speculate that this cell line can be a useful *in vitro* tool to investigate treatments that help to potentiate antiviral immunity. In this regard, using a porcine intestinal epithelial cell line developed by our group, we demonstrated that beneficial microorganisms with immunomodulatory capacities differentially regulate genes involved in antiviral defenses enhancing the ability of epithelial cells limit rotavirus replication (28–30). PBE cells could be used for the *in vitro* selection and characterization of beneficial microorganisms with the ability to regulate TLR3-signaling pathway in the respiratory tract allowing an improved epithelial innate antiviral immune response. Research on this topic is ongoing in our laboratories.

We also detected the up-regulation of *RIG-I* and *MDA5* in PBE cells stimulated with poly(I:C). RIG-I and MDA5 are present in the cytoplasm and detect viral nucleic acids leading to the production of IFNs, cytokines and chemokines (31, 32). RIG-I stimulates IFNs production during IFV infection (14). It was shown that the stimulation of the respiratory cell lines NSBE or NHBE with dsRNA enhance the expression of RIG-I, which contributes to increased amplification of IFN responses (14). It was also demonstrated that IFV infection increase the expressions of MDA5 in both *in vivo* and *in vitro* studies (32, 33). Furthermore, the mRNA levels of *MDA5* were significantly increased after the challenge of MK1-OSU cells with SIV (34, 35). These results further highlight the potential of PBE cells for conducting detailed antiviral immunological studies. One limitation of our study is the lack of use of a real viral challenge such as IFV to evaluate the response of PBE cells. Studying the ability of PBE cells to allow the replication of respiratory viruses of importance for the porcine host as well as evaluating the immune responses that are triggered by viral infections are important topics for future research.

The production of inflammatory factors in PBE cells was also characterized considering that the respiratory epithelium is sensitive to the inflammatory damage. It was reported that TNF-α can damage the integrity of the epithelial barrier using a porcine tracheal epithelial cell model. TNF-α can disrupt both ZO-1 and occludin and induce the production of IL-6 and IL-8 (36). It was also shown that the activation of TLR3 pathway in the respiratory tract can have both protective and detrimental effects, the later associated with inflammatory-mediated damage. The nasal administration of poly(I:C) to mice induce the production of pro-inflammatory mediators and the recruitment of inflammatory cells in the respiratory tract, which mediate tissue damage and impairment of lung function (37, 38). *In vitro* studies reported that the treatment of RECs with poly(I:C) stimulate the secretion of multiple inflammatory cytokines and chemokines including TNF-α, IL-6, IL-8, and MCP-1 (39, 40). Similarly, the stimulation of RECs with LPS can trigger the activation of the innate immune response characterized by an improved production of inflammatory factors. It was shown that human alveolar epithelial cells (A549) and bronchial epithelial cells (NHBE) activate the NF-κB inducing the production of the inflammatory cytokines TNF-α, IL-6, and IL-8 (41, 42). In line with these previous studies, we showed here that the stimulation of PBE cells with poly(I:C) or LPS significantly augmented the expression of *TNF-α, IL-6, IL-8*, and *MCP-1*.

Interestingly, we also detected variations in the expression of negative regulators of the TLR signaling pathway in PBE cell stimulated with TLR3 or TLR4 agonists, particularly in *A20* (encoded by *Tnfaip3*) and *Bcl-3*. Research have demonstrated that TLR negative regulators may have a relevant role in the development of inflammatory diseases of the respiratory tract. The chronic exposure to low-doses of LPS protected mice from developing house dust mite-induced asthma. LPS treatment diminished the production of cytokines by RECs that activate dendritic cells and potentiate type 2 immunity. Of note, *A20* knockdown in lung epithelium abolished the protective effect of LPS (43). The chronic and exaggerated inflammation in the airways in cystic fibrosis has been also associated to the reduced expression of A20 in the respiratory epithelium (43). Moreover, A20 protein production is induced in the lung from mice and human bronchial epithelial cells upon IFV infection and its overexpression in bronchial epithelial cells results in the protection of host against inflammatory damage (44). Human NCI-H292 airway epithelial cells stimulated with LPS significantly increase their production of IL-8 as well as the level of *Tnfaip3* mRNA (45). Furthermore, overexpression of *A20* inhibited activation of both NF-kB and the IL-8 promoter. Similarly, tracheobronchial epithelial cells (TBEC) showed a strong production of IL-8 and IP-10 (CXCL10) in

response to poly(I:C) treatment, which was accompanied with the upregulation of *A20* and *IRAK-M* (39). As the A20 protein, IRAK-M is involved in immunoregulation of airway inflammation. Although the role of IRAK-M in the respiratory tract immune responses was demonstrated by its influence on macrophages, dendritic cells, and T cells, recent studies highlighted its role in RECs (46). It was demonstrated that the knockdown of IRAK-M in EAS-2B and A549 cells significantly increased their ability to produce IL-6, IL-8, CXCL10, and CXCL11 in response to IL-1β, TNF-α, or IL-33 stimulation. On the other hand, it was shown that the high upregulation of *IL-8* expression induced by respiratory syncytial virus (RSV) infection in A549 cells is terminated by Bcl-3 in the late-phase of infection. In contrast to wild-type mice, Bcl-3-deficient mice exhibited significantly increased susceptibility toward the Gram-negative pathogen *Klebsiella pneumoniae* (47, 48). The loss of Bcl-3 generated a remarkable cytokine imbalance in the lungs, which was characterized by increased production of the neutrophil-attracting chemokines. Taken together, our results suggest that the expression of inflammatory cytokines and chemokines as well as TLR negative regulators in PBE cells is a valuable characteristic of this new cell line that may allow the evaluation of treatments that can regulate TLR-mediated inflammatory injury in the porcine airway.

The applications of the new porcine cell line developed in this work could be extended beyond its use in monolayers, for example it could be used in co-cultures with immune cells. Single cell RNA-seq and computational analysis (7) have started to reveal the complex epithelial–immune crosstalk that occurs in the respiratory tract in health and disease. Bi-directional interactions between RECs and alveolar macrophages help to maintain the homeostatic state of tolerance to innocuous antigens and the appropriate protective responses to pathogens when required (49). Most of these studies have been done in mouse models (50) while few studies investigated epithelial–macrophage crosstalk in humans (51). To the best of our knowledge, no studies have been performed in the porcine host. This new PBE cell line could be used with porcine alveolar macrophages (52) to evaluate their interactions in the context of the response to pathogens or PRRs activation.

A limitation of our work is that it was not possible to compare the immune responses mediated by TLR3 or TLR4 activation of PBE cells with those produced under the same conditions by primary cultures of porcine bronchial epithelial cells. Carrying out these studies would be of great value to propose this new cell line as a highly representative model of the immunological responses that occur in the bronchial epithelium *in vivo*. Furthermore, it would be of great interest to carry out these comparative studies with primary cultures of bronchial epithelial cells from pigs of different ages to assess whether the PBE cells represent only a limited age group. These are studies that we intend to do in the immediate future.

In conclusion, the PBE cell line developed in this work was characterized in terms of its expression of PRRs and its ability to respond to the activation of the TLR3 and TLR4 signaling pathways, which are key PRRs involved in the defense of the respiratory epithelium against pathogens. PBE cells stimulated with poly(I:C) were able to up-regulate the expression of *IFN-β*, *IFN-λ1* (*IL-29*), *IFN-λ3* (*IL-28B*), the antiviral factors *Mx1*, *OAS1*, and *PKR*, as well as the viral PRRs *RIG-1* and *MDA5*. In addition, poly(I:C) and LPS treatments increased the expression of the inflammatory cytokines *TNF-α, IL-6, IL-8*, and *MCP-1/CCL2* and differentially modulated the expression of negative regulators of the TLR signaling pathways. The expression kinetics studies of immune factors in PBE cells allow us to speculate that this cell line can be a useful *in vitro* tool to investigate treatments that help to potentiate antiviral immunity and/or regulate TLR-mediated inflammatory injury in the porcine airway, thereby protecting the host against harmful overresponses.

Data availability statement

The raw data supporting the conclusions of this article will be made available by the authors, without undue reservation.

Ethics statement

The animal study was reviewed and approved by Animal Experimentation of Tohoku University.

Author contributions

JV and HK designed the study and wrote the manuscript. KF, TZ, FR, ET, SS, and BZ did the laboratory work. KF, TZ, and FR performed statistical analysis. KF, WI-O, KN, HA, JV, and HK contributed to data analysis and interpretation. All authors read and approved the manuscript.

Funding

This study was supported by Grant-in-Aid for Scientific Research (A) (19H00965, 23H00354) from the Japan Society for the Promotion of Science (JSPS), and by the Japan Racing Association, and by the research program on development of innovative technology grants (JPJ007097) from the Project of the Bio-oriented Technology Research Advancement Institution (BRAIN) to HK, and by JSPS Core-to-Core Program, A. Advanced Research Networks entitled Establishment of international agricultural immunology research-core for a quantum improvement in food safety, and by AMED Grant Number JP21zf0127001. KF was supported by JST, the establishment of university fellowships towards the creation of science technology innovation, Grant Number JPMJFS2102.

Conflict of interest

The authors declare that the research was conducted in the absence of any commercial or financial relationships that could be construed as a potential conflict of interest.

Publisher's note

All claims expressed in this article are solely those of the authors and do not necessarily represent those of their affiliated organizations, or those of the publisher, the editors and the reviewers. Any product that may be evaluated in this article, or claim that may be made by its manufacturer, is not guaranteed or endorsed by the publisher.

Supplementary material

The Supplementary Material for this article can be found online at: https://www.frontiersin.org/articles/10.3389/fimmu.2023.1117102/full#supplementary-material

References

1. Baker RE, Mahmud AS, Miller IF, Rajeev M, Rasambainarivo F, Rice BL, et al. Infectious disease in an era of global change. *Nat Rev Microbiol* (2022) 20(4):193–205. doi: 10.1038/s41579-021-00639-z

2. Sarli G, D'Annunzio G, Gobbo F, Benazzi C, Ostanello F. The role of pathology in the diagnosis of swine respiratory disease. *Vet Sci* (2021) 8(11). doi: 10.3390/vetsci8110256

3. Ma W. Swine influenza virus: current status and challenge. *Virus Res* (2020) 288:198118. doi: 10.1016/j.virusres.2020.198118

4. Opriessnig T, Gimenez-Lirola LG, Halbur PG. Polymicrobial respiratory disease in pigs. *Anim Health Res Rev* (2011) 12(2):133–48. doi: 10.1017/S1466252311000120

5. Villena J, Kitazawa H. The modulation of mucosal antiviral immunity by immunobiotics: could they offer any benefit in the sars-Cov-2 pandemic? *Front Physiol* (2020) 11:699. doi: 10.3389/fphys.2020.00699

6. Zelaya H, Alvarez S, Kitazawa H, Villena J. Respiratory antiviral immunity and immunobiotics: beneficial effects on inflammation-coagulation interaction during influenza virus infection. *Front Immunol* (2016) 7:633. doi: 10.3389/fimmu.2016.00633

7. Hewitt RJ, Lloyd CM. Regulation of immune responses by the airway epithelial cell landscape. *Nat Rev Immunol* (2021) 21(6):347–62. doi: 10.1038/s41577-020-00477-9

8. Rijsbergen LC, van Dijk LLA, Engel MFM, de Vries RD, de Swart RL. *In vitro* modelling of respiratory virus infections in human airway epithelial cells - a systematic review. *Front Immunol* (2021) 12:683002. doi: 10.3389/fimmu.2021.683002

9. Fu Y, Durrwald R, Meng F, Tong J, Wu NH, Su A, et al. Infection studies in pigs and porcine airway epithelial cells reveal an evolution of a(H1n1)Pdm09 influenza a viruses toward lower virulence. *J Infect Dis* (2019) 219(10):1596–604. doi: 10.1093/infdis/jiy719

10. Meliopoulos V, Cherry S, Wohlgemuth N, Honce R, Barnard K, Gauger P, et al. Primary swine respiratory epithelial cell lines for the efficient isolation and propagation of influenza a viruses. *J Virol* (2020) 94(24). doi: 10.1128/JVI.01091-20

11. Shin DL, Yang W, Peng JY, Sawatsky B, von Messling V, Herrler G, et al. Avian influenza a virus infects swine airway epithelial cells without prior adaptation. *Viruses* (2020) 12(6). doi: 10.3390/v12060589

12. Thomas M, Pierson M, Uprety T, Zhu L, Ran Z, Sreenivasan CC, et al. Comparison of porcine airway and intestinal epithelial cell lines for the susceptibility and expression of pattern recognition receptors upon influenza virus infection. *Viruses* (2018) 10(6). doi: 10.3390/v10060312

13. Elvert M, Sauerhering L, Maisner A. Cytokine induction in nipah virus-infected primary human and porcine bronchial epithelial cells. *J Infect Dis* (2020) 221(Suppl 4): S395–400. doi: 10.1093/infdis/jiz455

14. Hauser MJ, Dlugolenski D, Culhane MR, Wentworth DE, Tompkins SM, Tripp RA. Antiviral responses by swine primary bronchoepithelial cells are limited compared to human bronchoepithelial cells following influenza virus infection. *PloS One* (2013) 8 (7):e70251. doi: 10.1371/journal.pone.0070251

15. Li Q, Domig KJ, Ettle T, Windisch W, Mair C, Schedle K. Evaluation of potential reference genes for relative quantification by rt-qpcr in different porcine tissues derived from feeding studies. *Int J Mol Sci* (2011) 12(3):1727–34. doi: 10.3390/ijms12031727

16. Nygard AB, Jorgensen CB, Cirera S, Fredholm M. Selection of reference genes for gene expression studies in pig tissues using sybr green qpcr. *BMC Mol Biol* (2007) 8:67. doi: 10.1186/1471-2199-8-67

17. Iwasaki A, Foxman EF, Molony RD. Early local immune defences in the respiratory tract. *Nat Rev Immunol* (2017) 17(1):7–20. doi: 10.1038/nri.2016.117

18. Ziegler CGK, Allon SJ, Nyquist SK, Mbano IM, Miao VN, Tzouanas CN, et al. Sars-Cov-2 receptor Ace2 is an interferon-stimulated gene in human airway epithelial cells and is detected in specific cell subsets across tissues. *Cell* (2020) 181(5):1016–35.e19. doi: 10.1016/j.cell.2020.04.035

19. Reeves SR, Barrow KA, White MP, Rich LM, Naushab M, Debley JS. Stability of gene expression by primary bronchial epithelial cells over increasing passage number. *BMC Pulm Med* (2018) 18(1):91. doi: 10.1186/s12890-018-0652-2

20. Ferrari M, Scalvini A, Losio MN, Corradi A, Soncini M, Bignotti E, et al. Establishment and characterization of two new pig cell lines for use in virological diagnostic laboratories. *J Virol Methods* (2003) 107(2):205–12. doi: 10.1016/s0166-0934(02)00236-7

21. Seo SH, Goloubeva O, Webby R, Webster RG. Characterization of a porcine lung epithelial cell line suitable for influenza virus studies. *J Virol* (2001) 75(19):9517–25. doi: 10.1128/jvi.75.19.9517-9525.2001

22. Seo SH, Webster RG. Tumor necrosis factor alpha exerts powerful anti-influenza virus effects in lung epithelial cells. *J Virol* (2002) 76(3):1071–6. doi: 10.1128/jvi.76.3.1071-1076.2002

23. Silversides DW, Music N, Jacques M, Gagnon CA, Webby R. Investigation of the species origin of the st. Jude porcine lung epithelial cell line (Sjpl) made available to researchers. *J Virol* (2010) 84(10):5454–5. doi: 10.1128/jvi.00042-10

24. Xie X, Gan Y, Pang M, Shao G, Zhang L, Liu B, et al. Establishment and characterization of a telomerase-immortalized porcine bronchial epithelial cell line. *J Cell Physiol* (2018) 233(12):9763–76. doi: 10.1002/jcp.26942

25. Brune K, Frank J, Schwingshackl A, Finigan J, Sidhaye VK. Pulmonary epithelial barrier function: some new players and mechanisms. *Am J Physiol Lung Cell Mol Physiol* (2015) 308(8):L731–45. doi: 10.1152/ajplung.00309.2014

26. Mayer AK, Muehmer M, Mages J, Gueinzius K, Hess C, Heeg K, et al. Differential recognition of tlr-dependent microbial ligands in human bronchial epithelial cells. *J Immunol* (2007) 178(5):3134–42. doi: 10.4049/jimmunol.178.5.3134

27. Lehmann R, Muller MM, Klassert TE, Driesch D, Stock M, Heinrich A, et al. Differential regulation of the transcriptomic and secretomic landscape of sensor and effector functions of human airway epithelial cells. *Mucosal Immunol* (2018) 11(3):627–42. doi: 10.1038/mi.2017.100

28. Albarracin L, Garcia-Castillo V, Masumizu Y, Indo Y, Islam MA, Suda Y, et al. Efficient selection of new immunobiotic strains with antiviral effects in local and distal mucosal sites by using porcine intestinal epitheliocytes. *Front Immunol* (2020) 11:543. doi: 10.3389/fimmu.2020.00543

29. Albarracin L, Kobayashi H, Iida H, Sato N, Nochi T, Aso H, et al. Transcriptomic analysis of the innate antiviral immune response in porcine intestinal epithelial cells: influence of immunobiotic lactobacilli. *Front Immunol* (2017) 8:57. doi: 10.3389/fimmu.2017.00057

30. Ishizuka T, Kanmani P, Kobayashi H, Miyazaki A, Soma J, Suda Y, et al. Immunobiotic bifidobacteria strains modulate rotavirus immune response in porcine intestinal epitheliocytes Via pattern recognition receptor signaling. *PloS One* (2016) 11 (3):e0152416. doi: 10.1371/journal.pone.0152416

31. Wei L, Cui J, Song Y, Zhang S, Han F, Yuan R, et al. Duck Mda5 functions in innate immunity against H5n1 highly pathogenic avian influenza virus infections. *Vet Res* (2014) 45(1):66. doi: 10.1186/1297-9716-45-66

32. Wu W, Zhang W, Duggan ES, Booth JL, Zou MH, Metcalf JP. Rig-I and Tlr3 are both required for maximum interferon induction by influenza virus in human lung alveolar epithelial cells. *Virology* (2015) 482:181–8. doi: 10.1016/j.virol.2015.03.048

33. Lee N, Wong CK, Hui DS, Lee SK, Wong RY, Ngai KL, et al. Role of human toll-like receptors in naturally occurring influenza a infections. *Influenza Other Respir Viruses* (2013) 7(5):666–75. doi: 10.1111/irv.12109

34. Kim HJ, Kim CH, Kim MJ, Ryu JH, Seong SY, Kim S, et al. The induction of pattern-recognition receptor expression against influenza a virus through Duox2-derived reactive oxygen species in nasal mucosa. *Am J Respir Cell Mol Biol* (2015) 53 (4):525–35. doi: 10.1165/rcmb.2014-0334OC

35. Zhang J, Miao J, Hou J, Lu C. The effects of H3n2 swine influenza virus infection on tlrs and rlrs signaling pathways in porcine alveolar macrophages. *Virol J* (2015) 12:61. doi: 10.1186/s12985-015-0284-6

36. Bercier P, Grenier D. Tnf-alpha disrupts the integrity of the porcine respiratory epithelial barrier. *Res Vet Sci* (2019) 124:13–7. doi: 10.1016/j.rvsc.2019.01.029

37. Stowell NC, Seideman J, Raymond HA, Smalley KA, Lamb RJ, Egenolf DD, et al. Long-term activation of Tlr3 by Poly(I:C) induces inflammation and impairs lung function in mice. *Respir Res* (2009) 10(1):43. doi: 10.1186/1465-9921-10-43

38. Villena J, Chiba E, Tomosada Y, Salva S, Marranzino G, Kitazawa H, et al. Orally administered lactobacillus rhamnosus modulates the respiratory immune response triggered by the viral pathogen-associated molecular pattern Poly(I:C). *BMC Immunol* (2012) 13:53. doi: 10.1186/1471-2172-13-53

39. Mubarak RA, Roberts N, Mason RJ, Alper S, Chu HW. Comparison of pro- and anti-inflammatory responses in paired human primary airway epithelial cells and alveolar macrophages. *Respir Res* (2018) 19(1):126. doi: 10.1186/s12931-018-0825-9

40. Sha Q, Truong-Tran AQ, Plitt JR, Beck LA, Schleimer RP. Activation of airway epithelial cells by toll-like receptor agonists. *Am J Respir Cell Mol Biol* (2004) 31 (3):358–64. doi: 10.1165/rcmb.2003-0388OC

41. Kim HJ, Kim SR, Park JK, Kim DI, Jeong JS, Lee YC. Pi3kgamma activation is required for lps-induced reactive oxygen species generation in respiratory epithelial cells. *Inflammation Res* (2012) 61(11):1265–72. doi: 10.1007/s00011-012-0526-7

42. Hu Y, Lou J, Mao YY, Lai TW, Liu LY, Zhu C, et al. Activation of mtor in pulmonary epithelium promotes lps-induced acute lung injury. *Autophagy* (2016) 12 (12):2286–99. doi: 10.1080/15548627.2016.1230584

43. Schuijs MJ, Willart MA, Vergote K, Gras D, Deswarte K, Ege MJ, et al. Farm dust and endotoxin protect against allergy through A20 induction in lung epithelial cells. *Sci (New York NY)* (2015) 349(6252):1106–10. doi: 10.1126/science.aac6623

44. Onose A, Hashimoto S, Hayashi S, Maruoka S, Kumasawa F, Mizumura K, et al. An inhibitory effect of A20 on nf-kappab activation in airway epithelium upon influenza virus infection. *Eur J Pharmacol* (2006) 541(3):198–204. doi: 10.1016/j.ejphar.2006.03.073

45. Gon Y, Asai Y, Hashimoto S, Mizumura K, Jibiki I, Machino T, et al. A20 inhibits toll-like receptor 2- and 4-mediated interleukin-8 synthesis in airway epithelial cells. *Am J Respir Cell Mol Biol* (2004) 31(3):330–6. doi: 10.1165/rcmb.2003-0438OC

46. Li J, Zheng Z, Liu Y, Zhang H, Zhang Y, Gao J. Irak-m has effects in regulation of lung epithelial inflammation. *Respir Res* (2023) 24(1):103. doi: 10.1186/s12931-023-02406-5

47. Jamaluddin M, Choudhary S, Wang S, Casola A, Huda R, Garofalo RP, et al. Respiratory syncytial virus-inducible bcl-3 expression antagonizes the Stat/Irf and nf-kappab signaling pathways by inducing histone deacetylase 1 recruitment to the interleukin-8 promoter. *J Virol* (2005) 79(24):15302–13. doi: 10.1128/JVI.79.24.15302-15313.2005

48. Pene F, Paun A, Sonder SU, Rikhi N, Wang H, Claudio E, et al. The ikappab family member bcl-3 coordinates the pulmonary defense against klebsiella pneumoniae infection. *J Immunol* (2011) 186(4):2412–21. doi: 10.4049/jimmunol.1001331

49. Puttur F, Gregory LG, Lloyd CM. Airway macrophages as the guardians of tissue repair in the lung. *Immunol Cell Biol* (2019) 97(3):246–57. doi: 10.1111/imcb.12235

50. Westphalen K, Gusarova GA, Islam MN, Subramanian M, Cohen TS, Prince AS, et al. Sessile alveolar macrophages communicate with alveolar epithelium to modulate immunity. *Nature* (2014) 506(7489):503–6. doi: 10.1038/nature12902

51. Moon HG, Kim SJ, Jeong JJ, Han SS, Jarjour NN, Lee H, et al. Airway epithelial cell-derived colony stimulating factor-1 promotes allergen sensitization. *Immunity* (2018) 49(2):275–87 e5. doi: 10.1016/j.immuni.2018.06.009

52. Tomokiyo M, Tonetti FR, Yamamuro H, Shibata R, Fukuyama K, Gobbato N, et al. Modulation of alveolar macrophages by postimmunobiotics: impact on Tlr3-mediated antiviral respiratory immunity. *Cells* (2022) 11(19). doi: 10.3390/cells11192986

frontiers | Frontiers in Immunology

TYPE Case Report
PUBLISHED 14 September 2023
DOI 10.3389/fimmu.2023.1154448

OPEN ACCESS

EDITED BY
Paraskevi C. Fragkou,
Evaggelismos General Hospital, Greece

REVIEWED BY
Dimitra Dimopoulou,
Panagiotis & Aglaia Kyriakou Children's Hospital, Greece
Annefleur Langedijk,
University Medical Center Utrecht, Netherlands

*CORRESPONDENCE
Constance Bindernagel
cbindernagel@usf.edu

RECEIVED 30 January 2023
ACCEPTED 14 August 2023
PUBLISHED 14 September 2023

CITATION
Bindernagel C, Sotoudeh S, Nguyen M, Wetzstein G, Sriaroon P and Walter J (2023) Case Report: ASCENIV use in three young children with immune abnormalities and acute respiratory failure secondary to RSV infection.
Front. Immunol. 14:1154448.
doi: 10.3389/fimmu.2023.1154448

Case Report: ASCENIV use in three young children with immune abnormalities and acute respiratory failure secondary to RSV infection

Constance Bindernagel[1,2]*, Shannon Sotoudeh[1,2], Minh Nguyen[1,2], Gene Wetzstein[3], Panida Sriaroon[1,2] and Jolan Walter[1,2,3]

[1]Department of Pediatrics, Division of Allergy and Immunology, University of South Florida Morsani College of Medicine, Tampa, FL, United States, [2]Department of Allergy and Immunology, Johns Hopkins All Children's Hospital, Saint Petersburg, FL, United States, [3]ADMA Biologics (United States), Ramsey, NJ, United States

Respiratory syncytial virus (RSV) is the most common etiology of bronchiolitis in young children. While most children clinically improve with care at home, RSV is the leading cause of hospitalization among infants aged 12 months or less. Common modalities of treatment for children with immune dysregulation include respiratory support and best supportive care, which may include immunoglobulin therapy. All immunoglobulin therapies adhere to Food and Drug Administration (FDA) - established standards for antibodies against measles, polio, and diphtheria, but there are no required standards for problematic respiratory viral pathogens, including RSV and others. ASCENIV is an approved IVIG that is manufactured from blending normal source plasma with plasma from donors that possess high antibody titers against RSV and other respiratory pathogens of concern. ASCENIV was developed, in part, to the unmet need that exists in immunocompromised patients who lack sufficient antibodies against problematic viral pathogens. ASCENIV is not a currently approved treatment for severe RSV and other viral infections. There is a lack of research regarding its potential benefits in the acute treatment period for RSV and in the pediatric population. Therefore, this case series was developed to describe real-world experiences of ASCENIV use in this less well studied clinical scenario. This case series reviews three pediatric patients ≤ 5 years of age with immune dysregulation and who were severely ill with RSV. Despite receiving best supportive care, and standard immunoglobulin therapy for some, the patients' clinical status continued to decline. All patients received ASCENIV in an intensive care setting. Each patient had ultimately recovered due to the various medical interventions done. This case series demonstrated that ASCENIV (500mg/kg) administration may have contributed to the treatment outcomes of a less well studied age-cohort of patients. In addition, no adverse side effects were observed after ASCENIV administration. Further analysis of the benefits of ASCENIV for the acute and preventative treatment in patients younger than 12 years of age with immune dysregulation should continue to be explored.

KEYWORDS

RSV, ASCENIV, pediatric, immunodeficiency, immune dysregulation, respiratory viral infections, acute respiratory failure, IVIG

Introduction

RSV infects nearly all children by 2 years-of-age (1). Infectivity in the United States has historically peaked between mid-October to early May (2), however, social restrictions in response to the COVID-19 pandemic interrupted the normal respiratory virus circulation. In 2021 and 2022, RSV infections peaked in the summer months (3), indicating highly unpredictable seasonality.

RSV is the most common etiology of bronchiolitis in young children. Methods of testing for RSV include nasopharyngeal aspirate, real time polymerase chain reaction (RT-PCR), direct fluorescence antibody test, viral culture, and rapid antigen test (4). While most children clinically improve with care at home, RSV is the leading cause of hospitalization among infants aged 12 months and less (5). Common modalities of treatment for children with immune dysregulation include respiratory support and best supportive care, which may include immunoglobulin therapy. All immunoglobulin therapies adhere to FDA - established standards for antibodies against measles, polio, and diphtheria, but there are no required standards for problematic respiratory viral pathogens, including RSV and others.

Methods

Chart reviews of three children with severe courses of RSV infections were performed. All patients required mechanical ventilator or high frequency oscillatory ventilation (HFOV) support. The first two patients underwent a primary immune evaluation as there was concern for a new presentation of immune dysregulation. The evaluation included extended immune phenotyping for lymphocyte subsets (T, B, NK and naïve/memory T cells), immunoglobulin panel, pneumococcus titers, diphtheria and pertussis titers, lymphocyte proliferation to mitogens and antigens, and sequencing for 407 primary immunodeficiency genes (Invitae Primary Immunodeficiency Panel). The third patient had recently been diagnosed with specific antibody deficiency and was in the process of beginning immunoglobulin replacement. All three patients had a form of immune dysregulation and received one dose of ASCENIV at 500 mg/kg in the acute care setting.

Case description

Patient demographics, past medical history, primary immune evaluation, genetic testing (if applicable), relevant laboratory values, and clinical courses are provided in Table 1. Figure 1 presents a graphical depiction of patients' clinical course and timeline.

Patient 1 was a 12-month-old boy with a pertinent history of three previous hospitalizations for severe respiratory infections, including RSV (Table 1). On the most recent hospital admission, the patient presented with tachypnea and increased work of breathing. He tested positive for RSV on viral RT-PCR. Patient experienced acute respiratory decompensation, was intubated, and admitted to the pediatric intensive care unit (PICU) for acute respiratory failure. The patient received broad-spectrum antibiotics for suspected superimposed bacterial pneumonia but continued to remain ventilator dependent.

Primary immune evaluation (Day 4) results were consistent with hypogammaglobulinemia, with a total IgG of 190 mg/dL. Genetic testing revealed one pathologic heterozygous mutation of p.Cys104Arg in the TNFRSF13B (TACI) gene. This specific mutation has been reported to be associated with autosomal recessive common variable immunodeficiency (CVID) (6). One heterozygous mutation was found to cause an increased risk of CVID and to possibly induce a CVID-like picture in mice models (7). Mutations at p.Cys104Arg have been described as one of the most common genetic mutations found in CVID (8).

Considering the patient's immune abnormality and minimal clinical improvement with conventional therapy, ASCENIV was explored. On Day 10 of hospitalization, the patient received ASCENIV 500 mg/kg. Over the next several days, his clinical status improved. The patient was subsequently extubated, weaned to room air, and discharged from the hospital. Just prior to discharge, his IgG total was 210 mg/dL. In this patient, no adverse effects were observed after administration of ASCENIV. He has remained on monthly immunoglobulin replacement therapy for hypogammaglobulinemia and is followed closely by a clinical immunologist.

Patient 2 was a 15-month-old boy with history of recurrent viral and RSV infections (Table 1). Upon presentation, he was positive for RSV on viral RT-PCR. The patient was admitted to the PICU for respiratory failure requiring intubation. The patient received high-dose intravenous (IV) steroids, HFOV, nitric oxide, broad-spectrum antibiotics. Respiratory viral panel testing during his hospitalization demonstrated continued RSV, as well as rhinovirus and enterovirus, positivity.

Primary immune evaluation (Day 8) was suspicious for specific antibody deficiency (SAD), although the official diagnosis could not be made due to his inability to receive Pneumovax based on his age. The patient had received all age-appropriate pneumococcal vaccinations, but no pneumococcal titers were evident at initial evaluation. He also demonstrated progressive T-cell lymphopenia, thought to be partially attributable to steroid use since admission. Genetic testing revealed several variants, one including a heterozygous pathological mutation in CARD9 at p.Val13Ile. The mutation is associated with autosomal dominant and recessive immune disease and increased susceptibility to opportunistic fungal infections (2). Considering his low T-cell count and VUS in CARD9, he was started on prophylaxis for pneumocystis jirovecii pneumonia (PJP).

His presentation was concerning for an underlying immune dysregulation disorder because of the clinical context. He did not follow the standard disease course for an RSV infection, which is 5-7 days of respiratory distress followed by improvement afterwards. He was intubated for a prolonged period, which is not typical in standard severe RSV infections. In cases where the RSV course requires intubation, prolonged requirement for respiratory support, and persistent viral positivity, it raises concern for immune dysregulation (9).

TABLE 1 Clinical course of three pediatric patients who received ASCENIV.

	Patient 1	Patient 2	Patient 3
Demographics	Male, 12-months-old	Male, 15-month-old	Female, 5-years-old
Past medical/ respiratory history	Eczema, craniosynostosis Several hospital admissions for severe viral RTIs, including a previous RSV infection.	Bilateral ear infections Frequent viral upper RTIs Diagnosed with RSV lower RTI four months prior to hospitalization	Cerebellar ataxia (genetic form), global developmental delay, SAD Multiple upper RTIs, two PICU admissions for viral pneumonia Moderate persistent asthma
Primary immune evaluation/Relevant laboratory values	The patient is fully immunized for age Low immunoglobulin (Ig): IgG and IgG selective subclass deficiency consistent with hypogammaglobulinemia Out of range results: Hospital/PICU Day 4 IgG=190 mg/dL IgG1 = 129 mg/dL IgG3 = 14 mg/dL There were not out of range results for total lymphocytes.	The patient is fully immunized for age On initial evaluation, 0/23 pneumococcal titers and progressive T-cell lymphopenia Out of range results, absolute lymphocytes (cells/μL): Hospital/PICU Day 8 * Total lymphocytes: 1073 cells/μL Hospital/PICU Day 17 * Total lymphocytes: 773 cells/μL Hospital/PICU Day 28 * Total lymphocytes: 3495 cells/μL[a] RSV: positive on Days 0 and 19; negative on Days 8, 28, and 34 Rhino/enterovirus: positive on Days 0, 8, and 19; negative on Day 34.	The patient is fully immunized for age On initial immune evaluation, 0/23 pneumococcal serotypes. After vaccination, had 14/23 serotypes. 20 months later, repeat testing demonstrated 5/23 serotypes. After repeat vaccination, had 1/23 serotypes.
Genetic testing	On pathologic heterozygous mutation TNFRSF13B (TACI) in p.Cys104Arg Additional variants of unknown significance included ARMC4, CD79B, HPS3, JAK3.	One pathological heterozygous mutation in CARD9 in p.Val13Ile Additional variants of unknown significance included C7, EFL1, IL12RB2, SMAHD1.	In 6/2018, genomic testing showed chromosomal abnormality (18p11.22 and 13 mutation) 11/2018, heterozygous for the *De Novo* p.Q306R VUS in the POU4F1 gene.
Clinical course	* Tachypnea, increased work of breathing, positive for RSV * Acute respiratory decompensation, intubation * Admitted to the PICU * Broad-spectrum antibiotics for suspected superimposed bacterial pneumonia	* Hypoxia, increased work of breathing and grunting, positive for RSV and rhinovirus/ enterovirus * Acute respiratory decompensation, intubation * Admitted to the PICU * Persistent viral positivity * Diagnosed with superimposed bacterial and ventilator associated pneumonia secondary to Moraxella catarrhalis and MRSA * High-dose IV steroids * HFOV, nitric oxide * Broad-spectrum antibiotics with PJP prophylaxis * 500 mg/kg conventional IVIG	* Respiratory distress, positive for RSV * Required BiPAP * Admitted to the PICU * Persistent respiratory failure requiring intubation * RSV positivity persisted * 600 mg/kg of conventional IVIG
ASCENIV initiation (day of hospital course)	ASCENIV 500 mg/kg Day 10	ASCENIV 500 mg/kg Day 21	ASCENIV 500 mg/kg Day 6
Clinical course after ASCENIV	Respiratory status improved; was extubated, weaned to room air Discharged on Day 14 Has remained on monthly Ig therapy for hypogammaglobulinemia	Respiratory status improved; transitioned off HFOV support to conventional ventilation Steroids tapered off; improved T-cell populations. Consecutive PCR clearance of RSV and rhino/ enterovirus PJP prophylaxis discontinued as lymphocyte count normalized Discharged on Day 55 Was to remain on monthly Ig therapy due to concern for SAD	Respiratory status improved; was extubated RSV Rapid detection became negative. Discharged on Day 20 Has remained on monthly Ig therapy

MRSA, methicillin resistant staphylococcus aureus; VUS, variant(s) of unknown significance; SAD, specific antibody deficiency, Ig therapy, immunoglobulin replacement therapy
Reference ranges: 10-12 months: IgG 594 mg/dL (294-1069), 13-23 months: IgG 679 mg/dL (345-1213), 4-5 years old: IgG mg/dL 780 (463-1236) based off Harriet Lane Values, 22 edition, page 379. Total lymphocytes: 2.8-12.3 cells/μL.

The patient's clinical status improved marginally after 500 mg/kg conventional IVIG was given on Day 18. Three days later, the patient received ASCENIV 500 mg/kg. By Day 28, the patient's clinical condition improved. Two sequential viral tests, rapid detection and RT-PCR demonstrated clearance of RSV. No adverse effects were observed after administration of ASCENIV in this patient. He was to remain on immunoglobulin replacement therapy until he could be re-evaluated for SAD. Additionally, the patient demonstrated sustained improved T-cell counts outside of the acute care setting. PJP prophylaxis was ultimately discontinued.

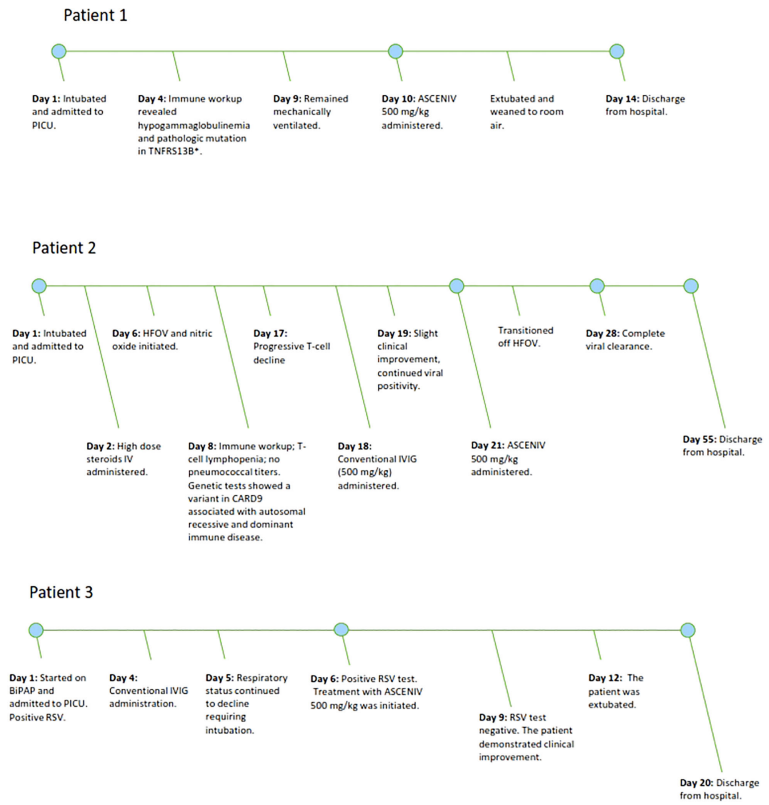

FIGURE 1
Figure 1 demonstrates the clinical timeline of three pediatric patients with severe courses of RSV lower respiratory tract infections. The timeline demonstrates the point in which ASCENIV 500 mg/kg was given during each patient's hospitalization.

Patient 3 was a 5-year-old girl with an extensive medical history including SAD with frequent viral infections and pneumonia requiring multiple PICU admissions, cerebellar ataxia, and moderate persistent asthma (Table 1). The patient presented to the hospital with increased work of breathing, decreased activity and poor urine output over the previous two days. Initial evaluation revealed RSV positivity using viral RT-PCR. Considering her prior history of rapid respiratory decline in the setting of respiratory infections and her current increased respiratory effort, the patient was subsequently admitted to the PICU on bilevel positive airway pressure (BiPAP).

She was started on a five-day course of azithromycin along with high-dose IV steroids. Other supportive measures including continuous albuterol, chest high frequency oscillations and a combination of an inhaled steroid and long-acting bronchodilator were also implemented.

On Day 4 of hospitalization, the immunology team was consulted due to her history of SAD. While admitted she received conventional IVIG, but despite this, the patient clinically decompensated requiring intubation and mechanical ventilation. On Day 6, viral RT-PCR testing again showed positivity to RSV; and ASCENIV 500 mg/kg was given. Three days later, repeat RSV rapid detection testing was negative. No adverse effects were observed after administration of ASCENIV in this patient. She was successfully extubated on Day 11 of hospitalization and gradually improved until discharge on Day 20. The patient has remained on IVIG therapy since discharge and has been clinically stable without any further hospitalizations.

Discussion

RSV is the most common etiology of bronchiolitis in young children. While most children clinically improve with care at home, RSV remains the leading cause of hospitalization among infants aged 12 months or less (5). Up to forty percent of children will experience lower respiratory tract infections during the initial RSV infection. Infection with RSV does not provide long-term immunity, with reinfections common throughout a patient's lifetime (10).

There have been prevention strategies for RSV in high-risk children, including palivizumab. Palivizumab is a monoclonal antibody that provides passive immunoprophylaxis to infants born at less than 32 weeks of gestation and/or in children less than 2 years-of- age with cardiopulmonary disease. It is given as monthly injections during the traditional months of the RSV season. The recent observation of the disruption in RSV seasonality since the COVID-19 pandemic has presented challenges with administration of palivizumab. Some have posed the consideration of giving more than the standard five consecutive

doses (11). There are additional monoclonal antibodies being evaluated, but they are still in clinical trials (12). Most recently in May of 2023, Arexvy became the first RSV recombinant vaccine approved by the FDA for adults 60 years and older (13). Currently, there are no approved vaccinations for the pediatric population.

Treatment for RSV disease is mainly supportive. In patients who have an immune dysregulation and a severe course of RSV, ribavirin and standard IVIG have been utilized. Ribavirin is a nucleoside analogue and is the only FDA-approved antiviral medication for the treatment of RSV. There have been concerns, though, about its high cost and effectiveness related to administration difficulties (11, 14). Regarding IVIG, there has historically been an unmet need for more direct neutralizing antibodies within the IVIG products. Therefore, ASCENIV poses a new consideration for possibly optimizing management.

ASCENIV is an approved IVIG that is manufactured from blending normal source plasma with plasma from donors that possess high antibody titers against a range of respiratory viral pathogens of concern. The efficacy and safety of ASCENIV has been documented in a Phase 3 study conducted in 59 patients. Patients were between the ages of 2 to 75 years with primary immunodeficiency disease. Each patient received ASCENIV 300-800 mg/kg every three or four weeks for 12 months. There were zero serious bacterial infections, thus meeting the primary endpoint. It was found in the study that the titer of anti-RSV neutralizing antibody increased by 5.47-fold and by 6.79-fold in subjects who received greater than 500 mg/kg (15).

In an investigation into the presence of antibody titers of ASCENIV versus other immunoglobulin therapies, ASCENIV was compared in aggregate to 10 different lots of commercially available standard polyclonal IVIG products. ASCENIV demonstrated consistently higher titers to nine respiratory pathogens assessed, including RSV, parainfluenza 1,2,3, influenza A and B, coronavirus OC43 and 229E, and human metapneumovirus. The mean titers of all antibodies were 1.5-fold higher in ASCENIV compared with standard IVIG and ranged from 1.4 to 1.9-fold higher depending upon the particular virus (16). Although it has high RSV anti-viral titers, ASCENIV does not currently possess the FDA-approved label for the treatment and prevention of RSV in immunocompromised individuals.

A study published by Falsey et al. (14), reported a series of 15 patients with immunosuppression/dysregulation and severe RSV infection. The patients ranged from 2 months-of-age to 71 years-of-age and received the ASCENIV precursor, RI-001, after failing standard care. Standard care included a variation of corticosteroids, standard IVIG, ribavirin, and/or palivizumab. In the analysis, the pre- and post-infusion neutralizing titers were measured. Each patient had a minimum of 4-fold increase in RSV-neutralizing antibody titers 5-10 days after the infusion. Seventy three percent of patients clinically improved and were discharged from the hospital.

This case series presents similar clinical findings. All three pediatric patients discussed were found had to have, or previous had, known immune abnormalities. Each patient experienced a severe course of RSV, which resulted in intubation and mechanical intubation. The concern for underlying immune dysregulation was validated because each presentation had a prolonged course of illness and failed best supportive care. In a large retrospective analysis at a tertiary care center, 73% of those who were admitted to PICU and required intubation from RSV had an immunodeficiency, hematologic, or oncologic process (17). ASCENIV was explored in each case as a possible adjunct to the current management strategy. Each patient did subsequently recover from the RSV illness and were discharged from the hospital. Although viral load studies were not collected, RSV RT-PCR was obtained on some of the patients and did demonstrate clearance. There was a mice model study done by Boukhvalova et al. (18) that demonstrated viral load reduction after treatment with the second generation product, RI-002 (ASCENIV). The mice were made immunodeficient with repeat exposure to cyclophosphamide, and subsequently infected with RSV. When RI-002 was given, it was observed that viral replication was inhibited, and that pulmonary inflammation and epithelial hyperplasia was minimized compared to the non-treated group.

The primary aim of this case series is two-fold. First is to propose the potential benefit of ASCENIV, in conjunction with best standard care, in the treatment of patients with severe RSV infections and immune dysregulation. It is important to note that true causality of ASCENIV in these patients' outcomes cannot be determined as that would need to be done in randomized controlled trials. Increasing awareness of this IVIG form may propel interest in future studies that investigate this specific question.

The second aim is to describe the minimal side effects of ASCENIV administration in pediatric patients. While ASCENIV has been approved for use in adults and adolescents (12-17 years of age), the safety and effectiveness of ASCENIV in children has not been well established in clinical trials (19). Compared to other IVIG forms, ASCENIV holds similar risks, including hypersensitivity reactions, aseptic meningitis, hemolysis, transmissible infectious agents, and interactions with medications. The top side effects reported include headache, sinusitis, nausea, and gastroenteritis (19). Each patient in the case series tolerated ASCENIV well and did not have any reported side effects. Falsey et al. (14) reported a similar finding with 53% of their cohort being less than 18 years-of-age.

Conclusion

The severity of RSV bronchiolitis in the three cases described raised concern for contributing primary immune dysregulation. Each patient did demonstrate immune abnormalities and suffered from clinical deterioration despite best standard care. This propelled the medical team to pursue ASCENIV as an additional treatment option. One dose of ASCENIV (500mg/kg) was given during the hospitalization which, in conjunction with the other medical interventions and natural course of the infection, resulted in the patients ultimately making a full recovery. None of the patients suffered from the adverse side effects described on the IVIG label. The potential causality of ASCENIV in the improved clinical outcomes should be explored as conclusions cannot not be reliably drawn from a case series. Future directions may include randomized

controlled trials to further investigate the question of ASCENIV being an effective RSV treatment in this less well studied age cohort.

Data availability statement

The original contributions presented in the study are included in the article/supplementary material. Further inquiries can be directed to the corresponding author.

Ethics statement

Written informed consent was obtained from the individual(s) for the publication of any potentially identifiable images or data included in this article.

Author contributions

All authors listed have made a substantial, direct, and intellectual contribution to the work and approved it for publication.

Acknowledgments

The editorial assistance of PPD was supported by funding from ADMA Biologics.

Conflict of interest

Author GW was employed by the company ADMA Biologics, Inc at the time of the study. Author JW served as consultant/advisor to the companies Takeda, X4- Pharmaceuticals,CSL-Behring, Grifols, ADMA Biologicals, Enzyvant, Regeneron, Pharming. Speaker's Bureau: Takeda and Pharming at the time of the study. Author JW received Grant/Research/Clinical Trial Support from Takeda, Janssen, Chiesi, MustangBio, ADMA Biologicals, Octapharma, X4-Pharmaceuticals, Novartis, Regeneron, Bristol-Myers Squibb.

The remaining authors declare that the research was conducted in the absence of any commercial or financial relationships that could be construed as a potential conflict of interest.

Publisher's note

References

1. U.S. Department of Health and Human Services - Centers for Disease Control and Prevention (CDC). *Respiratory syncytial virus (RSV)* (2020). Available at: https://www.cdc.gov/rsv/index.html.

2. Rose EB, Wheatley A, Langley G, Gerber S, Haynes A. Respiratory syncytial virus seasonality—United States 2014–2017. *Morbidity Mortality Weekly Rep* (2018) 67 (2):71. doi: 10.15585/mmwr.mm6702a4

3. Agha R, Avner JR. Delayed seasonal RSV surge observed during the COVID-19 pandemic. *Pediatrics* (2021) 148(3). doi: 10.1542/peds.2021-052089

4. Onwuchekwa C, Atwell J, Moreo LM, Menon S, MaChado B, Siapka M, et al. Pediatric RSV diagnostic testing performance: A systematic review and meta-analysis. *J Infect Dis* (2023), jiad185. doi: 10.1093/infdis/jiad185

5. U.S. Department of Health and Human Services - Centers for Disease Control and Prevention. *Increased interseasonal respiratory syncytial virus (RSV) activity in parts of the southern United States* (2021). Available at: https://emergency.cdc.gov/han/2021/han00443.asp.

6. Poodt AE, Driessen GJ, de Klein A, van Dongen JJ, an der Burg M, de Vries E. TACI mutations and disease susceptibility in patients with common variable immunodeficiency. *Clin Exp Immunol* (2009) 156(1):35–9. doi: 10.1111/j.1365-2249.2008.03863.x

7. Lee JJ, Jabara HH, Garibyan L, Rauter I, Sannikova T, Dillon SR, et al. The C104R mutant impairs the function of transmembrane activator and calcium modulator and cyclophilin ligand interactor (TACI) through haploinsufficiency. *J Allergy Clin Immunol* (2010) 126(6):1234–41.e2. doi: 10.1016/j.jaci.2010.08.017

8. Koopmans W, Woon ST, Brooks A, Dunbar PR, Browett P, Ameratunga R. Clinical variability of family members with the C104R mutation in transmembrane activator and calcium modulator and cyclophilin ligand interactor (TACI). *J Clin Immunol* (2012) 33:68–73. doi: 10.1007/s10875-012-9793-x

9. Piedimonte G, Perez MK. Respiratory syncytial virus infection and bronchiolitis. *Pediatr Rev* (2014) 35(12):519–30. doi: 10.1542/pir.35-12-519

10. Ralston SL, Lieberthal AS, Meissner HC, Alverson BK, Baley JE, Gadomski AM, et al. Clinical practice guideline: the diagnosis, management, and prevention of bronchiolitis. *Pediatrics* (2014) 134(5):e1474–502. doi: 10.1542/peds.2014-2742

11. Chuang YC, Lin KP, Wang LA, Yeh TK, Liu PY. The impact of the COVID-19 pandemic on respiratory syncytial virus infection: A narrative review. *Infect Drug Resist* (2023) 16:661–75. doi: 10.2147/IDR.S396434

12. Shang Z, Tan S, Ma D. Respiratory syncytial virus: from pathogenesis to potential therapeutic strategies. *Int J Biol Sci* (2021) 17(14):4073–91. doi: 10.7150/ijbs.64762

13. Federal Drug Association News Release. *FDA approves first respiratory syncytial virus (RSV) vaccine- arexvy approved for individuals 60 years of age and older* (2023). Available at: https://www.fda.gov/news-events/press-announcements/fda-approves-first-respiratory-syncytial-virus-rsv-vaccine.

14. Falsey AR, Koval C, DeVincenzo JP, Walsh EE. Compassionate use experience with high-titer respiratory syncytical virus (RSV) immunoglobulin in RSV-infected immunocompromised persons. *Transpl Infect Dis* (2017) 19(2). doi: 10.1111/tid.12657

15. Wasserman RL, Lumry W, Harris J3rd, Levy M, Stein M, Forbes L, et al. Efficacy, safety, and pharmacokinetics of a new 10% liquid intravenous immunoglobulin containing high titer neutralizing antibody to RSV and other respiratory viruses in subjects with primary immunodeficiency disease. *J Clin Immunol* (2016) 36(6):590–9. doi: 10.1007/s10875-016-0308-z

16. Orange JS, Du W, Falsey AR. Therapeutic immunoglobulin selected for high antibody titer to RSV also contains high antibody titers to other respiratory viruses. *Front Immunol* (2015) 6:431. doi: 10.3389/fimmu.2015.00431

17. Pham H, Thompson J, Wurzel D, Duke T. Ten years of severe respiratory syncytial virus infections in a tertiary paediatric intensive care unit. *J Paediatr Child Health* (2020) 56(1):61–7. doi: 10.1111/jpc.14491

18. Boukhvalova M, Blanco JC, Falsey AR, Mond J. Treatment with novel RSV Ig RI-002 controls viral replication and reduces pulmonary damage in immunocompromised Sigmodon hispidus. *Bone Marrow Transplant* (2016) 51(1):119–26. doi: 10.1038/bmt.2015.212

19. ADMA Biologics Inc. Boca Raton. *ASCENIV Human Immunoglobulin G Liquid [Package Insert]: Highlights of Prescribing information* (2019). Available at: https://www.asceniv.com/ASCENIV%2BPI.pdf.

Frontiers in Immunology

Explores novel approaches and diagnoses to treat immune disorders.

The official journal of the International Union of Immunological Societies (IUIS) and the most cited in its field, leading the way for research across basic, translational and clinical immunology.

Discover the latest Research Topics

See more →

Frontiers

Avenue du Tribunal-Fédéral 34
1005 Lausanne, Switzerland
frontiersin.org

Contact us

+41 (0)21 510 17 00
frontiersin.org/about/contact